Methane Hydrate Production from Alaskan Permafrost

Technical Progress Report

January 1, 2003 to March 31, 2003

by

Thomas E. Williams and William J. McDonald

(Maurer Technology Inc.)

Keith Millheim (Anadarko Petroleum Corp.)

Buddy King (Noble Corp.)

June 2003

DE-FC26-01NT41331

Maurer Technology Inc.
13135 South Dairy Ashford, Suite 800
Sugar Land, TX 77478

Anadarko Petroleum Corp.
1201 Lake Robbins Drive
The Woodlands, TX 77380

Noble Corp.
13135 South Dairy Ashford, Suite 800
Sugar Land, TX 77478

Disclaimer

Abstract

Natural-gas hydrates have been encountered beneath the permafrost and considered a nuisance by the oil and gas industry for years. Engineers working in Russia, Canada and the U.S have documented numerous drilling problems, including kicks and uncontrolled gas releases, in arctic regions. Information has been generated in laboratory studies pertaining to the extent, volume, chemistry and phase behavior of gas hydrates. Scientists studying hydrate potential agree that the potential is great – on the North Slope of Alaska alone, it has been estimated at 590 TCF. However, little information has been obtained on physical samples taken from actual rock containing hydrates.

This project is in the second year of a three-year endeavor being sponsored by Maurer Technology, Noble, and Anadarko Petroleum, in partnership with the DOE. The purpose of the project is to build on previous & ongoing R&D in the area of onshore hydrate deposition. We plan to identify, quantify and predict production potential for hydrates located on the North Slope of Alaska. We also plan to design and implement a program to safely and economically drill, core and produce gas from arctic hydrates. The current work scope is to drill and core a well on Anadarko leases in FY 2003. We are also using an on-site core analysis laboratory to determine some of the physical characteristics of the hydrates and surrounding rock. The well is being drilled from a new Anadarko Arctic Platform that will have minimal footprint and environmental impact. We hope to correlate geology, geophysics, logs, and drilling and production data to allow reservoir models to be calibrated. Ultimately, the goal is to form an objective technical and economic evaluation of reservoir potential in Alaska.

Table of Contents

List of Figures

1. Introduction

The purpose of this project is to plan, design and implement a program that will safely and economically drill/core and produce natural gas from arctic hydrates. A significant amount of research has been conducted on naturally occurring gas hydrates, and our team (Maurer, Anadarko and Noble) will adapt and apply laboratory R&D and technology in the field.

This is an aggressive project that will identify, quantify and predict production potential of hydrates by drilling the first dedicated hydrate well on the North Slope of Alaska in an area with hydrate potential. This project will utilize an Anadarko special purpose on-site laboratory to help analyze hydrate cores. Additionally, the well will be drilled from a special purpose-built arctic platform. Data generated in this project will also assist research organizations and technical teams as we begin to make an objective technical and economic assessment of this promising natural gas reservoir potential.

2. Executive Summary

METHANE HYDRATE PRODUCTION FROM ALASKA PERMAFROST

The objective of this project is to analyze existing geological and geophysical data and obtain new field data required to predict hydrate occurrences; to test the best methods and tools for drilling and recovering hydrates; and to plan, design, and implement a program to safely and economically drill and produce gas from hydrates in Alaska.

The overall scope of the work is to:

1. Evaluate geological and geophysical data that aid in delineation of hydrate prospects

2. Evaluate existing best technology to drill, complete and produce gas hydrates

3. Develop a plan to drill, core, test and instrument gas-hydrate wells in Northern Alaska

4. Characterize the resource through geophysics, logging, engineering and geological core and fluids analysis

5. Test and then monitor gas production from hydrate wells for one year

6. Quantify models/simulators with data for estimating ultimate recovery potential

7. Learn how to identify favorable stratigraphic intervals that enhance methane production

8. Assess commercial viability of developing this resource and ultimately develop a long-term production plan

9. Provide real hydrate core samples for laboratory testing

10. Develop and test physical and chemical methods to stabilize hydrate wellbores and improve core recovery

11. Step outside the well-known Prudhoe Bay/Kuparuk River area to further delineate hydrate deposits in Alaska

12. Report results to the DOE and transfer technology to the Industry

Phase I has been completed, which included well planning, site selection and equipment construction.

Phase II encompasses drilling and coring a hydrate well. During the first quarter of 2003, permits were issued and a permit application report was submitted to the DOE COR. The Anadarko Arctic Platform was completed, mobilized and assembled at the HOT ICE #1 well along with the rig, base camp and remote laboratory. The well was spudded on March 31, 2003. Drilling was suspended at 1400 feet (due to unseasonably warm weather) on April 24, 2003. Seven-inch casing was set through the base of the permafrost following logging of the upper section of the well. A report of the formation evaluation of the upper section was presented to the DOE on May 28. A report will be included in the next quarterly report. Some of the equipment (including the core and remote laboratory) were demobilized to Dead Horse, Alaska. Plans call for drilling to resume in the fourth quarter of 2003.

The well is being cored from top to bottom. Recovered cores are 3.25 inches in diameter and 10 ft long. Drilling fluids were chilled to -5°C. Approximately 92.5% of the core was recovered through the permafrost and is currently being analyzed. The UGNU sands (described in the modeling report) were encountered in the permafrost. It was determined that the base of the permafrost was at 1282 ft. The entire well will be thoroughly logged and tested. Core will be analyzed on site using an innovative mobile laboratory. This laboratory was constructed and the equipment tested in Tulsa, Oklahoma.

The USGS at Menlo Park provided hydrate core samples to test the equipment. Additional equipment that was effectively used on the ODP leg 204 has been provided at the well including the Lawrence Berkeley Laboratory CT Scanner and the Pacific NW Laboratory IR camera. A downhole temperature, pressure and inclination tool was also provided by Sandia Laboratory. Important modeling for well planning was conducted by Lawrence Berkeley Lab and the USGS. A report, "Dissociation Rates of Methane Hydrate at Elevated Pressures and of a Quartz Sand/Methane Mixture at 0.1 MPa," by Kirby and Stern of the USGS was utilized in the well planning (see **Appendix F**). CMR and NMR tools were provided by Schlumberger as well as scientists for evaluation and interpretation. The USGS provided equipment and personnel to take coal cores. A report on the coal from the USGS is included in **Appendix D**.

The advisory board met in March 2003 to review the well plans and complete the well-planning process. An overview of the project was provided by Anadarko. Reports of supporting work were presented by George Moridis of LBNL on Modeling (**Appendix E**) and Barry Freifeld on the CT for evaluation of hydrate cores. Other reports and presentations included the USGS report on Dissociation Rates (**Appendix F**), and three reports from University of Anchorage, Alaska ("Geologic Research of Well Records and Stratigraphy of the North Slope Region near Kuparuk, Alaska;" "Fundamental and Applied Research on Water Generated During the Production of Gas Hydrates (Phase 1);" and "Permafrost Foundations and Their Suitability as Tundra Platform Legs" (**Appendix C**)). Following this meeting Brad Tomer and Edith Allison from the DOE visited the well location. A number of other officials from the Department of Interior also visited the site. Assistant Secretary Mike Smith and Deputy Assistant Secretary Jim Slutz visited the well in April to prepare for a national Press Conference in Washington DC. Presentations by Anadarko and Maurer were provided, and a video of the Arctic Platform construction was shown. Noble Engineering and Development (NED) provided live data from the well. The DOE press release has generated numerous articles in oil and gas and scientific journals and magazines.

DOE NETL has also established a special web page for references to their support of gas-hydrate development. At their site (http://www.netl.doe.gov/scng/hydrate/) are posted updates describing the Hot Ice project as well as the latest version of “Fire in the Ice,” the National Energy Technology Laboratory Methane Hydrate Newsletter. The most recent version of the newsletter is Spring 2003.

After drilling has resumed at Hot Ice #1, the well will be drilled through sands that are expected to hold gas hydrates. The well will then be logged and shallow seismic (VSP) will be shot. A production test will be performed for 5-10 days, and the well will then be monitored for an extended period. An advanced hydrate simulator developed by Lawrence Berkeley National Laboratory will be calibrated with field data and used in the development of economic and production models for this and other hydrate accumulations.

3. Background and Statement of Work

3.1 BACKGROUND

Natural-gas hydrates (**Figure 1**) beneath the permafrost have been encountered by the oil and gas industry for years. Numerous drilling problems, including gas kicks and uncontrolled gas releases, have been well documented in the arctic regions by Russian, USA and Canadian engineers. There has been a significant volume of scientific information generated in laboratory studies over the past decade as to the extent, volume, chemistry and phase behavior of gas hydrates. However, virtually all of this information was obtained on hydrate samples created in the laboratory, not samples from the field.

Figure 1.
Methane Hydrate

Discovery of large accumulations around the world (**Figure 2**) has confirmed that gas hydrates may represent a significant energy source. Publications (Makogon and others) on the Messoyakhi gas-hydrate production in Siberia (which has produced since 1965), document that the potential for gas-hydrate production exists. Several studies have also addressed the potential for gas hydrates in the permafrost regions of North America. The results from the Mallik Hydrate, Mackenzie Delta Northwest Territories, Canada wells (hereafter, the "Mallik wells") drilled by JAPEX, JNOC and GSC, provide a significant amount of useful background information. The USGS made sizeable contributions to the Mallik project, as well as many other investigations on gas hydrates in the USA (especially Alaska), and has a tremendous amount of basic information on the presence and behavior of hydrates.

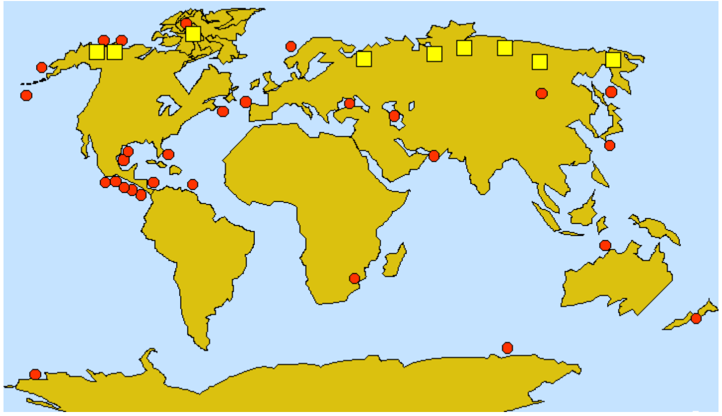

Figure 2. Methane Hydrate Deposits (USGS)

The project team now believes it is time to apply this knowledge to environmentally sound development of this resource. The first critical step is to drill and monitor wells in regions in the USA with the greatest likelihood of commercial quantities of methane hydrates. In fact, the project work represents the first attempt to drill, core and monitor hydrate wells in the USA. The specific objective of this effort is to obtain the field data required to verify geological, geophysical and geochemical models of hydrates and to plan, design and implement a program to safely and economically drill and produce gas from arctic hydrates. These "ground truth" data did not previously exist.

North America's emphasis on utilizing clean-burning natural gas for power generation has increased demand for gas and resulted in higher gas prices. A number of forecasts, including the NPC Study on Natural Gas (2000), indicate higher demand with prices in the range of $4 to $8/mcf. This is sufficiently high to allow investments in sources previously deemed uneconomic. The projected US demand for natural gas may grow to nearly 30 TCF by the end of the decade. This demand, particularly on the West Coast of the US, strongly suggests that a proposed Alaska Natural Gas Pipeline may now be economically feasible. This pending pipeline should provide a commercial market for natural gas, thereby allowing the necessary investments in new technology to develop and market the hydrate resource.

Anadarko is the one of the largest independent oil and gas exploration and production companies in the world, with 6.1 TCF of gas reserves and 1046 MMBO of oil reserves (more than 2 BBOE). Domestically, it has operations in Texas, Louisiana, the Mid-Continent and Rocky Mountains, Alaska and the Gulf of Mexico. Anadarko, one of the most active drillers in North America, is balancing its current exploration and production programs by investing in developing new gas resources in North America, including areas where the risks and potential rewards are high with the application of advanced technology. It is now one of the largest leaseholders in Alaska, with an ambitious program of exploratory drilling and seismic studies. Anadarko holds nearly 500,000 undeveloped acres under lease, many with the potential for commercial production from hydrates. Anadarko also has extensive holdings in the Mackenzie Delta region of the Northwest Territories of Canada, which also hold potential for hydrates. Thus, Anadarko is very interested in developing this resource.

With the amount of information on hydrates now available and the potential of developing this huge resource, this project makes good economic sense at this time. The best resources and ideas from around the world will be used to implement the technology in the field. Thorough planning of the test wells should allow avoiding some of the problems encountered in previous gas-hydrate wells.

This project will provide valuable information to the DOE, industry, and research community to identify key barriers and problems related to gas-hydrate exploration and production. This information will be highly useful in developing innovative, cost-effective methods to overcome these barriers. Close interaction will be maintained with an Advisory Board that includes Teresa Imm, Arctic Slope Regional Corp., Craig Woolard, University of Alaska Anchorage, Steve Kirby, USGS, Steve Bartz, Schlumberger, Timothy Colette, USGS, David Young, Baker Hughes Inteq, Rick Miller, Kansas Geological Survey, and Carl Sondergeld, University of Oklahoma.

3.2 OBJECTIVES

The objectives of this gas-hydrate project are to:

1. Analyze existing geological and geophysical data and obtain new field data required to predict hydrate occurrences

2. Test the best methods and tools for drilling and recovering hydrates

3. Plan, design, and implement a program to safely and economically drill and produce gas from hydrates.

3.3 SCOPE OF WORK

The overall scope of the work is to:

1. Evaluate geological and geophysical data that aid in delineation of hydrate prospects

2. Evaluate existing best technology to drill, complete and produce gas hydrates

3. Develop a plan to drill, core, test and instrument a gas-hydrate well in Northern Alaska

4. Characterize the resource through geophysics, logging, engineering and geological core and fluids analysis

5. Test and then monitor gas production from the hydrate wells for an extended period of time.

6. Quantify models/simulators with data for estimating ultimate recovery potential

7. Learn how to identify favorable stratigraphic intervals that enhance methane production

8. Assess commercial viability of developing this resource and ultimately develop a long-term production plan

9. Provide real hydrate core samples for laboratory testing

10. Develop and test physical and chemical methods to stabilize hydrate wellbores and improve core recovery

11. Step outside the well-known Prudhoe Bay/Kuparuk River area to further delineate hydrate deposits in Alaska

12. Report results to the DOE and transfer technology to the Industry

During **Phase I**, an effective plan was developed for drilling new hydrate wells in Alaska. This included geological and geophysical assessment, site selection, and developing well plans.

In separate reports we have provided DOE with the following Phase I Deliverables:

- Digital map of well locations
- Well log correlation sections
- Seismic maps and sections showing stratigraphic and lithologic units within gas hydrate stability zone
- Reservoir modeling report
- Well data for control wells used for site selection
- Site selection plan
- Testing and analytical procedures (Topical Report)
- Well plan
- Permit application
- NEPA requirements

Additional Phase I achievements beyond the original contract obligations include:

- Topical reports from University of Oklahoma and the Drilling Research Center on hydrate core apparatus and testing
- Support of other DOE hydrate projects including the Westport Core Handling Manual
- Three reports from the University of Alaska Anchorage
    1. Geological Research of Well Records
    2. Water Generated during Production of Gas Hydrates
    3. Permafrost Foundations/Suitability of Tundra Platform Legs
- USGS (Kirby et al.) report on dissociation of hydrates at elevated pressures
- LBNL Report on Hydrate Preservation in Cores
- Arctic Platform Video
- National Press Release and Conference in Washington DC

- First-ever North Slope coal cores provided to the USGS for coalbed methane study

- New equipment for measuring hydrates

Phase II encompasses drilling/coring a new hydrate well. After drilling, the well will be thoroughly logged and tested. Core will be analyzed on site using an innovative mobile laboratory. After completion, shallow seismic will be shot. The wells will then be monitored for an extended period and assessed for production potential. An advanced hydrates simulator will be calibrated with field data and used in the development of economic and production models for these and other hydrate accumulations.

3.4 STATEMENT OF WORK

Team organization is shown in Figure 3.

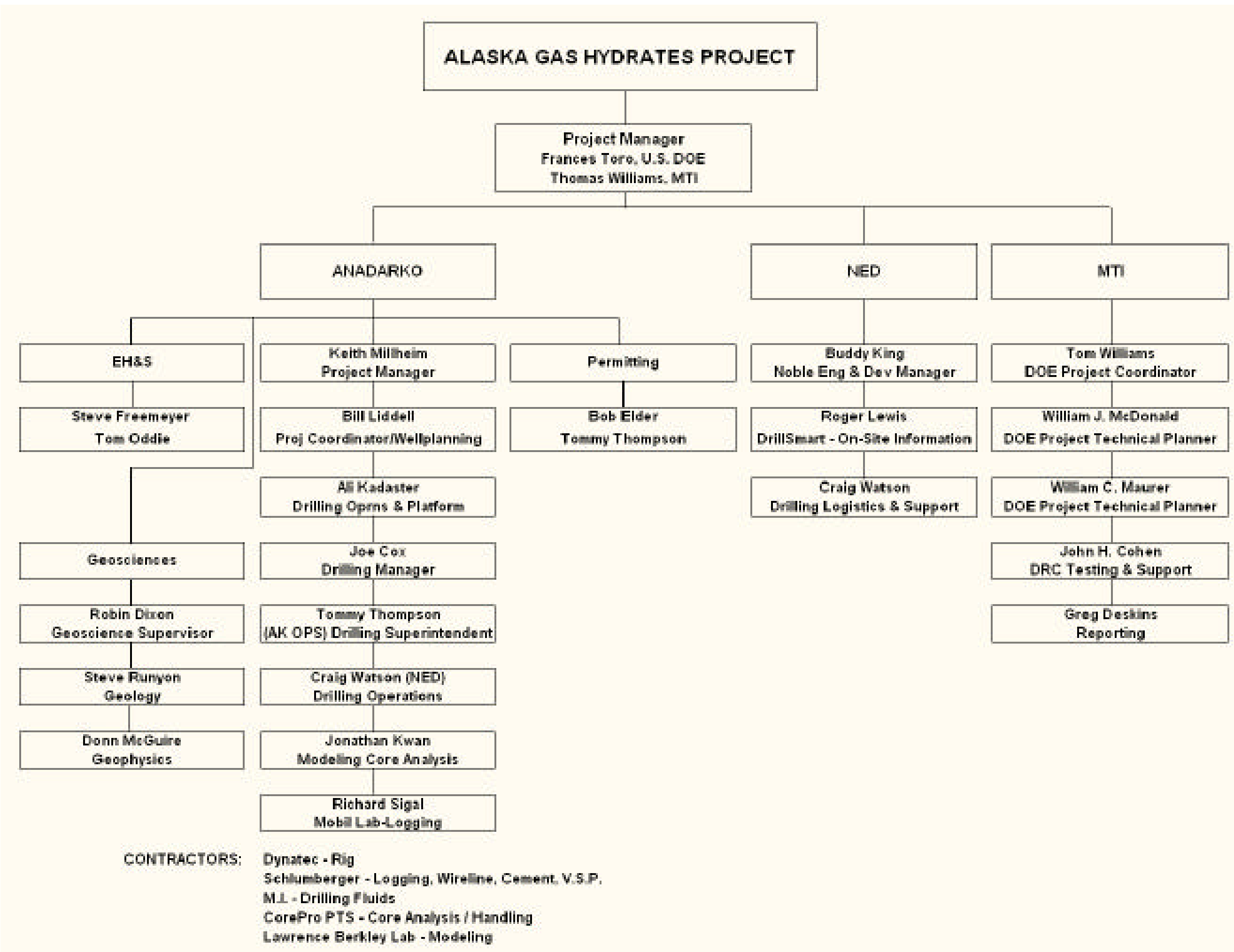

Figure 3. Project Team Structure

PHASE I

Phase I is now complete. Tasks 1-7 were completed as shown in the Phase I schedule in **Figure 4**.

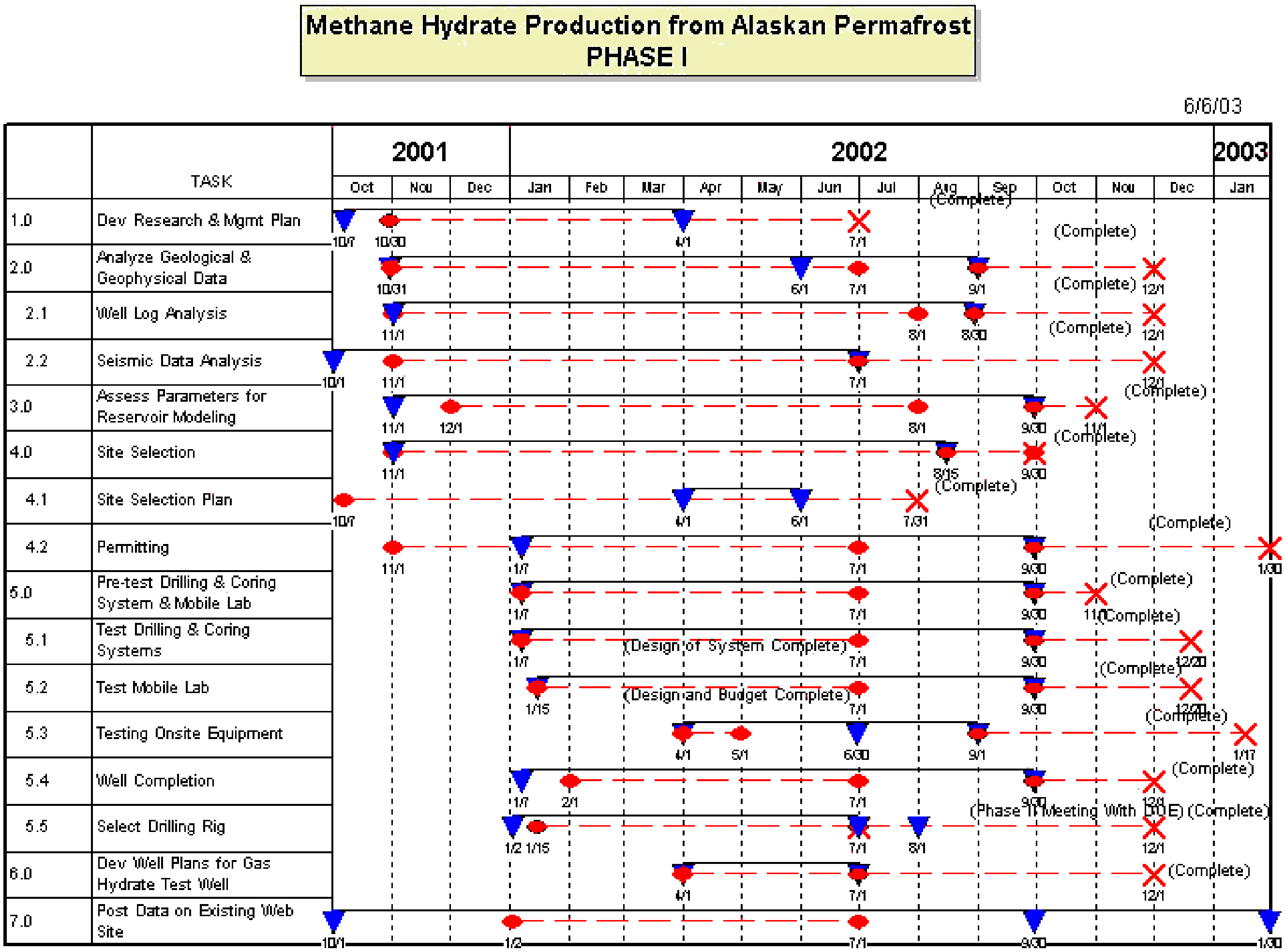

Figure 4. Phase I Project Schedule

PHASE II

The overall objective of Phase II will be to test exploitation techniques developed in Phase I by drilling/coring and completing one or more wells, and then performing a comprehensive battery of well tests and logs. Next, the well(s) will be monitored for a full year to develop long-term production options. Tasks to accomplish these objectives are described below. Phase II tasks are subject to change.

A comprehensive project management schedule (**Figure 5**) is used to track all the activities on-going in Phase II. These are tracked to assure this project is progressing properly. A "lessons learned" workshop is scheduled for June 12–17, 2003. This activity list may be revised at that meeting.

ID	Task Name	Start	Finish
	Alaska Hydrates DOE Project (Complete)	29-Dec-2001	30-May-2004
1	Phase I Continuation Planning/Preparation	29-Dec-2001	14-Feb-2003
15	Phase II - Alaska Hydrates Project	3-Sep-2002	30-May-2004
16	Modifications to Drilling/Coring Rig	1-Oct-2002	25-Jan-2003
21	Arctic Drilling Platform Testing/Construction	3-Sep-2002	8-Feb-2003
22	Leg Shipment/Install VSMs	25-Sep-2002	20-Oct-2002
23	Install Legs and Test Fixture/Freeze-in	21-Oct-2002	13-Nov-2002
24	Leg Testing - Proof Loading (Phase I)	8-Nov-2002	23-Nov-2002
25	Module Construction	3-Sep-2002	14-Dec-2002
26	Finish Out Platform/Rig Winterization	15-Dec-2002	18-Jan-2003
27	Ship to Deadhorse	19-Jan-2003	8-Feb-2003
28	Phase II Drilling, Completion, Testing	12-Oct-2002	7-Mar-2004
29	HAZOP Review - Task 9.1	14-Oct-2002	16-Oct-2002
30	Arctic Training - Task 8.1	12-Oct-2002	12-Mar-2003
31	Mobilization and Drilling	27-Jan-2003	24-Nov-2003
32	Set Template/Auger Holes for Legs	27-Jan-2003	2-Feb-2003
33	Set Legs/Freeze-In (Task 9.5)	3-Feb-2003	17-Feb-2003
34	Set Platform (Task 9.5)	18-Feb-2003	24-Feb-2003
35	Mob Personnel/Camp/Rig/Equip on to Platform	25-Feb-2003	3-Mar-2003
36	Install NED Drilling/Communications Equipment	1-Mar-2003	3-Mar-2003
37	SPUD and Drill HOT ICE #1 (Task 9.2)	31-Mar-2003	24-Nov-2003
38	Core to 1300'	31-Mar-2003	17-Apr-2003
39	Open Hole to 8.5"	18-Apr-2003	20-Apr-2003
40	Log Run and Cement 7" Casing	21-Apr-2003	22-Apr-2003
41	Core to ~2600 ft	23-Apr-2003	18-Nov-2003
42	Log and VSP (Tasks 10 and 12)	19-Nov-2003	22-Nov-2003
43	Run and Cement 4.5" Casing	23-Nov-2003	24-Nov-2003
44	Core and Fluid Diagnostics (Task 11.0)	31-Mar-2003	25-Nov-2003
45	On-site core and fluid analysis	31-Mar-2003	25-Nov-2003
46	Completion and Testing of Hydrates)	23-Nov-2003	5-Dec-2003
47	Run Completion Equipment (Task 13.0)	23-Nov-2003	24-Nov-2003
48	Installation of Surface Test Equipment	25-Nov-2003	27-Nov-2003
49	Production Test of Hydrates (Task 15.0)	28-Nov-2003	5-Dec-2003
50	Produce Well 5 days	28-Nov-2003	2-Dec-2003
51	Build up 2 days	3-Dec-2003	4-Dec-2003
52	Suspend Well	5-Dec-2003	5-Dec-2003
53	Demob Drilling Equipment	26-Nov-2003	11-Dec-2003
54	Demob Excess Equipment (Task 8.2)	26-Nov-2003	30-Nov-2003
55	Demob Rig (Task 8.2)	6-Dec-2003	7-Dec-2003
56	Demob Testing/Assoc Equip (Task 8.2)	6-Dec-2003	11-Dec-2003
57	Demob Platform (Task 9.5)	6-Dec-2003	11-Dec-2003
58	If Longterm Test is Approved by DOE:	6-Dec-2003	7-Mar-2004
61	Reservoir Characterization (Task 17)	23-Nov-2003	25-May-2004
65	Reservoir Modeling - Hydrate Potential (Task 18)	17-Dec-2002	1-Apr-2003
66	Quantification of Model (Task 19)	2-Jan-2004	31-Mar-2004
67	Economic Projection (Task 20)	5-Jan-2004	30-May-2004
68	Interim Economic Assessment	5-Jan-2004	5-Feb-2004
69	Create a Generic Development Plan	2-Mar-2004	15-Mar-2004
70	Develop Cost Schedule	16-Mar-2004	29-Mar-2004
71	Generate Stochastic Model for Reserves	1-Apr-2004	30-Apr-2004
72	Generate Stochastic Economics	1-May-2004	30-May-2004
73	Develop Well Plan for Future NS Hydrate Wells	2-Jan-2004	1-Mar-2004
74	Info Acquisition and Technology Transfer (Task 22)	12-Sep-2002	31-Mar-2004

Figure 5. Phase II Project Schedule

Subtask 4.2 – Permitting

Permitting has been completed. The first three wells permitted are named Hot Ice #1, #2 and # 3 (HOT ICE = High Output Technology Innovatively Chasing Energy). Following the Anadarko Geological and Geophysical assessment and the Site Selection task, the best location was selected in November and final permitting activity has focused on this location for HOT ICE #1. With the addition of the Arctic Platform, new permitting activities and costs have resulted. Meetings and inspections by State and Federal regulators have continued to take place. A number of positive reports complimentary of the operation have resulted.

The permit application was provided to the DOE (see below)

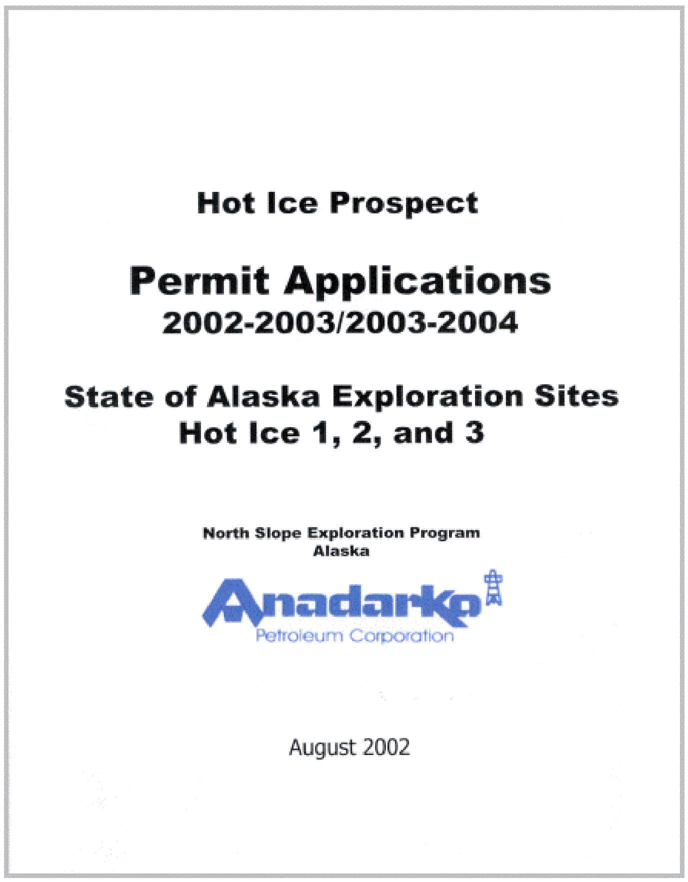
Hot Ice Prospect

Permit Applications
2002-2003/2003-2004

State of Alaska Exploration Sites
Hot Ice 1, 2, and 3

North Slope Exploration Program
Alaska

Anadarko
Petroleum Corporation

August 2002

A recent map showing the location of the site is presented in **Figure 6**.

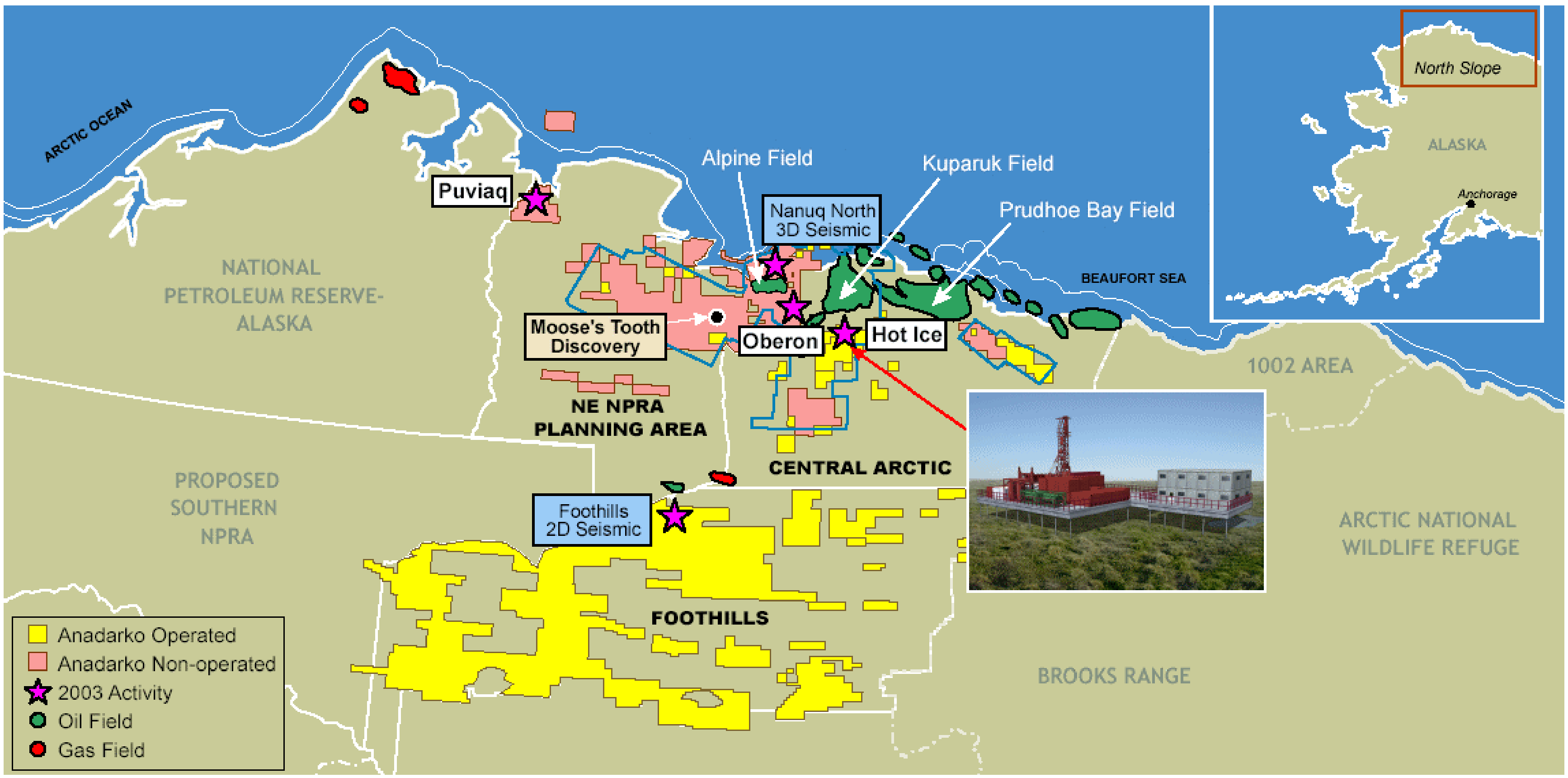

Figure 6. Map of North Slope Showing Hot Ice #1

Task 7.0 – Posting Data on Existing Web Sites

Maurer constructed an Internet web site (http://www.maurertechnology.com/index-hydrates.html) for hydrate project updates. It is linked to the NETL hydrate web site and displays presentations, progress highlights and photos. This site will continue to be updated to make results available to the R&D community. Special information is available to the project team (including DOE) through a password-protected page. Information about our project is being exchanged with other hydrate research organizations and meetings. Press releases have been issued, and the energy press has contacted Maurer and Anadarko for progress updates and information about the project. A number articles have appeared in Pe*troleum New Alaska, Hart's E&P, World Oil,* and others.

Task 8.0 – Preparation and Mobilization

Subtask 8.1 Arctic Training

The required training has been completed for all personnel who will be working on the North Slope overnight in support of this project. Training courses included: First Aid, Respiratory, FIT Test, H2S Training, NSTC Training, Hazcom/Hazwoper, PPE, Alaska Safety Handbook, Arctic Survival, Bear Awareness, NPRA Training, and Fire Extinguisher Training.

Subtask 8.2 Pad/Platform Preparation, Mobilization, and Construction

Permits have been issued, and we will erect an arctic platform at the well location in February. The recipient shall mobilize drill platform equipment to the well location, using an existing gravel road and a staging area at the end of the road.

Subtask 8.3 Personnel Mobilization

The recipient shall transport all project personnel to and from the well site. This task shall include transport of camp crew, catering staff, maintenance crew, rig crew, lab crew, logging crew, cementing crew, mud crew, and supervisory personnel.

Task 9.0 – Drilling and Coring

The recipient shall winterize the drill rig and mobilize it to Deadhorse and then to the well location. The recipient shall drill and core one or more wells from the arctic platform.

Subtask 9.1 Environmental Health and Safety

The recipient shall monitor and respond to environmental health and safety concerns, including monitoring and manifesting waste, in order to ensure compliance with regulations specified in permits.

Subtask 9.2 Drilling and Coring

The recipient shall drill and core one or more wells from the arctic platform constructed in Subtask 8.2. The recipient shall use the Noble Engineering and Development Drill Smart System to allow engineers to monitor and view drilling operations live from Houston.

Subtask 9.3 Maintain Camp Facilities

The recipient shall provide camp facilities to house and feed the crews rotating on a 12/12 shift schedule.

Subtask 9.4 Transportation of Drilling Supplies

The recipient shall transport by trucks and rolligons personnel, equipment, and supplies used in the drilling operations, including drilling fluids and drilling mud.

Subtask 9.5 Arctic Platform

The Anadarko Arctic Platform was constructed and tested in Houston, Texas. The structure is made of lightweight aluminum. It was mobilized to the base camp in January 2003, and inspected prior to mobilization to the well location in February (**Figure 7**). The legs were tested and put on location as soon as the freeze period began in January. A video of the transportation and construction was provided to the DOE. Legs were installed into the tundra permafrost and frozen into place. The platform can be mobilized by either helicopter and/or Rolligon from the base camp and assembled at the well location. Environmental monitoring equipment was also installed.

Figure 7. Arctic Platform at Hot Ice #1

The platform drilling area is 100 x 100 ft, and the base camp is 62.5 x 50 ft on an adjacent platform. The rig, equipment and base camp were installed on the platform by Rolligon and two cranes. After completion of drilling and completion operations, some of the equipment will be demobilized, with the remainder staying until well testing has been completed. The entire platform will be demobilized to Dead Horse. The platform will be thoroughly inspected by a third party and a post-analysis study conducted with recommendations on future operations. A thorough report will be provided after completion of this subtask.

Task 10.0 – Well Logging

The recipient shall run a suite of logs in the well(s) to characterize gas hydrate-bearing intervals, including the following: 1) electrical resistivity (dual induction), 2) spontaneous potential, 3) caliper, 4) acoustic transit-time, 5) neutron porosity, 6) density, and 7) nuclear magnetic resonance. Core data will be used to calibrate and quantify log information.

Task 11.0 – On-Site Core and Fluids Analysis

The recipient shall analyze core and fluids using a specially constructed mobile core laboratory, staffed by trained laboratory technicians. Core will be received in the cold module, where it will be photographed and assessed for the presence of hydrate. One-inch plugs will be removed from the core, and these plugs will be measured for porosity, permeability, compressional and shear wave velocity, resistivity, thermal conductivity, and NMR with specialized equipment specifically designed for making these hydrate core measurements, including a Schlumberger CMR tool. All of these measurements will be made under controlled pressure and temperature. Hydrate dissociation shall be monitored. Laboratory technicians will assist in preparing core for additional testing at other locations. Results of core and fluids handling procedures will be incorporated into the DOE-funded Westport Hydrate Core Handling Manual. The results of the analysis will be incorporated in Tasks 17, 18, 19 and 20.

Regarding the use of the LBNL CT (**Figure 8**) on site:

1. We are partitioning one end of a 20-ft Conex with a separate door to the outside for the X-ray room

2. There will be heater located in the room or an electrical outlet to add a portable heater

3. The x-ray room is adjacent to the station where the core will be cut to 3-ft lengths

4. Core sections will then be taken outside and then into the x-ray room

5. The x-ray machine can be started in a temperature-controlled environment

6. During shipment, the machine will be subjected to ambient temperatures as low as -40°F, (unless special measures are taken)

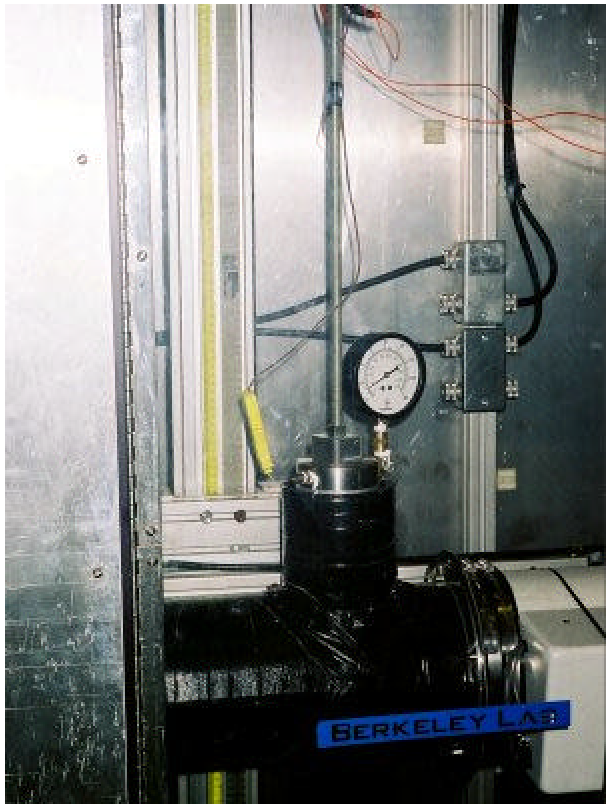

Figure 8. LBNL CT Scanner

The x-ray scanner is certified to be "cabinet safe." This means that any personnel can be near it for normal operation, and the user does not need to be fitted with a dosimeter. Only a certified "system maintainer" can use tools to perform maintenance and has the ability to modify or override interlock safety features.

This authority is granted from our EH&S department, and Victor will be the system maintainer. He will bring his own badge.

Regarding operation: the machine will need to be "tuned" to the samples that are collected. This means that adjustments must be made to both x-ray voltage and current depending on the density and composition of the samples. There could also be adjustments to the camera behind the image intensifier. It is hard to predict how often and when this task will need to be performed. Since we will be performing dual-energy scanning, both our hard and soft x-ray energies will need to be periodically readjusted depending on the collected core density and composition.

LBNL modified the machine so that it will hold a 3-ft piece of core. Four-ft long core holders were constructed since the extra space at the top of the core holder will be empty, preventing concern about core length. The quick scan will be performed in about two to three minutes from the time the sample in the sample holder is placed in the x-ray unit, to when it can be removed from the x-ray unit. A more detailed full 3-D CT characterization will take about 12 minutes for the entire 3-ft length. A shorter interval (i.e., 4 inches) can be scanned in full 3-D mode in about 2 minutes. We will have three to five core holders so that one can be loaded, while another one is being cleaned or prepped and a third can be in the scanner.

Task 12.0 – Shallow Seismic Survey(s)

After the well has been logged, a 3D vertical seismic profile (VSP) will be acquired to calibrate the shallow geologic section with seismic data and to investigate techniques to better resolve lateral subsurface variations of hydrate-bearing strata. Paulsson Geophysical Services, Inc. will deploy their 80 level 3C clamped borehole seismic receiver array in the wellbore to record samples every 25 feet. The surface vibrators will successively occupy 800 different offset positions arranged around the wellbore. This technique will generate a 3D image of the subsurface. Correlations of these seismic data with cores, logging, and other well data will be generated.

Task 13.0 – Well Completion

After the seismic data have been collected, the recipient shall complete the well. The completion method will be determined based on the results of drilling, coring, and logging. The base case is to produce one well completed in a single hydrate interval below the permafrost using tubing conveyed perforating guns and permanent downhole pressure gauges. The well shall be perforated in the hydrate interval after cementing 4-1/2 inch casing. The water and gas shall be produced into the production tubing after the hydrostatic pressure is reduced by swabbing. The well will be shut in downhole with a slickline plug to reduce wellbore storage volume. The well shall be equipped with multiple electronic BHP/temperature memory gauges near the perforations. A heat strip will be attached to the testing string to prevent fresh produced water from refreezing across from the permafrost when the well is shut in.

BHP/temperature gauges and heater cable shall be run into the well on 2-3/8 inch NU production tubing. Production facilities consisting of a two-phase vertical separator with gas and water measurement in a winterized enclosure will be hooked up. After testing, the well will be plugged and abandoned.

Task 14.0 – Well Instrumenting

The recipient shall equip the well(s) with downhole pressure and temperature transducers as part of the completion. This will allow the well(s) to be monitored during testing, and it will provide extended monitoring capabilities. It is anticipated that the well will be plugged and abandoned before tundra closure. At this time we do not have regulatory approval to work on the well after tundra closure. With the low anticipated production rates and the relatively short production time, there should not be a need for an extended pressure monitoring program.

Task 15.0 – Well Testing

The recipient shall commence well testing shortly after the well(s) has been perforated and the tubing run in the well(s). The well(s) will initially be produced with a large draw down to determine the productivity of a hydrate zone without thermal stimulation. The well(s) will be produced for a short time to determine if a stabilized rate is obtained. It will then be shut in and the bottomhole pressure recorded. The length of time the well(s) will be produced and shut in has not yet been determined. The total producing time will be approximately 5 days. Water and gas samples will be collected to determine composition.

Task 16.0 – Data Collection and Transmission

The recipient shall perform lab work and collect data on fluids captured during the well testing. The recipient shall also collect and transmit extended monitoring information.

Task 17.0 – Reservoir Characterization of the Core

The recipient shall characterize the hydrate reservoir, based on analyses of fluids, geology, engineering, logs, geophysics, and rock physics. All these data will be included in a well simulator. The recipient shall determine the percentage of gas contained in the hydrate zone that can be recovered from the reservoir, and the potential production rates. Core studies will be conducted to accurately predict reservoir producibility potential.

Task 18.0 – Reservoir Modeling

The recipient shall use information developed in reservoir characterization efforts to quantify Lawrence Berkeley National Laboratory's hydrate simulator. LBL's advanced simulator system is based on EOSHYDR2, a new module for the TOUGH2 general-purpose simulator for multi-component, multiphase fluid and heat flow and transport in the subsurface environment. Reservoir simulation during this phase of the project will focus on considering production schemes, both short and long term, for hydrate production on the North Slope based on all the reservoir characterization data obtained. Depressurization, injection and thermal methods are some of the production processes to be considered with the simulation.

Task 19.0 – Quantify the Model

This task will parallel Tasks 17 and 18. The reservoir model used will need to be continuously refined as well test data are acquired. This effort is an ongoing task required for making projections. Models will be enhanced iteratively to incorporate dynamic production data during the well test period.

Task 20.0 – Economic Projections and Production Options

After all model results are received, the recipient shall assess economic projections and production options. The recipient shall present the results of the program to the Advisory Board and DOE. Information from other gas-hydrate projects shall be reviewed and included in our recommendations. Model-based estimates and production options will then be developed. If it is determined that a significant volume of gas production from hydrates is technically possible, an economic analysis will be conducted.

Task 21.0 – Post Well Analysis

This task is designed for planning to conduct operations including an extended well production test in 2004 on another area of the North Slope of Alaska. A report and budget for an additional well and an extended well test will be produced based on the information generated from the Phase II activities (including lessons learned). It will be determined if an additional well and/or extended production test is warranted, and recommendations will be presented to the DOE in sufficient time for FY 2004 budget planning. We anticipate the additional well will be drilled in another lease area/region of Alaska. The production test plan will help determine the producibility of hydrate deposits. These plans will be valuable for future hydrate operations, even if this project is not extended into Phase III.

Task 22.0 – Information Acquisition and Technology Transfer

The recipient shall communicate and exchange information with experts in the field of hydrate well drilling, coring, and testing, including Advisory Board members, to stay abreast of the latest technology and preferred methodologies. The recipient shall also document results of the field tests and transfer this technology to the industry.

Subtask 22.1 Information Acquisition

The recipient shall identify and network with other experts in the field of hydrate well drilling, coring, testing, and analysis to gain insights into the latest methodologies and technologies. The recipient shall follow the latest developments related to hydrate wells by meeting with experts in the scientific and drilling communities.

Subtask 22.2 Technology Transfer

The recipient shall document project results and transfer the new information and technology to the industry, via web site postings, meetings, workshops, and at least one technical paper. The recipient shall also use the NED Smart Drill system to allow well activities to be viewed by scientists, engineers, and DOE project managers who are not present at the well site.

DELIVERABLES

The periodic, topical, and final reports shall be submitted in accordance with the attached Reporting Requirements Checklist and the instructions accompanying the checklist. In addition, the Recipient shall submit the following:

Phase I

1. Digital Map of all well locations in and adjacent to project area (Task 2.1)

2. Well log correlation sections showing lithologic and stratigraphic units that fall within the gas hydrate stability zone in and adjacent to the project area (Task 2.1)

3. Seismic maps and sections showing extent of stratigraphic and lithologic units that fall within the gas hydrate stability zone in and adjacent to the project lease area (Task 2.2)

4. Reservoir modeling report for proposed site (Task 3.0)

5. Well Data for individual control wells used for site selection (Tasks 2.1 & 4.1)

6. Site Selection Plan (Task 4.1)

7. Testing and analytical procedures report (Task 5.0)

8. Well plan(s) (Task 6.0)

Phase II

1. Drilling and Coring Report (Task 9.2)

2. Well Logging Report (Task 10.0)

3. Core and Fluid Analysis Report (Task 11.0)

4. Seismic Survey Report (Task 12.0)

5. Well Completion Report (Task 13.0)

6. Well Testing Report (Task 15.0)

7. Hydrate Reservoir Characterization and Modeling Report (Tasks 17, 18, &19)

8. Economic Projections (if production volumes dictate) and a Production Options Report (Task 20.0)

9. Plan for Future Hydrate Well on the North Slope (Task 21.0)

10. Technical Publications Summarizing Project Findings (All Tasks)

11. Final Report Summarizing Project Findings (All Tasks)

In addition to the required reports, the recipient shall submit informal status reports directly to the COR. These are preferred monthly with short descriptions of successes, problems, advances or other general project status information. The report should not exceed one (1) page in length and shall be submitted via e-mail.

The Contractor shall also provide the following to DOE: a copy of all non-proprietary data, models, protocols, maps and other information generated under the cooperative agreement, when requested by DOE, in a format mutually agreed upon by DOE and the participant.

Appendix A: Site/Rig Photos

Figure A-1. Hot Ice Well #2 Site

Figure A-2. Base Camp

Figure A-3. Setting the First Platform Module

Figure A-4. Assembling the Platform

Figure A-5. Complete Camp Ready for Drilling

Figure A-6. Team Members on the Rig Floor

Appendix B: Gas Hydrate Project Production Testing; North Slope, Alaska

Testing Objective

Naturally occurring hydrate formations are present as a solid in the hydrate-stability zone. Hydrate will remain a solid until formation conditions are moved outside of the hydrate-stability region. The hydrate-stability region is a function of pressure, temperature and composition of the gas and fluid in the pore space. The main purpose of the production test is to monitor production response from depressurizing a hydrate interval over a short period. It is not anticipated that production from the hydrate interval during the test would be economic even if there were a gas pipeline available and the gas could be sold. The main objective is to collect information on depressurization to calibrate the hydrate production simulator. The calibrated simulator can then be used to determine the most economical method of trying to commercially produce hydrates. It is anticipated that depressurization of the hydrate interval by depleting a free gas interval will be the most likely way to generate commercial quantities of gas from a hydrate interval. The testing objective is to gather information so that reservoir simulators in the future will be able to accurately predict hydrate dissociation that results from depressurization.

Completion Challenges

The completion of this well (**Figure B-1**) was designed to try to address all of issues that have been identified with producing hydrates at this location. Based on the rig capacity, the largest production casing that can be used below the permafrost has an outside diameter of 4.5 inches. This will have a drift diameter of approximately 4 inches. The location will not be accessible by ice roads during production testing. All equipment will be transported by rolligon or helicopter. As a result, size and weight of the equipment needs to be minimized. Completion and testing equipment need to be simple and require minimum support. With environmental regulations and cost constraints, the base plan will conclude testing before tundra closure occurs. The current plan is not to incorporate artificial lift in the base plan. There is also potential for formation sand production. Freeze protection has to be incorporated into the completion design. The fact that the well produces fresh water and predominately methane creates the possibility of forming hydrates or ice in both the tubing and tubing/casing annulus. The potential for having hydrate or freezing problems is greatest during shut-in periods.

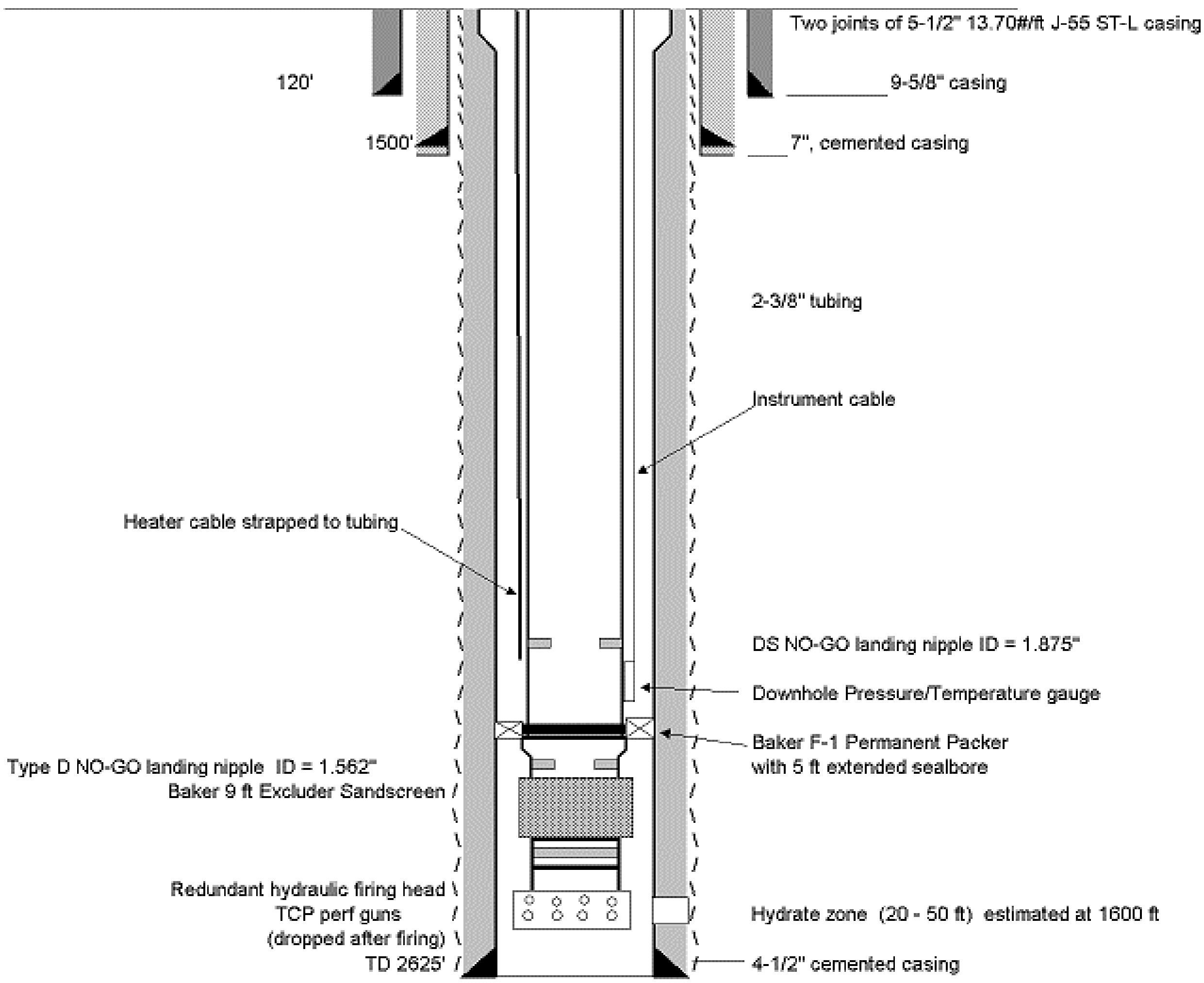

Figure B-1. Hot Ice #1 Completion

Completion Base Plan

There will be a number of uncertainties until we pull core from the well. We plan to perforate one hydrate interval after cementing 4-1/2 inch casing. The base case is to produce one well completed in a single hydrate interval using a tubing string, packer and permanent downhole pressure/temperature gauges. Water and gas will be produced into the tubing string. We will have the capability to swab the well to reduce bottomhole producing pressure. The well will be set up so that it can be shut in downhole by setting a plug in a profile to reduce wellbore storage volume. The well will be equipped with two electronic bottomhole pressure gauges and one temperature gauge near the perforations. A heat strip will be attached to the tubing string to prevent fresh produced water from refreezing across from permafrost when the well is shut in.

The base completion plan is to perforate one interval that is located at a depth with a reservoir temperature greater than 32°F. After the completion is run, production facilities consisting of a two-phase vertical separator with gas and water measurement in winterized enclosures will be hooked up.

A heater cable will be used to keep the water in the production tubing from freezing. It is anticipated that produced water will have a low salinity. The undisturbed surface temperature is approximately 12°F. As a result, there is a high probability that there will be a problem with water freezing or hydrate formation inside the tubing, if heat is not added. The heater cable is basically a flat ESP cable that is shorted above the packer. Electrical current flowing through the cable results in the generation of heat. The majority of the heat generated is transferred to the production tubing. Modeling results predicted that the heater cable would keep the temperature of the fluid inside the tubing above 50°F.

A heater cable should eliminate problems with water freezing, but adds other completion challenges. Using a heater cable requires the use of wellhead penetration. There is not enough room in a standard wellhead for 4-1/2 inch casing to have a high amperage penetration. To solve this problem, two additional casing spools will be used to allow the electrical penetrator. The top two joints of casing will be 5-1/2 inch so that there is enough room for the splices and the pigtail connection. With the heater cable and standard 2-3/8 inch EUE tubing, there is very little clearance inside of the 4-1/2 inch casing. The weight of 4-1/2 inch was reduced to 9.5 pounds per foot to give the largest possible internal diameter. This results in a clearance of slightly more than 0.25 in. between the heater cable over the coupling and drift of the 4-1/2 inch casing. This is especially tight since Range 1 tubulars (15-24 ft/joint) will be utilized for this project since a continuous coring rig is being used to run the completion equipment. 2-3/8 inch NU (10rd) tubing will be used in place of 2-3/8 inch EUE (8rd) tubing to increase the clearance by approximately 0.20 inch at each connection.

The well will be set up so that bottomhole pressure and temperature measurements can be made from the surface. Because of the large cost to come back and plug the well in an isolated Arctic environment, it is planned to plug the well at the end of the production test. This will also minimize the need to mobilize equipment at a later time to the well and reduce environmental impact.

Testing Base Plan

The well will be swabbed down to initiate flow. Produced gas will be vented or flared after being measured. Produced water will be pumped into a holding tank and later hauled to disposal using a rolligon at the end of the test. The well will initially be produced to determine productivity of a hydrate zone with only depressurization. The well will be produced for a short time to determine if a stabilized rate is obtained. The well will then be shut in. If necessary, a plug can be set in a profile to minimize the wellbore storage during the build-up test. The total test time will be approximately 5 days. A water and gas sample will be collected.

The testing plan outlined in this document is the current base plan. Simulation modeling is currently being performed that will estimate production for different reservoir conditions. Production and shut-in periods may have to be altered based on the actual reservoir parameters observed and the amount of time that is available before tundra closure.

Contingencies

As mentioned previously, there are a number of contingencies that have been considered in the completion design. At this time, we are not sure what production rate the well will be capable of producing as a result of uncertainty about reservoir parameters. There is also a contingency related to sand control. It is currently assumed that the formation is not completely unconsolidated. The base plan is to use a sand screen below the packer. This should be sufficient as long as low production rates are encountered. A contingency of using expandable sand screens was investigated. An expandable sand screen will be extremely difficult to install at this shallow depth. It would require that special 20-foot drill collars be manufactured to have enough setdown weight to expand the sand screen. Using an expandable screen would also require that the zone be perforated prior to running tubing.

Regulatory permit approvals for gas/emissions and fluids disposal will also be factored into contingency plans.

Longer Term Testing Option

The current Phase 2 proposal incorporates funding for a testing period of about 5 days without artificial-lift equipment. A scenario was also developed to produce the hydrate interval for an extended time period. The longer-term test is based on one well completed in a single hydrate interval with a progressive cavity pump set below the perforations. The completion plan would include a fiber-optic line embedded inside the instrument cable for the downhole gauge. The fiber-optic cable will give temperature every meter along the wellbore from the surface to below the hydrate region.

The base completion plan is to perforate one interval that is located at a depth with a reservoir temperature of greater than 32°F. The torque anchor, sand screen, progressive cavity pump, bottomhole pressure/temperature gauges and heater cable could be run into the well on the production tubing. The rotor for the progressive cavity pump will be run into the well on 7/8-inch steel sucker rods with rod guides. The rotor will be spaced out and the drivehead assembled. The progressive cavity pump has the advantage that the drive head has a small footprint that can be enclosed to prevent the wellhead and lines from freezing. At this point, production facilities consisting of a two-phase vertical separator with gas and water measurement in winterized enclosures will be hooked up.

It is planned to produce water up the tubing and gas up the annulus. The well will be equipped with a BHP/Temp gauge near the perforations. A heat strip will be attached to the production tubing to prevent fresh produced water from refreezing across from the permafrost when the well is shut in. Produced gas will be vented or flared. Produced water will be pumped into a holding tank and later hauled to disposal using a rolligon. A complete automation system could be installed to monitor the wellhead and separator pressure and temperature, water and gas production and tank levels. The automation system would also allow pumping and ESD equipment to be operated remotely.

The well would initially be produced with a progressive cavity pump to determine productivity of a hydrate well without thermal stimulation. The bottomhole pressure gauge will interface with control equipment for the progressive cavity pump to control the variable frequency drive and turn equipment off when the fluid level is below the perforations. The well will be produced for a short time to determine if a stabilized rate is obtained. The well will then be shut in and bottomhole pressure observed. At the end of this build-up period, the progressive cavity pump will be restarted and production rate compared to the rate prior to shut-in. With the fluid level near the perforations, hot water will be pumped down the production tubing/casing annulus into the perforated interval. The well will be shut in for a short time to allow heat to be transferred to the hydrate interval. The pump will be set below the perforations to prevent elastomers in the progressive cavity pump stator from being exposed to hot fluid injected down the annulus. The well will then be returned to production, and bottomhole pressure will be monitored during the production test.

It is planned to repeat the hot water injection, production and shut-in sequence. The number of cycles will depend on total test time and production response from the hot water injection. We will attempt to use the same hot water volume, producing time and shut-in time so that results of different production cycles can be compared. Length of production and shut-in times may need to be adjusted based on production and build-up results. Water and gas samples would be collected during each production cycle to determine if composition is changing with time.

At this time, we are still trying to determine if it is possible to obtain regulatory approval to perform some extended production testing without anyone on location. Personnel would need to be at the well during initial start-up, while pumping hot water and start-ups after extended shutdowns. To minimize logistics costs associated with housing people at a remote arctic location, we would like to have someone monitor the well and facility automation equipment remotely in Deadhorse, Alaska. People monitoring the well information would have the ability to shut down the pumping equipment and shut in the well if there was a problem. Personnel could be sent out periodically on helicopter or rolligon to monitor or repair equipment at the location. It is possible that we will need to have people located at the well site the entire time the well is being produced.

The extended producing time would give information about long-term production characteristics of hydrates. The long-term test would provide data about effects of injecting multiple hot fluids into the hydrate interval. This would result in a more realistic simulator that could be used to determine production performance of different production scenarios (huff and puff, steam injection, depressurization, etc.).

We have not been able to obtain reservoir simulation results at this time. Based on several papers that have been published, it is anticipated that production rate will be extremely low.

It will be very difficult to support the testing operation after tundra closure. The well site is located within a caribou calving area. Based on environmental regulations, we will have to shut down operations from tundra closure until at least July 15. It is not known if permits could be obtained this year (2003) to support the operation after tundra closure. If rolligons are allowed, the amount of weight that they can move could be restricted to 20,000 pounds or less. This would make it extremely difficult to move produced water, move equipment or address other logistics after tundra closure. The main purpose of the Phase 2 of the hydrate project is to obtain information that will be used to calibrate the reservoir simulator. The proposed 5-day test using swabbing will provide this information. The swabbing configuration without the addition of heat will provide a situation that is most similar to the depressurization of a hydrate interval that results from depleting a downdip gas zone.

Appendix C: UAA-Anadarko Gas Hydrates Research Projects Progress Report

University of Alaska at Anchorage

Introduction

Anadarko Petroleum, Maurer Technology and Noble Drilling are conducting, in partnership with the Department of Energy (DOE), a project to core, characterize and produce a gas hydrate reserve on Alaska's North Slope (DOE project DE-FC26-01NT41331). As part of that project, Anadarko is sponsoring three research projects at the University of Alaska Anchorage (UAA). These projects include:

- North Slope Geological Characterization (Principal Investigators (PI's): LeeAnn Munk, Kristine Crossen, Department of Geology) (see **Appendix C-1**)
- Gas Hydrate Production Water Production/Water Handling Issues (PI's, Craig Woolard and Bill Schnabel, School of Engineering; LeeAnn Munk, Geology; Mark Hines, Biology; John Kennish, Chemistry) (see **Appendix C-2**)
- On-Shore Platform Pile Foundation Research (PI: Hannele Zubeck, School of Engineering) (see **Appendix C-3**)

Final reports for these three efforts are included in this appendix. A brief summary of the progress on these projects is presented below.

North Slope Geological Characterization

The UAA Geology Department has employed Christina Ross, a geologist with petroleum industry experience, to locate geologic data from the logs of existing wells. Ms. Ross and the PI's have been working with Richard Sigal, Donn McGuire and others Anadarko staff to identify data needs and compile relevant information. Ms. Ross is now in the process of creating a CD containing all of the information collected to date.

Gas Hydrate Water Production/Water Handling Issues

A draft report summarizing water production/water handling issues related to gas hydrate production was prepared by the PI's and submitted to Anadarko for review in August 2002. We have since completed the final draft. As part of that effort, Craig Woolard met with Bob Elder and Tommy Thompson from Anadarko's Anchorage office and discussed water requirements and disposal on exploration and production facilities in general and some of the issues specific to Alaska's North Slope. We are continuing to expand the report focusing on additional strategies and options for achieving a "zero-discharge" exploration and production facility.

Mark Hines left UAA for a position at the University of Massachusetts this fall. Although he will no longer be part of the UAA hydrates team, he would like to continue working on the project in his new position if possible.

UAA's Applied Science, Engineering and Technology (ASET) Laboratory is now fully operational and capable of performing a complete chemical analysis of samples collected during gas hydrate coring and production. A plan for sampling and analyzing core and water samples will be included in the final report.

On-Shore Platform Pile Foundation Research

Hannele Zubeck from UAA has been working with Scott Hagood from Anadarko and several local consultants to develop a test plan for leg tests that will be conducted in Deadhorse. Dr. Zubeck will be traveling to the North Slope in late October/early November for the first round of leg testing.

The PI's and UAA appreciate the opportunity to participate on these research projects. Please contact me if you have any questions.

Craig R. Woolard
Associate Professor
UAA School of Engineering
907-786-1863
afcrw@uaa.alaska.edu

Appendix C-1

Geologic Research of Well Records and Stratigraphy of the North Slope Region near Kuparuk, Alaska

Report to Anadarko Petroleum Corporation

Research and Database Completed by:
Zulmacristina Ross, Research Geologist

Research Supervised by:
Kristine Crossen, Co-PI
LeeAnn Munk, Co-PI

Geology Department
University of Alaska Anchorage

November 25, 2002

SCOPE OF RESEARCH

This project was designed to provide Anadarko Petroleum Corporation with information about data related to North Slope geology that resides in Anchorage facilities. The information of interest includes existing well logs and cores from the upper 5,000 feet of subsurface, in an area on the North Slope near Kuparuk, Alaska. The specific areas of interest were designated to Z. Ross by the Anadarko team of Richard Sigal, Steve Runyon, and Don McGuire. The primary area of interest lay within 10N/7E-10N/10E, 9N/8E- 9N/10E, 8N/7E – 8N/10E, and 7N/8E - 7N/8E, with a secondary area within 10N/10E – 10N/13E and 9N/11E – 9N/13E.

Data from the research area, including well records, well types, well locations, core depth, core cuttings and general information were obtained from the Alaska Geologic Materials Center of the Alaska Division of Geologic and Geophysical Surveys and from the Alaska Oil and Gas Conservation Commission. The Anadarko team requested all available data from: drilling reports, sidewall and chip core reports, geochemical reports, well logs, test production reports, drill stem tests, formation tests (wire line conveyed tests), deviation surveys, and general geological reports.

The research was completed by Z. Ross under the supervision of K. Crossen and L. Munk. Throughout the research, the UAA team met weekly to discuss the progress of the project and to gain additional background information concerning the geology of the North Slope. Progress was communicated on a regular basis to Craig Woolard, the UAA liason with Anardarko. Several meetings and discussions regarding the focus of the UAA geology project occurred between K. Crossen, L. Munk, and the Anadarko team during July and August, 2002. Z. Ross met with R. Sigal and S. Runyon in July, and L. Munk and Z. Ross communicated regularly with S. Runyon and R. Sigal in August and September.

WORK COMPLETED (by Z. Ross)

Alaska Geologic Materials Center in Eagle River – 6 hours research
This facility houses cores and associated cuttings as well as a database of Alaskan wells, including information on lithology, heavy minerals, clay mineralogy, kerogen, and vitrinite, as well as palynology, siliceous fossils, foraminifera, and thin sections. The database includes published reports, quadrangle maps, retrieval methods, and API (Identification Number). The database contains information for 51 wells within the research area.

Alaska Oil and Gas Conservation Commission – 204 hours
This facility houses the information for Alaskan wells including well drilling reports, lithology descriptions, chip core descriptions, sample description reports, drilling surveys, geological markers, well log lists and other general information. The well records contain variable information and are not all of equal length. Over 6,000 pages of information were examined, and 1,200 pages copied to organize the final information requested. The report concentrates on 55 wells that were available for viewing at the time this project was undertaken.

University of Alaska Anchorage – 284 hours
The data were organized and incorporated into a computer database. The "Kuparuk Project Database" contains the following information: well name, API, operator, location, latitude and longitude, unit or lease name, field and pool, measured depth, true vertical depth, type of well, status, well logs, thickness of permafrost, and links to files of well logs, geological markers, side core descriptions, and general information.

Over 600 pages of information were transmitted by FTP (file transmission protocol) to S. Runyon and R. Sigal at Anadarko Petroleum Corporation, Houston (Attachment 1 – sent in August and September, 2002). In culmination of the research, a database entitled the "Kuparuk Project Database" was prepared that includes all the previously transmitted FTP files on the 55 wells (Attachment 1), a list of all the files enclosed in the database (Attachment 2), and a database from the Alaska Geological Materials Center (within Attachment 3) that contains additional information from 51 of the 55 wells in the research area. This report includes a CD containing all the attachments, databases, and an electronic copy of this written document (Attachment 3).

FUTURE RESEARCH

The Anadarko team has requested that we continue the project by investigating 1) paleontological information from the wells of interest, 2) surficial maps and gravel resources from this area, and 3) any other helpful information to characterize the formations of interest. We would like to pursue additional cooperative research with Anadarko Petroleum Corporation.

ATTACHMENT 1
Files Transmitted By FTP By Date

<u>FTP 08-13-02</u>

CIRQUE 1:
Cirque 1 Blowout Summary Report
Well Logs Cirque 1

CIRQUE 2:
Sidewall Sample Description Cirque 2
Well Logs Cirque 2 (2 Files)

NARVAQ 1:
Well Logs Narvaq 1

TARN 2:
Well Logs Tarn 2

TARN 3:
Core Description Tarn 3
Geological Markers Tarn 3
Sample Description Tarn 3
Summary Lithology Description Tarn No.3
Lithology Description Tarn 3
Well Logs Tarn 3

TARN 3A:
Well Logs Tarn 3A

TARN 4:
Core Chip Description Tarn 4
Geological Markers Tarn 4
Well Logs Tarn 4

TOOLIK FEDERAL 2:
Well Logs Toolik Fed 2

TOOLIK FEDERAL 3:
Well Logs Toolik Fed 3

WINTER TRAILS 1:

Core Descriptions Winter Trails 1
Core Description Cores 1 To 25
Geological Markers
Well logs Winter Trails 1

WOLFBUTTON 25-6-9:

Well Logs Wolfbutton 25-6-9

WOLFBUTTON 32-7-8:

Well Logs Wolfbutton 32-7-8

FTP 08-15-02

RUBY STATE 1:

Drilling Record Ruby Prospect

FTP 08-30-02

CIRQUE 2:

Sidewall Sample Description Cirque 2
Well Logs Cirque 2

KRU STATE 1 14-10-9:

Sidewall Core Summary KRU State 1 14-10-9

KUPARUK RIVER UNIT 2G-9:

Geological Markers KRU 2G-9
Well Logs Kuparuk River Unit 2G-9

KUPARUK RIVER UNIT 2K-3:

Well Logs Kuparuk River Unit 2K-3

KUPARUK RIVER UNIT TARN 2N-307:

Geological Markers KRU2N-307
Well Logs Kuparuk River Unit 2N-307

KUPARUK RIVER UNIT TARN 2N-309:
Geological Markers KRU2N-309
Well Logs Kuparuk River Unit 2N-309

KUPARUK RIVER UNIT TARN 2N-320:
Geological Markers KRU2N-320
Well Logs Kuparuk River Unit 2N-320

NARVAQ 1:
Core Analysis Report Narvaq 1
Geological Markers Narvaq 1
Show Evaluation Reports Narvaq1
Well Logs Narvaq 1

ROCK FLOUR 1:
Geological Markers Rock Flour 1

RUBY STATE 1:
Core Analysis Results Ruby State 1
Core Description Ruby State 1
Geological Markers Ruby State
Drilling Record Ruby Prospect

TARN 2:
Well Logs Tarn 2

TARN 3:
Core Description Tarn 3
Geological Markers Tarn 3
Lithology Summary Tarn 3
Lithology Description Tarn 3
Sample Description Tarn 3
Well Logs Tarn 3

TARN 3A:
Geological markers Tarn 3A
Well summary report Tarn 3A
Well logs Tarn 3A

TARN 4:

Core Chip Description Tarn 4
Geological Markers Tarn 4
Well Logs Tarn 4

TARN 2, 3, 3A AND 4:

Well Logs Tarn 2, 3, 3A and 4

TOOLIK FEDERAL 2:

Geological Markers Toolik Federal 2
Well Logs Toolik Federal 2 (2 Files)

TOOLIK FEDERAL 3:

Geological markers Toolik federal 3
Well logs Toolik Federal 3

WEST SAK 5:

Geological Markers West Sak 5
Well Logs West Sak 5

WEST SAK 20:

Core Description West Sak 20
Geological Markers West Sak 20
Well Logs West Sak 20

WEST SAK 25667 4:

Core Description West Sak 25667 4
Geological Markers West Sak 25667 4
Well Logs West Sak 25667 4

WEST SAK 26:

Summary Core Description West Sak 26
Well Logs West Sak 26

WEST SAK RIVER STATE B 10:

Geological Markers West Sak River State B-10

WINTER TRAILS 1:

Core Descriptions Winter Trails 1
Geological Markers Winter Trails 1
Logs Winter Trails 1
Winter Trails 1 Core Description 1 to 25

WOLFBUTTON 25-6-9:

Well Logs Wolfbutton 25-6-9

WOLFBUTTON 32-7-8:

Well Logs Wolfbutton 32-7-8

<u>FTP 09-20-02</u>

HEMI SPRINGS STATE 1:

General Information Hemi Springs State 1
Sidewall Sample Descriptions Hemi Springs State 1

KRU STATE 1 14-10-9 :

Sidewall Core Description KRU State # 1 14-10-9

KRU STATE 1:

Graphic True Vertical Depth KRU State 1
Sidewall Core Analysis Report KRU State 1

KRU STATE 2:

Sidewall Core Analysis Report KRU State 2
Sidewall Core Summary KRU State 2

KUPARUK RIVER UNIT 2K-02:

Geological Markers Kuparuk River Unit 2K-02
Interpolated Values for Chosen Horizons Kuparuk River Unit 2K-02

KUPARUK RIVER UNIT 2K-03:

Geological Markers Kuparuk River Unit 2K-03
Interpolated Values for Special Survey Points-Geological Markers KRU 2K-03
Graphic True Vertical Depth Kuparuk River Unit 2K-03

KUPARUK RIVER UNIT 2K-04:

Interpolated Values for Special Survey Points KRU 2K-04
Graphic True Vertical Depth Kuparuk River Unit 2K-04

KUPARUK RIVER UNIT 2K-05:

Graphic True Vertical Depth Kuparuk River Unit 2K-05.
Interpolated Values for Special Survey Point Geological markers Kuparuk River Unit 2K-05.

KUPARUK RIVER UNIT 2K-06:

Interpolated Values for Special Survey Points KRU 2K-06

KUPARUK RIVER UNIT 2K-07:

Geological Markers Kuparuk River Unit 2K-07
Graphic True Vertical Depth Kuparuk River Unit 2K-07
Interpolated Values for Special Survey Points Kuparuk River Unit 2K-07
Well Logs Kuparuk River 2K-07

KUPARUK RIVER UNIT 2K-09:

Geological Markers Kuparuk River Unit 2K-09
Graphic True Vertical Depth Kuparuk River Unit 2K-09
Interpolated Markers Report Kuparuk River Unit 2K-09

KUPARUK RIVER UNIT 2K-10:

Geological Markers Kuparuk River Unit 2K-10
Interpoled Values for Chosen Horizons KRU 2K-10
Sidewall Core Description Kuparuk River Unit 2K-10
Well Logs KRU 2K-10
Well Logs Kuparuk River 2K-10

KUPARUK RIVER UNIT 2K-12:

Geological Markers Kuparuk River Unit 2K-12
Interpolated Values for Special Survey Points Kuparuk River Unit 2k-12
Well logs Kuparuk River Unit 2K-12

KUPARUK RIVER UNIT 2K-17:

Geological Markers Kuparuk River Unit 2K-17
Graphic True Vertical Depth Kuparuk River Unit 2K-17
Interpolated Values for Chosen Horizons Kuparuk River Unit 2K-17

KUPARUK RIVER UNIT 2K-23:

Geological Markers Kuparuk River Unit 2K-23
Graphic True Vertical Depth Kuparuk River Unit 2K-23
Interpolated Markers Report Kuparuk River Unit 2K-23

KUPARUK RIVER UNIT 2K-24:

Geological Markers Kuparuk River Unit 2K-24
Graphic True Vertical Depth Kuparuk River Unit 2K-24
Interpolated Markers Report Kuparuk River Unit 2K-24
Well Logs Kuparuk River Unit 2K-24

KUPARUK RIVER UNIT 2K-25:

Geological Markers Kuparuk River Unit 2K-25
Interpolated Markers Report Kuparuk River Unit 2K-25

KUPARUK RIVER UNIT 2K-26:

Geological Markers Kuparuk River Unit 2K-26

PLACID ET AL STATE 1 3-10-13:

Geological Markers Placid Et Al State 1 3-10-13

ROCK FLOUR 1:

Graphic 1 True Vertical Depth Rock Flour 1
Sidewall Core Descriptions Rock Flour 1
Well Logs Rock Flour 1

TARN 1:

Conventional Core Plugs and Samples Descriptions Tarn 1
Geological Markers Tarn 1
Sidewall Core Analysis Tarn1

TARN 2:

Core Description Tarn 2
Geological markers Tarn 2
Graphic True Vertical Depth Tarn 2
Sample Description Tarn 2
Lithology Summary Tarn 2

WEST SAK RIVER STATE 25606 13:

Completion Report West Sak River State 25606 13
Drilling History West Sak 25606 13

WEST SAK 25590 15:

Cluster Listing Dipmeter West Sak 25590 15
Core Description West Sak 25590 15
Core Summary West Sak 25590 15
Drilling History West Sak 25590 15
Geological Markers West Sak 25590 15

WEST SAK 20:

Core Description West Sak 20
Drilling History West Sak 20
Magnetic Multishot Directional Survey West Sak 20

WINTER TRAILS 2:

Sidewall Core Description Winter Trails 2
Well Logs Winter Trails 2

WINTER TRAILS 3:

Inclination Survey Winter Trails 3
Sidewall Core Descriptions Winter Trails 3

WINTER TRAILS 4:

Sidewall Core Description Winter Trails 4

WOLFBUTTOM 25-6-9:

Core Analysis Results Wolfbuttom 25-6-9
Brief Core Description Wolfbutton 25-6-9
Formation Evaluation Plot Wolfbutton 25-6-9
Geological Markers Wolfbuttom 25-6-9

WOLFBUTTON 32-7-8:

- Brief Core Description Wolfbutton 32-7-8
- Geological Markers Wolfbutton 32-7-8
- Sidewall Samples Descriptions Wolfbutton 32-7-8

SEQUOIA 1:

- Summary of Pertinent Data Sequoia 1

ATTACHMENT 2
Files In The Database

CIRQUE-1:

Cirque 1 Blowout Summary Report
Cirque 1 Blowout Summary Report.rtf
Cirque 1 Information
Lithology Description Cirque 1
Well Logs Cirque 1

CIRQUE-2:

Sidewall Sample Description Cirque 2
Well Logs Cirque 2

GETTY STATE 1:

Brief Description of Lithology Getty State 1
Geological Markers Getty State 1

HEMI SPRINGS STATE 1:

Core Analysis Results Report Hemi Springs State 1
Core Description Report Hemi Springs State 1
Geological Markers Hemi Springs State 1
Sidewall Sample Descriptions Hemi Springs State 1
Well Logs Hemi Springs State 1

KRU STATE 1 14-10-9:

Geological Markers Kru State 1 14-10-9
Graphic True Vertical Depth Kru State 1 14-10-9
Sidewall Core Analysis Report Kru State 1 14-10-9
Sidewall Core Description Kru State 1 14-10-9
Well Logs Kru State 1 14-10-9

KUPARUK RIVER 21-10-8 No.1:

Well Logs Kuparuk River 21-10-8 No.1
Well Logs Kuparuk River Unit 21-10-8 No.1

KUPARUK RIVER UNIT 2G-9:

Geological Markers Kru 2G-9
Well Logs Kuparuk River Unit 2G-9

KUPARUK RIVER UNIT 2G-16:

Geological Markers Kuparuk River Unit 2G-16
Well Logs Kuparuk River Unit 2G-16

KUPARUK RIVER UNIT 2K-02:

Geological Markers Kuparuk River Unit 2K-02
Interpolated Values for Chosen Horizons Kuparuk River Unit 2K-02
Well Logs Kuparuk River Unit 2K-02

KUPARUK RIVER UNIT 2K-03

Geological Markers Kuparuk River Unit 2K-03
Graphic True Vertical Depth Kuparuk River Unit 2K-03
Interpolated Values for Special Survey Points-Geological Markers Kru 2K-03
Well Logs Kuparuk River Unit 2K-3

KUPARUK RIVER UNIT 2K-04:

Graphic True Vertical Depth Kuparuk River Unit 2K-04
Interpolated Values (Geol. Markers) for Special Survey Points KRU 2K-04

KUPARUK RIVER UNIT 2K-05:

Graphic True Vertical Depth Kuparuk River Unit 2K-05
Interpolated Values for Special Survey Point Geological Markers Kuparuk River Unit 2K-05

KUPARUK RIVER UNIT 2K-06:

Interpolated Values for Special Survey Points KRU 2K-06

KRU STATE 2:

Sidewall Core Analysis Report KRU State 2
Sidewall Core Summary KRU State 2

KUPARUK RIVER UNIT 2K-07:

Geological Markers Kuparuk River Unit 2K-07
Graphic True Vertical Depth Kuparuk River Unit 2K-07
Interpolated Values for Special Survey Points Kuparuk River Unit 2K-07
Well Logs Kuparuk River 2K-07

KUPARUK RIVER UNIT 2K-09:

Geological Markers Kuparuk River Unit 2K-09
Graphic True Vertical Depth Kuparuk River Unit 2K-09
Interpolated Markers Report Kuparuk River Unit 2K-09
Well Logs Kuparuk River 2K-09

KUPARUK RIVER UNIT 2K-10:

Geological Markers Kuparuk River Unit 2K-10
Interpoled Values for Chosen Horizons Kru 2K-10
Sidewall Core Description Kuparuk River Unit 2K-10
Well Logs KRU 2K-10
Well Logs Kuparuk River 2K-10

KUPARUK RIVER UNIT 2K-12:

Geological Markers Kuparuk River Unit 2K-12
Interpolated Values for Special Survey Points Kuparuk River Unit 2K-12
Well Logs Kuparuk River Unit 2K-12

KUPARUK RIVER UNIT 2K-17:

Geological Markers Kuparuk River Unit 2K-17
Graphic True Vertical Depth Kuparuk River Unit 2K-17
Interpolated Values for Chosen Horizons Kuparuk River Unit 2K-17
Well Logs Kuparuk River 2K-17

KUPARUK RIVER UNIT 2K-23:

Geological Markers Kuparuk River Unit 2K-23
Graphic True Vertical Depth Kuparuk River Unit 2K-23
Interpolated Markers Report Kuparuk River Unit 2K-23
Well Logs Kuparuk River Unit 2K-23

KUPARUK RIVER UNIT 2K-24:

Geological Markers Kuparuk River Unit 2K-24
Graphic True Vertical Depth Kuparuk River Unit 2K-24
Interpolated Markers Report Kuparuk River Unit 2K-24

KUPARUK RIVER UNIT 2K-25:

Geological Markers Kuparuk River Unit 2K-25
Interpolated Markers Report Kuparuk River Unit 2K-25
Well Logs Kuparuk River 2K-25

KUPARUK RIVER UNIT 2K-26:

Geological Markers Kuparuk River Unit 2K-26
Well Logs Kuparuk River Unit 2K-26

KUPARUK RIVER UNIT TARN 2N-307:

Geological Markers KRU 2N-307
Well Logs Kuparuk River Unit 2N-307

KUPARUK RIVER UNIT TARN 2N-309:

Geological Markers KRU 2N-309
Well Logs Kuparuk River Unit 2N-309

KUPARUK RIVER UNIT TARN 2N-320:

Geological Markers KRU 2N-320
Well Logs Kuparuk River Unit 2N-320

NARVAQ 1:

Core Analysis Report Narvaq 1
Geological Markers Narvaq 1
Show Evaluation Reports Narvaq1
Well Logs Narvaq 1

PLACID ET AL STATE 1 3-10-13:

Geological Markers Placid Et Al State 1 3-10-13
Sidewall Descriptions Placid Et Al State 1 3-10-13
Well Logs Placid Et Al State 1 3-10-13

RAVIK STATE 1:

Core Description Ravik State 1
Well Logs Ravik State 1

ROCK FLOUR 1:

Geological Markers Rock Flour 1
Graphic 1 True Vertical Depth Rock Flour 1
Sidewall Core Descriptions Rock Flour 1

RUBY STATE 1:

- Core Analysis Results Ruby State 1
- Core Description Ruby State No. 1
- Drilling Record Ruby Prospect
- Geological Markers Ruby State
- Vitrinite reflectance Ruby State No.1

SEQUOIA 1:

- Summary of Pertinent Data Sequoia 1

TARN 1:

- Conventional Core Plugs and Core Descriptions Tarn 1
- Geological Markers Tarn 1
- Sidewall Core Analysis Results Tarn 1
- Well Logs Tarn 1

TARN 2:

- Core Description Tarn 2
- Geological markers Tarn 2
- Graphic True Vertical Depth Tarn 2
- Lithology Summary Tarn 2
- Sample Description Tarn 2
- Well Logs Tarn 2

TARN 3:

- Core Description Tarn 3
- Geological Markers Tarn 3
- Lithology Summary Tarn 3
- Sample Description Tarn 3
- Summary Lithology Description Tarn 3
- Well Logs Tarn 3

TARN 3A:

- Geological Markers Tarn 3A
- Well Summary Report Tarn 3A
- Well Logs Tarn 3A

TARN-4:

Core Chip Description Tarn 4
Geological Markers Tarn 4
Well Logs Tarn 4
Summary Tarn (2, 3, 3A and 4) Logging Operations

TOOLIK FEDERAL 2:

Geological Markers Toolik Federal 2
Well Logs Toolik Federal 2
Well Logs Toolik Federal 2

TOOLIK FEDERAL 3:

Geological Markers, shows, sidewall cores Toolik Federal 3
Well Logs Toolik Federal 3
Well History Toolik Federal 3

WEST SAK 25667 4:

Core Description West Sak 25667 4
Geological Markers West Sak 25667 4
Well Logs West Sak 25667 4

WEST SAK RIVER 5:

Geological Markers West Sak River 5
Well Logs West Sak 5

WEST SAK RIVER STATE 25606 13:

Completion Report Core 1 – 6 West Sak River State 25606 13
Drilling History West Sak 25606 13
Well Logs West Sak 25606 13
Well Test Summary West Sak River State 25606 13

WEST SAK 25590 15:

Cluster Listing Dipmeter West Sak 25590 15
Core Description West Sak 25590 15
Core Summary West Sak 25590 15
Drilling History West Sak 25590 15
Geological Markers West Sak 25590 15

WEST SAK 20:

- Core Description West Sak 20
- Drilling History West Sak 20
- Geological Markers West Sak 20
- Magnetic Multishot Directional Survey West Sak 20
- Summary Core Description West Sak 20
- Well Logs West Sak 20

WEST SAK RIVER STATE B 10:

- Geological Markers West Sak River State B 10
- West Sak River Unit B 10 Test Summary

WEST SAK 26:

- Summary Core Description West Sak 26
- Well Logs West Sak 26

WINTER TRAILS 1:

- Core Descriptions Winter Trails 1
- Geological Markers Winter Trails 1
- Winter Trails 1 Core Description 1 to 25
- Well Logs Winter Trails 1

WINTER TRAILS 2:

- Sidewall Core Description Winter Trails 2
- Well Logs Winter Trails 2

WINTER TRAILS 3:

- Inclination Survey Winter Trails 3
- Sidewall Core Descriptions Winter Trails 3
- Well Logs Winter Trails 3

WINTER TRAILS 4:

- Sidewall Core Description Winter Trails 4
- Well Logs Winter Trails 4

WOLFBUTTON 32-7-8:

- Brief Core Description Wolfbutton 32-7-8
- Geological Markers Wolfbutton 32-7-8
- Sidewall Samples Descriptions Wolfbutton 32-7-8
- Well Logs Wolfbutton 32-7-8

WOLFBUTTON 25-6-9:

- Brief Core Description Wolfbutton 25-6-9
- Core Analysis Results Wolfbuttom 25-6-9
- Formation Evaluation Plot Wolfbutton 25-6-9
- Geological Markers Wolfbuttom 25-6-9
- Well Logs Wolfbuttom 25-6-9

ATTACHMENT 3 (contained on CD)

Kuparuk Project Database
Alaska Geological Materials Center Database
Final Report

Appendix C-2
Final Report

Fundamental and Applied Research on Water Generated During the Production of Gas Hydrates (Phase 1)

Prepared for

Anadarko Petroleum Corporation

Dr. Keith Millheim
Manager, Operations, Technology and Planning

By
Craig R. Woolard, Associate Professor, School of Engineering
William Schnabel, Assistant Professor, School of Engineering
LeeAnn Munk, Assistant Professor, Department of Geology
Mark Hines, Professor, Department of Biology

UAA University *of* Alaska Anchorage

February 17, 2003

Executive Summary

As part of Department of Energy project DE-PS26-01NT41331), Anadarko Petroleum contracted with the University of Alaska Anchorage (UAA) to conduct research projects related to the construction of an on-shore platform, hydrate geology and characteristics and hydrate exploration and production water handling and treatment. This report provides a review of hydrate water production and handling, hydrate geochemistry and hydrate microbiological activity.

A review of the available conceptual and numerical models for hydrate production indicates that significant amounts of water will be generated during the production of hydrate reserves. In most of the production scenarios cited in the literature, it is reasonable to assume that unless the water generated during hydrate dissociation is removed, the relative permeability of the formation to gas flow the ability to maintain gas production rates will be reduced. The one numerical modeling effort reviewed for this report that explicitly considered the water phase indicates that the single well depressurization production approach will generate water slugs as water is displaced from the formation by expanding gas. The major components of the produced water will be salts and dissolved gasses and potentially some sediment. Brine or steam injection production options may require water beyond that provided by hydrate dissociation to meet production demands.

The water generated during gas hydrate dissociation suggest that water handling will be critical component of the production process. And as such, the infrastructure designed to process water and wastewater will become a more important factor to the success of individual well or field than most conventional oil and gas operations. Under these conditions, the approach used to design and operate water systems may need to be modified from current methods used in the oil and gas industry. A more effective approach would be to design the w/ww infrastructure using a regional approach based on the following three principals. First, the design of w/ww systems at a particular installation should be integrated with the exploration and production activities and consider all water requirements and wastewater generation activities that occur at each site. Second, to increase efficiency and reduce complexity, w/ww systems should be designed on a field wide or region wide basis and not at a site-by-site basis. Finally, the w/ww systems designs should be robust enough to handle a variety of conditions and permit requirements. Membrane technologies represent some of the best systems commercially available to implement this approach.

Understanding the geochemical characteristics of gas hydrates and associated pore waters may lead to enhanced exploration and development techniques. Gas chemistry, pore water salinity, and isotopic composition of gases and water associated with gas hydrates are the current areas of interest related to developing and exploring for gas hydrates. Most of the literature focuses on marine gas hydrates because they have been studied more extensively than terrestrial gas hydrates. However, it is possible that some of the same principles used to understand marine gas hydrates could be related to terrestrial gas hydrates.

The existence and activity of microorganisms in the deep subsurface is important in relation to gas hydrate research since these organisms are responsible for much of the gas formation, their activities affect the distribution and fate of gases, and their populations in strata adjacent to hydrate deposits may be useful as bioindicators of the presence of hydrates. Recent studies have determined that microorganisms are ubiquitous in the deep marine and terrestrial subsurface and that the biomass of these bacteria exceeds the sum of all other biomass on Earth including all marine and terrestrial plants and animals.

The presence of gas hydrates greatly affects the abundance, composition, and activities of bacterial communities. To date, interactions among hydrates, geochemical conditions, and microbial processes have only been ascertained in oceanic settings. However, it is clear that microbial life influences the formation of hydrates and vice versa. Hydrates that intersect the marine sediment-water interface at methane seeps can support complex animal and microbial communities that are similar in composition to submarine communities at hydrothermal vents. Virtually nothing is known of microbiology of terrestrial hydrates and what types of microbial consortia are present, but it has been suggested that the terrestrial deposits may be comprised of a higher proportion of thermogenic methane than in their marine counterparts but little is known of these hydrates. Whatever the source, it seems clear that a better understanding of bacterial populations associated with hydrates will prove useful in locating and retrieving hydrate gases since microbial communities seem to respond strongly to the presence of the hydrates or at least to the free gas trapped under them.

Based on the results of the literature review conducted for this report, a number of data gaps were identified that include:

1) Evaluation of the water production volume and rate from gas hydrate reserves
2) Analysis of the organic and inorganic composition of hydrate produced water,
3) Quantification of water use and consumption on drilling platforms and possible incorporation of produced waters into platform operations,
4) Evaluation of the use of microbial populations as bioindicators for hydrate deposits,
5) Assessment of core material as a record of past biological activity, and
6) Evaluation of oxygen and hydrogen isotope ratios as indicators of hydrate dissociation rates.

These issues should be considered for further study as a part of the Anadarko gas hydrates research effort.

Table of Contents

Introduction

Anadarko Petroleum Corporation (Anadarko), Maurer Technology and Noble Drilling are conducting a 3-year Department of Energy project (DE-PS26-01NT41331) to drill, core and produce gas from hydrates on Alaska's North Slope. As part of that effort, Anadarko contracted with the University of Alaska Anchorage (UAA) to conduct research projects related to the construction of an on-shore platform, hydrate geology and characteristics and hydrate exploration and production water handling and treatment. This report provides a review of hydrate water production and handling, hydrate geochemistry and hydrate microbiological activity. The report was prepared in accordance with the proposal titled "Fundamental and Applied Research on Water Generated During the Production of Gas Hydrates" approved by Anadarko on June 18, 2002 (a copy of the proposal is included in Appendix A), and comments received from Anadarko during subsequent project meetings.

The report is divided into four main sections. The first section provides a review of the gas hydrate produced water quantity and quality as well as a review of potential treatment infrastructure strategies and options. Gas hydrate geochemistry and microbiology are reviewed in sections two and three, respectively. Finally, the report provides recommendations for future research.

Hydrate Water Production and Treatment

Hydrate Composition

Hydrates are ice-like structures that consist of a lattice of hydrogen-bonded water molecules with voids occupied by gas molecules. Many gasses can form hydrate structures but in natural gas hydrates the voids are occupied primarily by methane and propane. Hydrates on the North Slope of Alaska are composed primarily of methane (Collett, Kvenvolden et al. 1990; Collett 1993).

There are two basic types of hydrate structures. An ideal Structure I hydrate is a 1728 $Å^3$ unit cell consisting of 46 water molecules with 8 voids. These voids include 2 small dodecahedron voids that can hold gas molecules with a diameter of up to 5.2 Å and 6 large tetradecahedra voids that con hold gas molecules with a diameter of up to 5.9 Å. An ideal Structure II hydrate is a 5268 $Å^3$ unit cell containing 136 water molecules and 24 voids. Sixteen of these voids are have a diameter of 4.8 Å. The 8 remaining voids are somewhat larger with a diameter of approximately 6.9 Å. The presence of the gas guest molecules results in an expansion relative to ice of 16% and 18% for Structure I and Structure II hydrates (Kuuskraa, Hammershaimb et al. 1983).

The number of water molecules divided by the number of gas molecules is termed the hydrate number. For an ideal Structure I hydrate, the hydrate number is 46/8 or 5.75. An ideal Structure II hydrate has a water to gas ratio of 136:24 and a hydrate number of 5.67. In naturally occurring hydrates, hydrates numbers range from 6 (95% void occupancy) to 8 (70% void occupancy). Hydrates formed at lower pressures tend to have higher hydrate numbers (Kuuskraa, Hammershaimb et al. 1983).

The basic structure defines the relationship between gas and water generated during hydrate production. One cubic foot of an ideal Structure I hydrate completely saturated with methane would yield approximately 179 ft^3 of methane at 14.7 psia and 60^oF and 0.78 ft^3 of water. These values represent the maximum theoretical volumes of gas and water that could be produced during Structure I hydrate dissociation (Kvenvolden 1993).

Hydrates in Porous Media

Naturally occurring hydrates contain somewhat less favorable ratios of water and gas. The formation temperature and pressure as well as the gas composition, formation porosity and pore water chemistry all influence the composition and extent of a hydrate reserve.

The presence of dissolved solids in the pore water lowers the equilibrium temperature and the capillary forces present in porous media increase the equilibrium pressure at which hydrates form relative to pure water (Collett 1997; Klauda and Sandler 2001). As a result, naturally occurring hydrates occur in only a fraction of the voids present in the porous media. For example, in laboratory experiments conducted with a well sorted natural sand with an average grain size of 0.75 mm, deBoer et al (1985) observed that only 50% of the available pore space was filled with hydrates. Hydrate saturation values of less than 50% are often cited in the literature (Kamath, Godbole et al. 1987; Goel, Wiggins et al. 2001). Additionally, not only are the pore spaces in naturally occurring systems often unsaturated with respect to hydrates, but the hydrate structures themselves are often unsaturated with respect to gas. Naturally occurring hydrates range from 6.0 to 8.0, which correspond to a void occupancy of 95-70% (Kuuskraa, Hammershaimb et al. 1983; Collett, Bird et al. 1988).

When hydrates form, water molecules are incorporated into the hydrate lattice. Any ions present in the pore water during hydrate formation are excluded. As a result, hydrate formations can contain pore water with elevated salt contents. Increased salt concentration in the pore water will decrease the hydrate formation temperature and eventually inhibit hydrate formation creating hydrate filled pores interspersed with pores filled with saline water exist in a formation. Enrichment of salt concentrations to the solubility limit of approximately 26 wt% (260 g/L) is theoretically possible (Sloan 1990), however, field data from the North Slope indicate that pore water salt contents range from 5 to 15 parts per thousand (5 to 15 g/L) (Kamath, Godbole et al. 1987).

Several different forms of gas hydrates have been observed in porous media. Massive gas hydrates deposits contain only a small amount (e.g., 5%) of sediment. In layered hydrate formations, thin lenses of sediment separate hydrate layers. Nodular hydrate formations contain granules of hydrates up to 5 cm in diameter. Small hydrate inclusions are dispersed throughout the formation in disseminated hydrate formations. Several researchers have proposed that disseminated hydrates can grown into nodules, layers and eventually into to massive hydrate deposits if enough gas, pore water and the proper soil conditions exist (Kuuskraa, Hammershaimb et al. 1983; Sloan 1990).

In their evaluation of hydrate resources in the Prudhoe Bay-Kuparuk River area, (Collett, Bird et al. 1988) identified six laterally continuous sandstone and conglomerate formations that contained hydrates. The porosity of these units was difficult to measure due to a lack of hydrate samples, however, porosities were estimated to range from 22 to 48%. These estimates were consistent with the work of other researchers who measured porosities in the permafrost interval (0-610 m) at Prudhoe Bay of 40-45% and the estimated porosity of the West Sak sandstones in the 1000-1300 m interval to range between 25 and 35% (Collett 1993). Intervals containing hydrates ranged from 3-24m. Due to the lack of hydrate samples the form of the hydrate deposits (i.e, massive, layered, etc.) from the North Slope is not currently known. Figure 1 provides a schematic representation of hydrates formed in North Slope formations.

As shown schematically in Figure 2, two basic types of hydrate reserve configurations have been reported in the literature. A confined hydrate deposit exists when a hydrate bearing formation is located between two relatively impermeable layers. A hydrate cap on top of a free gas reservoir can also occur. Since the formation of hydrates significantly reduces formation permeability, hydrates can also act as a free gas cap (deBoer, Houbolt et al. 1985; Sloan 1990).

Figure 3 schematically illustrates the multiphase nature of a hydrate deposit before and after dissociation. In the most general case, a total of four phases can be present in the hydrate formation: the solid phase (i.e., the sediment grains), the hydrate phase, a brine phase with an initial salt concentration of C_1 and a free gas phase with a initial pressure P_1. Gas production requires the dissociation of the hydrate structure creating a three-phase system. The solid sediment grain phase volume remains unchanged. An increase in the volume of the brine phase and a reduction in the salt concentration would be expected in the closed system. An increase in the gas phase volume and pressure would also be expected. An example calculation for a hydrate formation where no free gas exists is also shown in Figure 3.

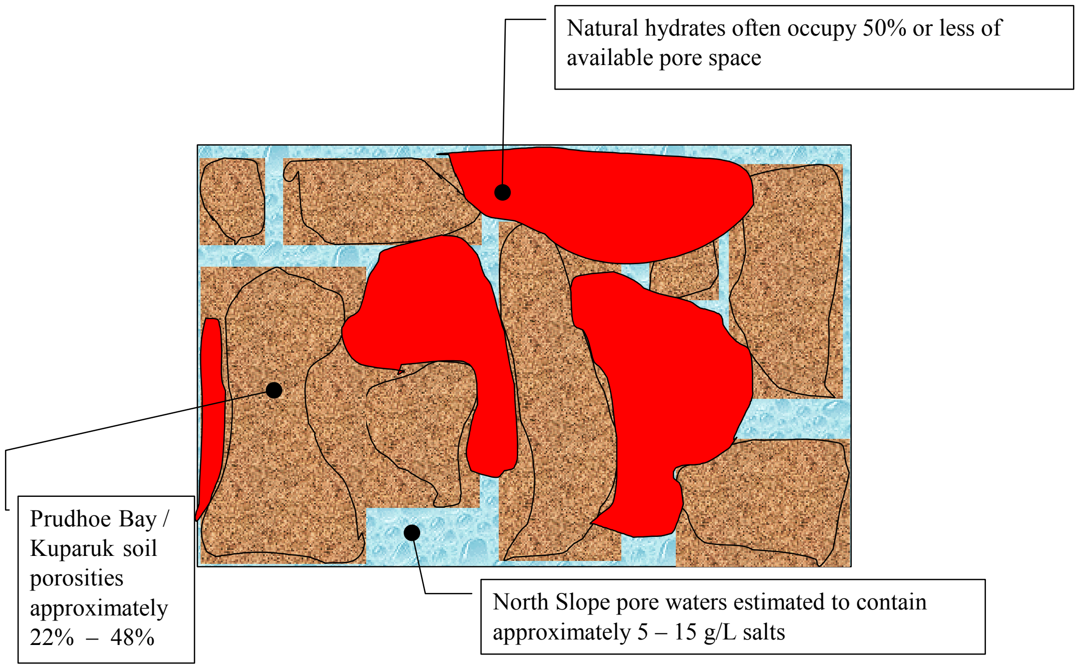

Figure 1 – Schematic of Hydrates in North Slope Porous Media

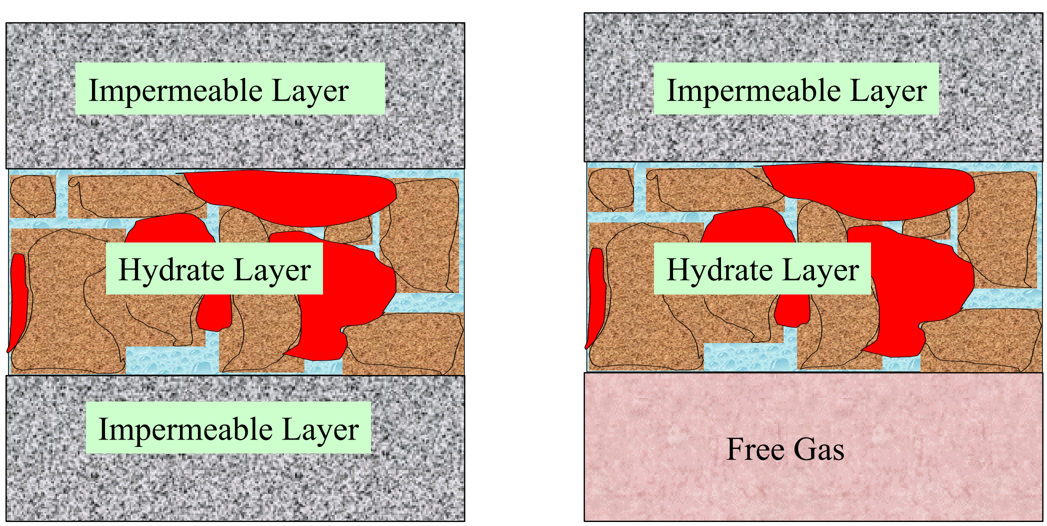

Figure 2 – General Types of Hydrate Reservoirs

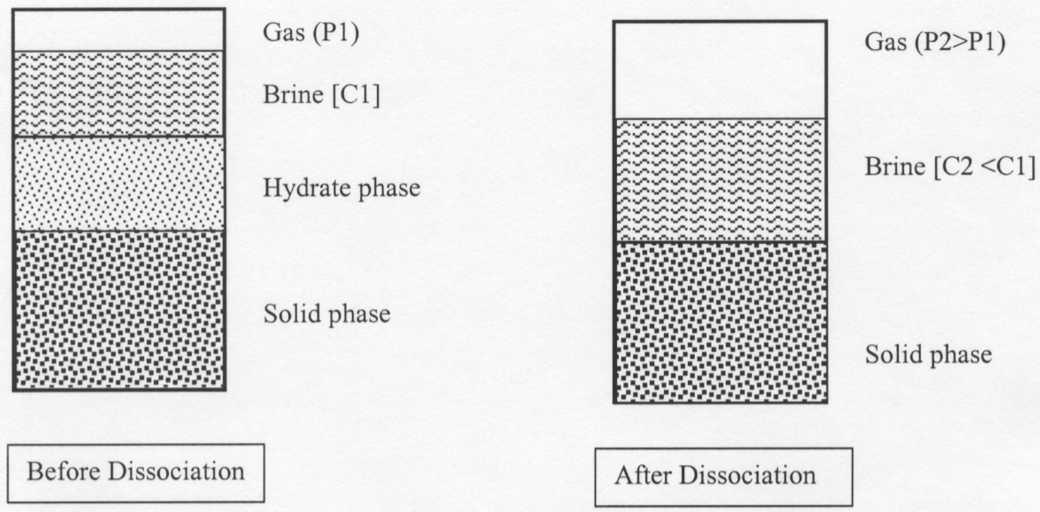

Example (for 1 ft^3 of formation):
Formation porosity = 30%
Hydrate saturation = 50%
Brine saturation = 50% at a concentration of 1 wt.% (10g/L)
No free gas
Hydrate number = 6.3 (90% occupancy)
Temperature = 2^oC

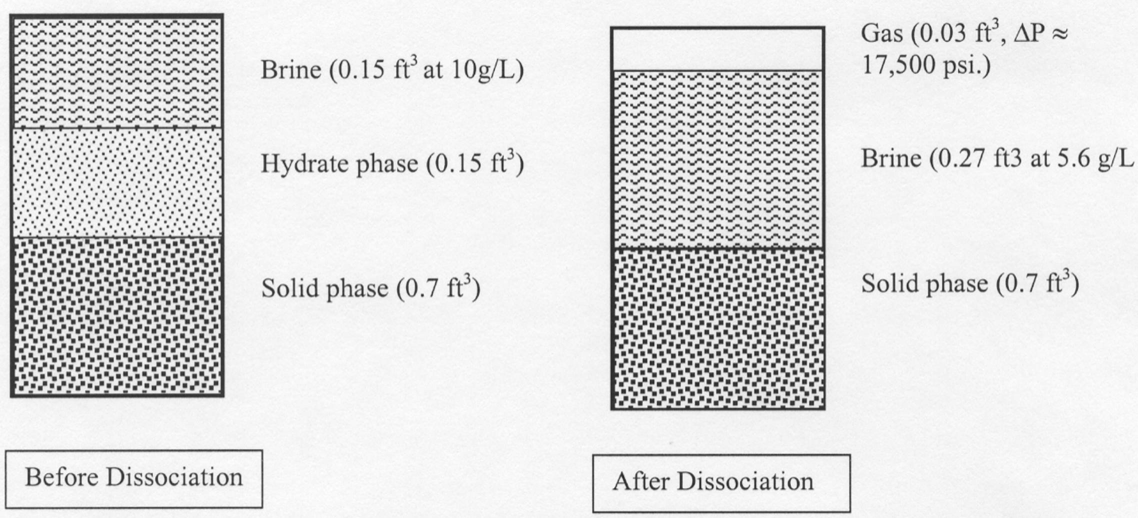

Figure 2 – Schematic Representation of the Phases Present in a Hydrate Reservoir Before and After Dissociation.

Hydrate Production Techniques

Hydrate dissociation can be accomplished using thermal stimulation, depressurization or the injection of hydrate inhibitors. A number of conceptual models of potential production techniques have been proposed in the literature. These include:

- A single well depressurization model where formation pressure is reduced to stimulate hydrate dissociation. (Kuuskraa, Hammershaimb et al. 1983; Kamath, Mutalik et al. 1991; Yousif, Abass et al. 1991; Goel, Wiggins et al. 2001)

- A single well, cyclic thermal injection model where hot brine or steam is injected into the hydrate formation, hydrates are allowed to dissociate during a "soak" period and then gas and water are produced from the well (Kuuskraa, Hammershaimb et al. 1983).

- Injection of methanol or glycol to lower the hydrate formation temperature (Sira, Patil et al. 1990; Patil 2002)

- A multi-well continuous thermal injection model where two or more interconnected wells are use. Hot brine or steam are injected into one well and gas and water are produced from the other well(s) in the system. Wells are connected by a network of fractures that facilitate gas and water flow (Kuuskraa, Hammershaimb et al. 1983).

- A reservoir depressurization model in which the reservoir pressure in a fracture in the hydrate deposit is maintained at a low value to cause hydrate dissociation (Kuuskraa, Hammershaimb et al. 1983).

- Depressurization of the free gas reservoir located beneath the hydrate cap (Makogon 1981).

- Use of down-hole heaters or the use of electromagnetic heating (Islam 1994; Patil 2002).

Since only depressurization of the free gas reservoir in the Messoiakh field in Western Siberia has been implemented at full scale (Makogon 1981), very limited information on the full-scale application of gas hydrate production approaches is available. Most of the research conducted to date consists of lab scale experiment to evaluate stimulation techniques (Sira, Patil et al. 1990; Kamath, Mutalik et al. 1991; Ershov and Yakushev 1992) and the development of numerical models to simulate thermal stimulation and depressurization production techniques (Holder, Angert et al. 1982; Kamath, Holder et al. 1984; Das and Srivastava 1991; Yousif, Abass et al. 1991; Goel, Wiggins et al. 2001).

Unfortunately, most of the hydrate production experiments and numerical models reviewed for this report fail to specifically address the water phase. The models typically assume that the water phase is immobile and will not impact gas production although several researchers agree that this is not a good assumption (Wittebolle and Sego; Sloan 1990; Yousif, Abass et al. 1991). Due to the lack of information on the fate of the water phase during hydrate production, only a conceptual evaluation of the water production issues can be offered at this time.

The volume and flow rate water generated during hydrate production will fundamentally be a function of the hydrate dissociation rate. (Kim, Bishnoi et al. 1987) determined that the intrinsic hydrate dissociation rate is proportional to the hydrate surface area and the difference between the fugacity of gas phase at the equilibrium and the decomposition pressure. Not all of the water liberated during hydrate dissociation will be produced. Formation type (i.e., confined, gas cap, etc.), formation characteristics (i.e., porosity, permeability, hydrate content, residual saturation) will also impact the amount of water produced. Capillary forces exerted by the formation will hold a fraction of the water produced during hydrate dissociation. Only water at saturations above the residual saturation will be mobile. (Makogon 1981) reported that residual water saturation in the Messoiakh field ranged from 29 to 50%. As discussed in the following paragraphs, each production technique would be expected to have unique water production characteristics.

Water production during depressurization of a single well.

Hydrate production using the depressurization approach using a single well can be accomplished by reducing the pressure in the well bore or formation fracture below the hydrate stability pressure. Figure 4 is a schematic representation of single well depressurization hydrate production.

A previous study (Goel, Wiggins et al. 2001) modeled hydrate dissociation via depressurization by assuming a cylindrical reservoir geometry. Hydrate production created an undissociated hydrate/dissociated gas interface. The position of this interface varied as hydrates dissociated during production. The model assumed a radial flow of fluids and that the water formed during dissociation had no effect on gas flow (i.e., water would not reduce the relative permeability to gas flow). Table 1 summarizes the parameters used in the Goel model. The model was used to generate pressure profiles in the formation for various production times and gas flow rates. Examples of data generated by the Goel model are provided in Figure 5. A large pressure drop is predicted at the undissociated/dissociated hydrate interface with very little change in pressure predicted in the dissociated portion of the formation. Gas production rates of 0.5 standard cubic meters per day (SCMD) were predicted from the model.

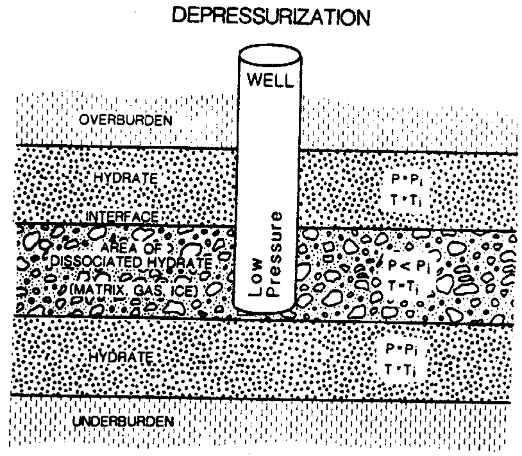

Figure 4 – Schematic Representation of Single-Well Depresssurization Hydrate Production from (Kuuskraa, Hammershaimb et al. 1983).

Table 1 – Hydrate Formation Parameters Used in the (Goel, Wiggins et al. 2001)Model.

Parameter	Value
Hydrate reservoir area	10 acres
Hydrate reservoir thickness	30 m
Porosity	30%
Hydrate saturation	20%
Hydrate reservoir temperature and pressure	56 atm/280 K
Hydrate equilibrium pressure	54 atm
Hydrate dissociation constant	124 e $^{(-9400/T\ (K))}$ kmol/(s m^2 Pa)
Gas viscosity	1.5 x 10-5 Pa s
Dissociated zone permeability	0.01 and 10 milldarcy

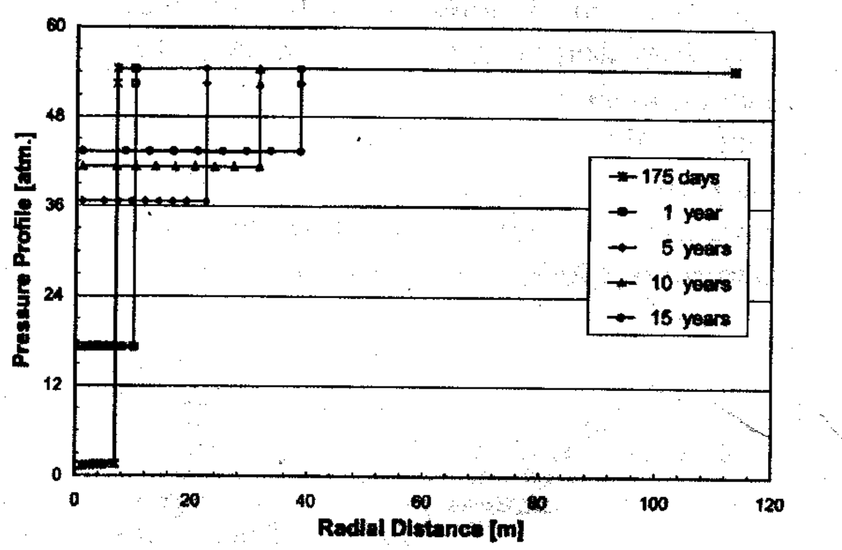

Figure 5 – Formation Pressure Profile Model Results from (Goel, Wiggins et al. 2001)

Yousif et al. (1991) also created a one-dimensional model to simulate the production of gas hydrates using the depressurization approach. This model explicitly addressed the mobile water phase and, as shown in Figure 6, the results indicated that a localized water content maximum would be created in the formation during hydrate production. The expanding gas forces all but the immobile water from the formation near the undissociated hydrate interface creating a water front. In this work, water saturations above approximately 40% would be mobile and create a produced water flow. These results suggest that dissociated water would reduce the relative permeability of the formation to gas flow and limit the ability to maintain gas production rates. A reduction in the relative permeability of the formation to gas would result in a reduction in gas flow and an increase in pressure that may inhibit hydrate dissociation. Using this production technique, the produced water would have to be removed to maintain hydrate production (Wittebolle 1985).

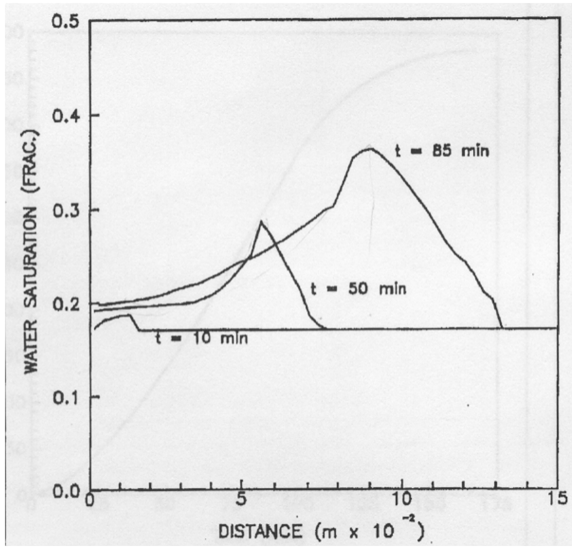

Figure 6 – Water Saturation Predictions from the (Yousif, Abass et al. 1991) Model

Water Production during the cyclic injection of hot fluids in a single well

Consider the cyclic single well production approach shown schematically in Figure 7 in which hot fluid (steam or brine) is cyclically injected into the hydrate formation to cause dissociation. In this production scenario, the sum of the formation water, the hot fluid (brine or the hot water condensate formed by from injected steam) and the water from dissociation of the hydrates would be present in the formation. In order to force hot fluids to the undissociated hydrate face, the dissociated formation would need to be flooded. At least a portion of this water must be removed if gas is to be produced using this approach to restore permeability to gas flow.

As the radius of dissociated hydrates expands, water will be required to fill the formation. Since the volume of water produced by hydrate dissociation is approximately 22% less than the volume occupied by the hydrate, additional water will be necessary to flood the formation.

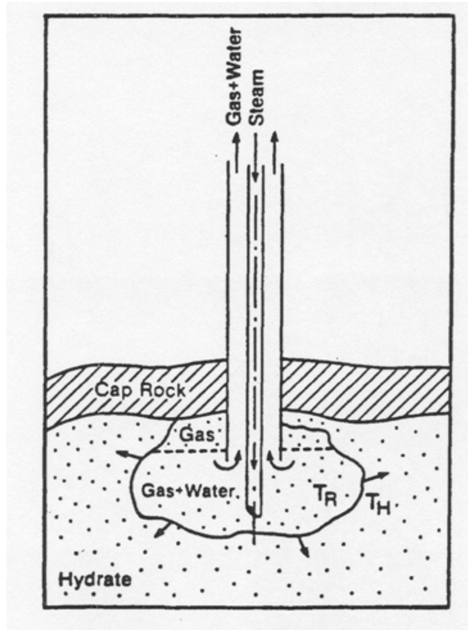

Figure 7 – Schematic Representation of Cyclic Single-Well Hydrate Production Using Injected Steam from (Kuuskraa, Hammershaimb et al. 1983)

In addition, the dissociation of hydrates will add pure water to the formation diluting the brine concentration. (Kamath, Mutalik et al. 1991) conducted laboratory experiments on hydrate dissociation using the brine injection methods. Salinity of the brine used to dissociate the hydrates was reduced by approximately 3 to 5% as the hydrates dissociated. Since the rate of gas production using the brine injection method is a function of temperature, pressure, brine concentration (as well as temperature, pressure and hydrate dissociation interface area) the continual addition of salts and/or the concentration of the recovered water (if it is to be reinjected) may be required to maintain the brine concentration and gas production rates.

Water production during depressurization of an associated free gas reservoir

Hydrate dissociation induced by the depressurization of an associated free gas reservoir may represent the best case scenario for the production of hydrate formations. This scenario also represents the case where minimal amount of produced water may be expected. Gas produced from the hydrate formation will be in contact with the water generated during the dissociation of the hydrate and connate water in the free gas formation. As a result, the gas stream should be saturated with water but water generated from the dissociation of hydrates may not load the well bore in this situation.

Water production during continuous thermal stimulation

Hydrate production during continuous thermal stimulation with hot brine, hot water or steam would use a combination of injection and recovery wells linked by fractures as shown schematically in Figure 8.   Hot fluid would be injected into the fractures causing hydrate dissociation. This water, along with the water generated during the dissociation of the hydrate formation, would be drain from the undissociated hydrate interface. The gas generated during hydrate dissociation may also displace water. Unless it is removed, the water generated during hydrate dissociation would reduce the relative permeability of the formation to gas flow and potentially load the production well.

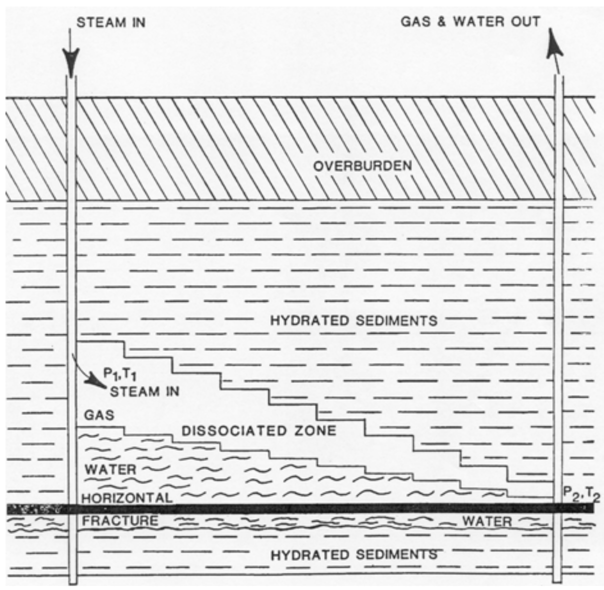

Figure 8– Schematic of Continuous Hydrate Production Using Steam Injection from (Kuuskraa, Hammershaimb et al. 1983)

Summary of Water Production Issues

A review of the available conceptual and numerical models for hydrate production indicates that significant amounts of water will be generated during the production of hydrate reserves. In most of the production scenarios cited in the literature, it is reasonable to assume that unless the water generated during hydrate dissociation is removed, the relative permeability of the formation to gas flow the ability to maintain gas production rates will be reduced. The one numerical modeling effort reviewed for this report that explicitly considered the water phase indicates that the single well depressurization production approach will generate water slugs as water is displaced from the formation by expanding gas. The major components of the produced water will be salts and dissolved gasses and potentially some sediment. Brine or steam injection production options may require water beyond that provided by hydrate dissociation to meet production demands.

Water and Wastewater Infrastructure Strategies

The water generated during gas hydrate dissociation suggest that water handling will be critical component of the production process. And as such, the infrastructure designed to process water and wastewater will become a more important factor to the success of individual well or field than most conventional oil and gas operations. Under these conditions, the approach used to design and operate water systems may need to be modified from current methods used in the oil and gas industry.

In most oil and gas operations today, the water and wastewater (w/ww) infrastructure is not considered as an integral part of planning process for field development. Water and wastewater systems are often designed separately from the main oil and gas handling facilities by oil-field service providers, term engineering contractors or camp system manufacturers contracted to perform design and construction tasks. Since many of these contractors do not specialize in w/ww processes, designs that are not fit for purpose frequently occur. Under the best circumstances, this approach produces designs that meet all the regulatory requirements for a particular installation. However, under almost all circumstances, the design of the w/ww infrastructure is completed on a site-by-site basis which can result in an eclectic collection of treatment technologies, each with its own specific operations and maintenance requirements.

A more effective approach, and one that the increased water generated expected during gas hydrate production may demand, would be to design the w/ww infrastructure using an regional approach based on the following three principals. First, the design of w/ww systems at a particular installation should be integrated with the exploration and production activities and consider all water requirements and wastewater generation activities that occur at each site. Second, to increase efficiency and reduce complexity, w/ww systems should be designed on a field wide or region wide basis and not at a site-by-site basis. Finally, the w/ww systems designs should be robust enough to handle a variety of conditions and permit requirements. Additional information on each of these design principals are provided in the following paragraphs.

__Exploration and Production Water Demands and Wastewater Generation__

Table 2 summarizes the water requirements and wastewater generation anticipated for a hydrates exploration and production platform and the associated water quality requirement (when known).

Table 2 - Summary of Water Demands and Wastewater Generation Activities on Gas Hydrate Exploration and Production Sites.

Water Use	Quantity and/or Rate	Required Water Quality
Personal use of potable water (drinking, personal hygiene, cooking)	65-70 gal/capita/day	Potable
Heat Generation and Cooling (boiler makeup water, steam generation, cooling water)	Function of types of system used	Hardness limitation (to prevent scaling)
Air Pollution Control Facilities	Function of type of systems used	Function of type of system used
Drilling Fluids Makeup Water	Function of drilling mud used	Function of drilling muds used
Washdown Water	Minimal	unknown
Wastewater Generation		
Backwash and concentrate from water treatment systems	1-5 gal/cap/day	Function of water treatment system utilized
Domestic Wastewater (gray water from kitchens/showers/sinks, etc. and blackwater from toilet facilities)	60-65 gal/cap/day	Function of location of discharge (i.e, injected, surface discharged, reused, etc.)
Hydrate and connate produced water	Function of type of hydrate formation produced	Unknown, although flow is not expected to be uniform (surge flow is expected

Arctic oil field camps typically must provide 65-70 gallons per capita per day of potable water. Most camps have a single plumbing system and as a result, potable water is supplied to all sinks, showers and toilet facilities in the camp. The remaining demands for water are process demands including the formulation of certain drilling fluids, water for heating and cooling system and washdown water used for cleaning process equipment and spaces. Some installations may also use water in the scrubbers used to meet air pollution discharge requirements.

Since most camps are prefabricated modules plumbed with high integrity water distribution and wastewater collection systems, nearly all of the potable water produced is collected as wastewater. Additional wastewater flows (e.g., backwash, concentrate, spent cleaning solutions) can be generated by the water treatment system. However, the largest waste stream will likely be the produced water generated during hydrate production. Although the basic nature of hydrate deposits suggests that the gas and water production rates should be related, good estimates of the volume and rate of water production do not exist.

Remote Operation

The Alaska Department of Environmental Conservation (ADEC) classifies water and wastewater treatment systems into one of four classes based on complexity (i.e., a class one system would be simple and a class four system complex). ADEC further requires that the supervising operator responsible for a public water or wastewater system be actively supervised each day by an operator with a level of certification equal to or greater than the system classification. Thus a class 4 system would require at least a Level 4 operator to be in compliance. Although the current regulations specify that the supervising operator be on-site during normal working hours, the ADEC does provide a process for evaluating alternate methods of system supervision.

One alternate method to operate water and wastewater systems is to implement a remote operations strategy shown schematically in Figure 9. Using this approach, water and wastewater treatment systems are distributed throughout the region (e.g., the North Slope) each have their own water and wastewater infrastructure. However, rather than have a full crew of operators on-site as is now the practice, a low level operator on-site would be supported by more experienced, higher level operators at a central monitoring and operations and support facility.

This type of approach would result in an overall reduction in the number of high level personnel required to operate the water and wastewater infrastructure. Fewer personnel may reduce operating costs, but as importantly, it will also reduce the need for high level operators that are currently in short supply. A number of rural Alaska communities are attempting this remote operations support approach because they cannot find and/or adequately compensate trained operators.

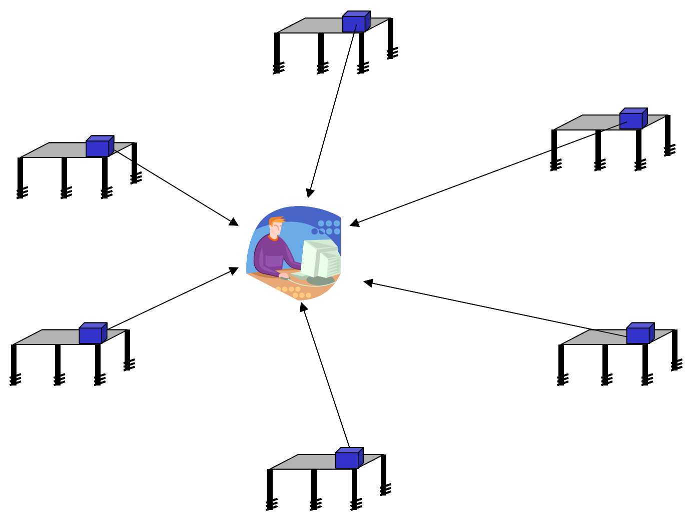

Figure 9 - Distributed Operation of Water and Wastewater Treatment Systems

To implement a remote operations and monitoring strategy, the ADEC and the Governor's Water/Wastewater Advisory Board must convinced that any operations strategy that deviates from that stated in the regulations is adequate to protect public health and the environment and the capital invested in the system. The general framework for the O&M strategy that must be reviewed and approved by the Board and the ADEC is summarized in Table 3.

Table 3 - General Framework for a Remote Operations and Maintenance Plan

Framework Elements
Statement of proposed O&M strategy
Description of the system involved including current classification, O&M requirements and the status of system compliance with current regulations
Qualifications of the operating personnel including current certification level, work history and job responsibilities
Duration of the proposed O&M change
For off-site supervising with on-site custodial care strategies include the qualifications and duties of the custodial personnel, the method of communications, the frequency of on-site visitation by supervising personnel and methods of emergency response.
Consequences of system malfunction and/or system failure and the methods of detection, safeguard and response
Compliance plan (if applicable)

Technology Characteristics

The final principal of an effective water and wastewater infrastructure strategy is to select treatment technologies that are robust enough to provide high performance under a wide variety of conditions yet flexible enough to be readily adaptable to different installations. Table 4 summarizes the major technology requirements required for oil and gas exploration and production operations and the corresponding design features.

One of the most important features for any water and wastewater treatment technology in the oil and gas industry is the flexibility. The normal design process for water and wastewater infrastructure consists of forecasting the design life needs and sizing process tanks and equipment to meet the needs of the installation throughout the design life. Unfortunately, the very nature of oil and gas exploration and production activities makes accurate prediction of water and wastewater flow rates difficult at best. Camp populations predictions are of loose estimates subject to changes in field production capability and economic factors beyond the control of individual project managers. As a result, estimates of treatment requirements are, in the author's experience, inherently unstable and subject to change.

Table 4 - Water and Wastewater Technology Requirements and Design Features

Technology Requirement	Design Feature
Variable camp population, Uncertain flows (need for flexibility)	Modular, scalable design
Sensitive receiving environments	High quality (tertiary) effluent
Poor source waterwater characteristics	Ability to remove organics and pathogens
Scarcity of qualified operators	Ease of operation. Capable of automated, remote operation
Space limitations	Small foot print
High transportation costs	Limited chemical use, limited sludge production

Many of the conventional technologies commonly used in the oil and gas industry to provide water and wastewater infrastructure are not well suited to match changing demands. Tanks must be sized to accommodate a certain range of flows/demands and significant variations, either above or below the design flow, can result in poor performance. Ideal infrastructure would be flexible enough to provide good performance over a wide range of flows and be easily expandable if additional capacity was required.

Remote, roadless exploration and production installations (i.e., the on-shore platform) will also make small footprint a premium. Systems that can operate with a minimum of tank space and be easily transported and assembled will be necessary.

Finally, wastewater systems should be capable of producing high quality effluent that will maximize the number of potential disposal options (i.e., surface discharge, reinjection, reuse, etc.). Water systems must be able to produce potable water from local sources, which on the North Slope are typically tundra ponds containing high concentrations of natural organic material. For both water and wastewater systems, high transportation costs require that the use of chemicals and the production of residuals be minimized to the extent possible.

Membrane technologies represent some of the best available systems commercially available to implement this approach. Selection of one or two membrane technologies capable that meet the criteria in Table 4 and standardization of designs could result in significant savings in permitting construction and operational costs. In the following paragraphs, conceptual designs of water and wastewater treatment systems for hydrate production platforms are presented along with preliminary technical information and cost estimates for these technologies.

Conceptual Design of Hydrates Water and Wastewater Infrastructure

Figures 10 provides a conceptual layout for an integrated water treatment systems for a gas hydrate production facility. Produced water from the hydrate formation would first pass through a separator to remove any dissolved gasses and entrained sediments. Depending upon the quality of that water, it may be suitable for use in other processes on pad (e.g., drilling mud makeup water, washdown water, etc.). Hydrate produced water could then be processed through a membrane treatment system to remove colloidal solids and reduce the total dissolved solids content. If necessary, surface water could also be processed through the membrane treatment system.

Several disposal options are possible for permeate and concentrate streams generated by the membrane treatment system. The permeate could be used for potable water uses on the platform and to satisfy other demands for high quality water. Permeate from the membrane system will be of high quality and also may be suitable for surface discharge, a factor which may be important in hydrate production of large amounts of water are generated that cannot be reinjected. The concentrate from the membrane system will be a concentrated brine that could be used to stimulate hydrate production. Other options for this stream include reinjection or evaporation.

Overview of Membrane Water Treatment Processes

Membrane processes involve the use of species selective membranes for the concentration of dissolved solids into smaller volumes. The utility of membrane systems is related to their mobility and flexibility, as well as their treatment capacity. As described in Figure 11, microfiltration (MF) technology typically provides removal of particles larger than 0.1 to 0.4 microns. Ultrafiltration (UF) technology is a tighter membrane providing removal of macromolecular particles and compounds with a size of 1,000 to 100,000 atomic molecular units (AMU). Nanofiltration (NF) membranes can reject compounds with a size of between 100 and 1,000 AMU and reverse osmosis (RO) can reject constituents in the water with less than 100 AMU. Unlike MF and UF however, factors other than molecular size including electrical charge can play a significant role in whether a compound is rejected at the membrane surface in RO and NF systems.

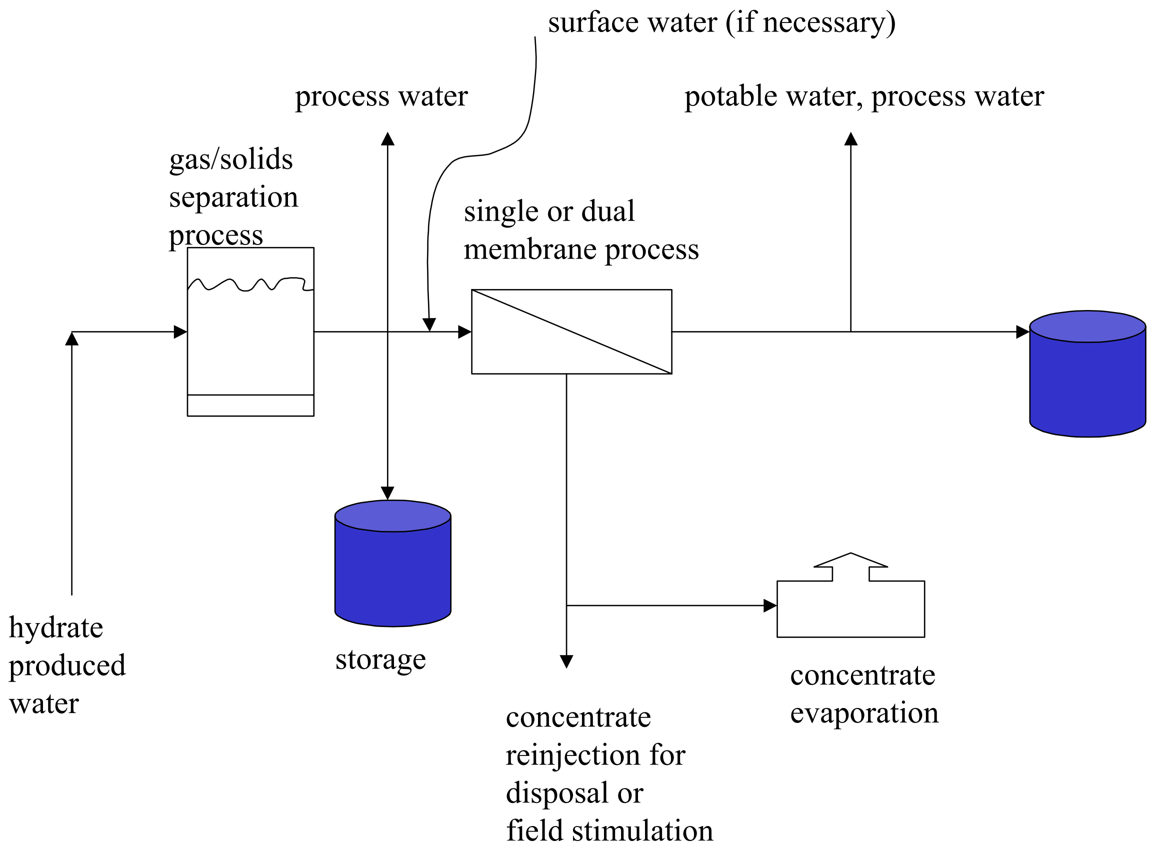

Figure 10 - Conceptual Design of an Integrated Water Treatment Facility for Gas Hydrate Production

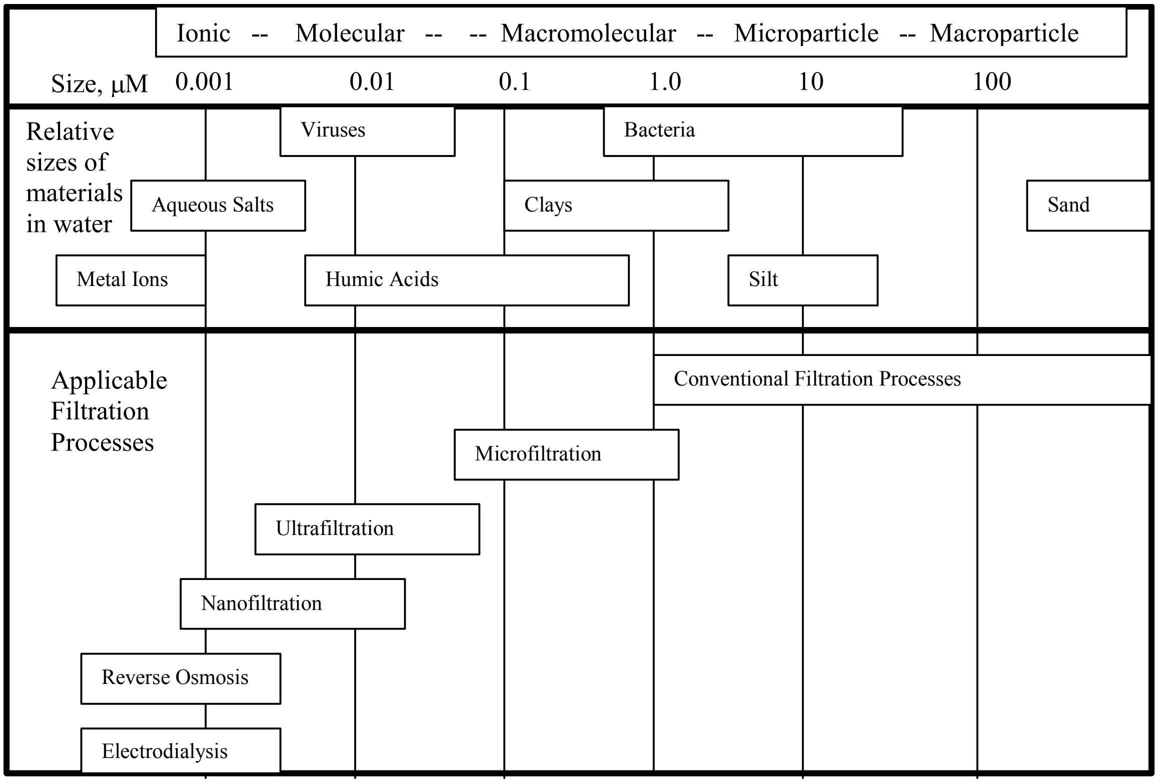

Figure 11 - Membrane Filtration Processes and Relative Sizes of Materials in Water

Since the dissolved inorganic compounds present in hydrate produced water will be typically smaller than the nominal pore size, MF and UF will not effectively reduce the total dissolved solids concentration. NF and RO membranes, however, will reject inorganic ions present in hydrate produced water. Of these two processes, RO membranes remove a higher fraction of the inorganic total dissolved solids. However, NF membranes will remove a fraction of the TDS at a lower operating pressure and can be an appropriate choice when large reductions in TDS are not required.

Types of Commercially Available Membrane Systems

Two basic types of NF and RO systems are commercially available. Spiral wound nanofiltration systems, as shown schematically in Figure 12, consists of a sandwich of flat sheets of NF membrane material and spacer channel wrapped around a central perforated tube to form a membrane element. These elements are inserted in to a pressure vessel end to end. Individual pressure vessels are then operated in hydraulic arrays configured to produce permeate with a minimum of fouling. Spiral wound construction yields membrane filtration systems with large membrane surface areas relative to the volume of the pressure vessels.

Spiral wound NF treatment systems will easily foul if supplied with water that is not adequately pretreated to remove particles. As a result, spiral wound nanofilters are typically preceded by one or more pretreatment processes intended to provide removal of colloidal particles. Pretreatment for NF processes include cartridge filtration, direct filtration, or conventional filtration. More recently microfiltration (MF) membrane or ultrafiltration (UF) filtration has been deployed as pretreatment to NF membranes to provide better pretreatment and extend the useful life of NF membranes. The use of both MF and NF membranes has been termed integrated dual membrane treatment, or MF/NF treatment.

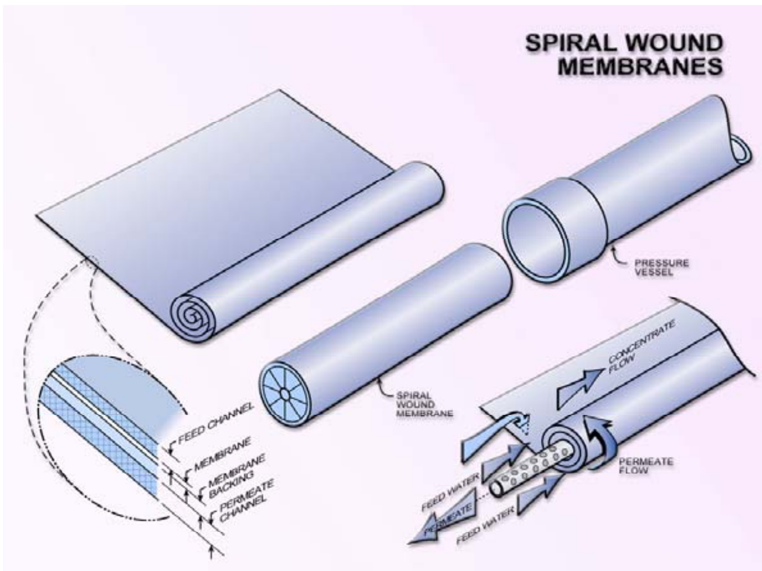

Figure 12 - Spiral Wound Membrane Module Construction

Tubular membranes are the second type of NF configuration used in drinking water treatment. In this type of treatment system, tubular membrane elements which are typically on the order of ½” in diameter are inserted into a pressure vessel to create a membrane module. A cutaway section of a typical tubular membrane module is shown in Figure 13.

In a full-scale tubular membrane NF system, raw water is pumped through the tubular elements. A recirculation pump is typically used to obtain the water pressures and flow rates necessary for the system to operate effectively. Permeate is collected in the module shroud. A small fraction of the concentrate stream is wasted, but the majority is recycled and combined with the raw water stream. Unlike spiral wound systems, tubular membrane systems are not easily fouled by particulates and only limited pretreatment (e.g., a strainer or bag filter) is required for their use. Certain manufacturers also employ an automated cleaning process where a foam ball is periodically run through the membrane elements to scour off the foulants that accumulate on the membrane surface. High flow velocities are also maintained through the membrane elements to reduce fouling.

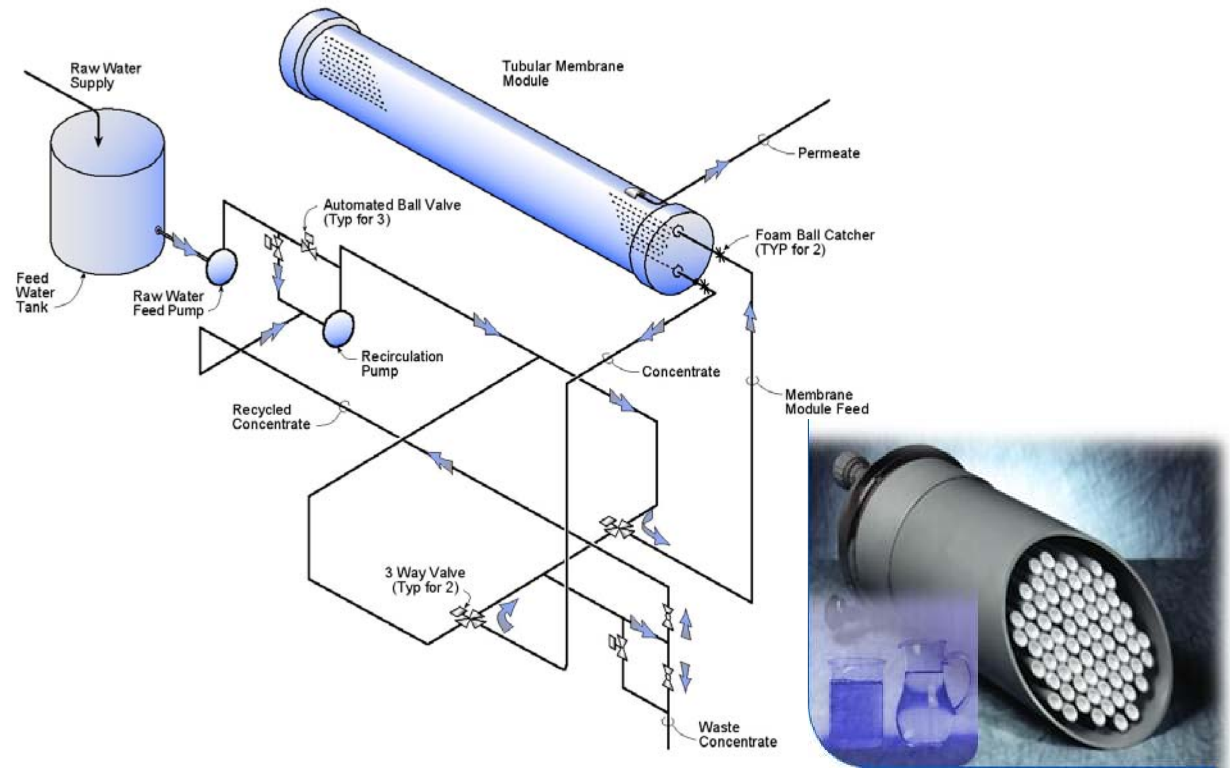

Figure 13- Cutaway section of a Tubular Membrane NF or RO Module (PCI Membrane Systems) and a Schematic of a Tubular Membrane NF or RO System.

The ED process is based upon the premise that most solutes in water are ionic species. Through the application of a direct current across the solution, cations are conveyed towards the anode, while anions migrate towards the cathode. As these ions move through solution, they are routed through charge-specific membranes, and flushed out of the system in concentrated brine solutions. In a fashion similar to the RO process, purified water would be surface applied or employed for beneficial uses, while concentrated brines would be re-injected or subjected to further treatment/disposal. A schematic of a typical ED process is provided in Figure 14.

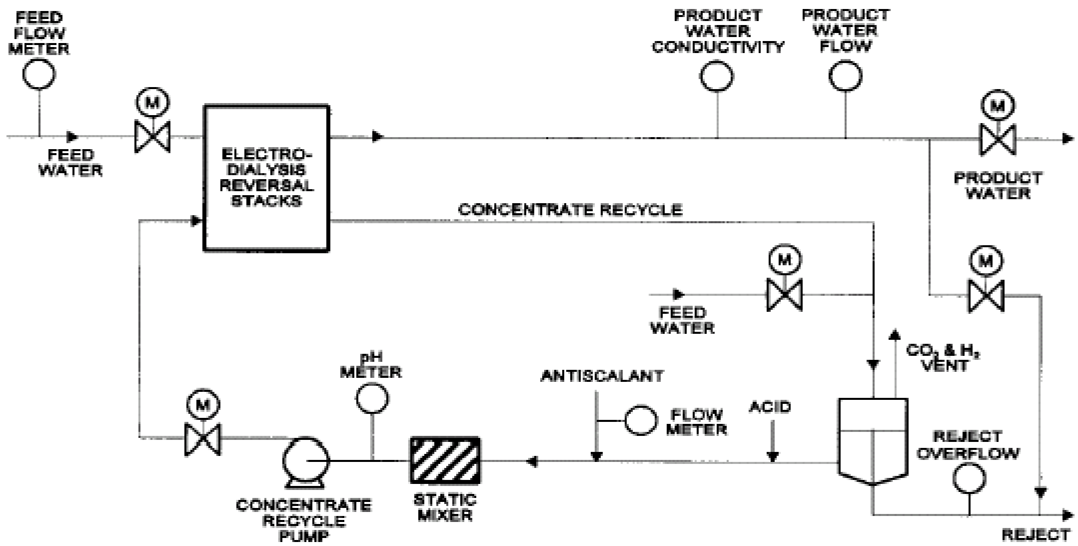

Figure 14 - Schematic of an ED Treatment Process from (Leitz and Boegli 2001).

Use of Membrane Systems for Hydrate Produced Water Treatment

Since both spiral wound and tubular membranes can effectively remove TDS, selecting the appropriate system depends on a number of factors including:

- Reduction in suspended and dissolved solids required for discharge
- Capital costs of the treatment equipment
- Footprint (which impacts overall building costs)
- Operating costs
- Complexity, redundancy and other factors

Although no membrane systems have been specifically designed for hydrate produced water treatment, reasonable estimates of capital and operations and maintenance costs can be obtained by evaluating drinking water membrane treatment systems. Jones and Woolard (2001) compared the costs of integrated MF/NF and tubular NF system for treating a hypothetical Alaskan drinking water source for system with a capacities ranging from 30,000 to 120,000 gal per day. The cost estimates compiled for this work should be reasonable estimates of costs for treating hydrate produced water with low pressure RO or NF membranes. It is important to note that the flux rates assumed by the NF membrane manufactures are approximately 6 gallons per day per square foot (gfd) for both the tubular and spiral wound membranes (see Table 2). This is a relatively low flux rate that could be met in a hydrate produced water RO or NF system.

Table 5 - Membrane System Design Parameters and Scope of Supply

Hollow Fiber MF Equipment	
Approximate MF Flux Rate	20 gfd
Membrane	Hollow Fiber PVDF
Module Surface Area	538 sf
Membrane Nominal Pore Size	0.1 micron
MF Recovery	96 percent
Sprial Wound NF or RO Equipment	
Approximate NF Flux Rate	6.1 gfd
Membrane	Composite Polyamide
Hydraulic Array	Single Pass with Recycle
NF System Overall Recovery	85 percent
Membrane Element Size	8 x 40 inch
Individual Membrane Element Area	350 sf
Tubular NF or RO Equipment	
Approximate Flux Rate	6 gfd
Membrane	Tubular Polyamide
Hydraulic Array	Single Pass with Recycle
NF System Overall Recovery	80 -90 percent
Individual Membrane Module Area	115 sf

MF Equipment Scope of Supply	Spiral Woun Membrane Equipment Scope of Supply
Backwashable Strainer	8-inch Pressure Vessels
Feed Water Tank	8-inch x 40-inch membrane elements
Feed Pump	NF Feed Pump
Membrane Modules	Stainless Steel High Pressure Piping, Valves and Fittings
Membrane Skid	PVC Schedule 80 Low Pressure Piping
Valve Assembly Block	PLC Process Controller
Integrity Test System	Flow, Pressure, Temperature, Conductivity Instruments
Reverse Flow (RF) Pump	Modem Process Monitoring Capability
Compressed Air System	Automatic Concentrate Flushing System
Interconnecting Piping for Furnished Equipment	Chemical Dosing System for Scale Inhibitor
Process Instrumentation and Controls	CIP System Components
Variable Frequency Drives for RF and Feed Pumps	Start Up Assistance and Training
Filtrate Turbidimeter	
Clean in Place System	
Chemical Dosing Pumps for CIP	
Spent Cleaning Solution Neutralizing System	
Start Up Assistance and Training	

Table 6 summarizes the budgetary equipment capital costs for the integrated MF/NF and tubular NF systems. It is important to note that these are costs for the membrane treatment skids only. These data indicate that tubular membrane systems exceed the cost of an integrated MF/NF system for the range of capacity sizes evaluated for this report, and that the difference increases as increases with design flow. As design flow rates increase, additional membrane area can be added to a spiral wound system in far fewer pressure vessels than with a tubular membrane system, and the capital costs for larger tubular membrane equipment reflect this.

Table 6 - Budgetary Capital Costs for Membrane Skids

	Tubular NF or RO System			Integrated MF/NF or MF/RO Membrane System						
				MF			NF or RO			
Capacity (gpd)	Modules	Membrane Area (ft^2)	Capital Cost	Modules	Membrane Area (ft^2)	Capital Cost	Membrane Elements	Membrane Area (ft^2)	Capital Cost	Integrated System Capital Cost
30,000	44	5,060	$320,000	4	2153	$145,000	7	4,900	$79,000	$224,000
60,000	88	10,120	$464,000	7	3766	$183,000	21	9,800	$123,000	$306,000
90,000	132	151,080	$604,000	11	5918	$215,500	28	14,700	$143,000	$358,500
120,000	176	20,240	$742,000	13	6994	$227,200	36	19,600	$164,000	$391,200

Another factor that is often a significant contribution to overall project capital costs, especially in cold climates, is the size of the structure needed to house the treatment system. To determine the relative areas required for MF/NF systems and tubular membrane systems, preliminary floor plans for both were prepared for the process equipment, and compared for the four system capacities presented above. The assumptions made in the preparation of the floor plans to determine system footprint included:

- Floor space for a strainer was provided for both the MF and tubular NF equipment.
- Interior ceiling height for the process floor was limited to 14 feet.
- MF and spiral wound NF membranes were configured as single skids without parallel redundancy. By contrast, tubular NF membranes were configured with multiple parallel modular stacks all operating in parallel and able to maintain production if one stack were out of service for CIP or maintenance.
- Minimum clearances of 2.5 feet were provided around at least three sides of all membrane skids.
- Four feet of clearance on each end of the spiral wound membrane skid was provided on each end for loading and unloading membrane elements. By contrast, an overhead door was provided on one end of the building for removal and replacement of the 12-foot long tubular membrane modules.
- Common clean in place (CIP) equipment including chemical solution tank, tank heater, circulation pump, solution flow meter, and micron filter would be used for both the MF and NF or RO equipment in the dual membrane system configuration.
- Floor space for control panels with a minimum of 36 inches clearance at the front of the panel was provided for each membrane skid.
- An MF backwash surge tank was included to prevent sewer hydraulic overload.
- For the MF/NF alternative, floor space was included for the membrane skids, air compressors, feed pumps, reverse flow pump, raw water break tank, an intermediate break tank for MF filtrate, an MF reverse flow surge tank, and the CIP equipment.
- For the tubular membrane alternative, floor space was included for the membrane module stacks, the recirculation pump, a raw water strainer, system control panel, and CIP equipment.
- No floor space allocations were made for any post treatment chemical addition or chemical storage for fluoridation or chlorination.

Table 7 summarizes the floor space required for the MF/NF system and the tubular NF system for each of the four capacities considered. The dual membrane MF/NF treatment system occupies a somewhat larger floor area for the 30,000 gpd plant capacity than the tubular NF system. However, for larger capacity systems, the MF/NF system occupies a smaller area due again to the fact that spiral wound membrane elements are more compact in terms of available surface area per unit volume than are the tubular membranes.

Table 7 - Process Equipment Floor Space Requirements

Capacity (gpd)	MF/NF Equipment Floor Space (sq ft)	Tubular NF Equipment Floor Space (sq ft)
30,000	392	352
60,000	542	640
90,000	636	928
120,000	660	1,216

Operating costs for the membrane filtration options are the sum of multiple components that include labor, energy, chemicals, and replacement membranes. Factors used to compute these costs are summarized in Table 8 for the MF/NF(or RO) and tubular NF or RO membrane alternatives. The following assumptions were made in estimating system operating costs:

- Labor costs were based on past experience with integrated MF/NF and tubular NF membrane systems and reflect the time required to operate (i.e., make process adjustments, mix chemicals, perform cleaning, monitor process parameters) the treatment system only. Other operator duties like maintaining the disinfection system, performing general housekeeping functions and preparing monthly reports are not included in the labor estimates.
- A power cost of $0.07 per kW-hr assuming that power is generated on-site using recovered gas.
- Annual membrane replacement costs were calculated assuming a 5-year life. No interest was accrued on money set aside each year for membrane replacement.

- Operating costs not considered in this comparison include the expenses of repair and replacement of equipment and components, and their associated depreciation costs.

Table 8 - Preliminary Estimates of Operating Costs

MF/NF or MF/RO Filtration System					
System Capacity	**30,000**	**60,000**	**90,000**	**120,000**	**gpd**
Labor					
Labor Manhours	50	50	50	50	hrs/month
Labor Costs Including Benefits	$50	$50	$50	$50	$/hr
Annual Labor Cost	$30,000	$30,000	$30,000	$30,000	$/yr
Energy					
Energy Used	5.8	11.3	17.2	21.8	kW
Energy Cost	$0.07	$0.07	$0.07	$0.07	$/kWH
Annual Energy Cost	$3,557	$6,929	$10,547	$13,368	$/yr
Chemical Costs	$6,039	$10,781	$15,617	$23,663	$/yr
Annual Membrane Replacem	$4,240	$7,980	$12,220	$15,460	$/yr
Total Annual Cost	$43,836	$55,690	$68,384	$82,491	$/yr

Tubular NF or RO Filtration System					
System Capacity	**30,000**	**60,000**	**90,000**	**120,000**	**gpd**
Labor					
Labor Manhours	15	15	15	15	hrs/month
Labor Costs Including Benefits	$50	$50	$50	$50	$/hr
Annual Labor Cost	$9,000	$9,000	$9,000	$9,000	$/yr
Energy					
Energy Used	5.6	11.3	16.9	22.6	kW
Energy Cost	$0.07	$0.07	$0.07	$0.07	$/kWH
Annual Energy Cost	$3,434	$6,929	$10,363	$13,858	$/yr
Chemicals					
Chemical Costs	$230	$460	$690	$920	$/yr
Annual Membrane Replacem	$17,600	$35,200	$52,800	$70,400	$/yr
Total Annual Cost	$30,264	$51,589	$72,853	$94,178	$/yr

Overall system complexity and redundancy should also be considered when selecting a membrane treatment processes. Larger water systems typically have the resources to effectively operate more complex systems and can handle the added complexity of an integrated membrane process that uses both MF and NF or RO membrane filtration. The tubular NF or RO process uses a single membrane filtration process. There is physically more hardware to maintain with the dual membrane alternative than the single membrane alternative, and commensurately more operational labor required to keep the system running.

System complexity will also impact installation costs. Because there is physically more hardware associated with the dual membrane alternative, the costs associated with process piping, mechanical and electrical work required to install the integrated system will likely exceed the costs for a tubular membrane system.

The MF/NF alternatives considered for this analysis were configured with only a single skid for each filtration process. If there is a failure in the performance of an MF module, most MF manufacturers provide for isolating the faulty module and operating with less than full capacity until corrective action is taken. However, if an NF element fails, the faulty equipment cannot be temporarily isolated. By contrast, with tubular NF equipment, a faulty NF module can be isolated, removed from service, and the remainder of the equipment operated until corrective action is taken. If dual NF skids are considered for the MF/NF alternative, the capital cost of that alternative would increase.

In summary, capital costs, footprint, operating costs and complexity and redundancy are factors that should be considered when evaluating NF processes. In the analysis conducted to prepare this report:

- Capital equipment costs for MF/NF treatment were lower than for tubular NF treatment over the 30,000 gpd to 120,000 gpd capacity range assuming only a single NF skid is used for the MF/NF alternative.

- Floor space requirements for the tubular NF process equipment were lower for the 30,000 gpd system. The integrated MF/NF system required less area for the large capacity systems.

- Operating costs computed as the sum of labor, chemical, energy, and membrane replacement costs are lower for the smaller 30,000 gpd tubular NF system. Somewhere between 30,000 and 60,000 gallons per day capacity, the operating costs become lower for the MF/NF system.

- An integrated MF/NF system is typically more complex than a tubular system and as a result, will have additional operation and installation costs relative to a tubular NF system. These costs are offset by the lower capital cost of the integrated MF/NF system at higher flow rates.

Conceptual Design of Hydrates Water and Wastewater Infrastructure

Figure 15 is a conceptual schematic of a wastewater treatment system for a gas hydrate production platform. Domestic and certain industrial wastes are treated biologically in a membrane bioreactor (MBR) or other appropriate treatment system. Effluent from an MBR would be of a quality that it could be used for certain process applications. Reuse is also an option.

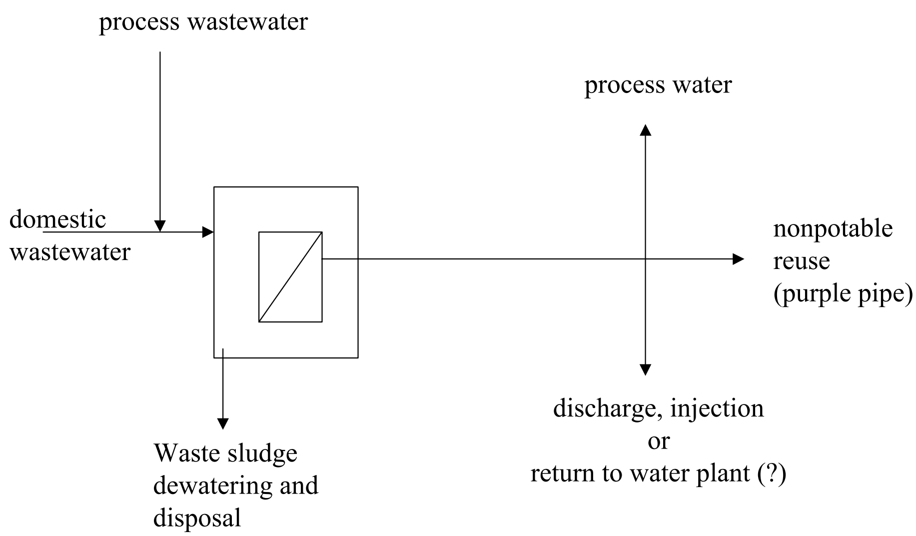

Figure 15 - Conceptual Design of an Integrated Wastewater Treatment System for Gas Hydrate Exploration and Production

Overview of Membrane Wastewater Treatment Processes

The membrane bioreactor (MBR) wastewater treatment systems are a suspended growth activated sludge treatment process that uses a mixed culture of microorganisms to treat wastewater. The MBR system uses banks of microfiltration (0.085-0.2 micron pore size) membranes suspended in the aeration chamber provide solids separation. Membrane modules eliminate the need for a separate secondary clarifier. These membranes, which resemble large bundles of “spaghetti” or flat sheets, are immersed at the end of the aeration basin. A vacuum is applied that draws treated wastewater through the membrane unit leaving the solids in the aeration basin. An aerator located at the base of each membrane units agitates the membranes and scours the membrane surface to prevents the accumulation of solids on the membrane surface. Several times each hour, the membrane units are backwashed with stored permeate (i.e., treated effluent) or allowed to agitate without vacuum applied to dislodge any accumulated solids. MBR’s require only a primary screen for pretreatment. As a result of this positive clarification process the system is easily automated and maintained, while providing an extremely consistent tertiary quality reclaimed water

MBR's are extremely compact because biological treatment, clarification and digestion all occur within the same aerated bioreactor. MBR's also typically operate at much higher mixed liquor concentrations (i.e. 12,000 to 15,000 mg/L) than the other treatment processes. As a result, the size of the reactor is 3 and 5 times smaller than more conventional treatment processes. The membrane units also provide solids separation that is largely independent of influent flow rate, strength and sludge properties making the system easy to operate and extremely reliable.

The MBR process produces a state-of-the-art treated effluent that exceeds secondary treatment standards. A system with a hydraulic residence time of less than 6 hours has been proven to be able to consistently produce an effluent with less than 5 mg/L BOD and suspended solids. A several log reduction in fecal coliforms (prior to disinfection) can also be achieved. The membrane modules allow MBR's to operate at long sludge ages that reduce the amount of waste sludge produced, and will significantly reduce the costs associated with hauling sludge. Nutrient removal is possible with minor modifications.

The MBR process requires very little operator attention. Unlike other processes, the physical separation of solids from the final treated effluent is accomplished by the membranes and does not require the operator attention or training necessary for other biological treatment systems. Many MBR plants are operated remotely with only daily local inspection and operator attention every several weeks. Some additional advantages the MBR technology has for oil and gas exploration and production include:

- Ease of operation with highly variable flows: The MBR is also a robust system that is easy to operate under variable wastewater flow conditions without deterioration in effluent quality.

- High quality effluent: The MBR produces an effluent of such quality that if can often be discharged to sensitive receiving environments without further treatment.

- Reduced Size: The use of membrane modules within the reactor reduces the size of the reactor. Small footprint systems require less space at the site and reduce the cost of heating the treatment facility.

- Packaged Systems: Modular MBR systems can be constructed off-site and delivered as a fully functional, containerized unit ready for connection to the influent and effluent piping and power.

A general process schematic for a typical MBR wastewater treatment system is shown in Figure 16. Screened wastewater is pumped from the primary treatment process directly into the MBR basins for secondary treatment. Treated effluent from the MBR is decanted into an effluent equalization basin and then pumped through a dsinfection system (if necessary) to the final discharge location. Waste sludge produced during biological treatment is pumped to an aerobic digester. Digested sludge is dewatered prior to final disposal. Screenings collected from the rotary drum screen are dewatered and compacted prior to final disposal.

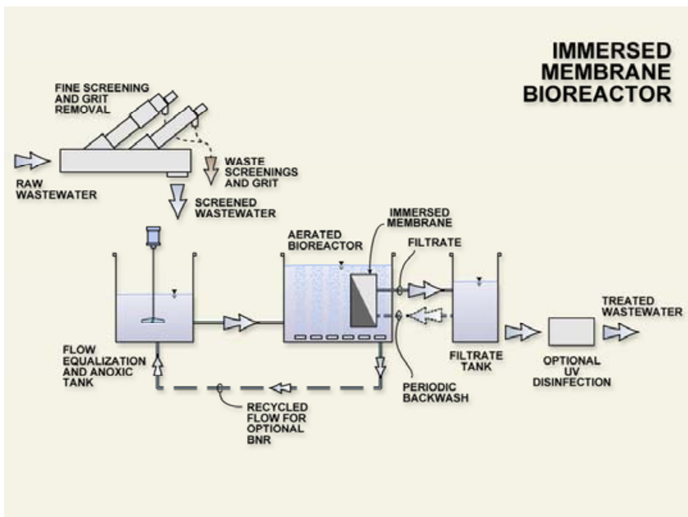

Figure 16 - Flow Schematic for a Typical MBR

Three types of submersible membranes are commercially available at this time. As shown in Figure 17, immersed hollow several manufacturers provide fiber membranes with either a vertical or horizontal orientation. Kubota, Inc manufactures a system of submersible flat sheet membranes.

Table 9 provides a rough order or magnitude capital cost estimate for a MBR system designed to treat an average daily wastewater flow of 45,000 gallons per day. In addition to the MBR treatment equipment, an equipment cost estimate for a sludge press has also been included in the estimate. Note that the costs listed in Table 9 are for equipment only. Additional costs for engineering, construction and startup would also be incurred.

Table 9 - ROM Equipment Cost Estimate for a 45,000 gpd MBR Wastewater Treatment System

Description	Quantity	Units	Unit Cost	Total Cost
Fine Screen	1	Each	$25,000	$25,000
Sreenings Chute and Hopper	1	Each	$5,000	$5,000
Sreenings Transfer Pump w/spare	2	Each	$3,000	$6,000
Equalization Basin (30k gal)	1	Each	$38,000	$38,000
Blowers	2	Each	$6,000	$12,000
Level Sensors	2	Each	$5,000	$10,000
Screened Influent Transfer Pumps	2	Each	$12,000	$24,000
MBR Equipment Package (includes control system, blowers, membranes and membrane tank(s), process pumps and associated instrumenation for the MBR process)	1	Each	$500,000	$500,000
On-Line Suspended Solids Analyzer	1	Each	$5,000	$5,000
Effluent Holding Basin (4k gal)	1	Each	$8,500	$8,500
Effluent Transfer Pumps	2	Each	$3,000	$6,000
Effluent UV	1	Each	$20,000	$20,000
Effluent Flow Meter	1	Each	$5,500	$5,500
Sludge Holding Tank (4k gal)	1	Each	$8,500	$8,500
Sludge Transfer Pump w/spare	2	Each	$3,000	$6,000
Sludge Decant Pumps	3	Each	$1,500	$4,500
Sludge Flow Meter	1	Each	$5,500	$5,500
Sludge Press and Appurtenances (20-30% dry solids)	1	All Inclusive	$160,000	$160,000
Refrigerated Samplers	2	Each	$4,000	$8,000
Drain Pump/Sump	1	Each	$4,000	$4,000
Laboratory Equipment (oven, scale, kits, glassware, misc)	1	All Inclusive	$10,000	$10,000
TOTAL				**$871,500**

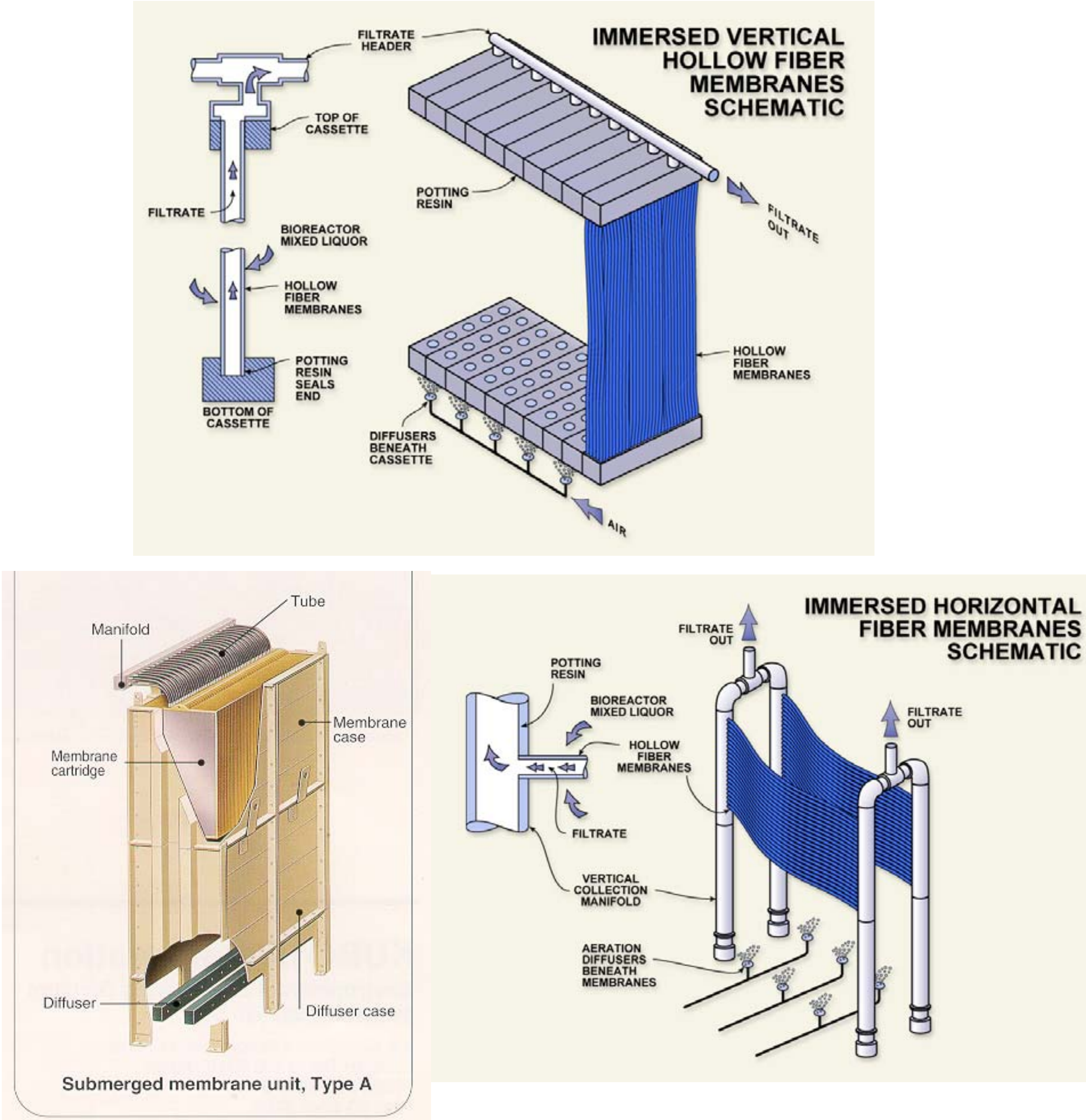

Figure 17 – Types of Membranes Commercially Available for Wastewater Treatment (Zenon, Inc. manufactures vertical immersed hollow fiber membranes. Mitsubishi, Inc. manufactures horizontal hollow fiber membranes, which are sold in the US market through Ionics, Inc. Kubota, Inc. manufactures immersed flat sheet membranes, which are sold in the US market through Enviroquip)

Produced Water and Wastewater Disposal Options

There are several potential disposal options for handling the water generated during hydrate production and the effluent from the wastewater treatment facilities. Reinjection of the wastewater and produced water into a separate formation will likely be the preferred option when available. Depending upon the type of reinjection technology used and the characteristics of the injection formation, little to no treatment may be required. In locations where reinjection is not feasible, surface discharge may be an option. Based on the anticipated water quality, treatment of the produced water would be required for surface discharge on the North Slope of Alaska. Finally, evaporation of produced water and wastewater is also an option for locations where neither reinjection nor surface discharge are options. The following sections summarize the technical and regulatory considerations for hydrate produced water disposal.

Reinjection

In reinjection, water produced during hydrate generation is pumped into a formation isolated from the hydrate-bearing zone. Since produced water from hydrate reserves is anticiapted to contain only dissolved salts and gasses and limited suspended solids, the feasibility of reinjection depend upon the proximity of a suitable formation to the hydrate-bearing strata.

Regulatory Considerations

Water generated during hydrate production is waste uniquely associated with the production of natural gas from hydrate reserves and as such, it should be classified as an exempt from regulation under Subtitle C of the Resource Conservation and Recovery Act (RCRA). Reinjection of this produced water would be regulated under the Underground Injection Control program of the Safe Drinking Water Act. Hydrate related produced water could be injected into a Class II D disposal well. Injection of produced water in a Class IID well will require demonstration that the practice will not adversely impact any underground sources of drinking water.

Injection Technology

Reinjection of produced water can be accomplished using surface reinjection pumps or down hole injection systems. Surface injection pumps require that produced water be lifted to the surface, treated to remove dissolved gasses and suspended solids if necessary, and then reinjected into a separate formation.

Down hole injection systems utilize pumps located in the production well bore to separate produced water and reinject this fluid into a deeper formation. Down hole technology eliminates the need to lift produced water to the surface and the associated handling costs and environmental issues. Hand et al. (1999), in a technical evaluation of down hole injection technology for the Gas Research Institute, indicated that gas wells that are proximate to the injection zone and have minimal sand production and tendency to scale are good candidates for down-hole injection technology. Down-hole gas/water separation technologies were determined to be economical in wells that generate 25-50 barrels of produced water per day and have produced water disposal costs of more than $1/barrel.

Hand et al. (1999) evaluated 4 types of down hole pumping equipment. Bypass tools (see Figure 17) allow produced water to flow from the formation and accumulate in the casing-tubing annulus. The pump draws water into the pump chamber during the upstroke, pushes it through the standing valve and into the tubing. The standing valve acts as a check on the pump downstroke preventing the water from draining out of the tube. When sufficient hydrostatic head has accumulated in the tube, the produced water drains into the injection formation by gravity. Bypass tools typically pump between 200 and 400 barrels of water per day.

Modified plunger rod pumps draw water into the pump barrel during the upstroke and then discharge the barrel contents into the disposal formation located below the production zone. Modified plunger pumps typically move between 800 and 1000 barrels of water per day. Electric submersible pumps and progressive cavity pumps can also be located down hole.

Surface Discharge

In circumstances where produced waters must be surface discharged, the major components of concern will likely be dissolved salts. Consequently treatment technologies to reduce the salt content will constitute the primary unit process in a treatment train.

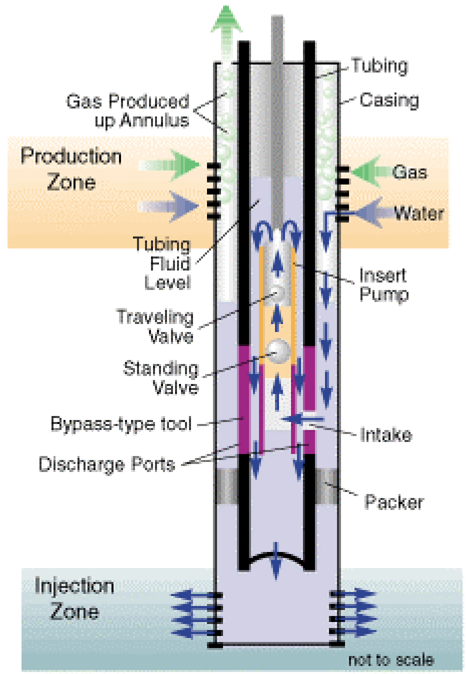

Figure 17 - Schematic of a Down-Hole Bypass Pump (From Hand et al. , 1999).

Regulatory Considerations

If treated produced water is to be discharged onto the tundra or into North Slope waterbodies, permits will be required from Alaska Department of Natural Resources (DNR), Alaska Department of Fish and Game (ADF&G), and Alaska Department of Environmental Conservation (ADEC). A DEC official (Kukla 2002) explained that all three agencies will likely grant a discharge permit if the effluent meets the Alaska Water Quality Standards stipulated in 18 AAC 70. Unless a variance is authorized, effluent water will be required to satisfy the most stringent standard applied for water use classes 1(A) and 1(b), water supply and water recreation respectively. The applicable standards and most stringent use classification are listed in Table 2.

The Alaska Water Quality Standards do provide for the utilization of mixing zones, as described in 18 AAC 70.240 through 18 AAC 70.270. Consequently, discharge waters could potentially exceed the standards listed above within a freshwater mixing zone, provided an appropriate permit is obtained.

Table 9 – Alaska Water Quality Criteria

Standard	Criteria	Class
Dissolved Oxygen	Not less than 7.0 mg/l.	1(A)iii
pH	Not less than 6.5 or greater than 8.5. Must not alter baseline by more than 0.5 units.	1(A)iii
Turbidity	Not greater than 5 NTU above baseline when baseline is 50 NTU or less. Not greater than 10% above baseline for baselines greater than 50%, not to exceed a maximum increase of 15 NTU. Not greater than 5 NTU increase in lakes, regardless of baseline.	1(B)i
Temperature	May not exceed 15 degrees Celcius.	1(A)i
Dissolved Inorganic Substances	TDS from all sources may not exceed 500 mg/l. Neither chlorides nor sulfates may exceed 250 mg/l.	1(A)i
Sediment	No measurable increase in settleable solids above baseline conditions, as determined by Imhoff cone method.	1(A)i
Toxic and Other Deleterious Organic or Inorganic Substances	Standards may not exceed Alaska Drinking Water Standards (18 AAC 80), or where those standards do not exist, EPA *Quality Criteria for Water*	1(A)i
Color	May not exceed 15 color units or the natural condition, whichever is greater	1(A)i
Petroleum Hydrocarbons, Oil and Grease	May not cause a visible sheen upon the surface of the water	1(A)i
Radioactivity	May not exceed Alaska Drinking Water Standards (18 AAC 80): Gross alpha radioactivity (including ^{226}Ra, but excluding Rn and U): 15 pCi/l; Combined ^{226}Ra and ^{228}Ra: 5 pCi/l; ^{90}Sr: 8 pCi/l; Tritium: 20,000 pCi/l; Gross beta radioactivity: 4 mrem. Also may not exceed standards in 10 CFR 20, or National Bureau of Standards Handbook 69.	1(A)i
Residues	May not, alone or in combination with other substances or wastes, make the water unfit or unsafe for the use, cause a film, sheen, or discoloration on the surface of the water or adjoining shorelines, cause leaching of toxic or deleterious substances, or cause a sludge, solid, or emulsion to be deposited beneath or upon the surface of the water, within the water column, on the bottom, or upon adjoining shorelines.	1(A)i

*Table exerpted from 18 AAC 70.020

If tundra discharge is determined to be a viable disposal option and large-scale disposal is planned, it is possible to petition for inclusion onto the National Pollutant Discharge and Elimination System (NPDES) General Permit for North Slope oil and gas extraction facilities (NPDES Permit # AKG-31-0000). An EPA official familiar with the permit indicated that although inclusion of tundra discharge is indeed possible, the negotiated standards would likely be similar to the standards stipulated by the Alaska water quality standards (Godsey 2002).

Evaporation

Evaporation represents a potential mass reduction technique for produced waters and wastewaters at North Slope well sites. The primary benefit of employing evaporation is that it allows for the possibility of near zero waste discharge. Additionally, a clear advantage to evaporation techniques is that the fuel necessary to drive the process can be readily obtained from gas produced at the wellhead.

The quantity of fuel required to evaporate wastewaters (produced, industrial, or domestic) will likely dictate the cost effectiveness of the process. It was stated previously that an ideal Structure I hydrate will produce approximately 0.78 ft^3 of water per 179 ft^3 of methane (229 ft^3 methane/ ft^3 water at 60 °F). As the hydrate numbers of naturally occurring hydrates are most often between 6 – 8, a natural system will likely produce between 165 – 220 ft^3 methane/ ft^3 water (assume 189 ft^3 methane/ ft^3 water).

Assuming a 100% efficient evaporation system, it would require approximately 68 ft^3 methane/ ft^3 water, or 36% of the total gas produced, to completely evaporate all of the associated hydrate water. Assuming a process efficiency of 70% (a frequent manufacturer's claim), 98 ft^3 (52% of total) would be required to totally eliminate the hydrate water from a well producing 189 ft^3 methane/ ft^3 water.

As the amount of methane necessary to evaporate hydrate waters constitutes a large fraction of the methane produced at any given well, evaporation only becomes cost effective if the volume of hydrate waters requiring disposal is significantly less than the theoretical volume of water dissociated during production. If the volume of connate water actually retrieved is less than the amount dissociated, then evaporation could be weighed against re-injection, filtration, or offsite disposal as a treatment option. If, on the other hand, large volumes of connate waters were retrieved, then evaporation could be used in conjunction with membrane systems to reduce the waste volume to a minimum. This multi step waste reduction process could be optimized to maximize cost savings resulting from lower disposal costs of reduced waste volumes.

Commercial evaporative treatment systems vary considerably by mechanism, design, capacity, and cost.

- Forced air type evaporators (e.g. Synthermic Wastewater Evaporator) are relatively energy efficient, as they rely on atmospheric input to overcome the latent heat of vaporization. Such systems would not likely be effective on the North Slope, however, due to the extremely cold temperatures.

- Steam pipe evaporators (e.g. Landa Water Blaze) force hot gasses through a water filled evaporation chamber. Due to the presence of hot gas bubbles in the liquid, the heat transfer efficiency of these systems is theoretically higher than efficiencies for bottom heated or submersed coil type systems. Although boiler-type systems (e.g. steam pipe, bottom heated, or submersed coil) require more energy than forced air evaporators in order to overcome the latent heat of vaporization, boiler systems are less dependant on atmospheric conditions. Corrosion can be a problem in any boiler type system, as the increased temperatures tend to amplify the corrosive effects of the fluids.

- Thermal oxidation systems (e.g. Thermo Oxidizer) subject an atomized flow stream to an open flame, thus vaporizing the stream and elevating the steam temperature to 800 – 1200 °C. The primary advantage of this type of system is that solids in the influent fluids are reduced to a dry ash. Additionally, dissolved components (e.g. methane, TPH, etc.) are oxidized in the process, thus minimizing hazardous stack emissions. Finally, corrosion is theoretically minimized in these systems compared to boiler systems, as there is no requirement for hot liquid water to be in contact with metal surfaces. The primary disadvantage of such systems is that energy is consumed in raising the temperature of the steam, and consequently these systems require more energy that boiler type systems.

Geochemistry Related to Gas Hydrate Exploration and Development in the North Slope Permafrost Regions, Alaska

Review of geologic setting and occurrence of gas hydrates in the Prudhoe Bay-Kuparuk River areas

The focus of traditional exploration for both petroleum and gas hydrates focuses on subsurface traps and the play concept in sedimentary basins described according to tectonic style (Collett 1993). A play consists of prospects and fields with similar geology (reservoir, cap rock, style of trap). The general concept of a play is to use the characteristics of discovered accumulations to predict similar undiscovered accumulations. However, basing interpretations mainly on tectonic style may be somewhat limiting to the discovery of new play types especially related to methane gas hydrates that exist in the North Slope because little is known about the geologic parameters controlling their distribution(Collett 1993).

Direct evidence for gas hydrates on the North Slope of Alaska comes from a core test and other indirect evidence comes from drilling and open-hole well logs that suggest many gas hydrate layers in the area of Prudhoe Bay and Kuparuk River oil fields(Collett 1993). Other locations including the Mackenzie River Delta and the Arctic Islands have inferred gas hydrates as well(Judge 1988; Judge 1992). The combined data from arctic gas hydrate studies shows that in permafrost regions, gas hydrates may exist between a range of depths of 130 to 2,000 m (Kvenvolden 1993) Global estimates of the amount of natural gas in permafrost related hydrate deposits range from 5.0×10^2 to 1.2×10^6 trillion cubic feet (TCFG) (Kvenvolden 1993).

In the case of the North Slope gas hydrates, two plays have been identified as the Topset play and the Fold Belt play (Collett 1993). Both of these plays are generalized due to the lack of knowledge of the size and distribution of individual gas hydrate accumulations that may exist within each of the plays defined. Collett (1993) defines the Alaska gas hydrate province as an area extending 950 km from the Chukchi Sea on the west to the Canadian border on the east with a maximum width of 320 km with a total area of 140,000 km^2.

General Geology

Extensive studies of the geology and petroleum geochemistry of the northern Alaska region have been done by(Lerand 1973; Grantz 1975; Carman 1983; Bird 1987; Gyrc 1988). In summary the sedimentary rocks of northern Alaska are divided into three sequences, which indicate major episodes of tectonic development in the region as well as the lithologic characteristics (Collett, 1993). In terms of source area according to Lerand (1973) and application to northern Alaska by Grantz et al. (1975) the three sequences are the Franklinian (Cambrian through Devonian), the Ellesmerian (Mississippian to Lower Cretaceous), and the Brookian (Lower Cretaceous to Holocene).

According to Collett (1993), the only confirmation of natural-gas hydrates in the Alaska gas hydrate province was obtained in 1972 by ARCO and Exxon when a core containing gas hydrates was recovered. Well-log data from an additional 445 Alaska wells were examined for gas hydrate occurrences (Collett, 1993), which showed that gas hydrates occurred in approximately 50 of the surveyed wells. These wells have multiple gas hydrate units that range in thickness from 3 to 31 m. There appear to be six laterally continuous sandstone and conglomerate units to the east of the Kuparuk River production unit and to the west of the Prudhoe Bay production unit. In addition, there is evidence from open-hole logs that a large free-gas accumulation exists downdip below four (C-F) of the hydrate units. The total estimated gas hydrates excluding the associated free gas in the Prudhoe Bay-Kuparuk River is approximately 37 to 44 trillion cubic feet (at STP) (Collett, 1993).

Two gas hydrate plays have been defined for the northern Alaska region; the Topset play and the Fold Belt play. The Topset play consists of stratigraphic traps and sandstone reservoirs of Creatceous and Tertiary age and is indicated structurally as a clinaform sequence on seismic records, which are relatively undeformed rocks that exist north of the Brooks Range fold belt. These rocks are part of the Nanushuk Group and the Sagavanirktok Formation that include marine and nonmarine deltaic sandstone, siltstone, shale, conglomerate, and coal. The methane-hydrate stability zone is up to 1,000 m within the area of the Prudhoe Bay field and the northern offshore limit of the stability zone corresponds to the 50 m bathymetric contour. Reservoir rocks consist of sandstone and conglomerate with beds up to 20m and may account for up to 75% of the total gas-hydrate stability zone. Probable source rocks within the play are immature interbedded deltaic shales and mudstones. Below the stability zone are thermally mature gas sources, which likely contribute to the known gas-hydrate accumulations in the Prudhoe Bay-Kuparuk River area (Collett, 1993). Expected traps are mostly stratigraphic and are related to facies changes, or traps formed against small-displacement normal faults, both of which would provide only fair to poor conventional caps (Collett, 1993).

The Fold Belt play consists of anticlinal traps in Cretaceous and Tertiary sandstone reservoirs in the northern part of the Brooks Range fold belt. This play is sandwiched between the Brooks Range thrust belt to the south and the rocks of the undisturbed deposits of the Topset play. The Chukchi Sea borders on the west and the eastern border extends offshore to the 50-m bathymetric contour in the Beaufort Sea. The eastern part of the play exists in rocks of the Sagavanirktok and Canning Formations, Hue Shale, a pebble shale unit, and Kemik Sandstone. The western part of the play includes parts of the Nanushuk Group and Torok Formation. The methane-hydrate stability zone reaches a maxiumum thickness of about 500 m and only half of the play has appropriate thermal conditions for the existence of gas hydrates. Potential reservoirs are sandstone units of deltaic and shallow-marine environments with expected porosities of 5 to 20%. Source rocks include gas-prone shale units of the Nanushuk Group and the Sagavanirktok, Torok, and Canning Formations. These source rocks range from immature to mature. Fault-cored anticlines related to Brooks Range thrusting form traps in this play and updip stratigraphic pinchouts on the flanks of anticlines may provide traps as well. The shales likely provide fair to good seals, although due to faulting the effectiveness of these seals may be reduced.

Geochemistry

The four main areas of technological contributions of modern geochemistry to petroleum exploration include 1) petroleum systems and exploration risk, 2) biomarkers, isotopes, and multivariate statistics for genetic oil-oil and oil-source rock correlation, 3) calibrated three-dimensional (3D) basin modeling, and 4) controls on petroleum occurrence and composition related to secondary processes(Peters 2002). These four areas may be applied in some fashion to the exploration of methane gas hydrates since their sources are often related, however, the occurrence of on-shore methane hydrates in the North Slope permafrost regions of Alaska are generally much shallower than petroleum deposits and therefore will likely pose different problems.

Understanding the geochemical characteristics of gas hydrates and associated pore waters may lead to enhanced exploration and development techniques. Gas chemistry, pore water salinity, and isotopic composition of gases and water associated with gas hydrates are the current areas of interest related to developing and exploring for gas hydrates. Most of the literature focuses on marine gas hydrates because they have been studied more extensively than terrestrial gas hydrates. However, it is possible that some of the same principles used to understand marine gas hydrates could be related to terrestrial gas hydrates.

Gas Chemistry

Analyses of gas hydrates that have been recovered indicate that the gas composition is predominately methane (>99%) and biogenic. However, gas hydrates may contain mostly thermogenic gas or mixture of thermogenic and biogenic gases. Thermogenic gases generally migrate from deep reservoirs along structurally controlled paths and form gas hydrates within in the appropriate temperature-pressure regime that is controlled primarily by the presence of permafrost in the North Slope region. Biogenic gas produced by microbial activity generally forms at more shallow depths. Thermogenic and biogenic gases can be distinguished based on their carbon isotopic compositions. A $\delta^{13}C$ in methane of –60 per mil or lighter relative to PDB standard suggests microbial formation and $\delta^{13}C$ heavier than about –50 per mil indicates a thermogenic source(Kvenvolden 1993). This depletion in δ^{13} occurs as bacteria metabolize CO_2 and release CH_4 as a product. In marine sedimentary sections from DSDP cores the carbon isotopic composition of CH_4 and CO_2 increases with depth (ie. ^{12}C is depleted with depth). The range of δ^{13} CH_4 is from –94 permil to –66 permil and that for CO_2 is from –25 permil to –4 permil with almost parallel changes(Kvenvolden 1993). Analyses from a corehole (92GSCTAGLU) in the McKenzie River Delta show that that $\delta^{13}C$ values range from –89.94 to –77.96 per mil indicating a microbial origin (Dallimore and Collett 1995)

Pore Water Salinity and Isotopic Composition

As gas hydrates form and water molecules crystallize, ions in solution are excluded from the crystal structure through a process referred to as ion exclusion (Ussler and Paull 1995) This results in pore waters associated with gas hydrates becoming concentrated in ion salts. The results from 55 analyses of pore waters from the North Slope region collected between depths of 400 to 2000 m range in salinity from 0.5 to 19.0 parts per thousand (ppt) (Collett, 1993) with no apparent correlation between depth and salinity. Pore water salinity affects the stability zone of gas hydrates because the presence of salts lowers the freezing temperature of water and therefore shifts the stability to higher pressure and lower temperatures.

During gas hydrate decomposition, pore waters would tend to be diluted as pure water is released from ice in the hydrate phase. Therefore, distinct geochemical gradients may exist during production of gas hydrates, which may establish a chemical model for drilling hydrates because the gradients may depend on the distance to and the amount of gas hydrate rich areas in sediment. The same principle applies to the $\delta^{18}O$ composition of pore water. As hydrates form ^{18}O is preferentially included in the crystalline structure of the hydrate and therefore the pore waters become depleted in ^{18}O. Hence, as the gas hydrates dissociate the pore water becomes progressively enriched in ^{18}O. Therefore, another geochemical gradient may be established by the oxygen isotopic composition of the pore water as gas hydrates dissociate. This may also be used as a tool to indicate a relative amount of gas hydrate in a given sedimentary formation or layer. These concepts have been modeled as closed systems and indicate that pore water salinities will increase and become isotopically fractionated during hydrate formation and that during decomposition, the pore waters will be diluted and enriched in ^{18}O. However, the oxygen, hydrogen, and carbon fractionation factors in the methane-water-methane gas hydrate system are unknown and may lead to complications of applying the models (Ussler and Paull 1995).

Microbiology of Gas Hydrate Formations

The existence and activity of microorganisms in the deep subsurface is important in relation to gas hydrate research since these organisms are responsible for much of the gas formation, their activities affect the distribution and fate of gases, and their populations in strata adjacent to hydrate deposits may be useful as bioindicators of the presence of hydrates. Recent studies have determined that microorganisms are ubiquitous in the deep marine and terrestrial subsurface and that the biomass of these bacteria exceeds the sum of all other biomass on Earth including all marine and terrestrial plants and animals (Pedersen 2000). These bacteria are attached to soil and rock matrices and are free living in groundwater (Pedersen 2001; Haveman and Pedersen 2002). To date, boreholes have been drilled that exceed 10,000 m, but living bacteria have been found to depths slightly over 5000 m (Gold 1992; Huber, Huber et al. 1994). Deeper depths are restrictive to life due to intolerable temperatures. The highest temperature at which hyperthermophilic bacteria have been cultured is ~113°C (Stetter 1996) and temperature seems to set the ultimate limit for life in the subsurface. However, pore space can also limit the abundance of bacteria since compaction is severe at high pressures and sediment loads (Ingebritsen, Sanford et al. 2000). Since microorganisms are adept at utilizing a variety of energy sources, it is not surprising that they occupy virtually every niche on Earth that does not surpass their extreme limits.

Oceanic Environments

The sub-sea floor and underlying basement rocks have been studied in increasing detail since 1985 due to the technology afforded by the drilling ship JOIDES Resolution of the Ocean Drilling Program (ODP). Until these studied were initiated, it was thought that that microbial life was restricted to the upper few meters of sediments in the deep sea since early studies failed to detect culturable species (Morita and ZoBell 1955). Microbial life has been found to be abundant in deep-sea sediments and rocks (Wellsbury, Goodman et al. 1997; Fisk, Giovannoni et al. 1998) and these microorganisms appear to be actively involved in the weathering of these rocks (Thorseth, Furnes et al. 1995; Thorseth, Torsvik et al. 1995). Hence, the continued search for microbial life in deep-sea deposits and rocks is a priority of the ODP.

The accumulation of bacterial end products within sediments indicates that bacteria are active throughout the sediment column even when the sediments are hundreds to thousands of meters thick, and these products are direct precursors of bacterially produced methane (Kvenvolden 1995; Kvenvolden 1995). Culturing and molecular studies have demonstrated the abundance and diversity of bacteria within deep layers of deep-sea sediments (Wellsbury, Goodman et al. 2000; Marchesi, Weightman et al. 2001; Inagaki, Sakihama et al. 2002). Bacterial abundance in marine sediments as determined primarily by microscopic counts of cells stained with fluorescent DNA dyes were over 10^6 cells/cm^3 at depths exceeding 500 m below the sediment surface (Cragg, Wimpenny et al. 1990; Cragg, Parkes et al. 1992; Cragg 1994; Cragg and Parkes 1994; Parkes, Cragg et al. 1994; Cragg, Parkes et al. 1996; Wellsbury, Goodman et al. 1997; Cragg, Law et al. 1999; Parkes, Cragg et al. 2000). In addition, other evidence exists that a high biomass of microbial life occurs deep within sediments and that these populations are active including 1) the presence of high molecular weight DNA that can be amplified using molecular techniques (Rochelle, Cragg et al. 1994; Bidle, Kastner et al. 1999; Li, Kato et al. 1999; Vetriani, Jannasch et al. 1999; Lanoil, Sassen et al. 2001; LopezGarcia, LopezLopez et al. 2001; Marchesi, Weightman et al. 2001); 2) rapid growth of bacteria in mixed cultures (Getliff, Fry et al. 1992); 3) isolation of bacteria that are uniquely adapted to the deep-sea environment such as barophiles (Bale, Goodman et al. 1997; Barnes, Bradbrook et al. 1998), and; 4) rapid activities determined by growth and radiotracer techniques (Cragg, Parkes et al. 1992; Parkes, Cragg et al. 1994; Patching and Eardly 1997). In addition, rates of bacterial processes within deep sediment samples vary vertically with mineralogical and geochemical changes, suggesting that the measured activities reflect *in situ* activities (Cragg, Parkes et al. 1992; Parkes, Bale et al. 1995). Some of these deposits are millions of years old yet still support relatively active bacterial communities (Ingebritsen, Sanford et al. 2000). Bacterial abundance does decrease with depth and with sediment age, but these decreases are far smaller than what would be expected simply due to the age of the deposit, indicating that other sources of energy may be involved.

Continental Habitats

Less work has been conducted on continental boreholes, but considerable work has appeared including studies using appropriate aseptic technique to isolate subsurface bacteria without surface contamination. Diverse microbial communities exist down to the deepest levels studies (~3000 m) (Chandler, Li et al. 1997; Crozier, Agapov et al. 1999; Onstott, Phelps et al. 1999). Sediments and soil/rocks become anoxic with depth and much of the microbial communities discovered within these deep regions are comprised of anaerobic communities living at high temperatures and pressures. Cultured species can be salt tolerant and heat loving, and may be either fermenting or respiring species. Metal and sulfate-reducing, acetogenic, autotrophic, and methanogenic bacteria have been isolated among others (Kotelnikova and Pedersen 1998; Onstott, Phelps et al. 1999; Pedersen 2001; Haveman and Pedersen 2002). Deep subsurface bacteria are capable of significant weathering of rocks (Petsch, Eglinton et al. 2001). Presently there are two lines of thought regarding the source of energy for these deep bacteria, the degradation of organic matter originally produced near the surface and transported or buried to depth over time, or the *in situ* formation of hydrogen or other inorganic energy sources at depth (Gold 1992; Stevens and McKinley 1995; Pedersen 1997; Stevens and

McKinley 2000). Although it has been shown that hydrogen can be produced from water-granite interactions, the potential for this process to support significant life has been questioned (Anderson, Chapelle et al. 1998). However, recent data have shown that some igneous rocks can support active microbial hydrogen-utilizing methane-forming bacterial communities that lack input of significant electron donors from the surface (Chapelle, ONeill et al. 2002). It has been suggested that deep-sea sediments are able to support bacterial activities through the heat-driven generation of acetic acid from buried organic within the sediments (Wellsbury, Goodman et al. 1997). Hence, recalcitrant organic matter left over from material deposited millennia earlier can be converted to labile organic compounds later due to the heat within deep deposits. It is unknown if this mechanism occurs in continental deposits.

The deep subsurface harbors microbial communities with abilities to conduct a variety of processes including the complete recycling of elements (Krumholz, McKinley et al. 1997; Abdelouas, Nuttall et al. 2000; Fujita, Ferris et al. 2000; Colwell 2001; Fredrickson and Onstott 2001; Grossman and Desrocher 2001; Lovley 2001). Studies of deep sites for the storage of spent nuclear waste have lead to discoveries of active and diverse microbial communities in deep aquifers in the Fennoscandian Shield (Haveman and Pedersen 2002) and the Canadian Shield (Stroes-Gascoyne and Sargent 1998). It was also found that these bacteria are quite active *in situ* (Pedersen and Ekendahl 1992; Ekendahl and Pedersen 1994; Kotelnikova and Pedersen 1998). Molecular studies determined the vast diversity of bacteria within deep subsurface continental aquifers and rocks (Chandler, Li et al. 1997; Krumholz, McKinley et al. 1997; Chandler, Brockman et al. 1998), and interesting new species have been recovered (Kotelnikova, Macario et al. 1998; Motamedi and Pedersen 1998; Krumholz, Harris et al. 1999). Like marine sediment, pore space is limiting and affects the distribution and activity of subsurface bacteria (Pedersen 2001). The deep subsurface harbors microbial communities with abilities to conduct a variety of processes including the complete recycling of elements (Krumholz, McKinley et al. 1997; Abdelouas, Nuttall et al. 2000; Fujita, Ferris et al. 2000; Colwell 2001; Fredrickson and Onstott 2001; Grossman and Desrocher 2001; Lovley 2001)..

Effects of Hydrates on Microbial Populations

The presence of gas hydrates greatly affects the abundance, composition, and activities of bacterial communities. To date, interactions among hydrates, geochemical conditions, and microbial processes have only been ascertained in oceanic settings. However, it is clear that microbial life influences the formation of hydrates and vice versa. Hydrates that intersect the marine sediment-water interface at methane seeps can support complex animal and microbial communities that are similar in composition to submarine communities at hydrothermal vents. These seep communities are common in the Gulf of

Mexico and are fueled by methane and reduced sulfur species (Sassen, MacDonald et al. 1994; Sassen, DeFreitas et al. 1999). However, while hydrates that are located well within sediments do not support rich communities of animals, they do seem to support rich bacterial populations that are often unique compared to bacteria in sediments devoid of methane.

It has been estimated from isotopic studies that much of the methane confined in hydrates in the sea is of microbial rather than thermogenic origin (Galimov and Kvenvolden 1983; Waseda 1998). However, some sites, like those studied in the Gulf of Mexico, have hydrate deposits that are derived from both thermogenic and biogenic methane, and these may be separated (Sassen, Sweet et al. 1999). It has also been suggested that even deposits derived solely from thermogenic methane may contain methane that has been recycled through methanogenic bacteria to yield a redefined microbial isotopic signature (Coleman, Risatti et al. 1981; Sassen, MacDonald et al. 1994; Sassen, DeFreitas et al. 1999).

It is not surprising that studies of microbial communities in hydrate-containing sediments have often focused on methanogenic bacteria and all studies that have searched for methanogens have easily found them. In some cases, unique species of methanogenic bacteria have been discovered in hydrate-containing strata (Hinrichs, DeLong et al. 1999) and these bacteria differ markedly from those found in sediments situated directly above and below the hydrate stability zone (Thomsen, Finster et al. 2001). Isotopic data indicate that the bulk of methane in marine hydrates is from the bacterial reduction of CO_2 via H_2 oxidation as opposed to the formation of methane from the methanogenic fermentation of acetic acid (Wellsbury, Goodman et al. 1997). The latter process accounts for 67% of methane in most anaerobic habitats (Conrad 1999), but appears to be of less importance in these deep-sea sediments. It is also possible that methane formed in much deeper sediments moves into hydrate-forming regions. However, to date, data show that methane carbon in hydrates has an isotopic signature similar to CO_2 at those depths suggesting that hydrate methane is derived from methane generated within or near the hydrate stability zone (Ingebritsen, Sanford et al. 2000). However, the anaerobic oxidation of methane (discussed in detail below) can be several orders of magnitude more active than the *in situ* production of methane from H_2/CO_2 suggesting that most of the methane was derived from sites well away from the hydrate stability zone (Cragg, Rochelle et al. 1996).

Besides methanogenic bacteria, hydrate deposits also contain large populations of other bacteria typical of active marine sediments, i.e., methane-oxidizers, sulfate reducers, acetogenic bacteria, nitrogen transforming species, sulfur oxidizers, metal reducers, and a suite of fermentative species (Bidle, Kastner et al. 1999; Ingebritsen, Sanford et al. 2000; Lanoil, Sassen et al. 2001). Waseda (1998) suggested that the total organic carbon of adjacent sediments needs to be 0.8-2.3% by weight to supply sufficient methane to create a significant hydrate deposit and hydrate methane is derived from sediment organic carbon. This level of organic carbon is not uncommon even in rather deep sediments in the deep ocean (Berner 1982; Emerson 1987; Waseda 1998).

When the global deep ocean is examined, it is possible to generate a relationship between sediment depth and microbial parameters such as biomass or activity (Wellsbury, Goodman et al. 2000; D'Hondt, Rutherford et al. 2002) in which microbial processes tend to decrease with sediment depth. However, bacterial biomass and activity increase greatly within the hydrate-stability zone. In fact, it is becoming clear that microbial activities increase greatly at the base of hydrate-containing strata (Ingebritsen, Sanford et al. 2000; Wellsbury, Goodman et al. 2000; Lanoil, Sassen et al. 2001). Lanoil et al. (2001) found that bacterial abundance was low within hydrate samples that lacked any noticeable sediment particles, but that these populations contained a relatively diverse bacterial community yet only a few types of methanogenic bacteria. They did find that bacterial populations in sediments adjacent to hydrates were nearly three orders of magnitude more abundant than in the hydrate itself. Wellsbury et al. (2000) conducted a detailed study of the depth distribution of bacterial biomass and several types of microbial activities and found that bacteria were unusually abundant and active in strata immediately below the hydrate-containing region (determined from bottom-simulating reflection data (BSR)). In particular, rates of bacterial growth (from nucleic acid uptake measurements), methane formation, methane oxidation and sulfate reduction peaked just below the BSR. Cell abundances were 10-100 times higher than predicted from average depth distributions indicating the stimulation of bacteria just below the hydrate-stability zone. Hence, this region represents a biogeochemically dynamic zone in which a complete carbon cycle occurs. In addition, ODP sites with the highest amounts of hydrates and underlying free gas supported the largest and most active bacterial populations (Cragg, Parkes et al. 1995; Cragg, Rochelle et al. 1996). It is also interesting that acetic acid concentrations increase to extremely high levels (>10 mM) at and below the hydrate-containing zone in deep-sea sediments and this acetate is oxidized to methane and CO_2 (Wellsbury, Goodman et al. 1997; Wellsbury, Goodman et al. 2000). In fact, it their studies, acetate conversion to methane greatly exceeded the rate of methane formation from the oxidation of H_2 coupled to CO_2 reduction. The elevated rates of microbial activity within these sediments appears to be due to consumption of free gases just below the hydrate zone as opposed to the direct use of hydrate-associated methane (Wellsbury, Goodman et al. 1997; Wellsbury, Goodman et al. 2000; Lanoil, Sassen et al. 2001).

Anaerobic Methane Oxidation

One of the mot interesting and perhaps useful discoveries within hydrate-containing sediments is the active rate of anaerobic methane oxidation. Although the oxidation of methane by aerobic bacteria has been studied for decades, it has only been recently that details of the bacterial oxidation of methane in the absence of oxygen have become known. It was proposed nearly 30 years ago that vertical profiles of dissolved methane within marine sediments were due to the consumption of methane at the base of the sulfate reduction zone (Reeburgh 1967; Barnes and Goldberg 1976; Martens and Berner 1977; Reeburgh 1977; Reeburgh and Heggie 1977; Reeburgh 1980; Reeburgh 1982) according to the following reaction:

$$CH_4 + SO_4^{2-} \rightarrow HS^- + HCO_3^- + H_2O$$

It is well known that methanogenesis and sulfate reduction are mutually exclusive processes in nature since the microorganisms involved compete for the same growth substrates (Martens and Berner 1974). However, methane produced in deeper methanogenic strata does not diffuse to aerobic layer where it is consumed, but rather disappears near the base of the sulfate-containing region immediately above the methane production zone (Reeburgh and Heggie 1977). The fact that the anaerobic oxidation of methane is microbially mediated is supported by tracer experiments using ^{14}C-methane (Reeburgh 1980; Iversen and Blackburn 1981) and from stable isotope ratios of methane and CO_2 (Blair and Aller 1995; Popp, Sansone et al. 1995). In addition, lipid biomarkers of microbes within the zone of anaerobic methane oxidation tend to be unusually depleted in ^{13}C indicating that these bacteria are consuming isotopically light carbon such as biogenic methane (Hinrichs, DeLong et al. 1999; Orphan, House et al. 2001). Isotopically light lipids from both sulfate-reducing and methane-producing bacteria have been found (Elvert and Suess 1999; Boetius, Ravenschiag et al. 2000; Elvert, Whiticar et al. 2000; Pancost, Damste et al. 2000; Orphan, Hinrichs et al. 2001). Sulfate-dependent anaerobic methane oxidation probably occurs to some extent in all sediments, especially those that have sufficient sulfate to support the sulfate-reducing partner. Studies noted increased rates of sulfate reduction and degradation of radiolabeled methane occurring in samples collected from the base of the sulfate-containing layers suggesting that methane was a source of energy for this process (Devol and Ahmed 1981; Alperin and Reeburgh 1984; Alperin and Reeburgh 1985; Iversen and Jørgensen 1985; Alperin, Reeburgh et al. 1988; Blair and Aller 1995; Hansen, Finster et al. 1998). Recent studies have demonstrated in vivo the stochiometric reduction of sulfate to sulfide during the oxidation of methane (Nauhaus, Boetius et al. 2002). It appears that anaerobic methane oxidation occurs in freshwater environments too, including lakes and flooded rice paddy soils (Panganiban, Patt et al. 1979; Murase and Kimura 1994; Murase and Kimura 1994), and has been noted in salt lakes as well (Iverson, Oremland et al. 1987).

Although it has been assumed that sulfate-reducing bacteria were responsible for this anaerobic methane loss, no sulfate reducer has ever been isolated that has this capacity. It was suggested later that the anaerobic oxidation of methane was occurring via a cooperative effort between methane-producing and sulfate-reducing bacteria in which the methanogen acts in reverse and consumes methane followed by a transfer of electrons to a sulfate reducer that then reduces sulfate to sulfide (Hoehler, Alperin et al. 1994). This type of bacterial cooperation termed syntrophy (Biebl and Pfennig 1978) is similar to what has been studied for over 30 years involving interspecies H_2 transfer between cooperating bacteria (Bryant, Wolin et al. 1967). However, in classical syntrophy, the methanogenic bacterium accepts H_2 from the partner and then reduces CO_2 to methane. It appears that methanogenic species involved in syntrophy during anaerobic methane oxidation are consuming methane and donating electrons via some carrier to a sulfate reducer. It was first suggested that the carrier molecule was H_2 since reverse methanogenesis could yield the following reaction (Hoehler, Alperin et al. 1994):

$$CH_4 + 2H_2O \rightarrow CO_2 + 4\,H_2$$

This reaction, which is endergonic at standard temperature and pressure can be exergonic if the H_2 levels are maintained extremely low by the H_2-consuming partner, i.e.,:

$$SO_4^{2-} + 4H_2 + 2H^+ \rightarrow H_2S + 4H_2O$$

More recent studies have suggested that this reaction may not be energetically favorable and acetate transfer is more likely (Valentine and Reeburgh 2000). However, additional study of molecules that could potentially shuttle electrons between the methanogen and the sulfate reducer tends to rule out acetate as well and suggests that formate is a more likely shuttle molecule and that the two partners must be in close physical contact with each other for the process to generate sufficient energy for both (Sorensen, Finster et al. 2001). Despite the fact that it seems clear that anaerobic methane oxidation is due to a bacterial partnership, little is known of these organisms

Molecular studies have shown that bacteria, especially methanogenic and sulfate-reducing species that are dominant within the methane-oxidizing region in anoxic sediments are distinct compared to species located above or below this region (Hinrichs, DeLong et al. 1999; Orphan, Hinrichs et al. 2001; Orphan, House et al. 2001; Thomsen, Finster et al. 2001). The fact that these physiologic groups dominate further supports the notion that these two bacterial groups are responsible for anaerobic methane oxidation. The finding that they are unique species or even genera suggests that this process is unique and is well designed for bacterial survival when using a low energy yielding reaction in a distinct environment.

Further studies utilizing molecular probes have investigated micro-colonies of sulfate-reducing and methanogenic bacteria that show that the methane-producer (which is actually consuming methane in this instance and is therefore a methanotrophic bacterium) is located in a small group that is surrounded by sulfate-reducers on the outside (Boetius, Ravenschiag et al. 2000; Orphan, Taylor et al. 2000). Secondary ion mass spectrometry in which an ion beam is passed directly through a microbial aggregate demonstrated that the aggregate was extremely depleted in ^{13}C, indicative of methane oxidation (Orphan, House et al. 2001). These aggregates have been found in hydrate containing sediments and at the interface between the sulfate reduction and methane production zones in other sediments. Neither species involved has been isolated in culture, but they can be detected easily using molecular probes. The methanotrophic group has a unique ribosomal RNA sequence that tends to be found only in regions exhibiting anaerobic methane oxidation including sediments with gas hydrates.

Virtually nothing is known of microbiology of terrestrial hydrates and what types of microbial consortia are present, but it has been suggested that the terrestrial deposits may be comprised of a higher proportion of thermogenic methane than in their marine counterparts (Collett 1993; Kvenvolden 1995), but little is known of these hydrates. Whatever the source, it seems clear that a better understanding of bacterial populations associated with hydrates will prove useful in locating and retrieving hydrate gases since microbial communities seem to respond strongly to the presence of the hydrates or at least to the free gas trapped under them. Terrestrial sites are most certainly much more complicated than their marine counterparts since they are affected by a myriad of continental processes such as soil formation, tectonic forces and a complicated geology. Marine hydrates are located on or within marine deposits that have been accumulating for millennia. Although these latter deposits may change greatly over time due to physical, geochemical and climate conditions, they are still composed primarily of marine muds that exhibit predictable depth patterns. Continental deposits can be overlain by a variety of rock and soils types and are subject to extensive folding and compression. They are affected by lateral and vertical water movement and can be affected by both freshwaters and brines of varying ionic strengths and compositions. Hence, the microbial biogeochemistry of continental hydrate deposits may vary greatly from marine deposits, but they may also have many similarities. Terrestrial sites can still have significant sulfate contents (Collett 1997) and hydrate-containing regions may harbor stimulated microbial communities such as those responsible for anaerobic methane oxidation and acetate utilization.

Permafrost Bacteria

High latitude sites also contain tens to hundreds of meters of permafrost and this ice can bisect the hydrate stability zone. The frozen layer can maintain a record of past climate events including a frozen record of vegetation and presumably microbial communities. However, prolonged freezing probably selects for bacterial species that are the most resistant to long-term freezing (Friedmann 1994) and do not provide an unequivocal record of past population structure as might be expected from preserved spores or plant parts like pollen. However, permafrost samples have provided cells that are very ancient and do provide insights into past ecosystems (Gilichinsky, Vorobyov et al. 1992; Gilichinsky 1997; Wilson, Braddock et al. 1998). Frozen habitats have been largely ignored until the last few years and techniques for studying processes in permafrost are in their infancy (Finegold 1996). Electron microscopic analysis of permafrost that was up to 3 millions years old revealed the presence of intact, vegetative bacterial cells that were not frozen inside (Vorobyova, Minkovsky et al. 2001). These cells differed from those isolated from surface seasonally unfrozen materials in that they often exhibited surficial capsules that were unusually thick, probably for cell protection. Bacterial enzyme activities commenced immediately after thawing without a lag indicating that these activities were present *in situ*, and enzymes that are normally thought to be robust in soils were also found to be most active in permafrost (Vorobyova, Minkovsky et al. 2001). Interestingly, in very old permafrost, few bacterial spores are present and fungal biomass is high, but is mostly present as spore (Gounot 2001). Hence, the only cells that are viable *in situ* are bacterial. This is surprising since soils tend to contain large numbers of spores, yet these tend to disappear in permafrost.

The microbial biomass in permafrost can be quite high with 10^7 to 10^9 cells per gram even in samples that are millions of years old (Gilichinsky and Wagener 1995; Shi, Reeves et al. 1997; Vorobyova, Soina et al. 1997; Rivkina, Gilichinsky et al. 1998; Wilson, Braddock et al. 1998). Both aerobic and anaerobic bacteria are present and viable. Anaerobes tend to dominate in soils that were anoxic prior to freezing and vice versa (Rivkina, Gilichinsky et al. 1998). Although bacterial activity is greatly depressed at cold temperatures, studies have shown that bacteria are viable and metabolizing in samples as low as –20°C (Friedmann, Kappen et al. 1993; Rivkina, Friedmann et al. 2000). It is thought that viable bacteria in ancient permafrost are able to metabolize since even old and highly frozen soil still contains regions of unfrozen water (Ershov 1998). Hence, it is highly likely that deep permafrost like that found in N. Alaska would contain relatively high numbers of viable and metabolizing bacteria. One would expect that this bacterial activity would increase greatly in the deeper regions just below the permafrost layer and especially just below the hydrate stability zone that transects the base of the permafrost.

Recommendations for Future Research

1. Due to the lack of full-scale experience with produced water generated during hydrate production, experiments to determine the mass and flow rate of gas and water produced using various production techniques should be conducted once the hydrate well has been completed.

2. Extensive inorganic and organic analysis of the water produced during hydrate drilling and production should be conducted to provide fundamental information on produced water quality and how it can change during hydrate production. Recommended analysis includes major and trace elements, anions, and isotope analyses. The major and trace elements and ions will allow us to establish any geochemical signatures associated with the hydrates as well as provide essential supporting data for understanding the microbial activity. These signatures may include changes in salinity or changes in concentration of other elements that have not yet been investigated. In addition, the chemical composition of the water must be known in order to make any decisions about treatment and ultimate disposal of the water.

3. A careful analysis of all water uses on the hydrate exploration and production platform should be conducted. This analysis should include quantification of the volumes and flowrates and the associated water quality requirements for all processes used on site. The overall water balance generated from this analysis can then be used to develop appropriate strategies for treatment, reuse, reinjection and disposal of water generated on site.

4. Changes in the relative distribution of microbial species can potentially pinpoint the location of hydrate deposits in oceanic settings. This was exemplified by drastic increases in biomass and activity just below the hydrate-containing region. If this is also true in continental deposits then small samples of drilling materials can be investigated to determine the potential for hydrates to occur and perhaps even the size of the deposit in continental settings. Molecular phylogenetic and activity measurements within adjacent strata need to be investigated. These data, in conjunction with the isotopic measurements outlined above, may provide unique markers.

5. The acquisition of a continental core in northern Alaska provides a unique opportunity to investigate ancient bacteria in the Arctic. This would be the first opportunity to examine extremely old permafrost deposits in this manner and, together with geochemical information, could provide unique information on past climate history and the types of microorganisms that existed in the geologic past.

6. Oxygen and hydrogen isotopes may provide a useful tool in determining the rate of dissociation of hydrates during drilling. If gas hydrates and equilibrium pore water were removed from the subsurface, an initial oxygen and hydrogen isotopic composition from which to measure the relative changes in isotopic composition of pore water as the hydrates dissociate could be obtained. This application may help develop a model of hydrate dissociation that could be applied to other locations where there is potential to drill gas hydrates.

References

Abdelouas, A., E. H. Nuttall, et al. (2000). "Biological reduction of uranium in groundwater and subsurface soil." Sci. Tot. Environ. **250**(1-3): 21-35.

Alperin, J. J., W. S. Reeburgh, et al. (1988). "Carbon and hydrogen isotope fractionation resulting from anaerobic methane oxidation." Global Biogeochem. Cycles **2**: 279-88.

Alperin, M. J. and W. S. Reeburgh (1984). Geochemical observations supporting anaerobic methane oxidation. Microbial Growth on C-1 Compounds. R. S. Hanson. Washington, D.C., ASM**:** 282-289.

Alperin, M. J. and W. S. Reeburgh (1985). "Inhibition experiments on anaerobic methane oxidation." Appl. Environ. Microbiol. **50**: 940-945.

Anderson, R. T., F. H. Chapelle, et al. (1998). "Evidence against hydrogen-based microbial ecosystems in basalt aquifers." Science **281**(5379): 976-977.

Bale, S. J., K. Goodman, et al. (1997). "*Desulfovibrio profundus* sp. nov., a novel barophilic sulfate-reducing bacterium from deep sediment layers in the Japan Sea." Int. J. Syst. Bacteriol. **47**(2): 515-521.

Barnes, R. O. and E. D. Goldberg (1976). "Methane production and consumption in anaerobic marine sediments." Geology **4**: 297-300.

Barnes, S. P., S. D. Bradbrook, et al. (1998). "Isolation of sulfate-reducing bacteria from deep sediment layers of the Pacific Ocean." Geomicrobiol. J. **15**(2): 67-83.

Berner, R. A. (1982). "Burial of organic carbon and pyrite sulfur in the modern ocean: Its geochemical and environmental significance." Am. J. Sci. **282**: 451-473.

Bidle, K. A., M. Kastner, et al. (1999). "A phylogenetic analysis of microbial communities associated with methane hydrate containing marine fluids and sediments in the Cascadia margin (ODP site 892B)." FEMS Microbiol. Ecol. **177**: 101-108.

Biebl, H. and N. Pfennig (1978). "Growth yields of green sulfur bacteria in mixed cultures with sulfur and sulfate reducing bacteria." Arch. Microbiol. **117**: 9-16.

Bird, K. J., and Magoon, L.B. (1987). "Petroleum geology of the northern part of the Arctic National Wildlife Refuge, Northeastern Alaska." U.S. Geological Survey Bulletin **1778**: 324p.
Blair, N. E. and R. C. Aller (1995). "Anaerobic methane oxidation on the Amazon shelf." Geochim. Cosmochim. Acta **59**(18): 3707-3715.
Boetius, A., K. Ravenschiag, et al. (2000). "A marine microbial consortium apparently mediating anaerobic oxidation of methane." Nature **407**(6804): 623-626.
Bryant, M. P., E. A. Wolin, et al. (1967). "*Methanobacillus omelianskii*, a symbiotic association of two species of bacteria." Arch. Microbiol. **59**: 20-31.
Carman, G. J., and Hardwick, P. (1983). "Geology and regional setting of the Kuparuk oil field, Alaska." American Association of Petroleum Geologists Bulletin **67**(6): 1014-1031.
Chandler, D. P., F. J. Brockman, et al. (1998). "Phylogenetic diversity of Archaea and Bacteria in a deep subsurface paleosol." Microbial. Ecol. **36**(1): 37-50.
Chandler, D. P., S. M. Li, et al. (1997). "A molecular comparison of culturable aerobic heterotrophic bacteria and 16S rDNA clones derived from a deep subsurface sediment." FEMS Microbiol. Ecol. **23**(2): 131-144.
Chapelle, F. H., K. ONeill, et al. (2002). "A hydrogen-based subsurface microbial community dominated by methanogens." Nature **415**(6869): 312-315.
Coleman, D. D., J. B. Risatti, et al. (1981). "Fractionation of carbon and hydrogen isotopes by methane oxidizing bacteria." Geochim. Cosmochim. Acta **45**: 1033-1037.
Collett, T. S. (1993). "Natural gas hydrates of the Prudhoe Bay and Kuparuk River Area, North Slope, Alaska." The American Association of Petroleum Geologists Bulletin **77**(5): 793-812.
Collett, T. S. (1993). Natural gas production from arctic gas hydrates. The Future of Energy Gases: USGS Professional Paper 1570. D. G. Howell. Washington, USGPO**:** 299-311.
Collett, T. S. (1997). "Gas hydrate resources of northern Alaska." Bulletin of Canadian Petroleum Geology **45**(3): 317-338.
Collett, T. S., K. J. Bird, et al. (1988). Geologic interrelations relative to gas hydrates within the North Slope of Alaska. Menlo Park, CA, U.S. Geological Survey.
Collett, T. S., K. A. Kvenvolden, et al. (1990). "Characterization of hydrocarbon gas within the stratigraphic interval of gas-hydrate stability on the North Slope of Alaska, U.S.A." Applied Geochemistry **5**: 279-287.
Colwell, F. S. (2001). Constraints on the distribution of microorganisms in subsurface environments. Subsurface Microbiology and Biogeochemistry. M. Fletcher. New York, Wiley-Liss, Inc**:** 71-95.
Conrad, R. (1999). "Contribution of hydrogen to methane production and control of hydrogen concentrations in methanogenic soils and sediments." FEMS Microbiol. Ecol. **28**(3): 193-202.

Cragg, B. A. (1994). Bacterial profiles in deep sediment layers from the Lau Basin (Site 834). Proc. Scientific Results, ODP, Leg 153, Lau Basin. J. Hawkins. Texas A&M University, College Station, Odp**:** 147-150.
Cragg, B. A., K. M. Law, et al. (1999). "Bacterial profiles in deep sediments of the Alboran Sea, western Mediterranean, Sites 976-978." Proceedings of the Ocean Drilling Program: Scientific Results **161**: 433-438.
Cragg, B. A. and R. J. Parkes (1994). Bacterial profiles in hydrothermally active deep sediment layers from Middle Valley (NE Pacific), Sites 857 and 858. Proc. Scientific Results, ODP Leg 139, Middle Valley, Juan de Fuca Ridge. M. J. Mottl**:** 509-516.
Cragg, B. A., R. J. Parkes, et al. (1996). "Bacterial populations and processes in sediments containing gas hydrates (ODP Leg 146: Cascadia Margin)." Earth Planet Sci. Lett. **139**: 497-508.
Cragg, B. A., R. J. Parkes, et al. (1995). The impact of fluid and gas venting on bacterial populations and processes in sediments from the Cascadia Margin accretionary system (Sites 888-892) and the geochemical consequences. Proc. ODP, Sci. Results, 146 (Pt 1): College Station, TX (Ocean Drilling Programm). E. Suess**:** 399-411.
Cragg, B. A., R. J. Parkes, et al. (1992). Bacterial biomass and activity in the deep sediment layers of the Japan Sea, Hole 798B. Proc., scientific results, ODP, Legs 127/128, Japan Sea. K. Tamaki. Texas &Aamp;M University, College Station, Odp**:** 761-776.
Cragg, B. A., P. A. Rochelle, et al. (1996). "Bacterial populations and processes in sediments containing gas hydrates (ODP Leg 146: Cascadia Margin)." Earth Planet. Sci. Lett. **139**(3-4): 497-507.
Cragg, B. A., J. W. T. Wimpenny, et al. (1990). Bacterial biomass and activity profiles within deep sediment layers. Proc., scientific reports, ODP, Leg 112, Peru continental margin. E. Suess. UK distributors, IPOD Committee, NERC, Swindon, ODP Texas &Aamp;M University College Station**:** 607-619.
Crozier, R. H., P.-M. Agapov, et al. (1999). "Towards complete biodiversity assessment: an evaluation of the subterranean bacterial communities in the Oklo region of the sole surviving natural nuclear reactor." FEMS Microbiol. Ecol. **28**: 325-334.
Dallimore, S. R. and T. S. Collett (1995). "Intrapermafrost gas hydrates from a deep core in the Mackenzie River Delta, Northwest Territories, Canada." Geology **23**(6): 527-530.
Das, D. K. and V. Srivastava (1991). Application of a finite element model to hydrate reservoirs. International Symposium on Cold Regions Heat Transfer, Fairbanks, AK.
deBoer, R. B., J. J. H. C. Houbolt, et al. (1985). "Formation of gas hydrates in permeable medium." Geologie en Mijnbouw **64**: 245-249.

Devol, A. H. and S. I. Ahmed (1981). "Are high rates of sulphate reduction associated with anaerobic oxidation of methane?" Nature **291**: 407-408.
D'Hondt, S., S. Rutherford, et al. (2002). "Metabolic activity of subsurface life in deep-sea sediments." Science **295**(5562): 2067-2070.
Ekendahl, S. and K. Pedersen (1994). "Carbon transformations by attached bacterial populations in granitic groundwater from deep crystalline bed-rock of the Stripa research mine." Microbiology **140**: 1565-1573.
Elvert, M. and E. Suess (1999). "Anaerobic methane oxidation associated with marine gas hydrates: superlight C-isotopes from saturated and unsaturated C_{20} and C_{25} irregular isoprenoids." Naturwissnechaften **86**: 295-300.
Elvert, M., M. J. Whiticar, et al. (2000). "Archaea mediating anaerobic methane oxidation in deep-sea sediments at cold seeps of the eastern Aleutian subduction zone." Org. Geochem. **31**(11): 1175-1187.
Emerson, S., C. Stump, P.M. Grootes, M. Stuiver, G.W. Farwell and F.H. Schmidt. (1987). "Estimates of degradable organic carbon in deep sea sediments from 14C concentrations." **Nature 329:51-53.**
Ershov, E. D. (1998). General geocryology. Cambridge, Cambridge University Press.
Ershov, E. D. and V. Yakushev (1992). "Experimental research on gas hydrate decomposition in frozen rocks." Cold Regions Science and Technology **20**: 147-156.
Finegold, L. (1996). "Molecular and biophysical aspects of adpatation of life to temperatures below the freezing point." Adv. Space Res. **18**(12): 87-95.
Fisk, M. R., S. J. Giovannoni, et al. (1998). "Alteration of oceanic volcanic glass: Textural evidence of microbial activity." Science **281**(5379): 978-980.
Fredrickson, J. K. and T. C. Onstott (2001). Biogeochemical and geological significance of subsurface microbiology. Subsurface Microbiology and Biogeochemistry. M. Fletcher. New York, Wiley-Liss, Inc**:** 3-37.
Friedmann, E. I. (1994). Permafrost as microbial habitat. Viable microorganisms in permafrost. D. A. Gilichinsky. Pushchino, Institute of Soil Science and Photosynthesis, Russian Academy of Science**:** 21-26.
Friedmann, E. I., M. A. Kappen, et al. (1993). "Long-term productivity in the cryptoendolithic microbal community of the Ross Desert, Anarctica." Microb. Ecol. **25**: 51-69.
Fujita, Y., E. G. Ferris, et al. (2000). "Calcium carbonate precipitation by ureolytic subsurface bacteria." Geomicrobiol. J. **17**(4): 305-318.
Galimov, E. M. and K. A. Kvenvolden (1983). Concentrations of carbon isotopic compostion of CH4 an dCO2 in gas from sediments of the Blake Outer Ridge, Deep Sea Drilling Project Leg 76. Init. Res. DSDP, 76. R. E. Sheridan et al. Washington DC, U.S. Government Printing Office**:** 403-407.
Getliff, J. M., J. C. Fry, et al. (1992). The potential for bacteria growth in deep sediment layers of the Japan Sea, Hole 798B-Leg 128. Proc. Scientific Results, ODP, Legs

127/128, Japan. K. Tamaki. Texas A&M University, College Station, Odp**:** 755-760.
Gilichinsky, D. and S. Wagener (1995). "Microbial life in permafrost: a historical review." Permafrost Periglacial Processes **6**: 243-250.
Gilichinsky, D. A. (1997). Permafrost as a microbial habitat: extreme for Earth, favorable in Space. Instruments, Methods, and Missions for the Investigation of Extraterrestrial Microorganisms. R. B. Hoover, Proc. SPIE**:** 472-481.
Gilichinsky, D. A., E. Vorobyov, et al. (1992). "Long-term preservation of microbial ecosystems in permafrost." Adv. Space Res. **12**: 255-263.
Godsey, C. (2002). "Personal communication. Environmental Protection Agency. (907) 271-6561."
Goel, N., M. Wiggins, et al. (2001). "Analytical modelling of gas recovery from in situ hydrates dissociation." Journal of Petroleum Science and Technology **29**: 115-127.
Gold, T. (1992). "The deep hot biosphere." Proc. Natl. Acad. Sci. USA **89**: 6045-6049.
Gounot, A. M. (2001). Ecology of psychrophilic and psychrotrophic micro-organisms in cold and frozen soils. Permafrost response on Ecomonic Development, Environmental Security and Natural Resource. V. Melnikov. Amsterdam, Kluwer Academic**:** 543-551.
Grantz, A., Holmes, M.L., and Kososki, B.A. (1975). "Geologic framework of the Alaskan continental terrace in the Chukchi and Beaufort Seas. In: Canada's Continental Margins and Offshore Petroleum Exploration. C.J. Yorath, E.R. Parker, and D.J. Glass (eds.)." Canadian Society of Petroleum Geologists **Memoir 4**: 669-700.
Grossman, E. L. and S. Desrocher (2001). Microbial sulfur cycling in terrestrial subsurface environments. Subsurface Microbiology and Biogeochemistry. M. Fletcher. New York, Wiley-Liss, Inc**:** 219-248.
Gyrc, G. (1988). "Geology and exploration of the National Petroleum Reserve in Alaska, 1974 to 1982." U.S. Geological Survey Professional Paper 1399: 940p.
Hansen, L. B., K. Finster, et al. (1998). "Anaerobic methane oxidation in sulfate depleted sediments: effects of sulfate and molybdate additions." Aquat. Microb. Ecol. **14**(2): 195-204.
Haveman, S. A. and k. Pedersen (2002). "Distribution of culturable microoganisms in Fennoscandian Shield groundwater." FEMS Microbiol. Ecol. **39**: 129-137.
Hinrichs, K. U., E. F. DeLong, et al. (1999). "Methane-consuming archaebacteria in marine sediments." Nature **398**(6730): 802-805.
Hoehler, T. M., M. J. Alperin, et al. (1994). "Field and laboratory studies of methane oxidation in an anoxic marine sediment: evidence for a methanogen-sulfate reducer consortium." Global Biogeochem. Cycles **8**(4): 451-463.

Holder, G. D., P. F. Angert, et al. (1982). "A Thermodynamic Evaluation of Thermal Recovery of Gas from Hydrates in the Earth." Journal of Petroleum Technology **May**: 1127-1132.

Huber, H., R. Huber, et al. (1994). "Search for hyperthermophilic microorganisms in fluids obtained from the KTB pump test." Sci. Drill. **4**: 127-129.

Inagaki, F., Y. Sakihama, et al. (2002). "Molecular phylogenetic analyses of reverse-transcribed bacterial rRNA obtained from deep-sea cold seep sediments." Environ. Microbiol. **4**(5): 277-286.

Ingebritsen, A. E., W. E. Sanford, et al. (2000). "Recent studies on bacterial populations and processes in subseafloor sediments: A review." Hydrology J. **8**: 11-28.

Islam, M. R. (1994). "A New Recovery Technique for Gas Production from Alaskan Gas Hydrates." Journal of petroleum Science and Engineering **11**: 267-281.

Iversen, N. and T. H. Blackburn (1981). "Seasonal rates of methane oxidation in anoxic marine sediments." Appl. Environ. Microbiol. **41**: 1295-1300.

Iversen, N. and B. B. Jørgensen (1985). "Anaerobic methane oxidation at the sulfate-methane transition in marine sediments from the Kattegat and Skagerrak (Denmark)." Limnol. Oceanogr. **30**: 944-955.

Iverson, N., R. S. Oremland, et al. (1987). "Big Soda Lake (Nevada). 3. Pelagic methanogenesis and anaerobic methane oxidation." Limnol. Oceanogr. **32**: 804-814.

Judge, A. S. (1988). "Mapping the distribution and properties of natural gas hydrates in Canada (abs.)." Proceedings of the American Chemical Society Third Chemical Congress of the North American Continent, Toronto, Canada(abstract number 29).

Judge, A. S., and Majorowicz, J.A. (1992). "Geothermal conditions for gas hydrate stability in the Beaufort-Mackenzie area - The global change aspect." Global and Planetary Change **98**(2/3): 251-263.

Kamath, A., S. P. Godbole, et al. (1987). "Evaluation of the stability of gas hydrates in northern Alaska." Cold Regions Science and Technology **14**: 107-119.

Kamath, V. A., G. D. Holder, et al. (1984). "Three Phase Interfacial Heat Transfer During the Dissociation of Propane Hydrates." Chemical Engineering Science **39**(10): 1435-1442.

Kamath, V. A., P. N. Mutalik, et al. (1991). "Experimental Study of Brine Injection and Depressurization Methods for Dissociation of Gas Hydrates." SPE Formation Evaluation **December**: 477-484.

Kim, H. C., P. R. Bishnoi, et al. (1987). "Kinetics of Methane Hydrate Decomposition." Chemical Engineering Science **42**(7): 1645-1653.

Klauda, J. B. and S. I. Sandler (2001). "Modeling gas hydrate phase equilibria in laboratory and natural porous media." Ind. Eng. Chem. **40**: 4197-4208.

Kotelnikova, S., A. J. L. Macario, et al. (1998). "*Methanobacterium subterraneum*, a new species of Archaea isolated from deep groundwater at the Åspö Hard Rock Laboratory, Sweden." Int. J. Syst. Bacteriol. **48**: 357-367.

Kotelnikova, S. and K. Pedersen (1998). "Distribution and activity of methanogens and homoacetogens in deep granitic aquifers at Åspö Hard Rock Laboratory, Sweden." FEMS Microbiol. Ecol. **26**(2): 121-134.

Krumholz, L. R., S. H. Harris, et al. (1999). "Characterization of two subsurface H_2-utilizing bacteria, *Desulfomicrobium hypogeium* sp. nov. and *Acetobacterium psammolithicum* sp. nov., and their ecological roles." Appl. Environ. Microbiol. **65**(6): 2300-2306.

Krumholz, L. R., J. P. McKinley, et al. (1997). "Confined subsurface microbial communities in Cretaceous rock." Nature **386**(6620): 64-66.

Kukla, A. (2002). Alaska Department of Environmental Conservation. Personal communication. (907) 269-7523.

Kuuskraa, V. A., E. Hammershaimb, et al. (1983). Handbook of gas hydrate properties and occurence, U.S. Department of Energy.

Kuuskraa, V. A., E. Hammershaimb, et al. (1983). Conceptual Models for Gas Hydrates. Phase 1. Technical Directive 6. Final Report., Morgantown Energy Technology Center.

Kvenvolden, K. A. (1993). A primer on gas hydrates. The Future of Energy Gases: USGS Professional Paper 1570. D. G. Howell. Washington, USGPO**:** 279-291.

Kvenvolden, K. A. (1995). "Natural gas hydrate occurrence and issues." Sea Technol. **36**: 69-74.

Kvenvolden, K. A. (1995). "A review of the geochemistry of methane in natural gas hydrate." Org. Geochem. **23**(11-12): 997-1008.

Lanoil, B. D., R. Sassen, et al. (2001). "Bacteria and Archaea Physically Associated with Gulf of Mexico Gas Hydrates." Appl. Environ. Microbiol. **67**(11): 5143-5153.

Leitz, F. and B. Boegli (2001). Evaluation of the Port Hueneme Demonstration Plant: An analysis of 1 MGD reverse osmosis, nanofiltration, and electrodialysis reversal plants run under essentially identical conditions, U.S. Department of the Interior Bureau of Reclamation.

Lerand, M. (1973). "Beaufort Sea. In: Future petroleum provinces of Canada - Their geology and potential. R.G. McCrossen (ed.)." Canadian Society of Petroleum Geologists **Memoir 1**: 315-386.

Li, L. N., C. Kato, et al. (1999). "Bacterial diversity in deep-sea sediments from different depths." Biodivers. Conserv. **8**(5): 659-677.

LopezGarcia, P., A. LopezLopez, et al. (2001). "Diversity of free-living prokaryotes from a deep-sea site at the Antarctic Polar Front." FEMS Microbiol. Ecol. **36**(2-3): 193-202.

Lovley, D. R. (2001). Reduction of iron and humics in subsurface environments. Subsurface Microbiology and Biogeochemistry. M. Fletcher. New York, Wiley-Liss, Inc**:** 193-217.

Makogon, Y. F. (1981). Hydrates of Natural Gas, PennWell Publishing Company, Tulsa, Oklahoma.

Marchesi, J. R., A. J. Weightman, et al. (2001). "Methanogen and bacterial diversity and distribution in deep gas hydrate sediments from the Cascadia Margin as revealed by 16S rRNA molecular analysis." FEMS Microbiol. Ecol. **34**(3): 221-228.

Martens, C. S. and R. A. Berner (1974). "Methane production in the interstitial waters of sulfate depleted marine sediments." Science **185**: 1167-1169.

Martens, C. S. and R. A. Berner (1977). "Interstitial water chemistry of anoxic Long Island Sound sediments. 1. Dissolved gases." Limnol. Oceanogr. **22**: 10-25.

Morita, R. Y. and C. E. ZoBell (1955). "Occurrence of bacteria in pelagic sediments collected during the Mid-Pacific Expedition." Deep Sea Res. **3**: 66-73.

Motamedi, M. and K. Pedersen (1998). "*Desulfovibrio aespoeensis* sp. nov., a mesophilic sulfate-reducing bacterium for deep groundwater at Åspö Hard Rock Laboratory, Sweden." Int. J. Syst. Bacteriol. **48**: 311-315.

Murase, J. and M. Kimura (1994). "Methane production and its fate in paddy fields .7. electron accepters responsible for anaerobic methane oxidation." Soil Sci. Plant Nutr. **40**(4): 647-654.

Murase, J. and M. Kimura (1994). "Methane production and its fate in paddy soils. IV. Sources of microogansims and substrates responsible for anaerobic CH_4 oxdidation in subsoil." Soil. Sci. Plant Nutr. **40**: 57-61.

Nauhaus, K., A. Boetius, et al. (2002). "In vitro demonstration of anaerobic oxidation of methane coupled to sulphate reduction in sediment from a marine gas hydrate area." Environ. Microbiol. **4**(5): 296-305.

Onstott, T. C., T. J. Phelps, et al. (1999). "Observations pertaining to the origin and ecology of microorganisms recovered from the deep sufsurface of Taylorsville Basin, Virginia." Geomicrobiol. J. **14**: 353-383.

Orphan, V. J., K.-U. Hinrichs, et al. (2001). "Comparative analysis of methane-oxidizing archaea and sulfate-reducing bacteria in anoxic marine sediments." Appl. Environ. Microbiol. **67**: 1922-1934.

Orphan, V. J., C. H. House, et al. (2001). "Methane-consuming archaea revealed by directly coupled isotopic and phylogenetic analysis." Science **293**(5529): 484-487.

Orphan, V. J., L. T. Taylor, et al. (2000). "Culture-dependent and culture-independent characterization of microbial assemblages associated with high-temperature petroleum reservoirs." Appl. Environ. Microbiol. **66**(2): 700-711.

Pancost, R. D., J. S. S. Damste, et al. (2000). "Biomarker evidence for widespread anaerobic methane oxidation in Mediterranean sediments by a consortium of methanogenic archaea and bacteria." Appl. Environ. Microbiol. **66**(3): 1126-1132.

Panganiban, A. T., T. E. Patt, et al. (1979). "Oxidation of methane in the absence of oxygen in lake water semples." Appl. Environ. Microbiol. **37**: 303-309.
Parkes, R. J., S. J. Bale, et al. (1995). "A combined ecological and physiological approach to studying sulphate reduction within deep marine sediment layers." J. Microbiol. Methods **23**: 235-249.
Parkes, R. J., B. A. Cragg, et al. (1994). "Deep bacterial biosphere in Pacific Ocean sediments." Nature **371**(6496): 410-413.
Parkes, R. J., B. A. Cragg, et al. (2000). "Recent studies on bacterial populations and processes in subseafloor sediments: A review." Hydrogeol. J. **8**(1): 11-28.
Patching, J. W. and D. Eardly (1997). "Bacterial biomass and activity in the deep waters of the eastern Atlantic - evidence of a barophilic community." Deep Sea Res. Pt. I Oceanog. Res. **44**(9-10): 1655-1670.
Patil, S. L. (2002). Overview of Gas Hydrate Production Technology. SPE-AAPG Western Regional Meeting, Anchorage, Alaska.
Pedersen, K. (1997). "Microbial life in deep basaltic aquifers." FEMS Microbiol. Rev. **20**: 399-414.
Pedersen, K. (2000). "Exploration of deep intraterrestrial microbial life: current perspectives." FEMS Microbiol. Lett. **185**: 9-16.
Pedersen, K. (2001). Diversity and activity of microorganisms in deep igneous rock aquifers of the Fennoscandian Shield. Subsurface Microgeobiology and Biogeochemistry. M. Fletcher. New York, Wiley-Liss**:** 97-139.
Pedersen, K. and S. Ekendahl (1992). "Incorporation of CO2 and introduced organic compounds by bacterial populations in groundwater from the deep crystalline bedrock of the Stripa mine." J. Gen. Microbiol. **138**: 369-376.
Peters, K. E., and Fowler, M.G. (2002). "Applications of petroleum geochemistry to exploration and reservoir management." Organic Geochemistry **33**: 5-36.
Petsch, S. T., T. I. Eglinton, et al. (2001). "C-14-dead living biomass: Evidence for microbial assimilation of ancient organic carbon during shale weathering." Science **292**(5519): 1127-1131.
Popp, B. N., F. J. Sansone, et al. (1995). "Determination of concentration and carbon isotopic composition of dissolved methane in sediments and nearshore waters." Anal. Chem. **67**: 405-411.
Reeburgh, W. S. (1967). "An improved interstitial water sampler." Limnol. Oceanogr. **12**: 163-165.
Reeburgh, W. S. (1977). "Methane consumption in Cariaco Trench waters and sediments." Earth Plant. Sci. Lett. **28**: 337-344.
Reeburgh, W. S. (1980). "Anaerobic methane oxidation: rate depth distributions in Skan Bay sediments." Earth Planet. Sci. Letters **47**: 345-352.
Reeburgh, W. S. (1982). A major sink and flux control for methane in marine sediments: anaerobic consumption. The Dynamics of the Ocean Floor. F. T. Manheim. Lexington, MA, D.C. Heath and Co.**:** 203-218.

Reeburgh, W. S. and D. T. Heggie (1977). "Microbial methane consumption reactions and their effect on methane distributions in freshwater and marine environments." Limnol. Oceanogr. **22:1-9**.
Rivkina, E., D. Gilichinsky, et al. (1998). "Biogeochemical activity of anaerobic microorganisms from buried permafrost sediments." Geomicrobiol. J. **15**(3): 187-193.
Rivkina, E. M., E. I. Friedmann, et al. (2000). "Metabolic activity of permafrost bacteria below the freezing point." Appl. Environ. Microbiol. **66**(8): 3230-3233.
Rochelle, P. A., B. Cragg, et al. (1994). "Effects of sample handling on estimation of bacterial diversity in marine sediments by 16S rRNA gene sequence analysis." FEMS Microbiol. Ecol. **15**: 215-225.
Sassen, R., D. A. DeFreitas, et al. (1999). "Thermogenic gas hydrates and hydrocarbon gases in complex chemosynthetic communities, Gulf of Mexico continental slope." Org. Geochem. **30**(7): 485-497.
Sassen, R., I. R. MacDonald, et al. (1994). "Organic geochemistry of sediments from chemsynthetic communities, Gulf of Mexico slope." Geo.-Mar. Lett. **14**: 110-119.
Sassen, R., S. T. Sweet, et al. (1999). "Geology and geochemistry of gas hydrates, central Gulf of Mexico continental slope." Trans. Gulf Coast Assoc. Geol. Soc. **49**: 462468.
Shi, T., R. H. Reeves, et al. (1997). "Characterization of viable bacteria from Siberian permafrost by 16S rDNA sequencing." Microbial. Ecol. **33**(3): 169-179.
Sira, J. H., S. L. Patil, et al. (1990). Study of Hydrate Dissociation by Methanol and Glycol Injection. 65th Annual Technical Conference and Exhibition of the Society of Petroleum Engineers, New Orleans, LA.
Sloan, E. D. (1990). Chapter 7: Hydrates in the Earth. Clathrate Hydrates of Natural Gases. New York, Marcel Dekker.
Sorensen, K. B., K. Finster, et al. (2001). "Thermodynamic and kinetic requirements in anaerobic methane oxidizing consortia exclude hydrogen, acetate, and methanol as possible electron shuttles." Microbial Ecol. **42**(1): 1-10.
Stetter, K. O. (1996). "Hyperthermophilic procaryotes." FEMS Microbiol. Rev. **18**: 145-148.
Stevens, T. O. and J. P. McKinley (1995). "Lithoautotrophic microbial ecosystems in deep basalt aquifers." Science **270**: 450-454.
Stevens, T. O. and J. P. McKinley (2000). "Abiotic controls on H_2 production from basalt-water reactions and implications for aquifer biogeochemistry." Environ. Sci. Technol. **34**(5): 826-831.
Stroes-Gascoyne, S. and F. P. Sargent (1998). "The Canadian approach to microbial studies in nuclera waste management and disposal." J. Contam. Hydrol. **35**: 175-190.

Thomsen, T. R., K. Finster, et al. (2001). "Biogeochemical and molecular signatures of anaerobic methane oxidation in a marine sediment." Appl. Environ. Microbiol. **67**(4): 1646-1656.

Thorseth, I. H., H. Furnes, et al. (1995). "Textural and chemical effects of bacterial activity on basaltic galss: an experimental approach." Chem. Geol. **119**: 139-160.

Thorseth, I. H., T. Torsvik, et al. (1995). "Microbes play and important role in the alteration of oceanic crust." Chem. Geol. **126**: 137-146.

Ussler, W. and C. K. Paull (1995). "Effects of ion exclusion and isotopic fractionation on pore water geochemistry during gas hydrate formation and decomposition." Geo-Marine Letters **15**: 37-44.

Valentine, D. L. and W. S. Reeburgh (2000). "New perspectives on anaerobic methane oxidation." Environ. Microbiol. **2**(5): 477-484.

Vetriani, C., H. W. Jannasch, et al. (1999). "Population structure and phylogenetic characterization of marine benthic Archaea in deep-sea sediments." Appl. Environ. Microbiol. **65**(10): 4375-4384.

Vorobyova, E., N. Minkovsky, et al. (2001). Micro-organisms and biomarkers in permafrost. Permafrost response on Ecomonic Development, Environmental Security and Natural Resources. V. Melnikov. Amsterdam, Kluwer Academic**:** 527-541.

Vorobyova, E., V. Soina, et al. (1997). "The deep cold biosphere: facts and hypothesis." FEMS Microbiol. Rev. **20**: 277-290.

Waseda, A. (1998). "Organic carbon content, bacterial methanogenesis, and accumulation processes of gas hydrates in marine sediments." Geochem. J. **32**(3): 143-157.

Wellsbury, P., K. Goodman, et al. (1997). "Deep marine biosphere fuelled by increasing organic matter availability during burial and heating." Nature **388**(6642): 573-576.

Wellsbury, P., K. Goodman, et al. (2000). "The geomicrobiology of deep marine sediments from Blake Ridge containing methane hydrate (Sites 994, 995, and 997)." Proc. Ocean Drill. Prog.: Sci. Res. **164**: 379-391.

Wilson, G. S., P. Braddock, et al. (1998). "Coring for microbial records of Antarctic climate." Antarct. J U.S. 1996 Review **31**: 83-86.

Wittebolle, R. J. (1985). A laboratory facility for testing sediments containing gas hydrates. 4th International Offshore Mechanics and Arctic Engineering Symposium, Dallas, Texas.

Wittebolle, R. J. and D. C. Sego Analysis of a production well through sediments containing gas hydrates.

Yousif, M. H., H. H. Abass, et al. (1991). "Experimental and Theoretical Investigation of Methane-Gas-Hydrate Dissociation in Porous Media." SPE Reservoir Engineering **February**: 69-76.

DIRECT (832) 636-8879 • MAIN (832) 636-1000 • FAX (832) 636-8006 • E-MAIL keith_millheim@anadarko.com
ANADARKO PETROLEUM CORPORATION
1201 LAKE ROBBINS DRIVE • THE WOODLANDS, TX 77380
P.O. BOX 1330 • HOUSTON, TX 77251-1330

KEITH K. MILLHEIM
MANAGER
OPERATIONS, TECHNOLOGY AND PLANNING

June 18, 2002

Craig R. Woolard Ph.D.,P.E.
Associate Professor
University of Alaska Anchorage
School of Engineering
3211 Providence Drive
Anchorage, AK 99508

Re: UAA Gas Hydrate Research Proposals

Dear Dr. Woolard:

Anadarko Petroleum accepts your proposal of $30,544.00 for Phase I, "Fundamental and Applied Research on Water Generated during the Production of Gas Hydrates". Please go forward with your research on the above mentioned Phase.

We are aware that the additional Phases will come when the qualified individuals have been identified. At any time that you need to interface with us, David Copeland from our department will be glad to help you. His phone number is 832-636-3024

Regards,

Dr. Keith K. Millheim
Manager,
Operations, Technology & Planning

KKM/mal

cc: UAA Grants and Contracts Department
Department of Geology - Lee Ann Munk

Fundamental and Applied Research on Water Generated during the Production of Gas Hydrates

Research Proposal Prepared by:
Craig Woolard and Bill Schnabel, University of Alaska Anchorage, School of Engineering
LeeAnn Munk, University of Alaska Anchorage, Department of Geology
John Kennish, University of Alaska Anchorage, Department of Chemistry
Mark Hines, University of Alaska Anchorage, Department of Microbiology

Introduction

Anadarko Petroleum Corporation (Anadarko), Maurer Technology and Noble Drilling are conducting a 3-year Department of Energy project (DE-PS26-01NT41331) to drill, core and produce gas from hydrates on Alaska's North Slope. Anadarko and its project partners met with faculty from the University of Alaska Anchorage (UAA) on February 5, 2002 to explore potential areas of collaboration.

During that meeting, the composition, quantity and treatment/disposal of the water generated during gas hydrate production were identified as key issues in need of further study. This document is a proposal to provide research on water related issues. We recognize that research needs will change as the project team gains experience with gas hydrate exploration and production and as such, we have prepared a plan that contains short, medium and long term projects that can be funded in phases. The project consists of a short-term (Phase 1) study to collect background information on gas hydrate water quantity, composition and disposal options. The information collected in Phase 1 will be used to design a sampling and analysis plan for the core collected at the drill site. Finally, in Phase 3, we will conduct long-term studies on water related issues once the nature and scope of the required work has been clearly defined by the project team and UAA faculty.

A brief description of each project phase is provided in the following sections. A proposed schedule along with a firm budget for Phase 1 (and estimated budgets for Phase 2) have also been included. Brief resumes of key personnel have been included as an attachment.

Project Description

Phase 1 – Literature Review and Identification of Critical Water Related Issues

In the first phase of the project, faculty will work with UAA's research librarian to assemble a bibliography of previous research conducted on gas hydrate geology, drilling and core analyses as well as specific issues related to natural resource production on the North Slope. The literature will then be reviewed and summarized by an interdisciplinary team of UAA faculty to identify the critical water-related science and engineering issues involved in gas hydrate production on the North Slope.

The literature will be summarized in a report that will provide, at a minimum:

- A summary of the quantity and quality of water generated from gas hydrates.
- A summary of the available geochemical data (for water and sediments) from previous cores collected from the North Slope.
- A summary of literature related to the microbial production and use of methane from gas hydrates
- A summary of the water disposal regulations on the North Slope
- A summary of the water quality and quantity requirements for the construction of ice roads and surface discharge of water.
- A summary of potential treatment and disposal options for water generated during gas hydrate production.

The final report for Phase 1 will also identify knowledge gaps and potential long-term research opportunities. We anticipate that the Phase 1 report will serve as the basis for defining future University research activities for the remainder of the DOE project. A few examples of potential long-term research projects are included in the description of Phase 3.

Phase 1 will be conducted during the spring of 2002. Project deliverables will include a draft summary report and presentation of findings at the next advisory board meeting. A final report will submitted in June, 2002.

Phase 2 – Chemical Analysis of Core Samples

In Phase 2, an interdisciplinary team of UAA faculty will conduct analysis of the aqueous, solid and gas phases present in samples from the gas hydrate core collected during drilling. At a minimum, measurements will include a complete analysis of major and trace elements by inductively coupled plasma - mass spectrometry (ICP-MS) and by ion chromatography (IC) for the water and sediment samples. Organic constituents in the water, sediments and gas will be analyzed using gas chromatography-mass spectrometery (GC-MS). Additional important organic and inorganic constituents (e.g., isotopes) identified during Phase 1 will also be measured on core samples.

All analyses will be conducted in UAA's Applied Science, Engineering and Technology (ASET) Laboratory, a modern analytical facility capable of analyzing a broad range of inorganic and organic constituents in multiple matrices (A description of the ASET Lab is attached as an appendix to this proposal).

Phase 3 – Water Related Exploration and Production Studies

In Phase 3, research projects will be conducted to provide the project team with critical information on water related exploration and production issues. The project team will determine the nature and scope of these projects after a review of the Phase 1 and Phase 2 data. Some examples of long-term research projects include, but are not limited to:

- Development of a geochemical model using data from Phase 2 and various isotope analyses to determine the chemical equilibria that may exist between pore water and solids in the formation. Such a model will provide insights into the chemical reactions occurring within the formation which may aid in understanding the origin of the gas hydrates and exploration activities. For example, it may be possible to utilize hydrogen and oxygen isotope values to determine if the pore water and hydrate water are most similar to meteoric water, if the water has a different source such as pore water that has migrated from other geologic units, or if the water is some mixture of multiple sources Strontium isotopes can be used to determine if the water is a product of mixing of multiple sources and if dilution by meteoric water has occurred.

- Identification of microbial markers that indicate the location and extent of hydrate reserves.
- Bench, pilot and full scale testing of water treatment systems (if necessary) to treat water generated during the production of gas hydrates.
- Laboratory experiments on core samples to evaluate how various pressure and temperature regimes influence water and gas production quantities and rates.

A more comprehensive list of potential long-term research projects will be provided as part of the Phase 1 report.

Schedule

A tentative schedule for each project phase is summarized below. Phase 2 and Phase 3 project dates will depend upon the drilling program and the availability of core samples.

Phase 1 – Literature Review and Identification of Critical Water Related Issues

March 1, 2002 – Begin work
May 2002 – Presentation of findings at second advisory board meeting
June 15, 2002 – submission of final report, review of report by project team, development of long-term UAA research plan.

Phase 2 – Chemical Analysis of Core Samples

June 15, 2002 -July 15, 2002 – development and approval of core sampling and analysis plan
July 15, 2002 – December 1, 2002 (assumed date of core availability) – Development of sampling protocols and analytical quality assurance/quality control methods.
December 1, 2002 - April 1, 2003 (assumed) – Analysis of core samples in ASET lab.
April 1, 2003 – July 1, 2003 – Data reduction, analysis and report preparation.

Phase 3 – Water Related Exploration and Production Studies

June 15, 2002 – Adoption of UAA long-term research plan
June 15, 2002 – project completion – Data collection and report preparation for long-term studies conducted at UAA or on-site.

Budget

A firm budget for Phase 1 of the proposed project is provided in the attached table. Depending upon the number of core samples and the complexity of the analyzed, we anticipate that the Phase two budget could range from $50,000 to $150,000. Because the exact scope and duration of projects conducted during Phase 3 are unknown at this time, no estimates have been provided.

Budget - Phase 1		
Library Research Services	$	5,000
Salary, benefits and leave		
Craig Woolard	$	4,000
LeeAnn Munk	$	4,000
Bill Schnabel	$	4,000
John Kennish	$	2,000
Mark Hines	$	4,000
Total Direct Costs	$	23,000
University Indirect Costs (32.8% of direct costs)	$	7,544
Total Project Cost	$	30,544

Key Personnel

Five UAA faculty will be involved in Phase 1 of the proposed project. Craig Woolard will serve as the project manager. He and Bill Schnabel will be responsible for summarizing the environmental regulatory and water treatment/disposal issues for the final report. Mark Hines will be responsible for evaluating and summarizing the microbiological research related to gas hydrates. LeeAnn Munk will focus on geochemical research. John Kennish will provide a peer review of the final report and provide guidance on analytical methods and requirements for core analysis. Brief resumes of each investigator are provided as an attachment.

Appendix C-3

Permafrost Foundations and Their Suitability as Tundra Platform Legs

Prepared for Anadarko Petroleum Corporation

By Lynn Aleshire and Hannele Zubeck

February 10, 2003

University of Alaska Anchorage
School of Engineering
3211 Providence Drive
Anchorage, Alaska, 99508

ABSTRACT

Anadarko Petroleum Corporation (APC) requires Vertical Support Members (VSM's) to support its Tundra Platform. The Platform will be mobilized for the hydrate drilling project on Alaska's North Slope during the winter of 2002/2003. The VSM's must meet APC's requirements to adequately support the Platform and, after the project is complete, to leave behind little or no evidence of the foundation. Foundation design processes for the North Slope were reviewed as well as basic principles of frozen ground soil mechanics. A variety of permafrost pile design and installation possibilities were reviewed to make recommendations of practical VSM's to support the Platform.

TABLE OF CONTENTS

LIST OF FIGURES

LIST OF TABLES

INTRODUCTION

Background

Anadarko Petroleum Corporation (APC) has designed and developed the Tundra Platform that will serve as a land-based, all-season drilling platform for oil and gas exploration on Alaska's North Slope. Operation of the platform requires expeditious mobilization and demobilization without leaving any significant traces on the tundra.

The Tundra Platform requires 39 vertical support members (VSM's) to provide an adequate foundation for the horizontal operations surface. This Platform surface is designed to stand 14 feet (5 m) above the ground surface. The project design life is 2 years. During mobilization all of the VSM's must be installed and allowed to freeze back to provide adequate strength. After drilling is completed and the well is plugged and abandoned the horizontal members of the Platform are dismantled leaving the VSM's. The VSM's must then be removed with the goal of reusing them for the next drilling project.

Problem Statement

Designing the VSM's for this project presents several challenges. Axial design load for each of the VSM's is 667 kN (100 kips) with an anticipated bending moment of 68 kNm (600 kip-in).

While piles are routinely installed successfully as long-term foundations in permafrost they are not often inserted and then removed after only a few weeks. The design must allow for ease of removal.

Because there are so many piles required for the Tundra Platform the most economical design would call for the shortest piles possible. Shorter piles are cheaper, easier to transport and require less installation and removal time.

Design life for the Anadarko drilling projects is relatively short, less than 2 years, and thus pile-jacking due to frost heave cycles is not a critical design factor. Permafrost degradation from heat transfer is not a serious concern because the operations surface is an adequate height above the ground surface. Heat sources greater than 0.7 m above the ground surface have been found not to transfer the heat necessary to cause thermal degradation (Johnston, 1981). In addition to mobility, the important design factors are axial loads, primary creep and lateral loads.

Goals and Objectives

The purpose of this report is to describe different pile types, design methods, and installation methods in permafrost and evaluate their suitability as a foundation for the Tundra Platform. Based upon the results of this evaluation a course of action is recommended.

Scope of Work

This work will be accomplished by summarizing existing literature about piles in permafrost, considering new designs and methods, analyzing their suitability as Tundra Platform legs and formulating recommendations for future research.

DESIGN METHODS

The typical engineering design approach for foundations in permafrost is sketched in Figure 1. The primary determining factor is thaw stability of the soil. In other words, how does the soil behave throughout the seasonal freeze/thaw cycles? Stable soils are clean and granular without ice. They do not heave when frozen and do not subside when thawed. Most soils are classified as thaw unstable. Ice and fine-grained soils are very common in permafrost and, therefore, foundations are designed to accommodate their heaving and subsidence.

Once it is determined that a pile foundation is the best design choice the pile design follows a procedure outlined in Figure 2.

Piles carry loads in two different ways regardless of the installation method. They can mobilize adfreeze strength at the pile soil interface, which is analogous to a friction pile in warm soils, or they can utilize the shear strength of the soils (end bearing). Essential to any foundation in frozen ground is maintenance of the thermal regime, that is, the permafrost must be kept frozen and as cold as possible. Anadarko's Tundra Platform will not cause excessive heat to be added to the ground because it is elevated. It will also provide shade that is beneficial in keeping the thermal regime.

Pile Failure

Pile failure may be defined two ways:

1. Excessive creep displacement over the project life. An allowable cumulative movement of the foundation must be determined.

2. Sudden movement caused by failure of the soil in tertiary creep.

Creep

When frozen ground is subjected to a load it responds with instantaneous deformation followed by a time-dependent deformation. Very heavy loads will display a limiting strength (Andersland and Ladanyi, 1994). Model curves of the behavior of frozen soils under load are shown in Figure 3. The initial displacement, primary creep, is a very small portion of the total time and displacement. Secondary creep is the next part of the curve and is also called steady-state creep. The limiting strength of a soil is defined by the tertiary creep that always leads to failure. The pile may also fail in creep; the creep displacement exceeds the allowable displacement.

Johnston and Ladanyi (1972) visually examined the frozen soils, silty clays, surrounding grouted anchors which had been pulled out of the ground. They found two kinds of deformation: a thin zone of high shear strain at the soil-grout interface and an outer zone of uniform shear strain that decreased rapidly with distance from the anchor. They considered the former to be slip failure at the anchor-soil interface which coincides with the tertiary creep and failure. In other words it is visible evidence of the failure of the adfreeze bond under load. For slurried piles the failure will likely be between the pile and the slurry.

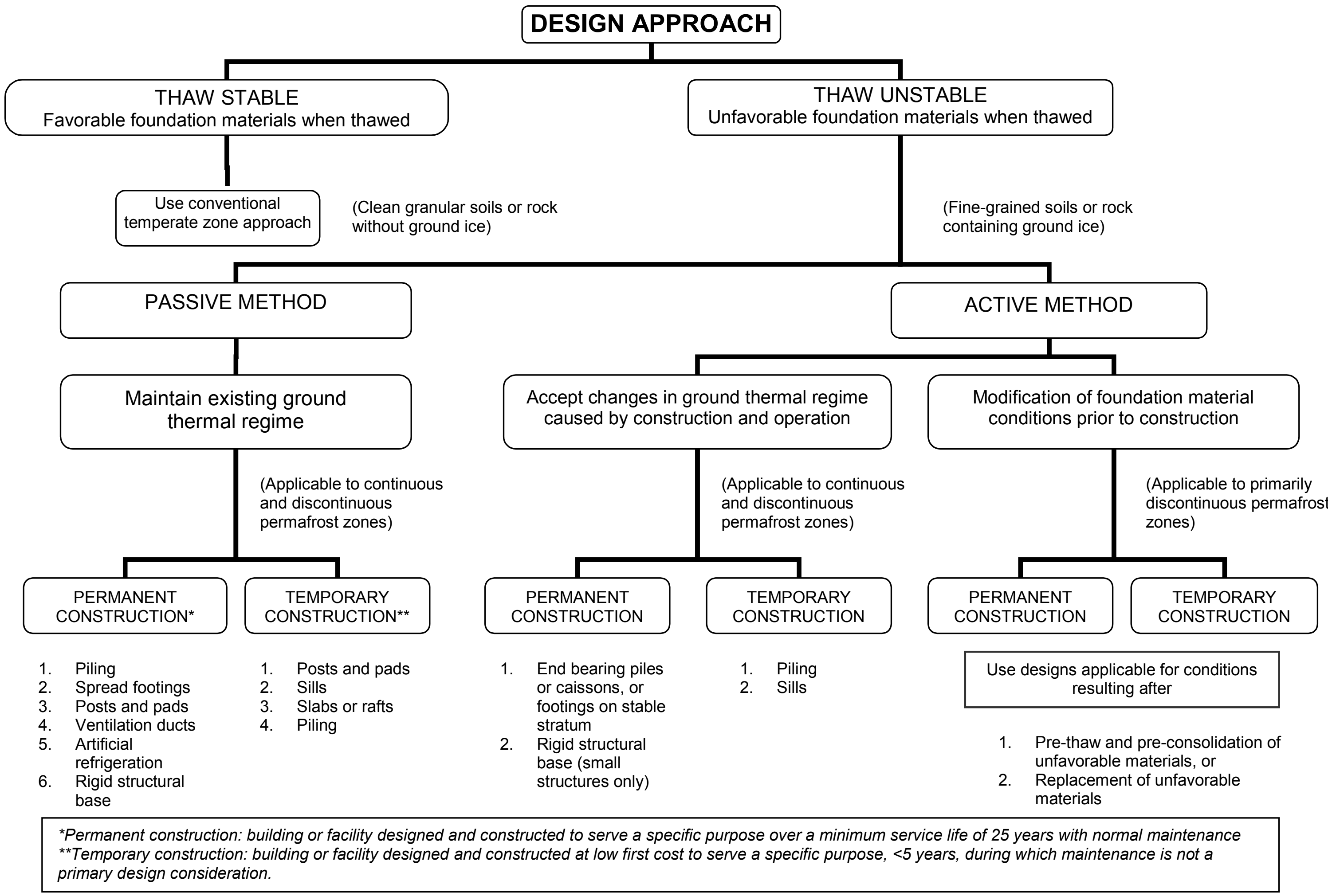

Figure 1 Foundation schemes for permafrost areas (modified from Linell and Lobacz, 1980)

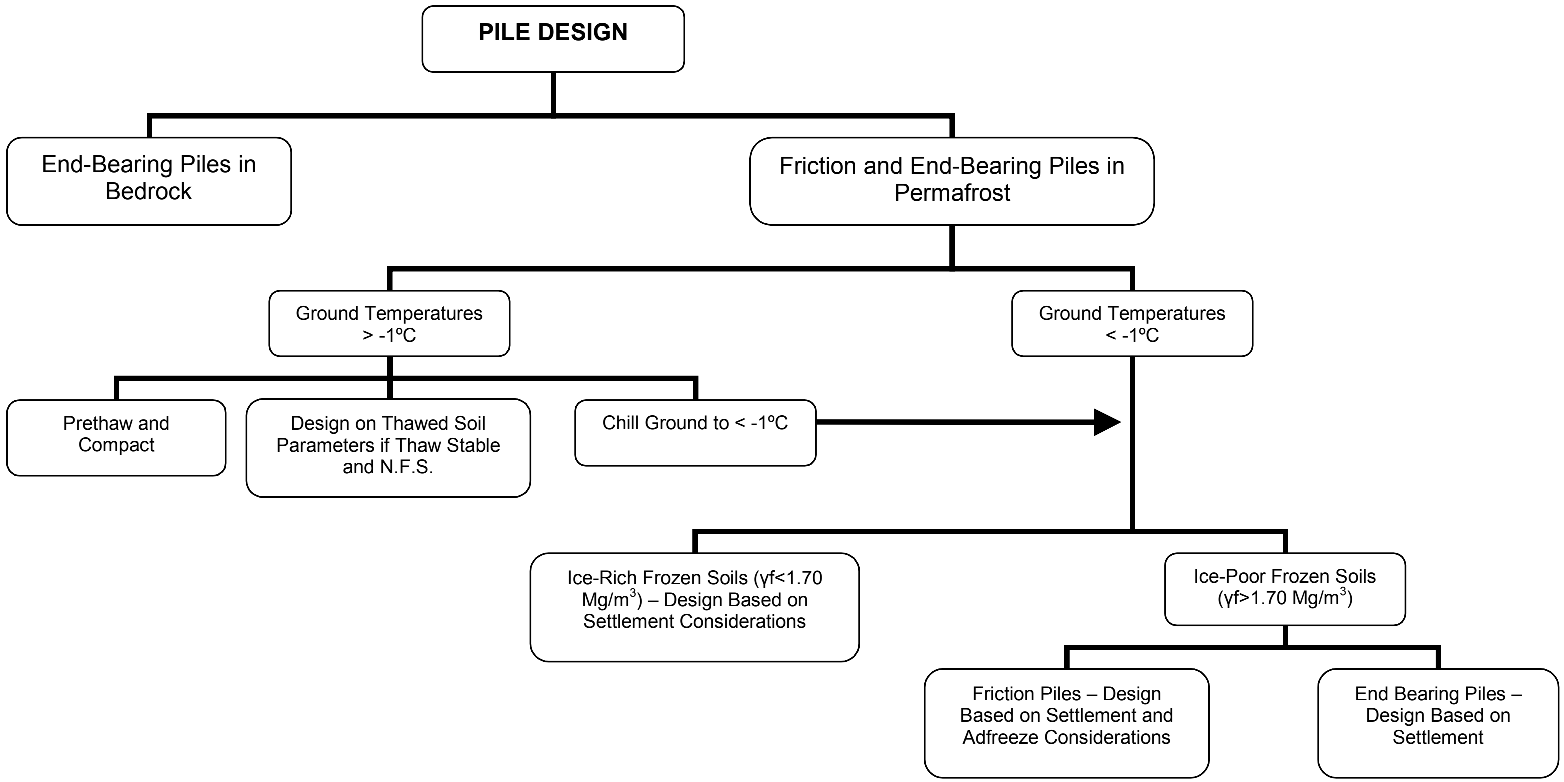

Figure 2 Pile design procedure for frozen ground (adapted from Weaver and Morgenstern, 1981)

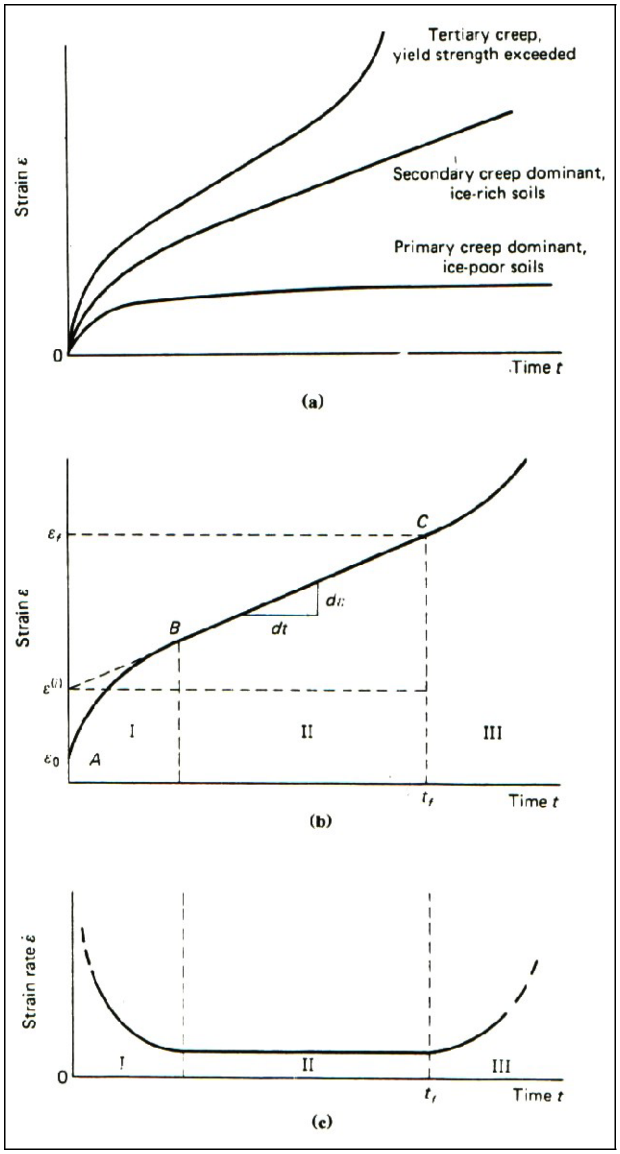

a) Creep-curve variations
b) Basic creep curve
c) True strain rate versus time

Figure 3 Model creep curves from constant-stress test (Andersland et al., 1978)

In design practice, the main concern is prediction of the displacement in secondary creep. Design load, allowable displacement and design temperature are required. Creep is directly related to ground temperature; displacement rates are much higher in warmer permafrost. Typically, predictions are made assuming ice-rich soils are present. Ice content of permafrost soils is highly variable within small areas. The presence of ice lenses and wedges is unpredictable and, therefore, a design based upon an ice-rich soil is conservative at best. For light structures, the resistance to pile jacking is the main concern.

There are numerous models used to predict creep in ice and ice-rich soils. Ladanyi (1972), Ladanyi and Johnston (1974), Nixon and McRoberts (1976), Nixon (1978), Morgenstern, Roggensack and Weaver (1980), Weaver and Morgenstern (1981), and Sego (1980) have each contributed to creep theory as it is practiced today and the reader is referred to these papers for a much more detailed discussion.

A result of the research listed above is the following equation (Equation 1) which predicts pile velocity in polycrystalline ice at temperatures below -1ºC assuming constant load. The constant, B, is temperature dependent and has been experimentally determined by Morgenstern et al (1980) and is defined by Equations 2 and 3.

Equation 1 $$\dot{u} = \frac{9}{2} aB\tau^3$$

Where: $\dot{u}$ *= pile velocity, (mm/yr)*

a = pile radius, (mm)

τ = constant shear stress, (kPa)

B = constant related to soil/ice structure and temperature, (kPa^{-3}/yr)

Equation 2 $$B = \frac{1.2x10^{-7}}{(1-T)^2} \text{ for } -2 < T \leq -1 \circ C$$

Equation 3 $$B = \frac{6x10^{-8}}{(1-T)} \text{ for } T \leq -2 \circ C$$

Using these three equations, curves can be generated to determine normalized pile velocity in terms of creep rate/year for various temperatures and loads (Neukirchner, 1984).

Adfreeze Design

Adfreeze forces are produced when the frozen ground bonds to the pile surface and resists movement due to the applied load. The magnitude of the adfreeze force is related to the surface area and roughness of the pile, soil type, and temperature.

There are several methods used to determine load capacity of a pile using adfreeze strength. All of these methods produce rough estimates of the adfreeze strength based upon experimental studies. For all adfreeze calculations the depth of the active layer does not contribute to the pile strength. In other words, the first several feet of soil that is the active layer is not included as part of the pile length.

An often used design method developed by Linell and Lobacz (1980), given in Figure 4,estimates strength as a function of temperature and applies various factors to compensate for pile roughness and soil types. It includes the correlation factors used to calculate load bearing capacity. “Sustainable” adfreeze strength relates to long-term adfreeze strength.

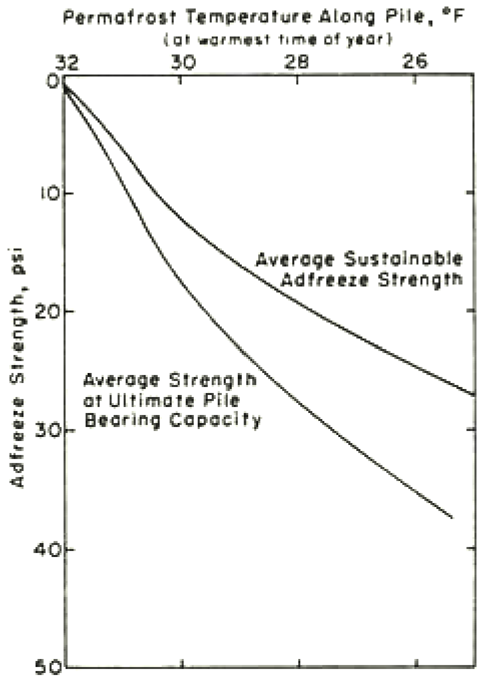

Tangential adfreeze bond strengths versus temperature for silt-water-slurried 0.22-m-O.D. steel pipe piles in permafrost, averaged over 5.50- to 6.40-m embedded lengths in permafrost. Correction factors for type of pile and slurry backfill (using steel in slurry of low-organic silt as 1.0).

Type of pile	Slurry soil	
	Silt	Sand
Steel	1.0	1.5
Concrete	1.5	1.5
Wood, untreated or light creosoted	1.5	1.5
Wood, medium creosoted (no surface film)	1.0	1.5
Wood, coal-tar-treated (heavily coated)	0.8	0.8

Notes:

1. Applies only for soil temperatures down to about -4°C (25°C).
2. Where factor is the same for silt and sand, the surface coating on the pile controls, regardless of type of slurry. In the remaining factors the pile is capable of generating sufficient bond, so that the slurry material controls.
3. Gradations typical of soils used for slurry backfill are as follows: silt—SFS, Fairbanks silt; sand—SM, McNamara concrete sand.
4. Pile load tests performed using 44.5 kN/day (10kips/day) load increment were adjusted to 44.5 kN/3 days (10 kips/ 3days) to obtain curves shown.
5. Clays and highly organic soils should be expected to have lower adfreeze bond strengths.

Figure 4 Adfreeze strength as a function of temperature (from Linell and Lobacz, 1980)

Another model that is commonly used on the North Slope was developed by the North Slope Task Group. It uses a step function to approximate increases in adfreeze strength with depth (ARCO, Sohio, et, al, 1982). Permafrost temperatures are assumed to be the highest encountered in the Prudhoe Bay area. It assumes a 100-year design life. Table 1 is a chart of the adfreeze design strengths developed by the North Slope Task Group. Pile capacity can then be calculated by multiplying the adfreeze strength by the surface area of the pile. This model does not consider pile roughness and the slurry properties.

Table 1 Adfreeze strengths as a function of depth and factor of safety (modified from ARCO Oil & Gas and Sohio, 1982)

Depth, m (ft)	Adfreeze Strength, kPa (psi)	
	F.S. = 2.0	F.S. = 3.0
0 to 2 (0 to 9)	15 (103)	10 (69)
2 to 4 (9 to 14)	20 (138)	15 (103)
>4 (>14)	25 (172)	20 (138)

Typically, end-bearing capacity is neglected in adfreeze designs. Linell and Lobacz (1980) considered piles backfilled with slurry to be friction piles with zero load at the tip. After reviewing long-term creep tests on frozen soils and proposed creep laws, Weaver and Morgenstern (1980) also concluded that end-bearing support is negligible for piles in all types of homogeneous permafrost. The fraction of load supported in end-bearing by a pile in frozen ground is less than 2%. However, both Ladanyi and Paquin (1978) and Sego (1980) determined experimentally that after settlement of 30% of the pile diameter there is some end-bearing capacity. The point resistance becomes proportional to the penetration rate. For low settlement rates, less than 1mm/yr, the end bearing is neglected.

Both driven piles and smooth freezeback piles are considered friction piles and are designed to carry their loads using the strength of the adfreeze bond.

Shear Strength Design

Piles can be designed with a helix or rings that change the way the pile mobilizes load-bearing capacity. Shear strength or bearing capacity of the frozen ground carries the load instead of adfreeze strength. Utilizing the soil shear strength greatly increases the allowable pile load. Estimates range from 3 to 7 times the adfreeze strength (Vialov 1959 and Newcombe 1973). As a result, screw piles can be much shorter than adfreeze piles.

Frozen soils are considered to be cohesive soils and, as described by Terzaghi (1943), the bearing capacity is dependent upon soil cohesion and the soil friction angle. Therefore, this type of design requires *in situ* soil analysis to obtain the required values. Ishlinskiy (1944) and Berezantsev (1949) developed the theoretical model for calculating bearing capacity, $P_{\lim}$, for two-dimensional circular footings as shown in Equation 4. Vialov (1959) compared the theoretical calculations with actual measurements of bearing capacity. Computed values compared favorably with measured bearing capacities. The bearing capacity equations produce the bearing length necessary to support the design load. The required helix length for the pile is calculated from the bearing length.

Equation 4 $$P_{\lim} \approx 5.65c_e + q$$

Where P_{lim} *=limiting stress of the soil (kg/cm²) or ultimate bearing capacity*

c_e*=measured value of soil cohesion which includes plasticity and internal friction angle (kg/cm²)*

$q = \gamma D_f$*, where* γ*=unit weight of the soil and* D_f*=depth of the footing*

PILE TYPES AND INSTALLATION METHODS

Driven Piles

Driven piles in permafrost are different from driven displacement piles used in warmer climates. Permafrost requires some type of preconditioning before any type of pile can be driven because of its strength and hardness. Original builders in cold regions used steam to thaw the frozen ground and then inserted the pile, usually timber, by gently driving it. Steam thawing is a process difficult to control; a uniform hole size is not easily obtained (Crory, 1982). The slurry produced by the thawing is forced to the surface during the driving process. Stones or rocks often displace piles driven in steam-thawed holes, as much as 300 mm (12 in), and then must be straightened by rethawing and wedging the pile until it freezes into place (Johnston, 1963).

According to Nottingham and Christopherson (1983) driven piles, usually steel pipe or reinforced H-piles, are inserted into thermally modified pilot holes. Piles cannot be driven efficiently at temperatures colder than –0.5 to -1.0°C (-31 to 30°C) without pilot holes. Holes are predrilled or augured at a diameter less than the pile and filled with a warm fluid to warm the soils. The undersized hole makes driving easier and control of vertical alignment is maintained. Piles are usually driven with impact or vibratory hammers. Driving rates range from 300 mm (1 ft) per minute for an impact hammer to 1,500 mm (5 ft) per minute for a vibratory hammer. If properly planned, installation rates for driven piles can be twice that of drilled and slurried piles. Driven piles require less freezeback time, typically less than 2 days, and thus can be loaded sooner (Nottingham and Christopherson, 1983).

ARCO Alaska conducted extensive testing and research and selected the thermally modified pile driving method as the fastest and most economical method of pile installation. As a result, all the piles installed for the aboveground oil pipeline in the Kuparuk Field were installed by this method. Recommended water temperature is 66°C (150°F) with a thaw time of 30 minutes for granular soils and 60 minutes for fine-grained soils. For the determination of adfreeze strengths, soil type is more important than installation method. Different methods produced comparable adfreeze strengths. However, piles driven in frozen gravelly soils indicate lower adfreeze values than ice-rich silty sands. The author suggested this is because gravelly soils are located near rivers and subject to warmer ground temperatures (Manikian, 1983).

Freezeback Piles

Freezeback piles, also called drill and slurry piles, are placed by drilling an oversized hole, inserting the pile, and backfilling with a sand or gravel slurry to fill annular voids while suspending the pile with a crane. Slurries are mixed according to ASTM standards.

Screw Piles

Screw piles, also called ring piles or helical piles, have rings or a helix added to the surface of the pile that are of a greater diameter than the pile itself. They are, therefore, utilizing shear strength rather than adfreeze. Screw piles are installed using the drill and slurry method and thus also require freezeback time before loading. Installation procedures must ensure that slurry is placed adequately in the helical portion of the pile.

Helical Piers

Helical piers have a 50 mm (2 in) shaft and typically a 200 or 250 mm (8 or 10 in) helix and are currently used as foundations in permafrost for light-weight structures. They are screwed into the permafrost with a backhoe or excavator with a rotation head. Usually a pilot hole is not necessary. However, if soils are very cold a pilot hole may be necessary along with extra weight on the rotating head when screwing in the pier. Using a factor of safety of 2.0, each pier can carry about 111 kN (25 kips) if the soil conditions permit. (Zubeck and Liu, 2002).

For the Tundra Platform project 4 helical piers would replace each VSM. They would be inserted at an angle with a common apex. A connection would then be made to a vertical member and then to the platform. This 4 member unit would supply the necessary strength for lateral loading as well as axial loading. Angular installation is very common in warmer soils where these devices are used also in tension as helical anchors.

Thermal Piles

Thermal piles or thermosyphons are VSM's that are self-contained passive two-phase liquid/vapor heat transfer units (Figure 6). They are widely used to maintain thermal regimes in permafrost. The heat transfer technology is also used for remediation of foundations that have failed because of permafrost degradation. Thermosyphons can significantly increase soil strength by reducing the soil temperatures.

Thermal piles can be smooth piles designed using adfreeze forces, but are more and more ring or helical piles utilizing soil shear strength. They are installed using the drill and slurry method. Freezeback times are reduced because the thermal pile increases the rate at which heat is removed from the soil.

EXPERIMENTAL FOUNDATION OPTIONS FOR TUNDRA PLATFORM

TPL-7

Anadarko along with Radoil Inc. have designed a pile specifically for its Tundra Platform, Figure 6. For the purposes of this report we will designate it TPL-7. Outside diameter (OD) of the pile in the 6.7 m (22 ft)-upper smooth portion is 0.35 m (13.625 in). Below that point the casing OD becomes 0.22 m (8.625 in); with the helix added the diameter of the lower portion of the pile becomes 0.334 m (13.135 in). Planned embedment depth is approximately 6.1 m (20 ft).

The large diameter of the upper portion is required to accommodate the expected moment caused by wind. This design was originally a helical pile that would mobilize the soil shear strength. Because of the increased diameter of the upper portion it is highly probable that the adfreeze strength will be mobilized before the shear strength and the helix will add any additional load capacity. A field test was conducted for the TPL-7 and is reported separately (Zubeck, et al. 2003). According to the test results, more testing is required before the TPL-7 can be used for the Tundra Platform foundation system.

Flat Loop Evaporators

Flat loop evaporators are not VSM's, but they utilize thermosyphon technology to allow for on-grade construction. Horizontal thermosyphons are installed on-grade and require no ground penetrations (Yarmak and Long, 2002). Similar designs are used successfully beneath pavement and building structures to maintain the thermal regime in areas of warm or discontinuous permafrost (Forsström et al., 2002).

Briefly, the plastic thermosyphons are 64 mm (2.5 in) in diameter and are laid out on the ground. The ground is sprayed with enough water necessary to saturate the tundra and to cover the tubes. The thermosyphons freeze in place and can be overlaid by insulation and the Tundra Platform. Because this installation is on-grade normal loads are not a critical design factor. The controlling design factor is the heat transfer from the Platform to the subgrade and thus a thermal analysis is required. The spacing of the thermosyphons is dependent upon the results of the analysis and allows for maintenance of the thermal regime of the permafrost beneath the Platform.

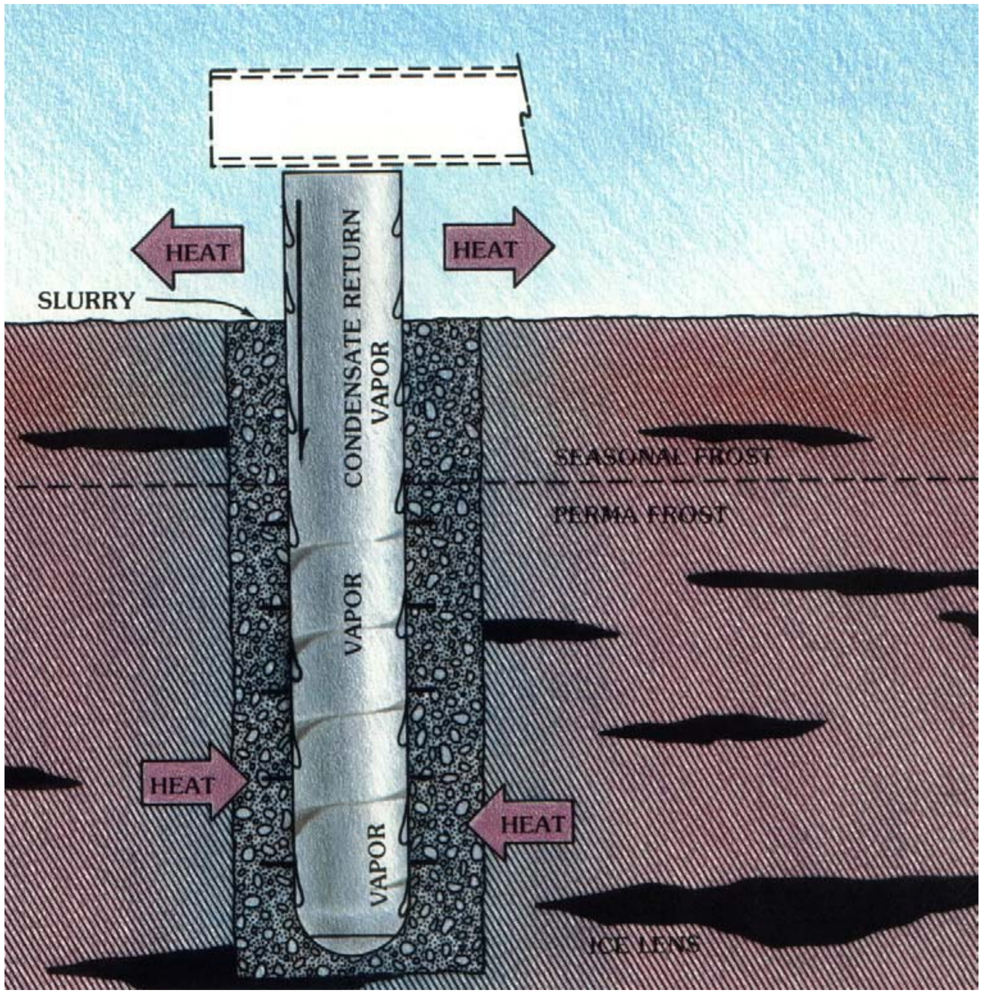

Figure 5 Thermal pile. Self-contained passive refrigeration system (from Arctic Foundations)

After drilling operations are complete and the well is plugged and abandoned the Platform components and the insulation are removed. The tubes are left behind and can be recovered when they have thawed in spring or summer temperatures. If the access to the site is limited in the summer period, steam could be circulated in the tubes to thaw them quickly.

It is understood that this type of foundation is not a consideration for this particular project. However, we do include this description to inform Anadarko of the state-of-the-art for possible application in future projects in cold regions.

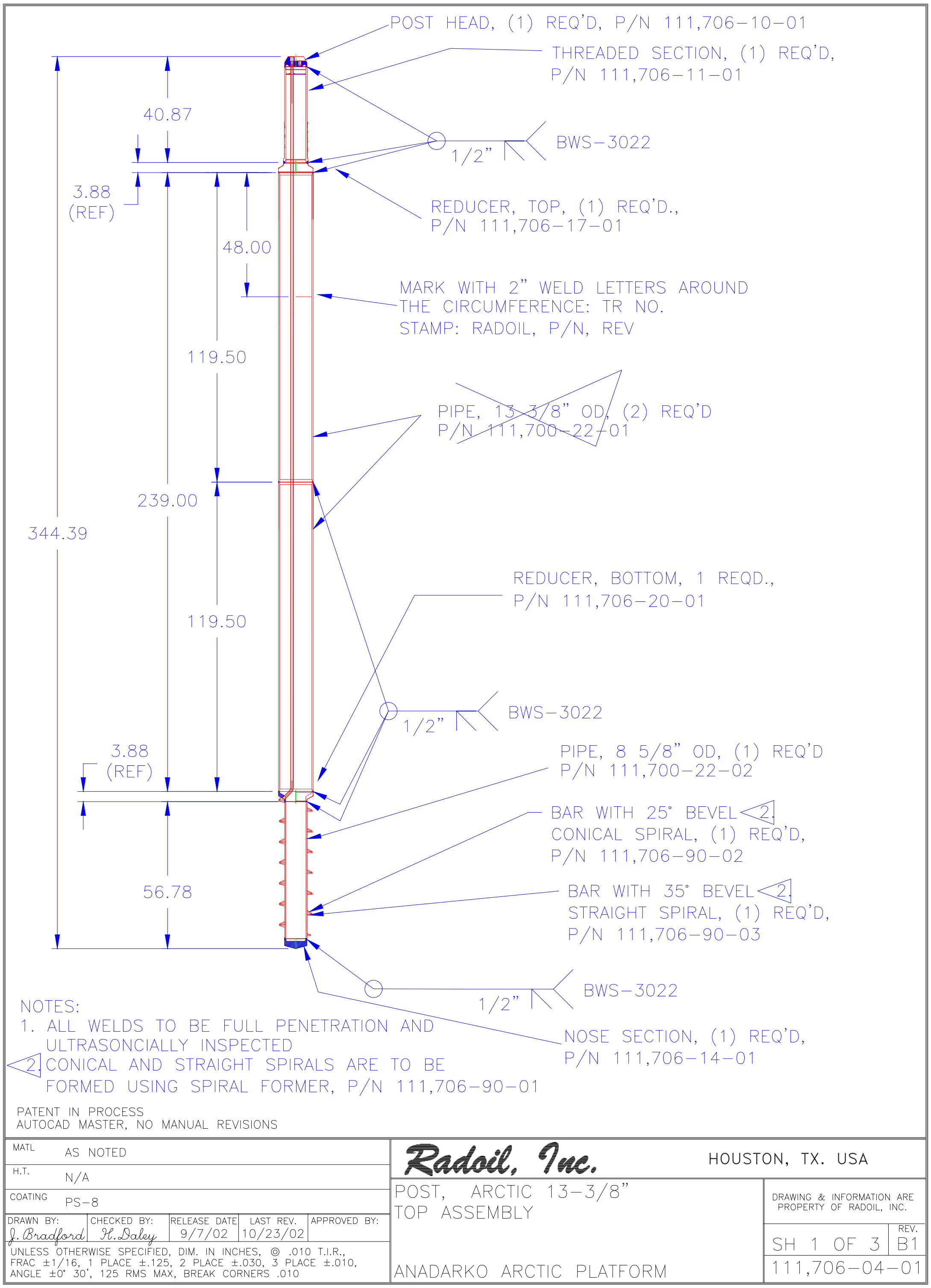

Figure 6 Diagram of Anadarko's Tundra Platform Leg, TPL-7

SUITABILITY OF FOUNDATION TYPES AS TUNDRA PLATFORM LEGS

Driven Piles

Advantages:

- Driven piles can be installed very quickly, as many as three per hour in warm permafrost (Phukan, 1998). Operationally, they would be relatively inexpensive to install.

- Because they require minimum thawing of the pilot hole, freezeback times are less than for drill and slurry piles.

- They can be cut off below the surface and left behind without removal.

Disadvantages:

- Driven piles utilize adfreeze design and are thus very long piles. Removal at the end of the project would be difficult.

- Precise placement is usually possible, but not always easily attained. The required tolerances for placement of the horizontal members must be compared with the expected placement precision.

Freezeback Piles

Advantages:

- Precise placement is easily achieved. Because the piles are inserted into oversized holes they can be accurately positioned before the slurry is poured.

Disadvantages:

- Temperature monitoring is required because adequate freezeback time is necessary before loading.

- Operationally, greater installation time is required.

- Adfreeze design requires pile lengths up to 10 m (30 ft).

- Pile removal by pullout will be difficult, because of the length and quantity.

- Pile removal will take more time because of the quantity

Screw Piles

Advantages:

- Because screw piles utilize the shear strength of the soil they can be much shorter than the piles mentioned above, and may be more economical.

- Operationally, shorter piles mean that less installation time is necessary. Shorter auguring time and fewer slurry materials are required.

- They can be placed precisely because they are installed using a drill/slurry method.

Disadvantages:

- They require freezeback time.
- Because they are usually shorter a lateral load or bending moment may require the pile to be lengthened.
- Because of the helix they are not easily removed. A mechanism to rotate and pull the pile to remove it from the ground will be necessary.

Helical Piers
Advantages:

- Fast and easy installation.
- Small size and weight.
- Ease of transportation.
- Resistance to frost jacking.

Disadvantages:

- The four piers required for each “leg” need to be connected to large-diameter legs at the ground surface.

TPL-7
Advantages:

- Shorter length than an adfreeze pile, if properly installed.
- Legs can be removed.

Disadvantages

- Uncertain load bearing capacity because of the unconventional diameter of the helix in relationship to the pile diameter. Need more research before an adequate design can be developed.
- Rotation for removal requires special equipment, which is an added expense.

Thermally Controlled Piles
Advantages:

- Short legs because the helices utilize soil shear strength.
- Capable of reducing soil temperatures and thus increasing soil strength.
- Have built-in capability for circulating fluids.

Disadvantages:

- Initial expense is greater than conventional piles.

Flat Loop Evaporators

Advantages:

- Allow for on-grade construction and thus eliminate VSM's.
- Relatively inexpensive and easy to install and remove.
- No ground penetrations. The siphon tubes can be recovered in the summer leaving no trace of a foundation.

Disadvantages:

- Requires some freezing time, but much less than a conventional ice pad.
- Design may require some insulation between structure and tundra.

RECOMMENDATIONS FOR IMPLEMENTATION AND FUTURE RESEARCH

General Recommendations for Design Choices

There are several feasible pile designs for Anadarko's Tundra Platform. Cost effectiveness and site impact are the most important factors. We can recommend two of the reviewed designs. Recommendations are based upon general economic understanding that may or may not agree with Anadarko's own specific economic and operational standards.

- Driven piles. These would use an adfreeze design. They would be the cheapest to purchase and their installation by driving is the quickest of all the piles reviewed. Because they would be relatively long, lateral loads are easier to accommodate. When the project is complete they would not be recovered, but cut off below the surface leaving little evidence of the project.
- Helical piles: The bearing capacity design would allow them to be much shorter and they would be easier to recover if equipment is available to rotate and pull them out. Initial expense would be greater but the piles would be available for reuse. Lateral loading needs to be considered in the design.
- Flat Loop Evaporators and Helical Piers: We believe that these options are also worth of considering as foundation systems for the Platform.

Future Research

The future research could be conducted in two fronts: Conduct more studies on TPL-7 or optimize the pile length for smooth adfreeze piles. Reduced scale laboratory and field tests are recommended for TPL-7. Outcome of this research would be more information on how much more capacity do the helixes add for the pile when compared to a smooth pile.

The length of a smooth adfreeze pile could be optimized using Finite Element Analysis and reduced scale laboratory testing. The current adfreeze design method assumes that the adfreeze strength is mobilized along the whole pile surface, whereas Dr. He Liu and Dr. Hannele Zubeck from the UAA hypothesize that it is only mobilized along a small section of the pile. The outcome of this research would be a method to design the length of an adfreeze pile in ice-rich silt with ground temperature.

REFERENCES

Andersland, O.B. and B. Ladanyi, *An Introduction to Frozen Ground Engineering*, Chapman and Hall, New York, 1994.

Andersland, O.B., F.H. Sayles, and B. Ladanyi, *Geotechnical Engineering for Cold Regions,* McGraw-Hill, New York, 1978.

ARCO Oil & Gas, Sohio Construction Co., Northwest Alaskan Pipeline Co., Panhandle Eastern, Ralph M. Parson Co., Exxon Production Research Co., *Members Sponsor Task Group Pile Design Report,* July 1982.

Arctic Foundations, *Frozen Assets,* brochure.

Berezantsev, V., *Some Problems of the Theory of Limiting Resistance of Soil to Stresses,* Doctoral dissertation. AN SSSR Permafrost Research Institute, 1949.

Crory, F.E., "Piling in frozen ground," *Journal of Technical Council on Cold Regions Engineering,* ASCE, 108(1), pp 112-124, 1982.

Forsström, A., E.L Long., J.P. Zarling, and S. Knutsson., "Thermosyphon Cooling of Chena Hot Springs Road," *Proceedings of the 11th International Conference on Cold Regions Engineering,* pp 645-55, Anchorage, Alaska, May 2002.

Ishlinskiy, A., "The Axio-symmetrical problem of the theory of plasticity and Brinell test," *Occurrences in Mathematics and Mechanics,* Vol. VIII, No. 3, 1944.

Johnston, G.H., "Pile construction in permafrost," *Proceedings of 1st International Conference on Permafrost*, Lafayette, Indiana, November 1963.

Johnston, G.H. (Ed.), *Permafrost Engineering and Design and Construction,* Wiley, Toronto, 1981.

Johnston, G.H. and B. Ladanyi, "Field test of grouted rod anchors in permafrost," *Canadian Geotechnical Journal*, Vol. 9, pp 176-194, 1972.

Ladanyi, B., "An engineering theory of creep of frozen soils," *Canadian Geotechnical Journal,* Vol. 9, pp 63-80, 1972.

Ladanyi, B. and G.H. Johnston, "Behavior of circular footings and plate anchors embedded in permafrost," *Canadian Geotechnical Journal,* Vol. 11, pp 531-553, 1974.

Ladanyi, B. and J. Paquin, “Creep behavior of frozen sand under a deep circular load,” *Proceedings of 3rd International Conference on Permafrost,* Edmonton, Alberta, Canada. Ottowa: National Research Council of Canada, Vol. 1 pp 670-86, 1978.

Linell, D.A. and E.F. Lobacz, *Design and Construction of Foundations in Areas of Deep Seasonal Frost in Permafrost,* Special Report 80-34, Cold Regions Research and Engineering Laboratory, Corps of Engineers, Hanover, NH, August 1980.

Manikian, V., “Pile driving and load tests in permafrost for the Kuparuk pipeline system,” *Proceedings*, Fourth International Conference on Permafrost, Vol. 1, Fairbanks, Alaska, pp. 804-810, 1983.

Morgenstern, N.R., W.D. Roggensack, and J.S. Weaver, “The behaviour of friction piles in ice and ice-rich soils,” *Canadian Geotechnical Journal*, Vol. 17(3), pp. 405-415, 1980.

Neukirchner, R.J., “Permafrost temperature profiles for design of piles by creep theory,” *Proceedings of 3rd International Specialty Conference Cold Regions Engineering*, Vol. 1, pp 53-67, Edmonton, Alberta, Canada, April 1984.

Newcombe, T., BP Alaska Pile Test Program, BP North Slope Project, Anchorage, Alaska, 1973.

Nixon, J.F., First Canadian Geotechnical Colloquium: “Foundation design approaches in permafrost areas,” *Canadian Geotechnical Journal,* Vol. 15, pp 96-112, 1978.

Nixon, J.F. and E.C. McRoberts, “A design approach for pile foundations in permafrost,” *Canadian Geotechnical Journal*, Vol. 13, pp. 40-57, 1976.

Nottingham, D. and A.B. Christopherson, “Driven piles in permafrost: state of the art,” *Proceedings of IV International Conference on Permafrost*, pp 928-933, Fairbanks, Alaska, 1983.

Phukan, A., “Driven piles in warm permafrost,” *Proceedings of the 7th International Conference on Permafrost,* Yellowknife, Canada, June 1998.

Sego, D.C., *Deformation of Ice Under Low Stress,* PhD. Dissertation, University of Alberta, Edmonton, Alberta, Canada, 1980.

Terzaghi, K., *Theoretical Soil Mechanics,* Wiley, New York, 1943.

Vialov, S.S., “*Rheological Properties and Bearing Capacity of Frozen Soils*,” Translation 74, translated for Cold Regions Research and Engineering Laboratory, Corps of Engineers, 1959.

Weaver, J.S. and N.R Morgenstern, “Pile design in permafrost,” *Canadian Geotechnical Journal*, Natural Resource Council Canada, 18(3), pp. 357-370, 1981.

Yarmak, E. and E.L. Long, “Recent developments in thermosyphon technology,” *Proceedings of the 11th International Conference on Cold Regions Engineering,* pp 656-62, Anchorage, Alaska, May 2002.

Zubeck, H. and H. Liu, “Design of Helical Piers in Frozen Silt,” *Proceedings of the 11th International Conference on Cold Regions Engineering,* pp 656-62, Anchorage, Alaska, May 2002.

Zubeck, H.K., Porhola, S. and Aleshire, L. "Tundra Platform Leg Test," submitted to Anadarko Petroleum Company, February 2003.

Tundra Platform Leg Test

Prepared for Anadarko Petroleum Corporation

by

Hannele Zubeck
Stan Porhola, and
Lynn Aleshire

University of Alaska Anchorage,
School of Engineering

February 19, 2003

ABSTRACT

The University of Alaska Anchorage, School of Engineering designed and analyzed a pile test in permafrost for Anadarko Petroleum Company. The two piles (Spiral Legs) tested were designed and built by Radoil, Inc. using a concept provided by the Anadarko. The goals for the testing were to assure that the piles can be installed and removed without major problems, to assure that the piles can carry the design load for the design life of 2 years without instantaneous failure or excessive creep displacement, and to provide information and experience for future testing. The test proved that the Spiral Legs could be installed and removed without major difficulties at the average temperature of –2°C (28°F) in the ice rich silty soil and pure ice. The observed pile displacement rate at this temperature and in this soil was about 0.025 mm/h (0.001 in/hr). With this rate, the allowable design displacement of 15 mm (0.60 in) would be reached in one month. More research is recommended before Spiral Legs are used in the field. Since the spirals did not seem to offer the benefit of providing an acceptable displacement rate, the future research is recommended in optimizing the length of smooth piles.

TABLE OF CONTENTS

TABLE OF FIGURES

TABLE OF TABLES

APPENDICES

INTRODUCTION

Background

Anadarko Petroleum Company (Anadarko) has designed a portable tundra platform and will field test the design during the 2003 drilling season on a gas hydrate coring well as part of their research into gas hydrate technologies. The design of the platform calls for ease of mobilization and demobilization without leaving significant damage to the existing tundra. An important part of the platform design is the foundation system. Anadarko has designed a pile with helixes (Spiral Leg) to carry the load from the superstructure to the permafrost. The function of the helixes was to possibly add additional pile capacity and to aid in removing the piles by circulating a heated liquid down the pile, through the helixes and back to the surface. Anadarko provided funding for the University of Alaska Anchorage (UAA), School of Engineering to design and analyze a pile test that would determine the suitability of the spiral legs as the tundra platform foundations and to provide information for further testing.

Problem Statement

The piles need to meet the following requirements:

- The design load per pile is 445 kN (100kips). The ultimate capacity of each pile is 667 kN (150 kips) using a factor of safety of 1.5 and a design life of 2 years. The allowable settlement is 15 mm (0.6 in) in 2 years and 25mm (1 in) in 40 years.

- The permafrost needs to remain frozen below the tundra platform. If degradation of the permafrost is anticipated, the foundation system needs to assist in keeping the permafrost from thawing.

- The foundation system needs to be removable so that the tundra will not be seriously damaged after the foundation has been removed.

Piles have not been removed in the past, and therefore, research needs to be conducted to make sure that the proposed pile design meets all the requirements for the capacity, permafrost protection and the ease of removal.

Goals and Objectives

The following objectives were set for the initial load testing conducted in November 2002 at the Alaska Telecom Inc. (ATI) site in Prudhoe Bay:

1. Assure that the piles can be installed and removed without major problems.

2. Assure that the piles can carry the design load for the design life of 2 years without instantaneous failure or excessive creep displacement.

3. Provide information and experience for future testing.

The purpose of this report is to describe the pile tests performed, analyze the test results and give recommendations for implementation and future research.

Scope of the Work

A testing plan was created based on ASTM D 5780 Standard Test Method for Individual Piles in Permafrost Under Static Axial Compressive Load (1995). The test results were analyzed and recommendations for implementation and future research were given.

MATERIALS

Test Legs

The two Spiral Legs tested were designed and constructed by Radoil Inc. A photo of the spirals is given in Figure 1 and a schematic picture is given in Figure 2. The total length of each leg was 8.839 m (29 ft), embedment depth into the permafrost was 4.27 m (14 ft), the inner diameter was 314 mm (12.347 in) and the outer diameter was 340 mm (13.375 in). The bottom 1.524 m (5 ft) had an inner diameter of 194 mm (7.625 in) and outer diameter of the smooth leg of 219 mm (8.625 in) with spirals extending the outer diameter to 333 mm (13.125 in). The spirals had a 152-mm (6-in) lead making the spiral angle 12.44°. The spirals were hollow having a 10-mm (0.375 in) wall thickness. A small pipe was designed to carry heated liquid from the top of the spiral to the bottom and back to the surface through the inside of the leg. The leg material was carbon steel with a Young’s modulus of 200,000 MPa (29,000,000 psi).

Additionally, a smooth leg and two Vertical Support Members (VSM’s) were installed. The smooth leg was used as a control leg for the removal experiment and the VSM’s provided reaction forces for the compressive test load.

Figure 1 Spiral legs

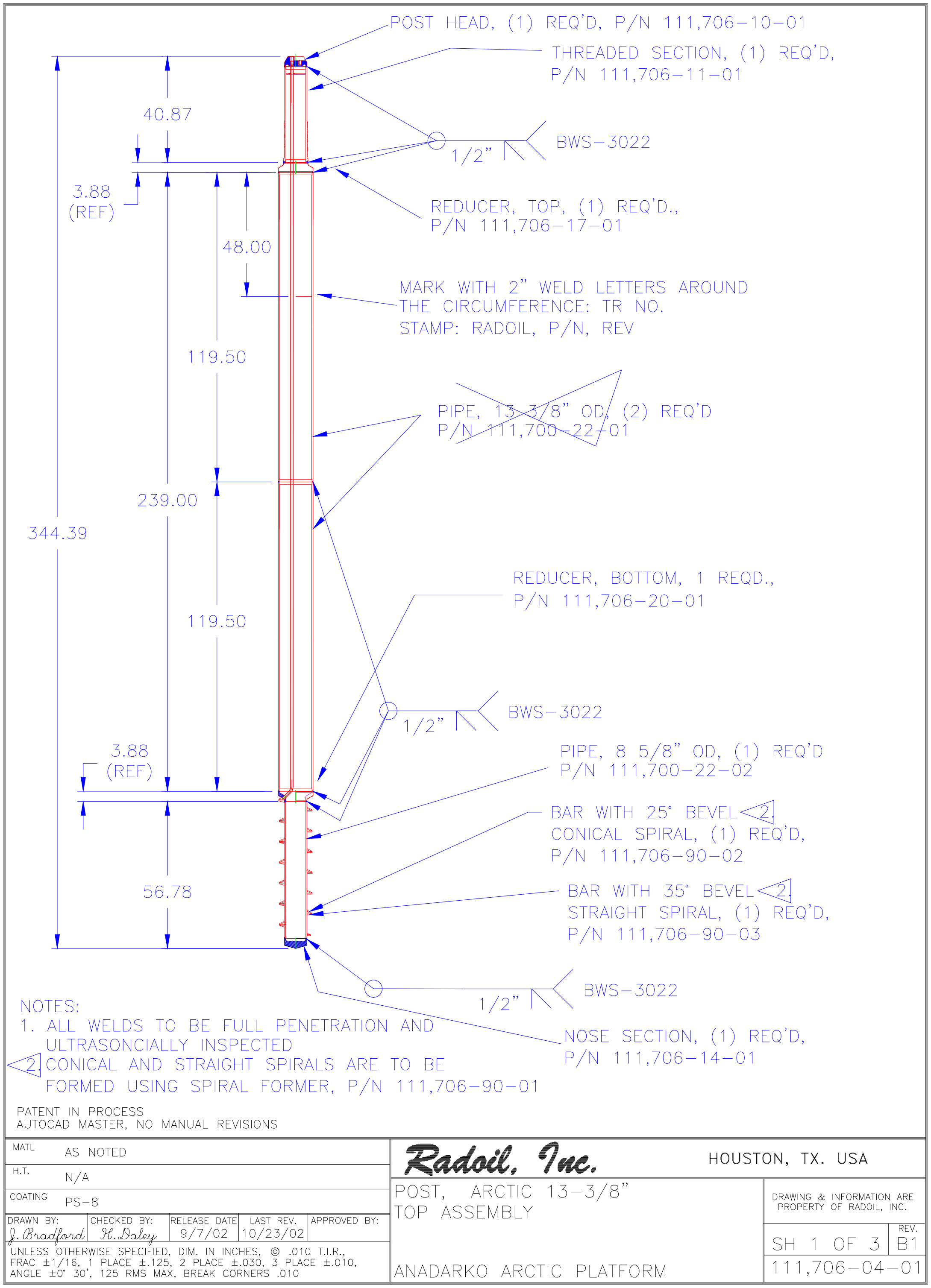

Figure 2 Schematic picture of spiral legs

Soils

The sand slurry used to backfill the holes was well graded sand with silt and gravel, SW-SM (Alaska Testlab, 2002) The gradation is given in Table 1. A water content of 7.6% was determined in the UAA Soils Laboratory and 7.7% by Alaska Testlab.

Table 1 Soil Gradation (Alaska Testlab, 2003)

U.S. Sieve (opening, mm)	Passing %	Sieve Size	Passing %
1/2 in (12.70 mm)	100	No. 40 (0.425 mm)	19
3/8 in (9.52 mm)	98	No. 60 (0.250 mm)	12
No. 4 (4.75 mm)	64	No. 100 (0.150 mm)	7
No.10 (2.00 mm)	40	No. 200 (0.075 mm)	5.3
No. 20 (0.85 mm)	29		

Michael Baker, Jr. Inc. (2002) logged the drilling of the piles and prepared a separate geotechnical report for the native soils. The following summarizes the soil strata shown in Figure 3.

The existing soil consisted of a 1.2 to 1.8-m (4 to 6 ft) thick fill and native soil beneath it. The fill material was poorly graded gravel with sand. The native soil around the spiral legs consisted of a organic to sandy silt layer of 0.6 m to 0.9 m (2 to 3 ft), beneath which Spiral Leg #2 had a 0.6-m (2ft) gravel layer and 2 m (7 ft) thick ice lens. Spiral Leg #3 had a 3.0-m (10ft) thick ice lens with air bubbles directly underneath the silt. A gravel layer with silt or sand started at a depth of 5.2 m to 5.8 m (17 to 19 ft) from the soil surface.

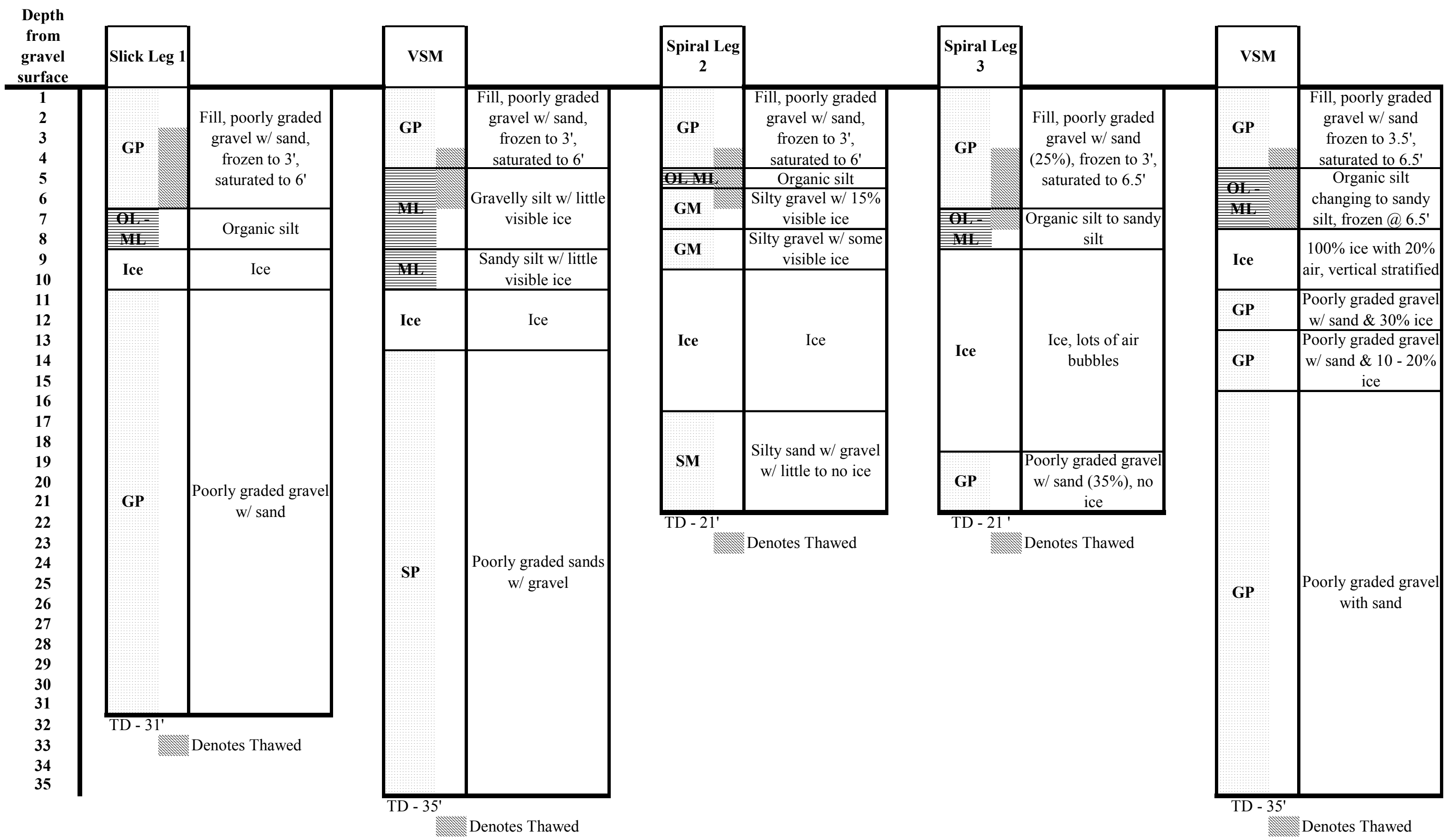

Figure 3 Soil logs (Baker)

TEST PROCEDURE

Test Setup

The test setup is shown in Figures 4 and 5. The test frame, load actuator and legs were designed by Radoil Inc. using a concept provided by Anadarko. The load was applied with two linear actuators at the top of the VSM's. The Radoil drawing number for the whole set up was 190,899-07-01 A4. A plan view of the test setup is given in Figure 6. The installation procedure by Anadarko is given in Appendix A and a report of pile removal by Federico Lier in Appendix B.

The Spiral Legs were suspended in augered holes with a 508-mm (20 in) diameter. The holes were backfilled with the sand slurry described earlier. The slurried legs were left to freeze for seven days. The top 1.8 m (6 ft) of each hole was not filled with slurry so that active layer forces would not affect the legs. Installation of the smooth leg and VSM's was similar to the Spiral Legs.

The testing followed the procedure outlined in ASTM D 5780 (1995). The following sections will summarize the testing and loading sequence.

Figure 4 Test setup

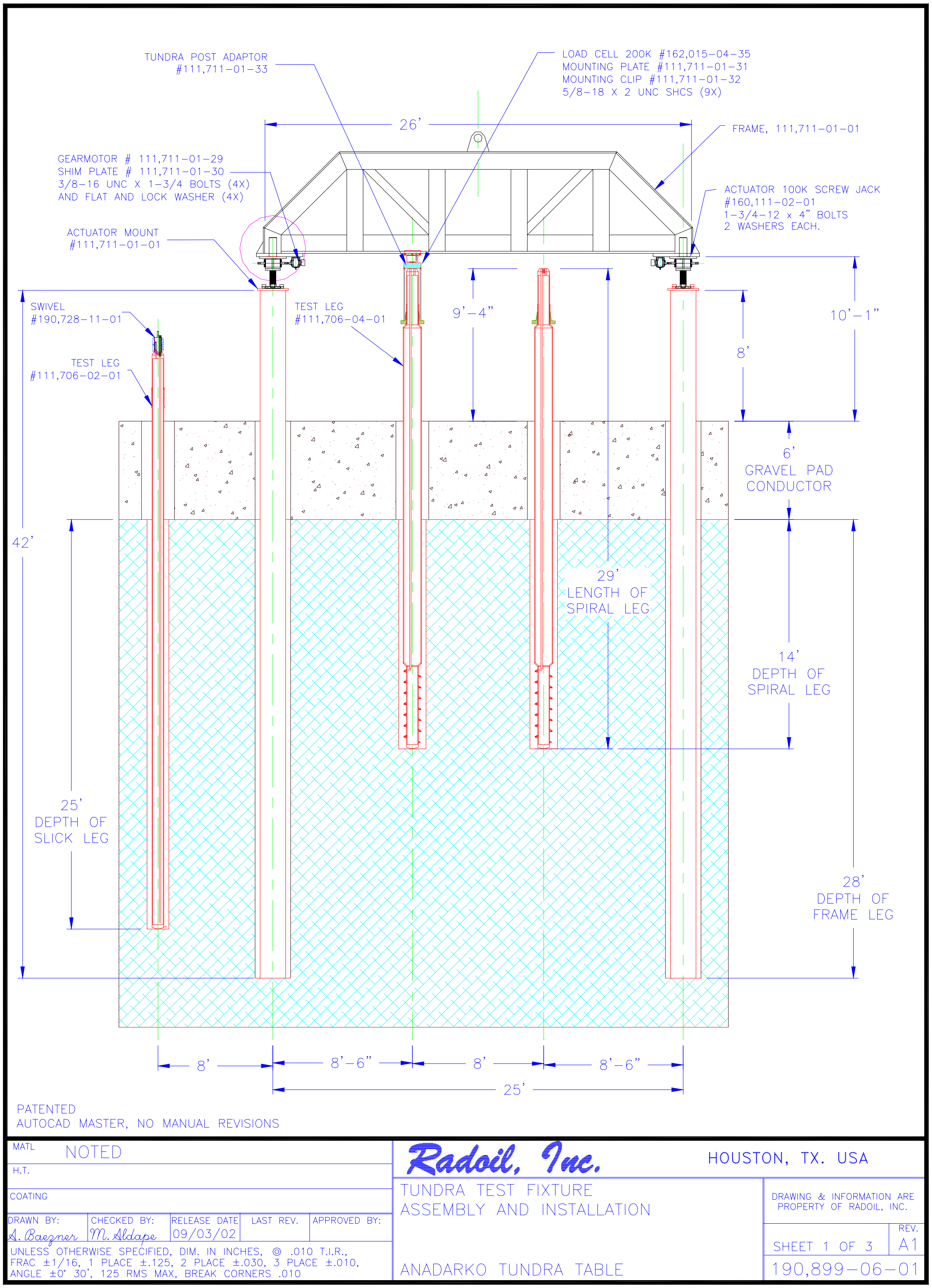

Figure 5 Schematic of test setup

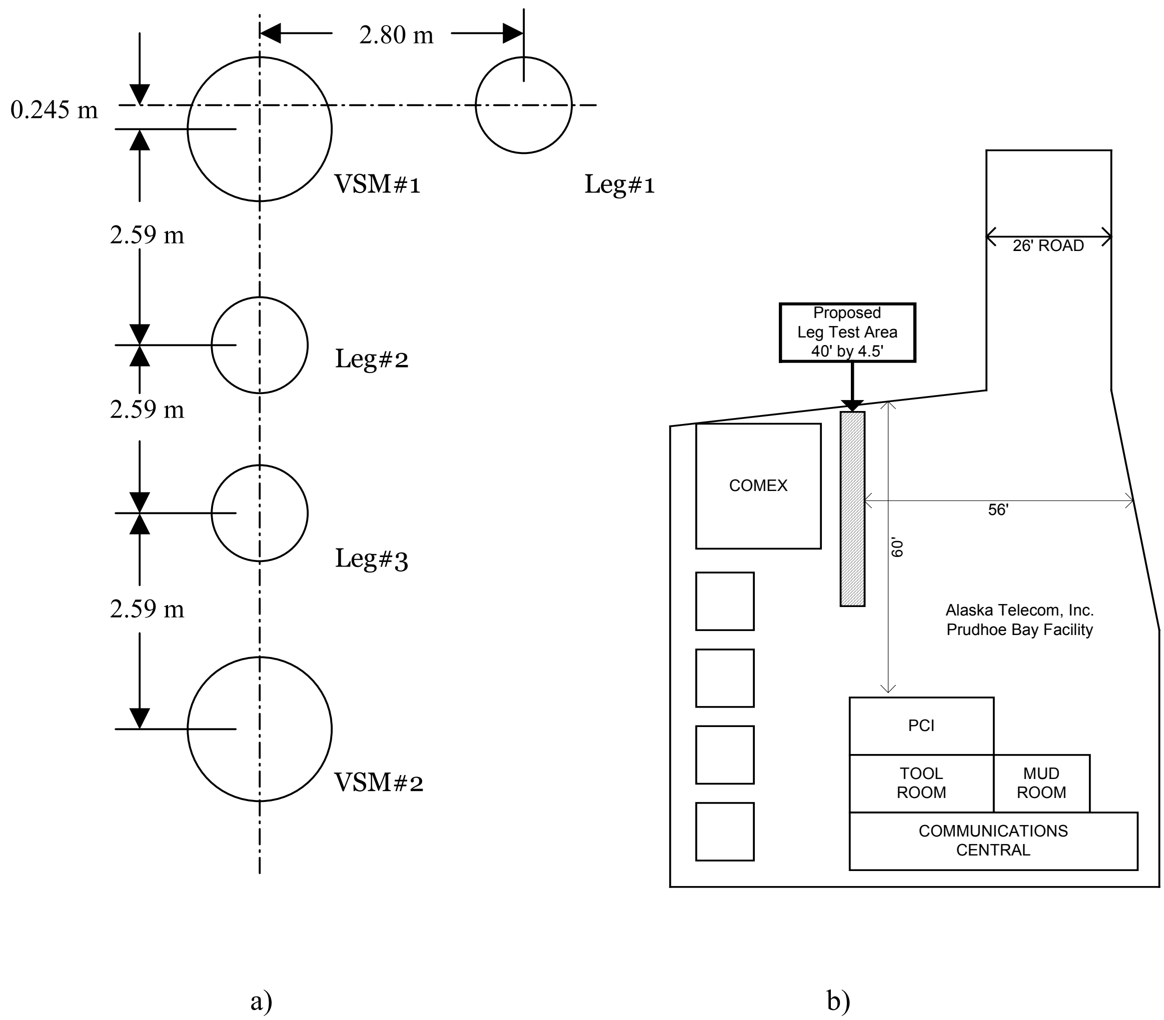

Figure 6 Plan view of test setup a) as built, b) site location (Radoil, Inc. 2002)

Apparatus for Measuring Movement

The primary method of measurement was a potentiometer (Figure 7) with an accuracy of 0.05 mm (0.001 in). ASTM D 5780 requirements call for an accuracy of 0.0025 mm (0.0001 in). The potentiometer accuracy was considered to be adequate for this phase of testing. The potentiometer was attached to a vertical carbon steel rod welded to a conductor that was used as a casing through the gravel pad at each hole (see Figures on page 3 and 4 in Appendix A).

Figure 7 Potentiometer for measuring displacement

Three secondary methods of measurements were used:

1. *A wire, scale and mirror (Figure 8).* A wire was stretched on the side of the test legs. The wire broke immediately and a thicker string was used instead. A scale and a mirror were mounted on the side of the leg such that the string passed clear of the face of the scale. The string was approximately 25 mm (1 in) from the scale. Vertical support angle irons were welded to the VSM conductors (see Figure on page 3 in Appendix A) that were considered to be as stable reference points as any other anchored reference system on the site. The other end of the wire was tied to one of the angle irons and the other end was hanging over the other angle iron and tied to a weight. The tension of the string was checked before each reading. The stainless steel scale had divisions up to 1/64 in. or 0.4 mm (0.016 in). The measurements were made by lining up the string, its mirror reflection and the scale. The length of the angle iron support at VSM #2 (closest to the smooth leg) was 1.585 m (5.2 ft) and at VSM #1 was 1.256 m (4.12 ft). The distance between the supports was 6.960 m (22.833 ft).

2. *A surveyor's level and a scale on the leg.* Permanent benchmarks were established outside the immediate test area. A transit was set up outdoors with a clear line of site to both the scale and the benchmarks (Figure 9).

3. *Dial gages.* The dial gages were accurate to 0.001 in. and two were used for the test. One to measure vertical movement and a second to measure horizontal or rotational movement (Figure 10).

Figure 8 Wire, scale and mirror for measuring displacement

Figure 9 Transit setup

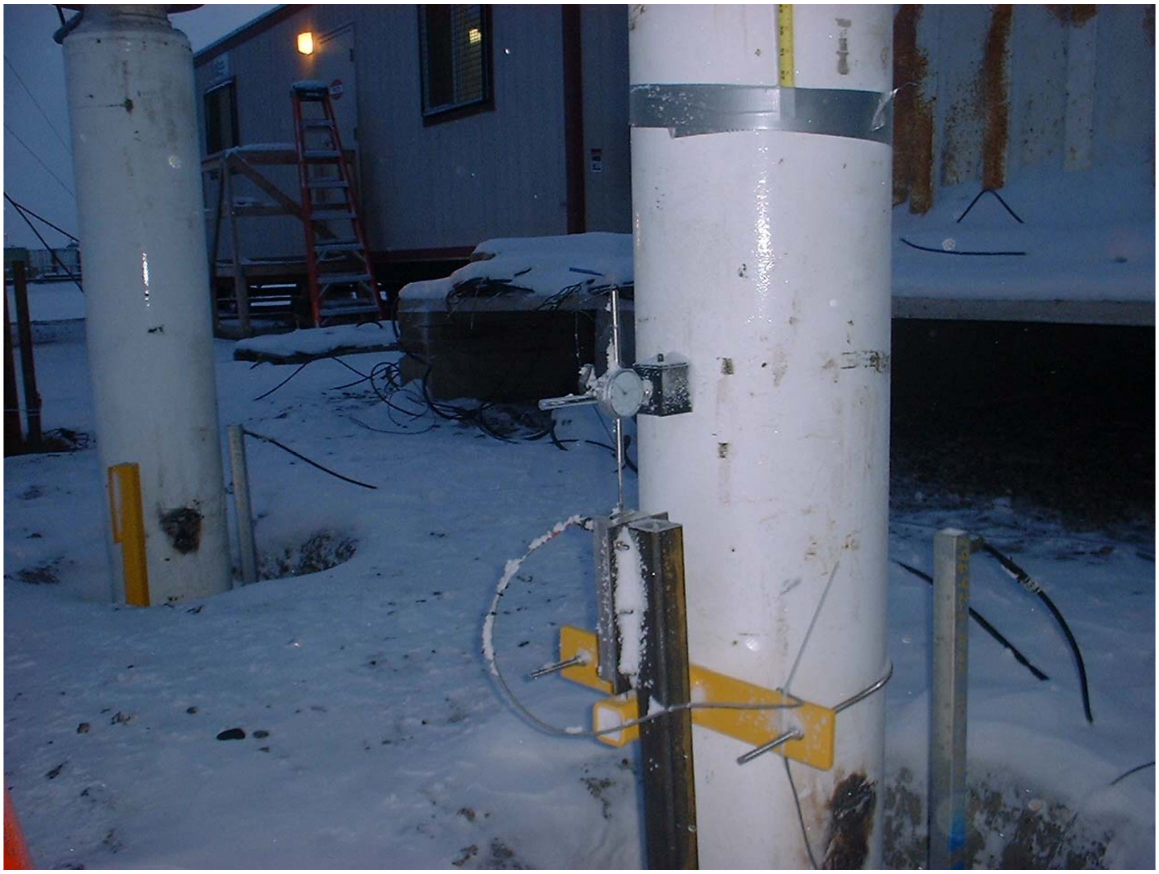

Figure 10 Dial gage

Apparatus for Measuring Temperature

The temperature was measured using thermistors. A string of thermistors was installed in the augered hole of the smooth leg and the two Spiral Legs. Figure 11 details the positions of the thermistors on each of the legs. The air temperature was also measured using a thermistor. The accuracy of the thermistors was 0.2 °C (0.4°F).

Apparatus for Measuring Load

The applied load was measured using a load cell with an accuracy of 1% of the load reading. The load cell can be seen in Figure 4 between the left most Spiral Leg and the testing frame.

Measuring and Recording Procedures

ASTM D 5780 requires displacement readings to be recorded at the following intervals: every 10 minutes during the first 30 minutes, every 20 minutes for the next 1 ½ hours, every hour for the next 10 hours, every 2 hours for the next 12 hours, every 6 hours thereafter. For the tests reported here, the displacement and the load were read ten times per second and stored once per second from the commencement of a test up to 24 hours after the load increment was removed.

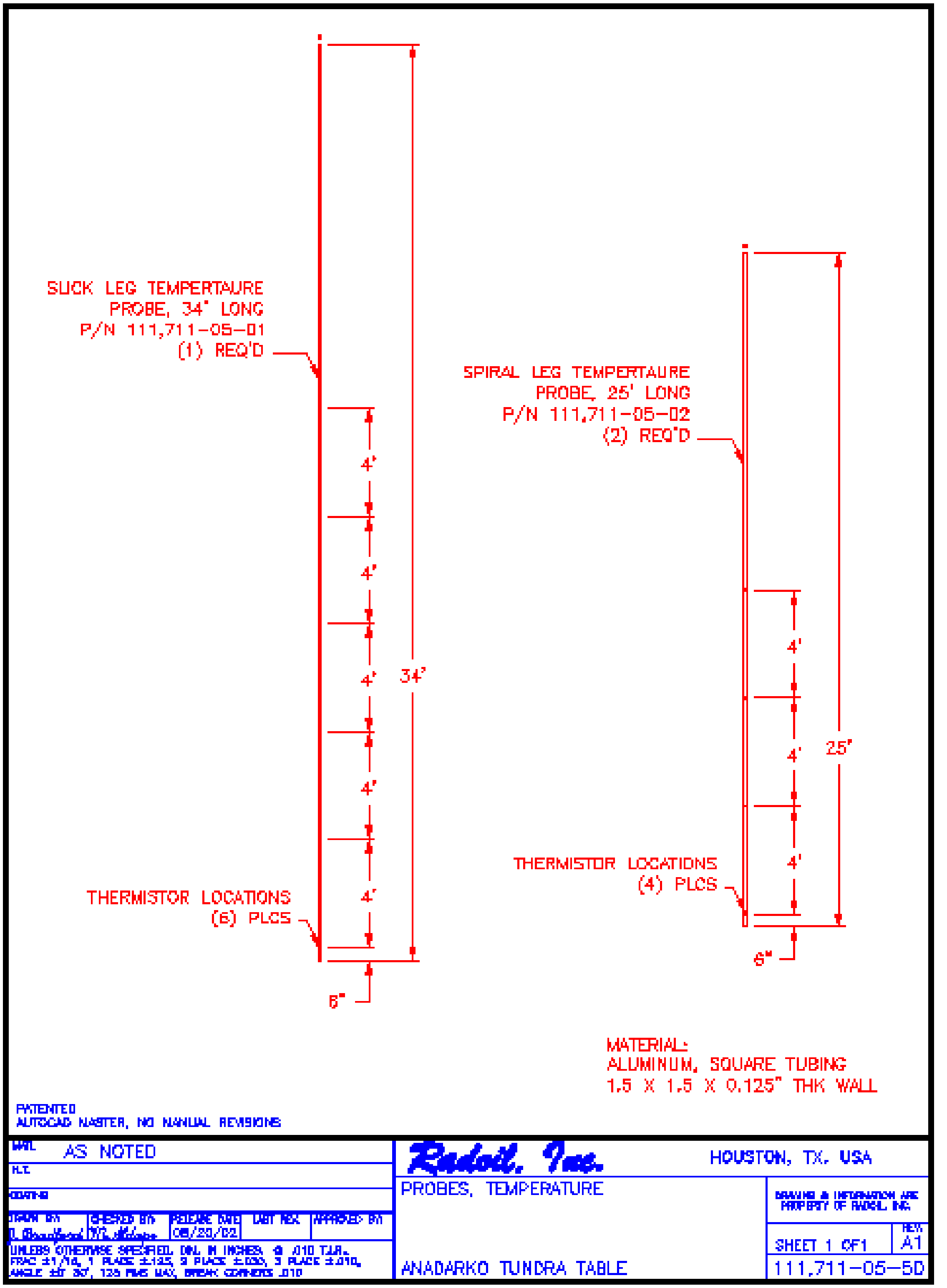

Figure 11 Thermistor strings

The secondary measurement devices were read periodically for backup data. The creep displacement readings were selected for plotting and analysis at each 0.0254 mm (0.001 in) during secondary creep and more often during the primary creep. ASTM D 5780 requests ground-temperature readings prior to the start of each load increment, after the completion of each load increment, and at least once per day during each load increment. For our tests, the air and ground temperatures were read 10 times per second and selected for analysis every 6.25 minutes.

Loading Procedure

The loads were applied in a continuous uniform manner until the test load was attained. The time to load was under 10 seconds except for the 445 and 667 kN (100 and 150 kips) loads. Since a mechanical actuator was used, it was not possible to maintain the load exactly at the designated level. The load ranges are given with the test results.

According to the ASTM D 5780 method, two types of loads are to be applied to the test legs: creep loads and failure loads. The creep load increments are maintained until a uniform rate of movement of the test leg is achieved for four consecutive measurement periods (at least 15 min apart) or for a minimum of 3 days (which ever is greater). If failure occurs before attaining uniform movement the load test on the leg may be terminated, or if after 7 days there is not uniform movement the test increment may be terminated. The failure load increments are maintained on the test leg until failure occurs. If failure is not reached in 7 days the test increment may be terminated. When failure occurs or the test increment is terminated the applied load is to be removed and rebound measurements are to be taken for 24 hours.

No soil data for the site were available prior to installation of the legs that would assist in selecting proper load levels. The load levels of 222, 445 and 667 kN (50, 100 and 150 kips) were chosen based on the 667-kN (150 kips) capacity of the test frame. It was unknown prior to testing whether or not any of the loads would lead to a failure.

LOAD TEST ON PILE 1 (Spiral Leg #3)

A nominal load of 67 kN (15 kips) was applied on Spiral Leg #3 at 20:00 on November 8 to make sure that the loading and measurement apparatus worked properly.

The actual testing started at 12:21 on November 9 by applying a load of 222 kN (50 kips). The program was set up to keep the load between 213 and 222 kN (48 to 50 kips). The test was terminated at 13:57 on November 10. The creep rate had been stable for 20 hours.

A load of 445 kN (100 kips) was applied at 15:15 on November 10. The program was set up to keep the load between 440 and 445 kN (99 to 100 kips). The test was terminated at 9:53 on November 12. The creep rate had been stable for 40 hours.

A load of 667 kN (150 kips) was applied at 11:49 on November 12. The program was set up to keep the load between 440 and 445 kN (99 to 100 kips). One of the actuators failed during the load application, but the other actuator was able to bring the system up to the target load. The test was terminated at 9:17 on November 15. The creep rate had been stable for 65 hours.

LOAD TEST ON PILE 2 (Spiral Leg #2)

After the rebound had been measured for 2 hours, the load cell, potentiometer, and dial gages were removed from Spiral Leg #3. The load cell was moved along the truss by hand over Spiral Leg #2. The leg was placed in contact with the load cell, and the potentiometer and a dial gage were attached to the leg.

The wire, scale and mirror were not used for the testing of Spiral Leg #2, as the potentiometer, dial gage and transit measurement systems were reliable for the data recording and verification. The dial gage for vertical displacement was read periodically to verify the potentiometer readings. However, blowing snow and freezing temperatures affected the gage readings, and therefore the dial gage was not relied upon during testing of Spiral Leg #2. No rotation was observed for Spiral Leg #3, and therefore the dial gage used to measure the rotation was not used for Spiral Leg #2.

A nominal load of 67 kN (15 kips) was applied on the Spiral Leg #2 at 13:10 on November 15 to make sure that the loading and measurement apparatus worked properly. The actual testing started at 14:03 on November 15 by applying a load of 445 kN (100 kips). The program was set up to keep the load between 440 and 445 kN (99 to 100 kips). The test was terminated at 14:02 on November 18. The creep rate had been stable for 40 hours.

A load of 667 kN (150 kips) was applied at 15:00 on November 18. The program was set up to keep the load between 658 and 667 kN (148 to 150 kips). The test was terminated at 15:00 on November 23. The creep rate had been stable for 40 hours.

TEST RESULTS

Temperature Data

The measured ground temperatures for Spiral Legs are given and analyzed below with the displacement data. Temperature data from for the smooth leg and the ambient air are given in Appendix C. The season of October - November is the warmest period for permafrost below the ground surface, which is desired for permafrost pile testing. The measured temperatures showed that the permafrost was about 1°C (2°F) warmer at the depth of 4 m (14 ft) than in November of 1969, a value reported by Neukirchner (1984).

Spiral Leg #3

Data for the displacement, displacement rate and temperatures are given in Tables 2 to 5. The pile displacement with time is plotted in Figure 12 and the soil temperature with time in Figure 13. In the first test, 222-kN (50 kips) load on Spiral Leg #3, the creep reached the secondary creep rate at approximately 40 minutes. The average creep rate was measured to be 0.023 mm/hr (0.0009 in/hr). The pseudo-instantaneous displacement (obtained by intersecting the best fit line for the secondary creep data and the ordinate) was 0.38 mm (0.015 in). When the load was removed, an immediate rebound of 0.38 mm (0.015 in) was observed. When the test started, only the bottom 2.29 m (7.5 ft) of the pile was in frozen soil. The average temperature over the frozen part of the leg was –2°C (28°F). At the end of the test, an estimated of 2.44 m (8 ft) of the pile was in frozen soil. The average temperature over the frozen part of the leg was still about –2°C (28°F). The load actuator increased the load from the minimum set value to the maximum set value twice, at 3 hours and 54 minutes, and at 23 hours 29 minutes, which explains the small changes in the displacement rates at those times.

In the second test, 444-kN (100 kips) load on Spiral Leg #3, the creep reached the secondary creep rate at approximately 3 hours. The average creep rate was measured to be 0.026 mm/hr (0.0010 in/hr). The pseudo-instantaneous displacement was 1.04 mm (0.041 in). When the load was removed, an immediate rebound of 0.84 mm (0.033 in) was observed. When the test started, only the bottom 2.44 m (8 ft) of the pile was in frozen soil. The average temperature over the frozen part of the leg was –2°C (28°F). At the end of the test, an estimated of 3.66 m (12 ft) of the pile was in frozen soil. The average temperature over the pile was still about –2°C (28°F). The load actuator increased the load from the minimum set value to the maximum set value at about 18 hours, which explains the small change in the displacement rate at that time.

In the third test, 667-kN (150 kips) load on Spiral Leg #3, the creep reached the secondary creep rate at approximately three hours. The average creep rate was measured to be 0.027 mm/hr (0.0011 in/hr). The pseudo-instantaneous displacement was 1.52 mm (0.060 in). When the load was removed, an immediate rebound of 1.270 mm (0.050 in) was observed. When the test started, the bottom 3.66 m (12 ft) of the pile was in frozen soil. The average temperature over the frozen part of the leg was –2°C (28°F). At the end of the test, entire pile length of 4.27 m (14 ft) was in frozen soil. The average temperature over the pile was still about –2°C (28°F).

Spiral Leg #2

Data for the displacement, displacement rate and temperatures are given in Tables 6, 7 and 8. The pile displacement with time is plotted in Figure 14 and the soil temperature with time in Figure 15. In the first test, 444-kN (100 kips) load on Spiral Leg #2, the creep reached the secondary creep rate at approximately 8 hours. The average creep rate was measured to be 0.024 mm/hr (0.00094 in/hr). The pseudo-instantaneous displacement (obtained by intersecting the best fit line for the secondary creep data and the ordinate) was 1.07 mm (0.042 in). When the load was removed, an immediate rebound of 0.74 mm (0.029 in) was observed. When the test started, only the bottom 3.35 m (11 ft) of the pile was in frozen soil. The average temperature over the frozen part of the leg was –2°C (28°F). At the end of the test, entire pile length of 4.27 m (14 ft) was in frozen soil. The average temperature over the pile was about –2.5°C (27°F).

In the second test, 667-kN (150 kips) load on Spiral Leg #2, the creep reached the secondary creep rate at approximately 11 hours. The average creep rate was measured to be 0.020 mm/hr (0.00078 in/hr). The pseudo-instantaneous displacement was 1.55 mm (0.061 in). When the load was removed, an immediate rebound of 1.17 mm (0.046 in) was observed. The entire pile length of 4.27 m (14 ft) was in frozen soil during the whole test. The average temperature over the pile was about –2.5°C (27°F) at the beginning of the test and about –3.0°C (26.6°F) at the end of the test. The load actuator increased the load from the minimum set value to the maximum set value at about 18 hours, which explains the small change in the displacement rate at that time.

Secondary Displacement Measurements

Displacements from the secondary measurement systems are given in Table 9. The wire and mirror system measurements were close to potentiometer readings for Leg #3. This system was not used for Leg #2, as the dial gages were more accurate and easier to read. The dial gage confirmed the potentiometer readings. Possible rotation of the piles was measured for Spiral Leg #3 at load levels of 444 and 667 kN (100 and 150 kips). No rotation was observed.

Table 2 Displacement data for Spiral Leg #3 with 222-kN (50 kips) load

Time	Displacement		Time	Displacement		Time	Displacement	
hrs	mm	0.001 in	hrs	mm	0.001 in	hrs	mm	0.001 in
0.00	0.000	0	6.96	0.559	22	19.55	0.813	32
5E-3	0.305	12	8.18	0.584	23	20.80	0.838	33
14E-3	0.330	13	9.81	0.610	24	21.81	0.864	34
0.08	0.356	14	10.96	0.635	25	22.93	0.889	35
0.65	0.381	15	12.36	0.660	26	23.36	0.914	36
1.65	0.406	16	13.45	0.686	27	23.58	0.940	37
2.81	0.432	17	14.88	0.711	28	24.53	0.965	38
3.90	0.483	19	16.15	0.737	29	25.31	0.991	39
4.56	0.508	20	17.13	0.762	30			
5.65	0.533	21	18.41	0.787	31			

Table 3 Displacement data for Spiral Leg #3 with 444-kN (100 kips) load

Time	Displacement		Time	Displacement		Time	Displacement	
hrs	mm	0.001 in	hrs	mm	0.001 in	hrs	mm	0.001 in
0.00	0.000	0	7.36	1.219	48	24.96	1.702	67
0.01	0.254	10	8.14	1.245	49	26.14	1.727	68
0.02	0.787	31	8.71	1.270	50	27.24	1.753	69
0.02	0.813	32	9.71	1.295	51	28.04	1.778	70
0.04	0.838	33	10.49	1.321	52	29.24	1.803	71
0.06	0.864	34	11.17	1.346	53	30.46	1.829	72
0.15	0.889	35	12.14	1.372	54	31.54	1.854	73
0.33	0.914	36	13.01	1.397	55	32.71	1.880	74
0.45	0.940	37	13.52	1.422	56	33.67	1.905	75
0.83	0.965	38	14.51	1.448	57	34.71	1.930	76
1.27	0.991	39	15.84	1.473	58	35.96	1.956	77
1.71	1.016	40	16.92	1.499	59	37.02	1.981	78
2.16	1.041	41	17.54	1.524	60	37.82	2.007	79
2.87	1.067	42	18.17	1.549	61	38.84	2.032	80
3.91	1.092	43	18.79	1.575	62	39.89	2.057	81
4.16	1.118	44	19.87	1.600	63	40.87	2.083	82
4.94	1.143	45	21.22	1.626	64	41.94	2.108	83
5.67	1.168	46	22.66	1.651	65			
6.69	1.194	47	23.66	1.676	66			

Table 4 Displacement data for Spiral Leg #3 with 667-kN (150 kips) load

Time	Displacement		Time	Displacement		Time	Displacement	
hrs	mm	0.001 in	hrs	mm	0.001 in	hrs	mm	0.001 in
0.00	0.000	0	15.81	1.956	77	42.53	2.692	106
0.03	1.245	49	16.69	1.981	78	43.79	2.718	107
0.04	1.270	50	17.48	2.007	79	44.68	2.743	108
0.05	1.295	51	18.66	2.032	80	45.73	2.769	109
0.07	1.321	52	19.23	2.057	81	46.63	2.794	110
0.10	1.346	53	19.98	2.083	82	47.98	2.819	111
0.17	1.372	54	20.93	2.108	83	48.78	2.845	112
0.29	1.397	55	22.06	2.134	84	49.56	2.870	113
0.40	1.422	56	23.26	2.159	85	50.53	2.896	114
0.64	1.448	57	24.16	2.184	86	51.41	2.921	115
0.88	1.473	58	25.56	2.210	87	52.49	2.946	116
1.38	1.499	59	26.68	2.235	88	53.49	2.972	117
1.83	1.524	60	27.91	2.261	89	54.76	2.997	118
2.26	1.549	61	28.84	2.286	90	55.73	3.023	119
3.01	1.575	62	29.83	2.311	91	56.36	3.048	120
3.41	1.600	63	30.36	2.337	92	57.28	3.073	121
4.23	1.626	64	31.19	2.362	93	58.34	3.099	122
4.98	1.651	65	32.01	2.388	94	59.49	3.124	123
5.49	1.676	66	32.99	2.413	95	60.49	3.150	124
6.36	1.702	67	34.09	2.438	96	61.59	3.175	125
7.39	1.727	68	34.98	2.464	97	62.58	3.200	126
8.11	1.753	69	36.09	2.489	98	63.59	3.226	127
9.23	1.778	70	36.56	2.515	99	64.59	3.251	128
10.09	1.803	71	37.51	2.540	100	65.48	3.277	129
11.26	1.829	72	38.43	2.565	101	66.43	3.302	130
12.34	1.854	73	39.34	2.591	102	67.44	3.327	131
13.14	1.880	74	40.16	2.616	103	68.63	3.353	132
14.46	1.905	75	40.91	2.642	104			
15.23	1.930	76	41.93	2.667	105			

Table 5 Temperature data for Spiral Leg #3, °C

Date	Time	Depth, m (ft)				Date	Time	Depth, m (ft)			
dd-mm	hrs	0.61 (2)	1.83 (6)	3.05 (10)	4.27 (14)	dd-mm	hrs	0.61 (2)	1.83 (6)	3.05 (10)	4.27 (14)
2-Nov	0	4.2	3.1	4.2	0.2		266	-0.7	-1.6	-3.1	-3.9
3-Nov	25.5	-0.1	1.0	-0.2	-0.7	14-Nov	280	1.1	-1.4	-3.2	-3.8
4-Nov	40	-0.3	1.0	-0.2	-0.7		290	0.2	-1.6	-3.2	-3.9
	50	0.0		-0.3	-1.6	15-Nov	304	1.8	-1.6	-3.3	-4.1
5-Nov	63	0.0	2.2	-0.5	-2.0		314	0.0	-2.1	-3.3	-4.2
	74	0.0		-0.6	-2.2	16-Nov	328	3.5	-1.9	-3.3	-4.0
6-Nov	88	-0.1		-0.8	-2.9		338	1.2	-1.8	-3.3	-4.0
	98	-0.1		-1.1	-3.4	17-Nov	352	0.6	-2.1	-3.4	-4.2
7-Nov	111	-0.1		-1.5	-3.6		362	-0.8	-2.1	-3.4	-4.3
	122	-0.1		-1.7	-3.7	18-Nov	376	-0.1	-2.2	-3.5	-4.3
8-Nov	136	-0.1		-2.0	-3.8		386	-1.6	-2.3	-3.4	-4.1
	146	-0.3	0.0	-2.1	-3.9	19-Nov	400	-0.1	-2.2	-3.5	-4.1
9-Nov	160	0.4	0.4	-2.3	-3.8		410	0.2	-2.1	-3.5	-4.0
	170		0.4	-2.4	-3.9	20-Nov	424	-0.7	-2.4	-3.5	-4.2
10-Nov	184	0.0	0.4	-2.6	-4.0		434	-0.8	-2.4	-3.6	-4.3
	194	-0.3	-0.1	-2.7	-3.9	21-Nov	448	-1.6	-2.6	-3.6	-4.3
11-Nov	208	0.6	-0.2	-2.9	-4.2		458	-1.6	-2.5	-3.5	-4.1
	218	1.0	-0.2	-2.9	-4.1	22-Nov	472	-1.9	-2.6	-3.6	-4.2
12-Nov	232	-0.6	-1.3	-3.0	-4.2		482	-1.8	-2.6	-3.6	-4.2
	242	-0.1	-1.4	-3.1	-4.2	23-Nov	496	-1.5	-2.5	-3.6	-4.1
13-Nov	256	0.0	-1.4	-3.1	-3.9						

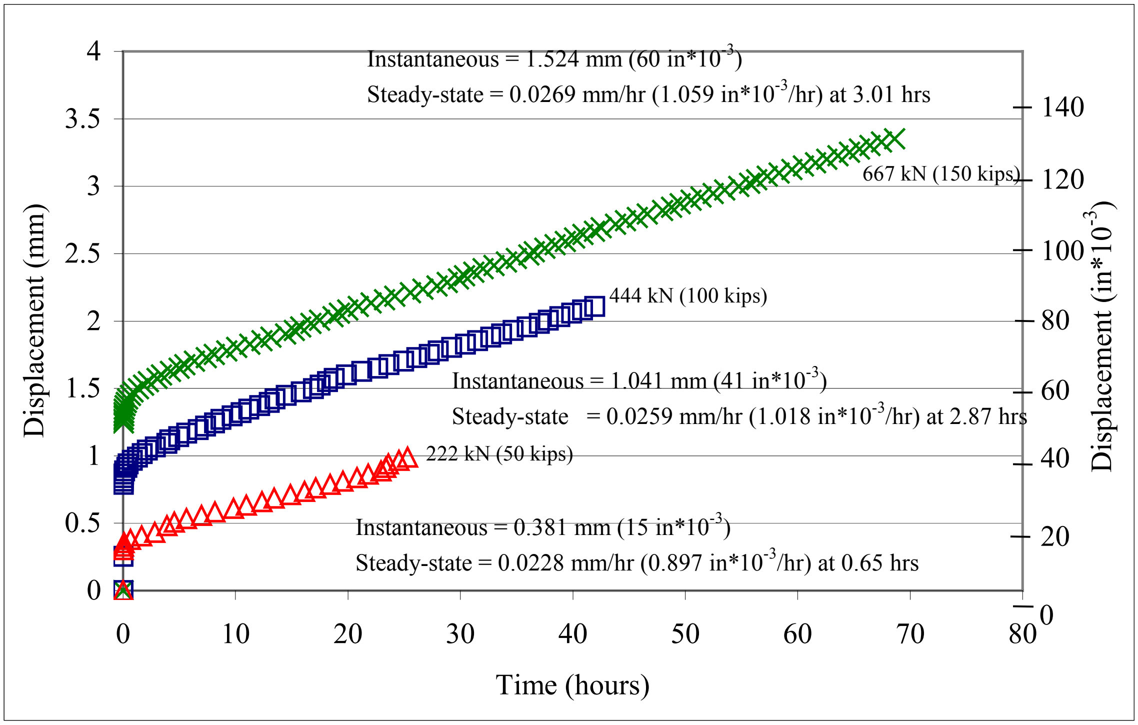

Figure 12 Pile displacement with time for Spiral Leg #3

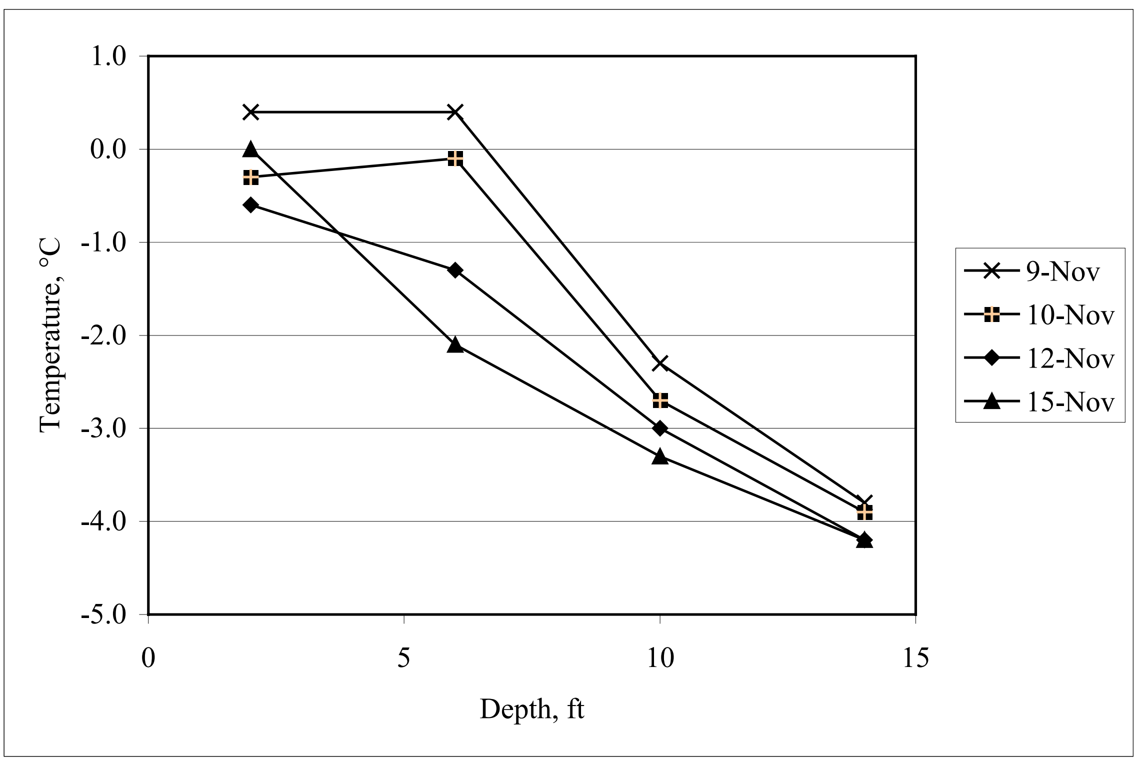

Figure 13 Pile temperature with depth for Spiral Leg #3

Table 6 Displacement data for Spiral Leg #2 with 442-kN (100 kips) load

Time	Displacement		Time	Displacement		Time	Displacement	
hrs	mm	0.001 in	hrs	mm	0.001 in	hrs	mm	0.001 in
0.00	0.000	0	1.06	0.914	36	30.03	1.803	71
0.0005	0.025	1	1.56	0.940	37	30.93	1.829	72
0.0017	0.051	2	1.78	0.965	38	31.88	1.854	73
0.0022	0.076	3	2.45	0.991	39	32.44	1.880	74
0.0030	0.102	4	3.25	1.016	40	33.13	1.905	75
0.0035	0.127	5	3.56	1.041	41	33.84	1.930	76
0.0042	0.152	6	4.26	1.067	42	34.68	1.956	77
0.0047	0.178	7	5.11	1.092	43	35.58	1.981	78
0.0052	0.203	8	6.05	1.118	44	36.56	2.007	79
0.0058	0.229	9	6.56	1.143	45	37.68	2.032	80
0.0060	0.254	10	7.16	1.168	46	38.43	2.057	81
0.0063	0.279	11	7.81	1.194	47	39.26	2.083	82
0.0072	0.305	12	8.85	1.219	48	40.11	2.108	83
0.0077	0.330	13	10.23	1.245	49	41.29	2.134	84
0.0085	0.381	15	10.96	1.270	50	42.21	2.159	85
0.0092	0.406	16	11.50	1.295	51	43.66	2.184	86
0.0093	0.432	17	12.65	1.321	52	45.03	2.210	87
0.0097	0.457	18	13.98	1.346	53	45.96	2.235	88
0.0102	0.483	19	14.91	1.372	54	47.08	2.261	89
0.0108	0.508	20	16.06	1.397	55	48.46	2.286	90
0.0110	0.533	21	17.16	1.422	56	50.38	2.311	91
0.0117	0.559	22	17.80	1.448	57	51.84	2.337	92
0.0133	0.584	23	18.45	1.473	58	53.3613	2.362	93
0.0163	0.610	24	19.46	1.499	59	54.4113	2.388	94
0.0183	0.635	25	20.24	1.524	60	55.1780	2.413	95
0.0230	0.660	26	21.24	1.549	61	57.2780	2.438	96
0.0352	0.686	27	22.24	1.575	62	59.4947	2.464	97
0.0430	0.711	28	23.13	1.600	63	62.0947	2.489	98
0.0463	0.737	29	24.08	1.626	64	64.2947	2.515	99
0.0963	0.762	30	24.73	1.651	65	65.9613	2.540	100
0.1630	0.787	31	25.31	1.676	66	67.5113	2.565	101
0.1963	0.813	32	26.09	1.702	67	69.1447	2.591	102
0.3130	0.838	33	26.96	1.727	68	70.2947	2.616	103
0.5963	0.864	34	27.71	1.753	69	71.8280	2.642	104
0.6797	0.889	35	28.93	1.778	70			

Table 7 Displacement Data for Spiral Leg #2 with 667-kN (150 kips) load

Time	Displacement		Time	Displacement		Time	Displacement	
hrs	mm	0.001 in	hrs	mm	0.001 in	hrs	mm	0.001 in
0.0000	0.000	0	23.52	2.007	79	69.49	2.972	117
0.0158	0.610	24	24.77	2.032	80	71.11	2.997	118
0.0233	0.787	31	25.64	2.057	81	72.74	3.023	119
0.0400	1.092	43	26.82	2.083	82	73.86	3.048	120
0.0567	1.143	45	28.49	2.108	83	75.24	3.073	121
0.0717	1.168	46	29.39	2.134	84	76.72	3.099	122
0.10	1.194	47	30.69	2.159	85	78.36	3.124	123
0.14	1.219	48	31.79	2.184	86	79.96	3.150	124
0.24	1.245	49	33.34	2.210	87	81.37	3.175	125
0.39	1.270	50	34.16	2.235	88	82.29	3.200	126
0.56	1.295	51	35.49	2.261	89	83.29	3.226	127
0.84	1.321	52	36.67	2.286	90	84.54	3.251	128
1.21	1.346	53	37.72	2.311	91	85.96	3.277	129
1.56	1.372	54	38.91	2.337	92	87.52	3.302	130
2.21	1.397	55	40.19	2.362	93	88.99	3.327	131
2.64	1.422	56	41.71	2.388	94	90.64	3.353	132
3.42	1.448	57	42.32	2.413	95	92.31	3.378	133
4.06	1.473	58	43.62	2.438	96	93.59	3.404	134
4.84	1.499	59	44.46	2.464	97	94.89	3.429	135
5.29	1.524	60	46.16	2.489	98	96.07	3.454	136
6.01	1.549	61	47.27	2.515	99	97.69	3.480	137
6.92	1.575	62	48.36	2.540	100	99.11	3.505	138
7.41	1.600	63	49.77	2.565	101	100.71	3.531	139
8.59	1.626	64	51.12	2.591	102	102.11	3.556	140
9.52	1.651	65	52.42	2.616	103	103.74	3.581	141
10.22	1.676	66	53.26	2.642	104	105.47	3.607	142
11.21	1.702	67	54.59	2.667	105	107.17	3.632	143
11.96	1.727	68	55.64	2.692	106	108.59	3.658	144
12.66	1.753	69	56.91	2.718	107	110.02	3.683	145
13.62	1.778	70	57.96	2.743	108	111.26	3.708	146
14.82	1.803	71	58.99	2.769	109	112.42	3.734	147
15.22	1.829	72	60.24	2.794	110	113.82	3.759	148
16.36	1.854	73	61.61	2.819	111	115.04	3.785	149
17.72	1.880	74	63.26	2.845	112	116.56	3.810	150
18.51	1.905	75	64.29	2.870	113	117.99	3.835	151
19.92	1.930	76	65.26	2.896	114	119.46	3.861	152
21.34	1.956	77	66.39	2.921	115			
22.19	1.981	78	68.04	2.946	116			

Table 8 Temperature Data for Spiral Leg #2, °C

Date	Time	Depth, m (ft)				Date	Time	Depth, m (ft)			
dd-mm	hrs	0.61 (2)	1.83 (6)	3.05 (10)	4.27 (14)	dd-mm	hrs	0.61 (2)	1.83 (6)	3.05 (10)	4.27 (14)
2-Nov	0	5.8	3.9	0.5	-0.3		266	0.4	-1.2	-1.6	-4.1
3-Nov	25.5	-0.1	0.1		-0.7	14-Nov	280	0.5	-1.3	-1.4	-4.1
4-Nov	40	0.0	-0.1	0.1	-1.0		290	0.5	-1.5		-4.1
	50	0.0	-0.1	0.5	-1.1	15-Nov	304	0.7	-1.5		-4.1
5-Nov	63	0.0	-0.1	-0.2	-1.7		314		-1.6		-4.2
	74	0.0	-0.1		-2.2	16-Nov	328		-1.7		-4.1
6-Nov	88	0.0	-0.1	-0.2	-2.7		338	0.1	-1.7		-4.1
	98	0.1	-0.1		-3.1	17-Nov	352	-0.1	-1.7		-4.2
7-Nov	111	0.1	0.0	-0.3	-3.3		362	-0.4	-1.9		-4.2
	122	0.1	-0.1	-1.0	-3.4	18-Nov	376	-0.7	-1.9		-4.2
8-Nov	136	0.5	-0.1	-1.6	-3.5		386	-1.1	-2.0		-4.2
	146	0.6	-0.2	-1.8	-3.6	19-Nov	400	-1.1	-2.1		-4.2
9-Nov	160	0.9	-0.2	-2.0	-3.8		410	-1.5	-2.1		-4.2
	170	1.2	-0.2	-2.0	-3.8	20-Nov	424	-1.7	-2.2		-4.2
10-Nov	184	0.0	-0.2	-2.1	-3.9		434	-1.9	-2.3		-4.2
	194	-0.1	-0.3	-2.5	-3.9	21-Nov	448	-2.1	-2.4		-4.2
11-Nov	208	-0.1	-0.4	-2.3	-3.9		458	-2.2	-2.4		-4.2
	218	0.0	-0.4	-2.1	-4.0	22-Nov	472	-2.4	-2.5		-4.2
12-Nov	232	-0.1	-0.6	-1.8	-4.1		482	-2.4	-2.5		-4.2
	242	0.1	-0.8	-1.6	-4.1	23-Nov	496	-2.5	-2.5		-4.2
13-Nov	256	-0.1	-1.0	-1.6	-4.1						

Table 9 Primary vs. Secondary Displacement methods

Leg 3 (All values are the change from the initial value)					
Time (hours)	Temperature °C	Potentiometer (in)	Transit (in)	Dial Gage (in)	Wire (in)
0	-17.0	0.000	0	-	0
21.81	-13.6	0.034	0.9375	-	0.016
27.35	-13.0	0.060	-	-	0.047
44.45	-17.0	0.083	-	-	0
Leg 2 (All values are the change from the initial value)					
Time (hours)	Temperature °C	Potentiometer (in)	Transit (in)	Dial Gage (in)	Wire (in)
0	-13.0	0	0	0	-
24.02	-10.6	.067	-	.067	-
91.55	-22.4	.153	-	.156	-
95.17	-22.8	.156	-	.1585	-

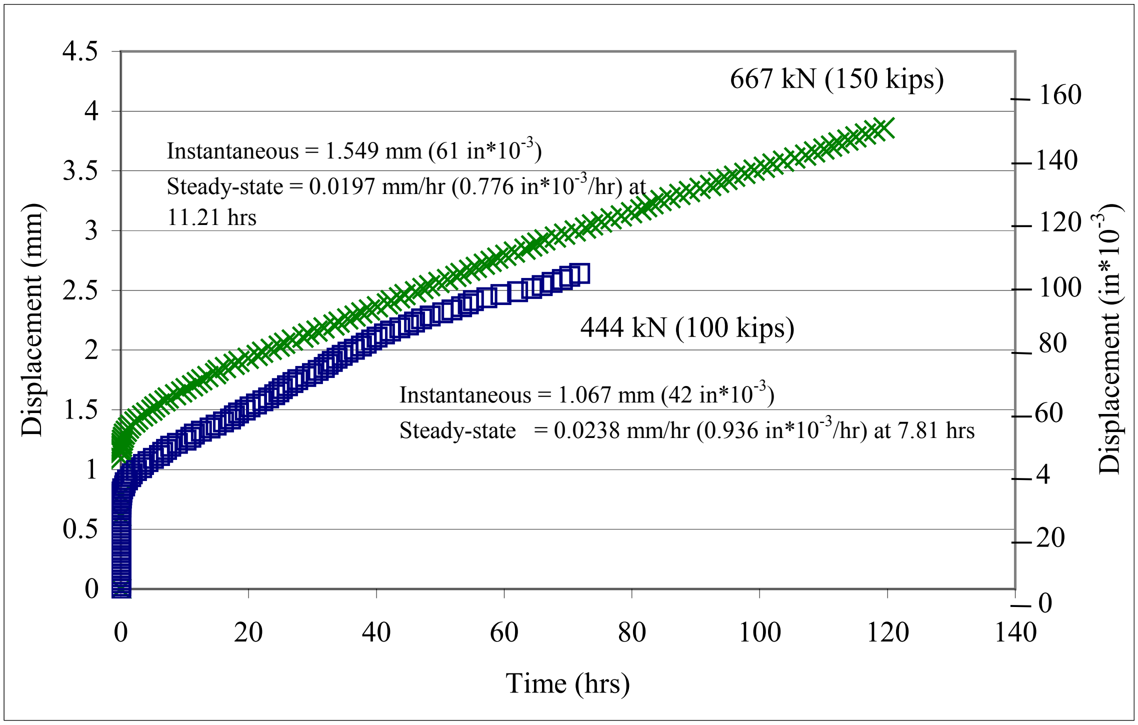

Figure 14 Pile displacement with time for Spiral Leg #2

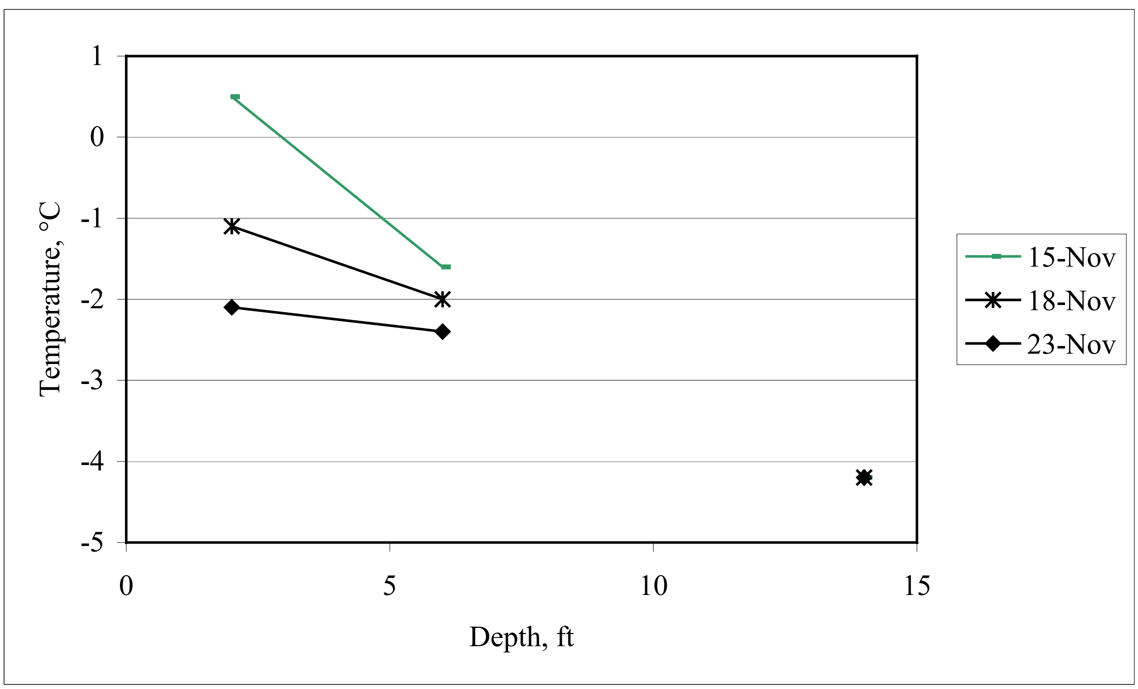

Figure 15 Temperature with time for Spiral Leg #2

PILE INSTALLATION AND REMOVAL

Accoring to Federico Lier (personal correspondence and report in Appendix B), the pile installation proceeded without any difficulties and did not differ from installation of smooth piles. The slurry was not vibrated when it was dropped to the oversized hole around the piles, which may have resulted in gabs directly below the helixes. Based on the tight schedule, the pile testing was started while the ground temperatures were still changing due to the freeze back of the warm slurry around the piles. The removal of piles was conducted by with a learning curve, but progressed mostly without difficulties. One of the legs had an obstruction in the fluid circulation system, refused to come out and was finally abandoned on the site. The pile was cut three feet below the ground surface.
Lier estimates that the total removal time per pile is estimated to be from 30 to 45 minutes and even less during production, as three to four piles can be hooked up to the steam plant at the same time.

CONCLUSIONS

The following conclusions that apply for the ice rich silty soil and pure ice found at the test site at the average temperature of –2°C (28°F) were obtained from the test results:

- The testing period represented the warmest permafrost temperatures, which is the worst case scenario for pile bearing capacity considerations and pile installation, and the best case scenario for pile removal.

- The Spiral Legs were installed with the same effort as smooth adfreeze piles. However, the slurry need to be vibrated during pouring to eliminate possible air gabs below the helixes. The Spiral Legs can be removed in an estimated 30 to 45 minutes assuming that the fluid circulation system works as designed.

- The test frame and the potentiometer functioned well for the given test period the air temperature being warmer than –23°C (-10°F). The dial gages worked well, too, and were handy in verifying the potentiometer readings.

- The observed pile displacement rate was about 0.025 mm/h (0.001 in/hr). With this rate, the allowable design displacement of 15 mm (0.60 in) would be reached in one month. The displacement rate was not affected significantly with the magnitude of the load. The capacity of the test frame did not allow for higher loads that would have led to a possibly higher displacement rates and failure.

- Vibration of the slurry during installation may improve the pile performance.

RECOMMENDATIONS

The following recommendations are made on the basis of the test results:

- More research before the Spiral Legs are used in the field.

- The following is recommended for possible future pile testing in the field: a larger capacity test frame (1334 to 1780 kN; 300 to 400 kips), a system that works down to –40°C (-40°F), and a flexible schedule to assure that the slurry around the pile is properly frozen. The slurry should be sampled at the plant, tested for gradation and water retention, and compared with the specifications. The slurry need to be vibrated around the piles.

- The idea of instrumentation of the actual Tundra Table Legs was considered. At this time, the authors and Dr. Helen Liu from the UAA consider that this data may not be usable for modeling purposes, because the piles will be installed in such a heterogeneous soil and the temperature is changing constantly. Laboratory testing in controlled environment would provide more valuable data. However, the instrumentation can be designed under a separate report if Anadarko wants to record a range of displacement for the Tundra Table sites.

- Since the spirals did not seem to offer the benefit of providing an acceptable displacement rate under the testing conditions, the future analytical and laboratory research should be optimizing the length of the smooth piles.

REFERENCES

Alaska Testlab, (2002), Laboratory Report for Michael Baker Jr. Inc for Anadarko Pile Test, reported 11/26/2002.

American Society for Testing and Materials, (1995). Designation: D 5780 Standard Test Method for Individual Piles in Permafrost Under Static Axial Compressive Load, West Conshohocken, PA.

Michael Baker Jr. Inc., (2002), Pile Test Geotechnical Investigation, submitted to Anadarko Petroleum Company.

Neukirchner, R. J., (1984) "Permafrost Temperature Profiles for Design of Piles by Creep Theory," Proceedings: Cold Regions Engineering Specialty Conference, April 4-6, 1984, Candadian Society for Civil Engineering, Montreal, Quebe

A. Leg Test Objectives

1. To test the vertical load bearing capacity of the leg in the permafrost.
2. To determine the response to cyclic loading of the leg.
3. To determine creep characteristics in both steady state and cyclic loading conditions.
4. To provide education and experience in the actual leg installation and removal process.
5. To establish the temperature profile outside of the leg during freeze-in, steady state, and melt-out conditions.
6. To establish the amount of energy required for the melt-out process by monitoring the temperature of fluid in and fluid out of the leg when fluids are pumped through the legs circulation system.
7. Establish a working relationship with the local agencies and universities for future support.

B. Preparation

1. Test Site
   a. The test site facility selected is the Alaska Telecom, Inc. Prudhoe Bay facility.

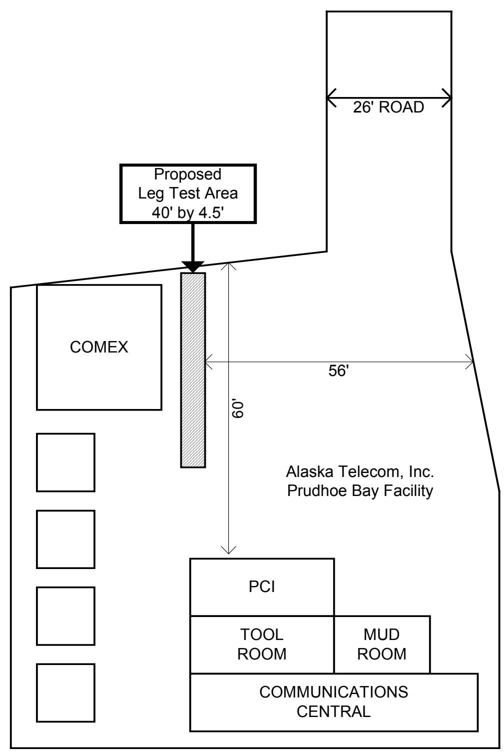

2. Survey and mark seven (7) hole positions as outlined below
   a. Insure area sufficient for maneuvering heavy equipment and handling thirty-five (35) foot long leg sections. **(Avoid risky areas with buried and/or aboveground power lines and guy wires).**
   b. Insure test fixture area selected is on level ground.

Anadarko Tundra Platform
Tundra Performance Test
Five Leg Test Fixture

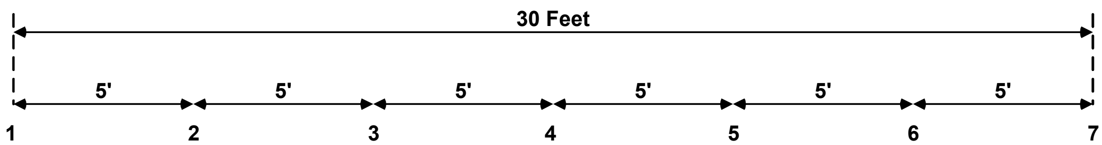

3. Insert five each twenty-four (24") inch screw in conductors as indicated below.

Anadarko Tundra Platform
Tundra Performance Test
Five Leg Test Fixture

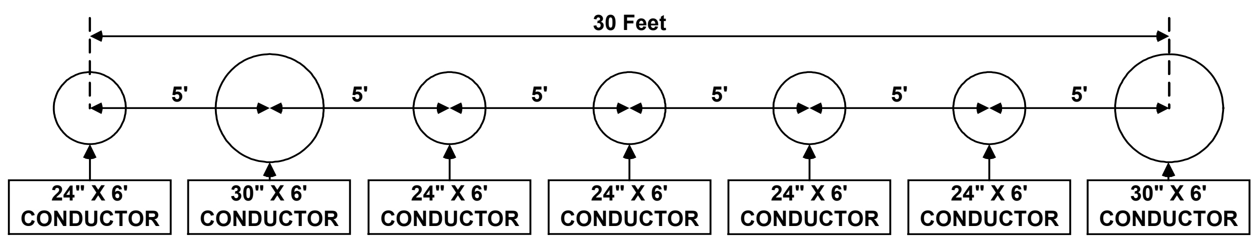

   a. Insertion shall be through the gravel pad until the surface of the tundra is encountered.
   b. Insure that Herculite or another suitable material is spread out to contain the soil/gravel removed from each hole, which will be in excess of three (3) cubic feet per linear foot of depth. The material removed should be stored on site for use in filling the excavated holes upon completion of the leg test project.

4. Insert two each twenty six (30”) inch screw in conductors as indicated below.

Anadarko Tundra Platform
Tundra Performance Test
Five Leg Test Fixture

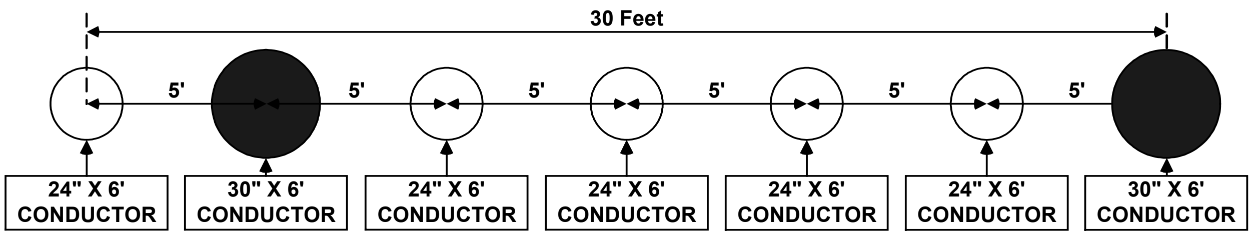

   a. Insertion shall be through the gravel pad until the surface of the tundra is encountered.
   b. Insure that Herculite or another suitable material is spread out to contain the soil/gravel removed from each hole, which will be in approximately five (5) cubic feet per linear foot of depth. The material removed should be stored on site for use in filling the excavated holes upon completion of the leg test project.

5. Drill two each twenty-six (26) inch diameter holes to a depth of thirty (30) feet below the tundra surface level.
   a. Sediment removed from each hole will be approximately one hundred and forty (140) cubic feet and should be stored on site to enable filling of excavated holes upon completion of the leg test project, or disposed of in accordance with local regulations.

6. Insert two each eighteen (18) inch diameter by forty (40’) feet length VSMs into the twenty-six inch holes to a depth of thirty feet below tundra surface. Stickup of the VSM of four (4’) feet is required above the gravel pad. (Reference drawing schematic on page 4).
   a. Slurry in place in the most optimum manner for quick freeze-in of the VSMs.

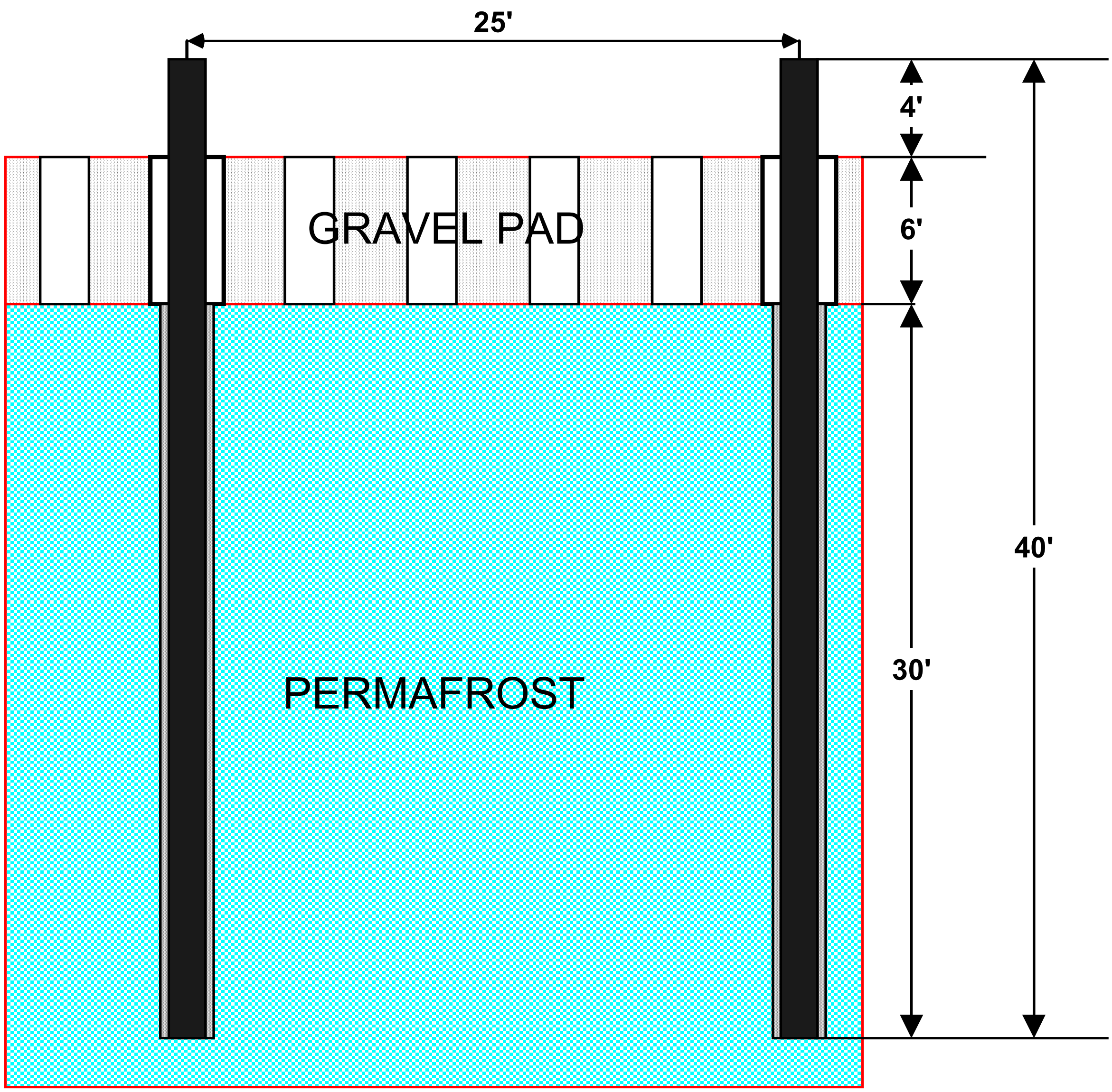
25'
4'
6'
GRAVEL PAD
40'
30'
PERMAFROST

C. Test Leg Installation

7. Installation of Non-Spiraled (Smooth OD) Leg.
   a. Drill (auger) the left hole (#1) a sixteen (16) inch diameter to a depth of twenty-five (25) feet below tundra surface level.
   b. Sediment removed from this hole will be approximately forty five (45) cubic feet and should be stored on site to enable filling of excavated holes upon completion of the leg test project, or disposed of in accordance with local regulations.
   c. Using a crane with a swivel connection between the leg and load line, pickup leg number 983 800 1 and insert into the hole.
   d. The leg should stop with the top four feet three inches (4' 3") above ground (gravel pad) level. Check to insure this measurement is accurate and also check with a level to ensure the leg is in a straight vertical position. Install wooden wedges between the leg and the caisson to ensure the leg remains true vertical.
   e. Lower temperature sensor probe, which is a thirty-four (34) foot length of 1 ½ inch square tubing, to a depth of twenty-five (25) feet below tundra surface and secure to the leg above the surface level of the gravel pad. (Top is painted blue with wire spool attached).
   f. Fill the annular void with sand and water slurry and allow leg to freeze in. Monitor temperature over time and observe and record when leg is firmly frozen in. (Reference drawing schematic on page 6).

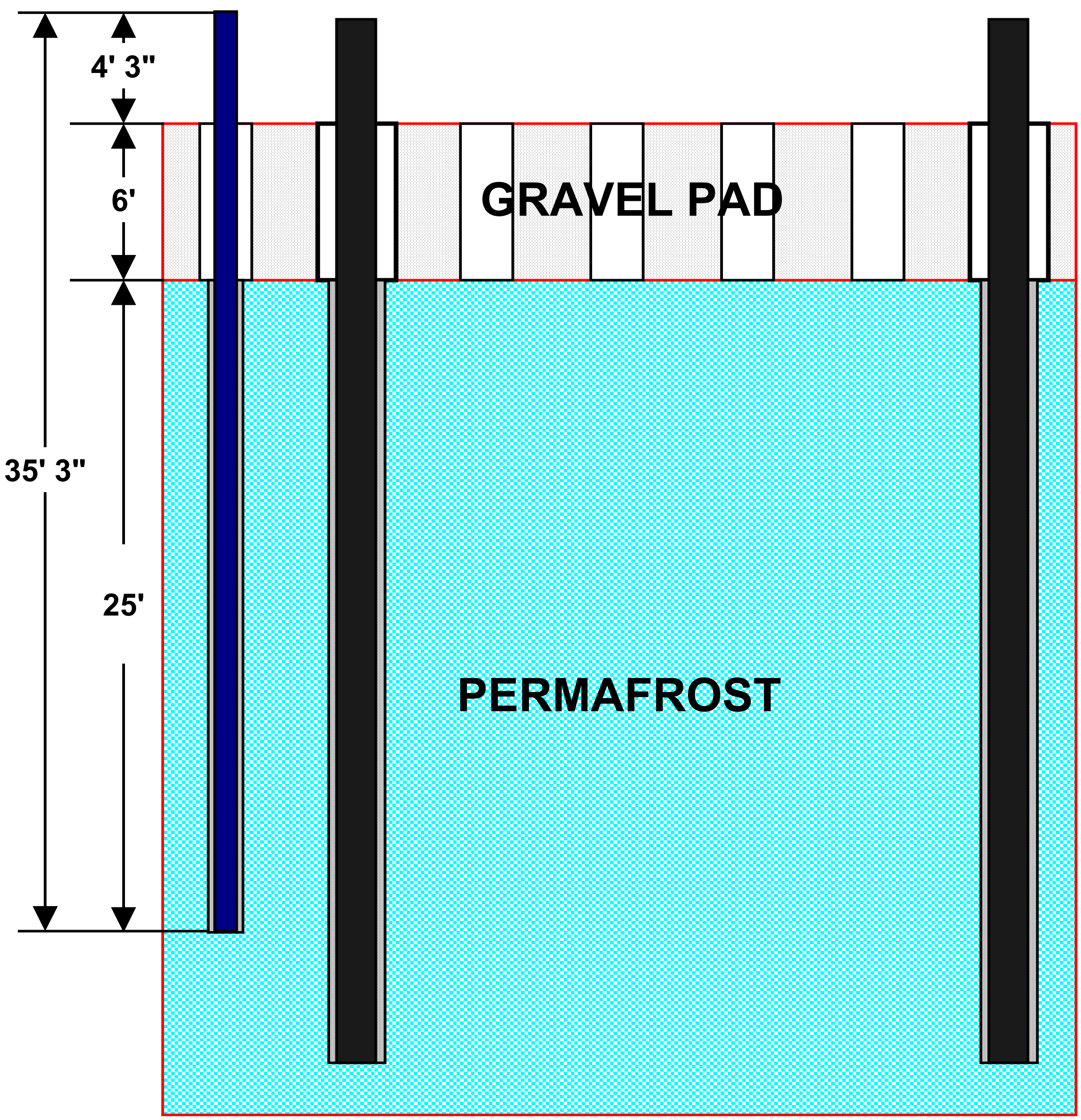
4' 3"
6'
35' 3"
25'
GRAVEL PAD
PERMAFROST

8. Installation of Helical Spiraled Leg(s).
    a. Drill (auger) the holes four (4) and five (5) a twenty (20) inch diameter to a depth of fourteen (14) feet.
    b. Sediment removed from this hole will be approximately twenty-five (25) cubic feet and should be stored on site to enable filling of excavated holes upon completion of the leg test project, or disposed of in accordance with local regulations.
    c. Using a crane with a swivel connection between the leg and load line, pickup leg number 983 800 2 and 983 800 3 separately and insert into the hole. The top of the legs should be six feet five inches (6’ 5”) above ground (gravel pad) level. Check to insure this measurement is accurate and also check with a level to ensure the leg is in a straight vertical position. Install wooden wedges between the leg and the caisson to inure the leg remains true vertical.
    d. Lower temperature sensor probe on each leg, which is a twenty-five (25) foot length of 1½ inch square tubing, to a depth of fourteen (14) feet below tundra surface and secure to the leg above the surface level of the gravel pad. (Top is painted blue with wire spool attached).
    e. Fill the annular void with sand and water slurry and allow leg to freeze in. Monitor temperature over time and observe and record when leg is firmly frozen in. (Reference drawing schematics on pages 8 and 9).

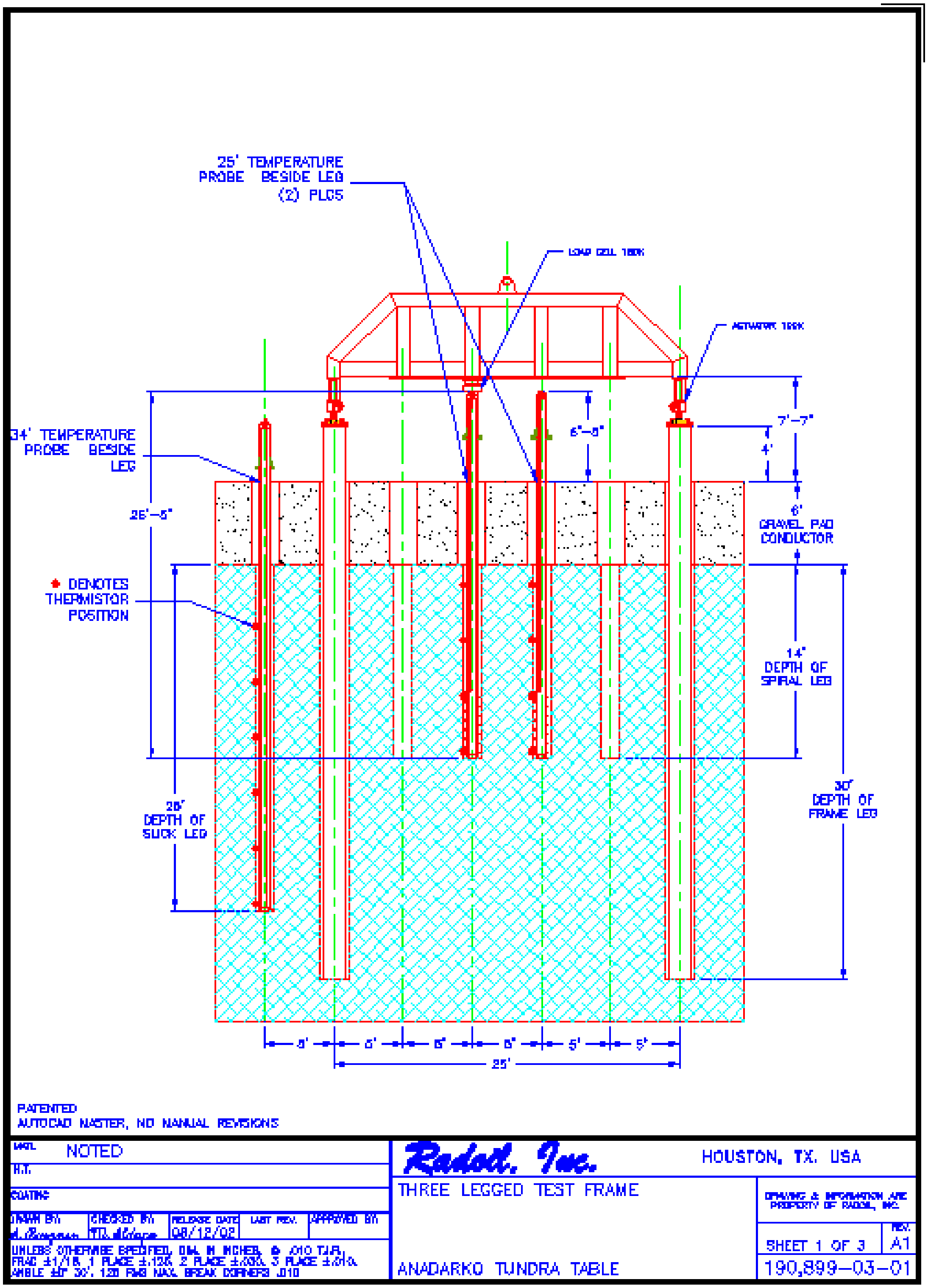
25' TEMPERATURE PROBE BESIDE LEG (2) PLCS
LOAD CELL 180K
ACTUATOR 180K
34' TEMPERATURE PROBE BESIDE LEG
6'-5"
7'-7"
4'
26'-5"
6' GRAVEL PAD CONDUCTOR
DENOTES THERMISTOR POSITION
14' DEPTH OF SPIRAL LEG
20' DEPTH OF SUCK LEG
30' DEPTH OF FRAME LEG
5'
5'
6'
6'
5'
5'
25'
PATENTED
AUTOCAD MASTER, NO MANUAL REVISIONS
MATL NOTED
H.T.
COATING
DRAWN BY
CHECKED BY
RELEASE DATE 08/12/02
LAST REV.
APPROVED BY
UNLESS OTHERWISE SPECIFIED, DIM. IN INCHES, ⊕ .010 T.I.R., FRAC ±1/16 1 PLACE ±.12X 2 PLACE ±.03X 3 PLACE ±.010 ANGLE ±0° 30', 120 RMS MAX. BREAK CORNERS .010
Radoil, Inc.
HOUSTON, TX. USA
THREE LEGGED TEST FRAME
DRAWING & INFORMATION ARE PROPERTY OF RADOIL, INC.
SHEET 1 OF 3
REV. A1
ANADARKO TUNDRA TABLE
190,899-03-01

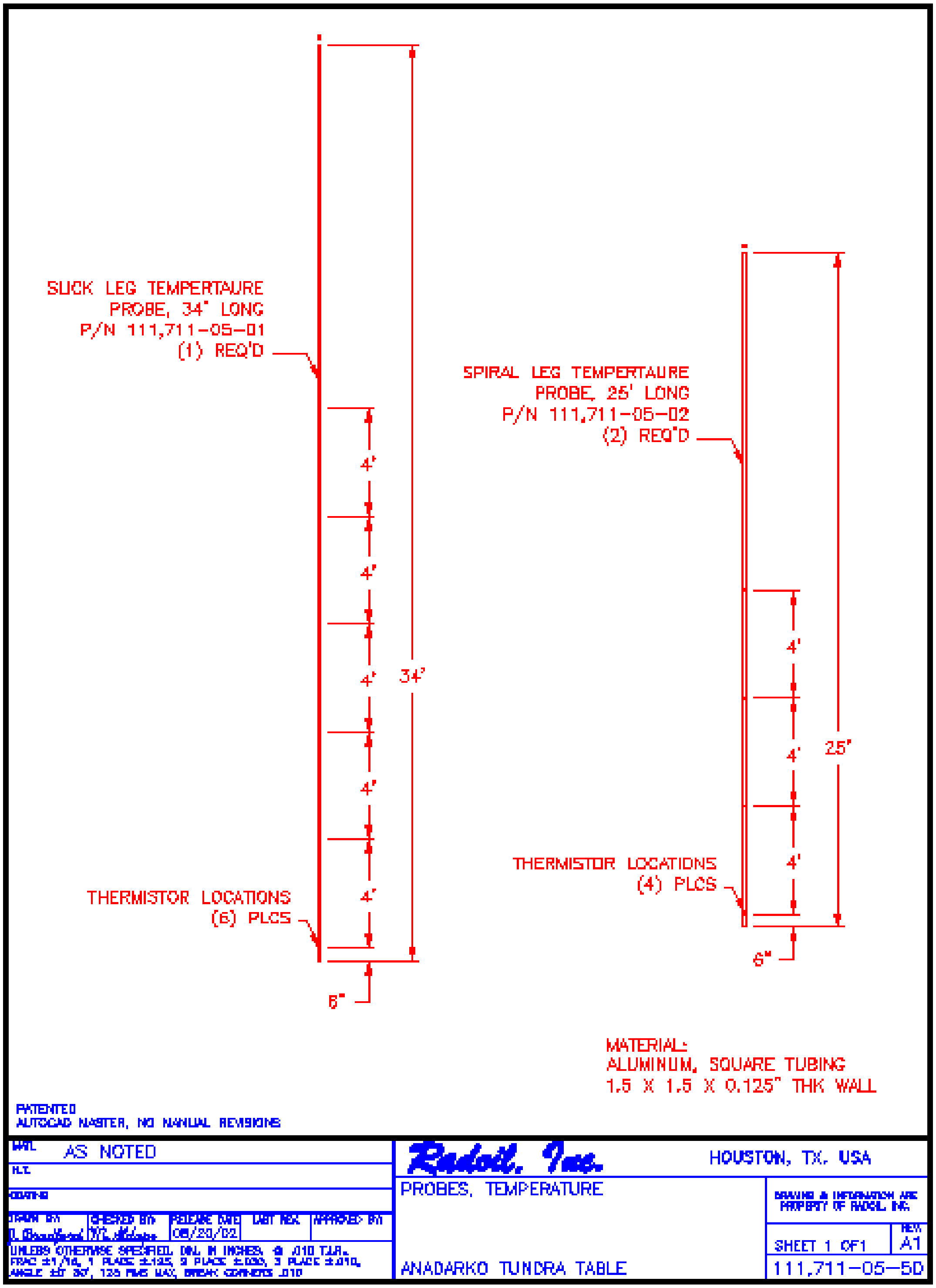
SUCK LEG TEMPERTAURE
PROBE, 34' LONG
P/N 111,711-05-01
(1) REQ'D
4'
4'
4'
34'
4'
4'
THERMISTOR LOCATIONS
(6) PLCS
6"
SPIRAL LEG TEMPERTAURE
PROBE, 25' LONG
P/N 111,711-05-02
(2) REQ'D
4'
4'
25'
4'
THERMISTOR LOCATIONS
(4) PLCS
6"
MATERIAL:
ALUMINUM, SQUARE TUBING
1.5 X 1.5 X 0.125" THK WALL
PATENTED
AUTOCAD MASTER, NO MANUAL REVISIONS
AS NOTED
08/20/02
Radoil, Inc.
HOUSTON, TX. USA
PROBES, TEMPERATURE
ANADARKO TUNDRA TABLE
SHEET 1 OF 1
A1
111,711-05-5D

D. Test Fixture Installation:

1. Lift the test fixture frame and set in position with the two connection plates landing on top of the 18 5/8 inch VSMs.
2. Weld the connection plates to the VSMs.
3. Connect the load cell to which ever leg is to be tested first.
4. Connect the data signal cables to the operators console.
5. Connect the electric cables to the electric supply circuit.

E. List of tools and equipment required:

1. Truck mounted auger drill with 12” and 16” augers available.
2. Crane with fifty-foot boom, load line, fast line, and minimum of 15-ton capacity.
3. Twenty-five foot tape measure.
4. Three-foot level.
5. Two each alignment strings.
6. Twelve eight inch wooden chocks with strap handles and safety lanyard attached.
7. Portable steam jenny and water supply.
8. Leg swivel and hoses to connect to steam jenny.
9. Appropriate hand tools to attach swivel and connections.
10. One eight-foot stepladder.
11. One twenty-foot telescoping ladder.

APPENDIX B

Observation, Conclusions & Recommendation for The Pile Load Test Leg Removal

by
Federico Lier P.E.
December 9, 2002

Observation

Background: Test Pile Leg#2 & 3 were tested for their load capacity. The bottom five feet is helical (spiral) and were placed 20 feet below existing ground surface of which 14 feet were embedded in gravel. Leg#1 is a slick pile and was placed 31 feet below ground surface of which 25 feet were embedded. The legs have internal piping to pump a cooling or heating media though it to speed the freeze back or their removal. Freeze back temperatures along the piles varied between 0 to –5 degrees Celsius. The steam applied had a temperature of 298 degrees Fahrenheit at 50 psi. The temperature will vary with pressure.

The piles were removed on December 8, 2002. (See Daily Field Report 12-08-02 for a minute-by-minute log of the removal.

Removal - Leg#2: A fitting was welded to one of the openings to the heat/cooling pipe. Also two ¾ inches thick steel ears with a hole were welded on both sides of all three legs. This was needed to be able to pull on the piles. The existing pull connecters could not be used as they inhibit the access to the heat/cooling coils. An air compressor was connected to Test Leg#2 pushing warm air through the heat/cooling coils. The air was connected at the end of the day and left there for approximately 14 hours. Steam from a portable steam plan was connected to the heat/cooling coil. For about two to three minutes the intake fitting was leaking and much steam escaped before entering the pile. Not much steam exited the end of the internal piping for about five minutes after which an ample amount of steam escaped. Initial low escape and excessive leaking of steam would indicate that the steam condensed quickly at the beginning. 34 minutes after commencing the steaming Leg#2 was pulled out with a Case 821 (Front-end-loader/Fork-lift) with no visual resistance. This would indicate that the leg could have been pulled faster. The pile could then be removed with a crane (Grover RT 745).

APPENDIX B

Removal - Leg#3: Compressed air was placed on this leg for about one hour. Steam was connected with no escape of steam from the outlet for approximately 5 minutes after which bubbling water escaped. The water was hot and at intervals sprayed into the air like a geyser. The Case 821 was hooked up to the leg after about 15 minutes but the leg would not move. The forklift was left with a constant pull so we would know when the leg was thawed sufficient to be pulled. This occurred after 22 minutes after connecting the steam.

Removal - Second VSM: As the top of both VSM's is open the steam hose was just lowered into the inside of the VSM's. Initially the hose, which hade a 7 feet long steel pipe at the end, was only lowered to about 15 feet below the top of the pipe. After 24 minutes the forklift tried to move the pile without success. The steam plant was then moved closer to the piles, as the hose from the steam plant was not long enough to lower it to the bottom of the pile. Nine minutes after lowering the steam hose to the bottom of the VSM the pile could be removed without any visible effort. Total removal time was 33 minutes and nine minutes after the steam was lowered to the bottom.

Removal – First VSM: Steam was lowered to the bottom of he VSM and pulled after 18 minutes without any visible effort of the forklift indicating that the pile could have been removed quicker.

Removal – Leg#3: As the air compressor was connected to the heat/cooling coil opening it became obvious that the heat/cooling pipe was plugged. The plug (ice, dirt or fabrication error) could not be removed even with high pressure. Steam was then connected with no steam escaping from the outlet. Most the steam escaped at the intake fitting. Pile got hot at the first five feet. Pile would not move even with constant effort of the forklift. After 75 minutes the steamer was disconnect from the top and lowered on the outside of the pipe to a depth of approximately 17 feet below the ground surface. The water level rose to approximately three feet of the existing ground surface. 60 minutes later we decided to cut the top of the pile to lower the steam to the inside. Only one side of the heat/cooling coil had a pipe connected. The Steam was lowered but could not get passes ten feet because of an obstruction. Almost got the hose stuck and it took a consederable effort to get it untangled. We continued to steam from the inside for another 60 minutes without success. It was then decided that we would cut the pipe and abandon it on site. The pile was cut three feet below the ground surface.

APPENDIX B

Other: The location for the test was marginal and the room to move equipment and piles was inadequate. At times the limited space was a safety hazard.
Equipment should be inspected and be in good working condition before moving to a remote location.

Conclusion

From the removal it became evident that steam is a quick and effective way to remove the pipe out of the frozen ground. Steam is easy to produce and applied. Steam plants are readily available on the North Slope and mobile. Heat and pressure can be increased up to ~400 Degree Fahrenheit at 175 psi. Total removal time per pile is estimated at 30 to 45 minutes and less during production as three to four piles can be hooked up to the steam plant at the same time.

Recommendation

Several important observations were made, which need to be taken in to consideration for the successful removal of the tundra legs.

- For the steam to work it has to applied at the bottom of the pile.
- Heat/cooling inlet and outlet on the pile should be better accessible and not interfere with pull fittings.
- In and outlet of the heat/cooling should be tested for plugs and obstruction before leaving the manufacturer.
- In and Outlet should be capped and have a connector to easily fit the steam fittings so no field welding and changes will be needed.
- In and Outlet to the heat/cooling coil should be just above the ground surface. This would help to lower the distance the steam has to travel to reach the bottom of the pile, which will increase the removal of the pile and decrease condensation.
- Fittings on the steam plant and into the pile need to be tight.
- If the steam can be moved quickly to the bottom of the pile no hot air is needed to pre-warm the steal.
- Piles should have a better mechanism for pulling and removal with the forklift/crane. The piles are to slick to be hoisted with a rope or chain. The existing mechanism is to cumbersome needing special tools and will slow down the removal process specially if temperatures are below freezing.

APPENDIX C

THERMISTOR DATA

Date	Time	Temperature, °C Depth, m (ft)						Air Temperature, °C
dd-mm	hrs	0.61 (2)	2.13 (7)	3.35 (11)	4.57 (15)	6.10(20)	7.62 (25)	
2-Nov	0	4.7	0.1	0.9	0.0	0.5	3.7	
3-Nov	25.5	3.1	0.5	-2.2	-3.8	-3.8	-2.3	
4-Nov	40	-0.4	-0.2	-2.7	-4.3	-3.9		
	50	2.6		-3.1	-3.6	-3.6		
5-Nov	63		-1.4	-3.3	-4.6	-4.2		
	74		-1.6	-3.3		-4.6		
6-Nov	88		-1.9	-3.4		-4.7	-4.3	
	98		-2.1	-3.4	-4.9	-4.5		
7-Nov	111		-2.3	-3.8	-4.0	-4.7		
	122		-2.4	-3.8	-4.9	-4.9	-4.6	
8-Nov	136			-3.7	-4.3	-4.9		
	146		-2.5	-3.8	-4.9	-4.9		
9-Nov	160		-2.7	-3.8	-4.7	-4.9		
	170		-2.4	-3.8	-4.3	-4.9		-17.0
10-Nov	184		-2.9	-3.8	-4.2	-5.0		-13.6
	194		-2.2	-3.9	-4.1	-5.0		-13
11-Nov	208	0.0	-2.5	-3.9	-4.2	-5.0	-5.5	-17.0
	218	-1.1	-3.2	-4.0	-5.2	-5.0	-5.5	-13.4
12-Nov	232	-1.1	-2.7	-3.9	-4.2	-5.0	-5.5	-13.06
	242	-1.4	-2.9	-3.9	-4.5	-5.0	-5.5	-13.92
13-Nov	256	-0.7	-2.5	-3.9	-4.3	-5.1	-5.6	-14.98
	266	-0.3	-2.2	-3.9	-3.8	-5.1	-5.6	-12.05
14-Nov	280	-0.5	-2.5	-4	-4.6	-5.1	-3.9	-14.31
	290	-0.7	-2.5	-4	-4.4	-5.1	-5.6	-14.43
15-Nov	304	-1.4	-3.1	-4	-5	-5.1	-4.9	
	314	-1.3	-2.7	-4	-4.3	-5.1	-5.6	-13.02
16-Nov	328	-1	-2.6	-4	-4.3	-5.1	-5.6	-7.67
	338	-0.9	-2.7	-4	-4.5	-5.1	-1.8	-10.57
17-Nov	352	-1.4	-3	-4	-4.7	-5.1		-18.23
	362	-1.3	-2.8	-4	-4.5	-5.1	-1.9	-20.84
18-Nov	376	-1.5	-3	-4	-4.7	-5.1	-5.6	-18.43
	386	-1.2	-2.9	-4	-4.3	-5.1	-4.2	-18.31
19-Nov	400	-1.4	-3.1	-4	-4.8	-5.1	-5.5	-22.36
	410	-1.2	-2.9	-4.1	-4.8	-5.2	-5.3	-22.83
20-Nov	424	-1.4	-3.1	-4.1	-4.6	-5.1	-5.2	-22.52
	434	-1.6	-3.1	-4	-4.8	-5.1	-4.8	-21.56
21-Nov	448	-1.6	-3.1	-4	-4.6	-5.1	-5	-22.31
	458	-1.3	-2.9	-4	-4.3	-5.2	-5.7	-20.88
22-Nov	472	-1.4	-2.9	-4	-4.3	-5.1	-5.6	-19.88
	482	-1.4	-2.9	-4.1	-4.5	-5.1	-5.6	-17.71
23-Nov	496	-1.5	-3	-4.1	-4.5	-5.1	-3.3	-14.45

Appendix D: Coalbed Methane Studies at Hot Ice #1 Gas Hydrate Well (USGS)

First Report

Charles E. Barker
US Geological Survey
Denver, CO 80225
barker@usgs.gov

Coal Gas Content Measurements

Six coal seams were sampled (160, 255, 650, 840, 960 and 1090 ft TVD) in the initial drilling phase to the casing point at 1400 ft. Canister desorption measurements indicate that coal samples from 160 to 960 ft TVD, taken from seams deeply embedded within the permafrost, did not contain significant sorbed coalbed gas. Somewhat dramatically, the last coal seam cored before the casing point at 1400 ft did have a measurable gas content. This coal seam (1090 ft TVD) yielded about 15 standard cubic feet of gas/ton of coal (SCF/ton).

Based on a streak test, the lack of complete gelification and the presence of still distinct tree limbs and so forth, these coals appear to be lignite to perhaps subbituminous C rank. In comparison, the somewhat higher rank subbituminous B to A coals of the prolific coalbed methane producing Powder River Basin of Wyoming contain about 25 SCF/ton. Gas content usually increases with depth and rank, so the deeper coals expected immediately below the 1400 ft TVD casing point will have higher gas contents.

Ice Veins in Coal

Coal studies also show that coarsely crystalline ice in veins (**Figure 1**), whose crosscutting relationship to coal bedding indicates they result from water injection and freezing in place. The injection and freezing process may occur in multiple episodes as indicated by layered vein structures (**Figure 2**). Injection of water (now seen as ice) is indicated by the ice crosscutting the coal seam bedding (**Figures 3 and 4**) in all seams encountered up to about 960 ft TVD and in, at least one case, has been injected in such a manner as to cause brecciation of coalbed (**Figure 5**). This injection and fracturing process is thought to be generated during initial stages of permafrost formation when cooling causes formation water to expand, pressuring the strata and inducing water movement. This pressurized water preferentially invades the structurally weaker coal seams within the more competent clay-rich siliciclastic sedimentary strata.

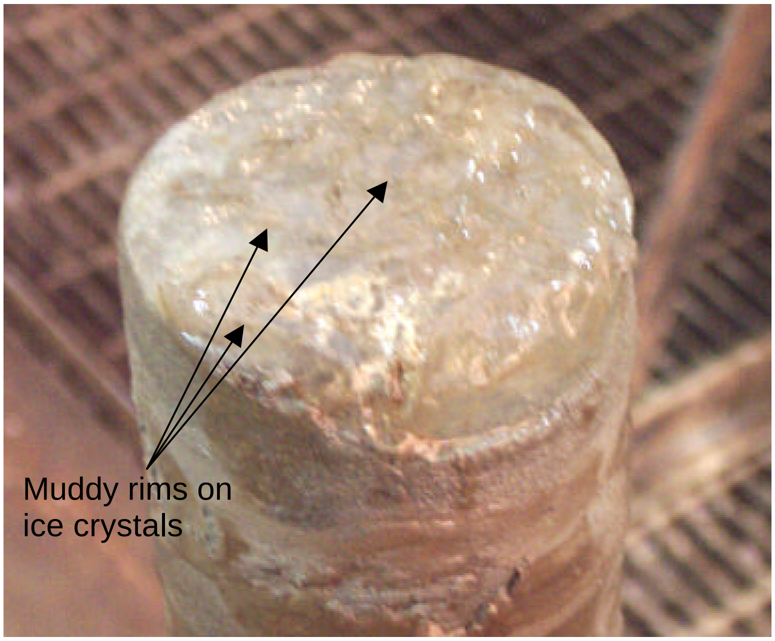

Figure 1. Broken core surface composed of coarsely crystalline ice crystals whose boundaries are delineated by muddy rims. Ice vein is cutting a matrix-supported conglomerate. Depth is about 520 ft TVD. When in gauge, core diameter is about 3.4 inches.

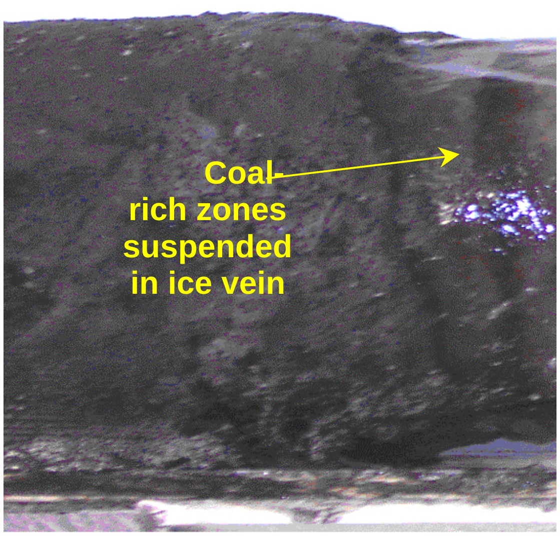

Figure 2. Layered ice vein, Anadarko Hot Ice #1 Well, 252.3 ft TVD. When in gauge, core diameter is about 3.4 inches.

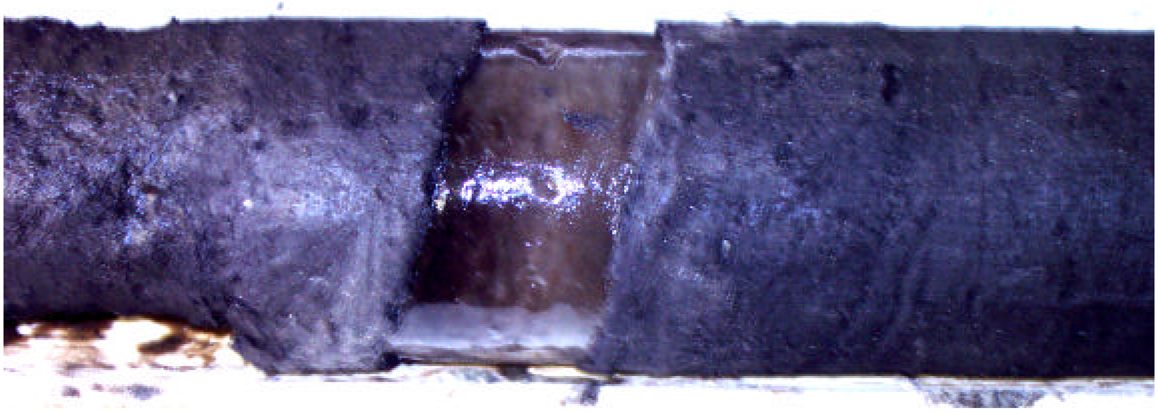

Figure 3. Ice vein, Anadarko Hot Ice #1 Well, 252.3 ft TVD. When in gauge, core diameter is about 3.4 inches.

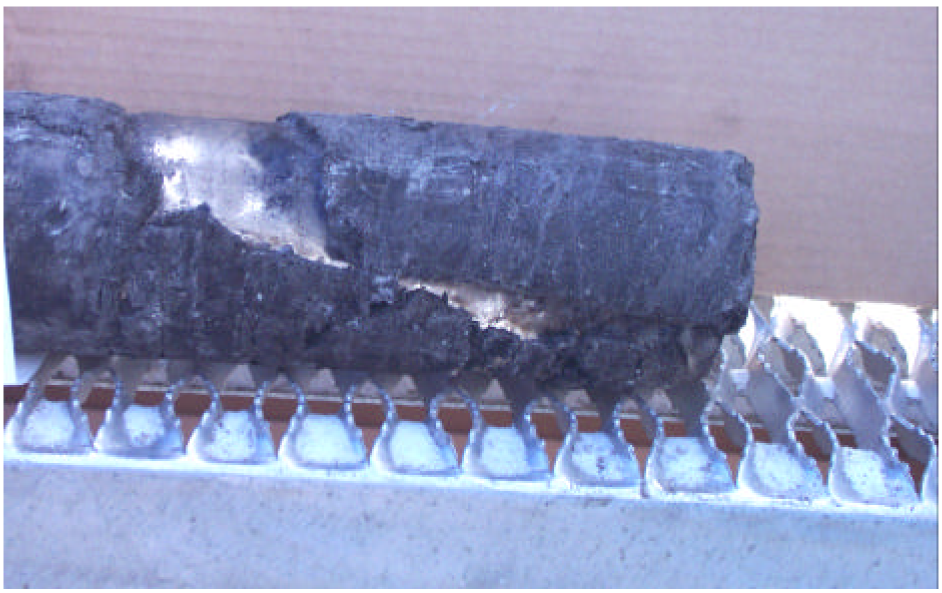

Figure 4. Ice vein cross-cutting coal, Anadarko Hot Ice #1 Well, 650-654 ft TVD. When in gauge, core diameter is about 3.4 inches.

Figure 5. Another view of core shown in Figure 4 showing brecciation of the coal by the injection and freezing process that forms ice veins in Hot Ice Well, 650-654 ft TVD. Note brownish-black coloration of the coal typical of low rank coal. When in gauge, core diameter is about 3.4 inches.

Discussions with Tim Collett (USGS, Denver) and a preliminary literature search indicate these ice-vein features observed in the Hot Ice well occur at a much greater depth than previously reported. The photographs of these features clearly show ice veins 5 to 10 cm thick crosscutting the coalseam bedding. This phenomenon was observed in all of the gas-barren coalbeds down to 960 ft TVD. The 15-inch thick gassy coal bed at 1090 ft TVD did not display ice veining.

The relationship between the gas-barren coal seams and ice veining disrupting the coal seams in particular and the rock seals in general throughout the sedimentary column that may a genetic relationship. The ice veins may act to disrupt the gas-tight seals needed to retain gas in shallowly buried coal seams. Further, the relationship suggests a mechanism for the nearly complete gas loss in permafrost bound coals by gas seal disruption followed by simple buoyant gas seepage. This process may be enhanced by forced gas migration from the coals by solution or, as entrained bubbles, in the initially mobile water phase still present within the forming permafrost and eventual loss to the atmosphere through the now disrupted gas seals.

Probably most intriguing to science in general is that if this ice formed during permafrost formation about 1.5 Ma, ice in the coal seams at the Hot Ice well is on the order of a million years old. Samples taken for composition and isotopic analysis of the ice may yield data that have interesting paleoclimate implications as well as contain information on permafrost formation processes.

Implications of Gas-Barren Coals within the Permafrost

The lack of gas in shallower coal seams deeply embedded in the permafrost was forecast from gas log studies in wells across the North slope basin (Collett and others,

1989) and coal desorption data measured by the USGS at the Tarn field in 2000 – but had not been confirmed by coal core sampling. Thus, in the Hot Ice well, for the first time, we obtained coal core data confirming our hypothesis about the loss of gas from shallowly buried coals embedded within the permafrost.

A question then arises: Why are these coals still barren of gas after their apparent depletion about 1.5 Ma when the permafrost formed? Chemically low rank coals are highly gas prone and capable of continued generation of copious amounts of microbial gas over the 1.5 Ma available since depletion. The coals are also prone to sorbing gas sourced from upward migration of deep basin gas. These gases can refill breached and depleted coalbed reservoir – if the gas seals are reconstituted when the permafrost forms and cements the sedimentary column. We conjecture that this process does not occur at the Hot Ice well for several reasons. One, biogenesis is likely markedly slowed at below-freezing temperatures. Second, upwardly seeping deep basin generated gases are likely bound up in the hydrate zone below the permafrost. Finally, perhaps the gas seals have not reconstituted above the coals and gas continues to escape to atmosphere.

Potential for Coal Seams after 1400-ft TVD Casing Point

The potential for coals when drilling recommences below 1400 ft is high. Log analysis for nearby wells indicates good chances for intersecting additional coal seams and carbonaceous shale (below the 1400 ft casing point) over a depth range of 1400 to 1550 ft TVD. Of particular interest to the coalbed methane study is a 5-ft thick coal bed indicated from log studies at 1525 to 1530 ft.

It cannot be stressed enough that collecting coal core from below the base of the permafrost is crucial to confirming the hypothesis for the mechanism for gas-barren coalbeds in permafrost.

Appendix E: FY2002 Studies—Hydrate Preservation in Cores (LBNL)

George J. Moridis
Earth Sciences Division, Lawrence Berkeley National Laboratory

1. INTRODUCTION

In support of a field test planned by the Maurer/Anadarko team, LBNL investigated hydrate preservation during core recovery by means of numerical simulation. In this report we discuss the simulated systems, their conditions, and the corresponding results. We identify important parameters controlling hydrate dissociation and preservation during core recovery from gas hydrate that are representative of typical permafrost accumulations.

2. SYSTEM DESCRIPTION

We considered cores 10 ft long, with a steel sleeve thickness of 1/8 in. We investigated the effects of the core diameter D (2.5 in and 3.345 in), hydrate saturation S_H (85% and 50%), initial hydrate temperature T (9 ^oC and 4 ^oC), permeability k (10 mD, 100 mD and 1000 mD), and mud temperature T_m (0 ^oC and –5 ^oC). In all the studies, the porosity ϕ = 0.30 and the initial pressure P = 1051 Psia. We assumed a uniform and isotropic porous medium and a kinetic dissociation model. The core boundaries are exposed to (a) a linearly decreasing hydrostatic pressure and the mud temperature T_m while it is being raised to the surface (740 m in 15 min), and (b) a constant atmospheric pressure and T_m during another 15 min of study/observation.

3. RESULTS AND CONCLUSIONS

A total of 48 simulation sets were conducted. The simulation results lead to the following conclusions:

A. Depressurization is the main dissociation mechanism during core recovery.

B. Due to the strong endothermic nature of the reaction, the cores experience significant cooling during dissociation.

C. Lower permeability leads to slower advancement of the radial dissociation front, a smaller dissociated zone, a steeper radial saturation gradient, and higher hydrate preservation in the core.

D. Hydrate preservation declines rapidly with time. The clear implication is that hydrate preservation can be maximized if the core is pressurized as early as possible.

E. The pressure distribution in the cores exhibits a remarkable radial uniformity, and is characterized by a rapid pressure decline with time and a narrow depressurized along the outer perimeter/boundaries of the core. The maximum pressure is observed at the bottom of the simulated half core. The implication is that better hydrate preservation is achieved in longer cores.

F. The temperature distribution in the core appears quite uniform in z, while significant radial variations (i.e., in the r direction) are observed. The core temperature declines continuously during the 30-min simulation period because of the strongly endothermic nature of the hydrate dissociation (leading to heat absorption from their surroundings and resulting in temperatures below freezing). The temperature decline follows the movement of the dissociation front, i.e., from the periphery (exposed to declining pressures and subject to dissociation through depressurization) toward the center of the cylindrical core.

G. The hydrate saturation profiles show that dissociation is initially limited to a narrow band along the outer surface of the hydrate-impregnated core. As time advances, the dissociated region keeps expanding by moving inward radially, while the high-saturation region shrinks continuously. The highest concentration of hydrates is encountered near the center of the core.

H. A lower mud temperature results in substantially (and consistently) higher hydrate recovery because the colder hydrates (in contact with the mud) will remain stable at a lower pressure. Thus, the coldest possible mud should be used for hydrate core recovery. It is important, however, that the mud should not contain large amounts of salts or alcohols because these substances are hydrate inhibitors and tend to promote dissociation.

I. Higher initial hydrate saturation leads to higher hydrate preservation in the cores because of the availability of larger amounts of hydrates and lower permeability.

J. Higher hydrate preservation is observed in samples with a larger core diameter because of the availability of larger amounts of hydrates.

K. Lower formation temperatures enhance hydrate preservation because of slower dissociation and lower effective permeabilities over longer times (as high hydrate saturations are maintained longer).

Thus, hydrate recovery in cores is enhanced by (i) a low intrinsic permeability, (ii) a low initial hydrate temperature, and (iii) a high hydrate saturation. For a given set of initial hydrate conditions, hydrate preservation is maximized by (iv) minimizing the time from coring to storage, (v) maximizing the core diameter, (vi) using long cores, (vii) using the lowest possible mud temperature, and (viii) by using a mud with no salts or alcohols.

FY2003 Studies
Scoping Analyses Of Gas Production From Hydrates

George J. Moridis
Earth Sciences Division, Lawrence Berkeley National Laboratory

1. INTRODUCTION

In support of a field test planned by the Maurer/Anadarko team, LBNL is conducting scoping studies involving possible preliminary scenarios of gas production from hydrate accumulations in the North Slope, Alaska. In this report we discuss the conditions and characteristics of the scenarios under investigation, the range of possible production strategies (as dictated by the geologic conditions), and the approach involved in the determination of (and sensitivity to) important parameters affecting gas production from hydrates.

2. SYSTEM DESCRIPTION

We are considering two different hydrate zones. The first belongs to the Ugnu formation, and is characterized by a pressure P = 700 psig and a temperature T = 36 ^{o}F at the bottom of the hydrate interval. The intrinsic permeability of this system ranges between 10 mD and 400 mD, and the water salinity (as indicated by the Cl concentration in the native water) is 1500 ppm. The second zone belongs to the West Sak formation, and is deeper and warmer (P = 970 psig and T = 45 ^{o}F at the bottom of the hydrate interval). This zone has an intrinsic permeability of 400 mD and a Cl concentration of 15,000 ppm in the native pore water.

In both cases, it is assumed that the thickness of the hydrate interval is 20 ft, the porosity ϕ = 0.30, and the initial pore fluids are just hydrate and water (i.e., there is no native gas initially in the hydrate interval). Two hydrate saturation S_H values are considered: 40% and 80%. Additionally, the hydrate interval is assumed to be bounded by no-flow boundaries. Thus, it is not in contact with an underlying free-gas zone or with an aquifer. The result of this combination of boundary conditions and initial hydrate saturation may severely affect flow-based dissociation (i.e., depressurization) in the case of S_H = 80% because of the corresponding very low water relative permeability.

3. APPROACH

At this early preliminary stage, only single-well production is being considered. The possible production strategies are dictated by the site geology and by the hydrate characteristics. Thus, the following production scenarios are being simulated:

A. Depressurization through water production. As previously indicated, this may be a challenging scenario because of the low relative permeability of water in such a system (especially at the S_H = 80% level). A possible mitigation strategy is hydrate fracturing. However, this approach involves significant uncertainty because of lack of knowledge on the behavior and characteristics of fractures in hydrate-bearing sediments and the low fracture volumes.

B. A huff-and-puff approach. The flow component of this approach may face the same challenges discussed in item (a). A possible adverse effect is the increase in pressure during the injection phase, which will lead to an increase in the dissociation temperature (and may even prevent dissociation until this elevated dissociation temperature is attained). Another potential challenge is the low injection rate and small injected volume (if fracturing is to be avoided) in accumulations with a significant hydrate saturation because of adverse permeability conditions.

C. Thermal dissociation through the circulation of hot water in the wellbore or continuous heat addition (e.g., electrical heating).

D. Combinations of thermal stimulation with inhibitor-induced dissociation (e.g., through the use of warm brines) may also be investigated if they are shown to offer significant advantages over simple thermal dissociation.

Evaluation of potential production methods will follow an interactive approach that will involve using the most recently updated information to focus on the most promising scenario(s). The production analysis strategy will be reassessed after completion of these preliminary simulations. Note that a significant realignment of this study will be necessary if field data show substantial deviations from our current assumptions on site geology and hydrate properties and conditions.

Appendix F:

Dissociation Rates of Methane Hydrate at Elevated Pressures and of a Quartz Sand-Methane Hydrate Mixture at 0.1 MPa

Report of the Menlo Park USGS Research in Support of

the Maurer/Anadarko/DOE Methane Hydrate Joint Industry Project

Under the National Methane Hydrate Research and Development Program

National Energy and Technology Program, Department of Energy

March 5, 2003

Stephen H. Kirby, Susan Circone, and Laura A. Stern
U.S. Geological Survey
345 Middlefield Rd. MS 977
Menlo Park, CA 94025

Report prepared by Susan Circone

Results Summary:

- The dissociation rate of porous, synthetic methane hydrate decreases with increasing pressure, and the pressure effect on the dissociation rate is reversible when the pressure is changed. The slowest dissociation rates at elevated pressures were observed at 268 K. Below 273 K the rates exhibit a complex temperature-dependence similar to that observed at 0.1 MPa. Our results suggest that optimum preservation of sI methane-rich hydrate will occur in drill cores maintained near 268 K during retrieval.

- The dissociation behavior of porous, synthetic methane hydrate is not significantly affected by the rate of depressurization, based on a slow depressurization experiment designed to emulate the depressurization pathway during retrieval of a drill core sample. Methane pressure was reduced over 13 minutes from 2.34 MPa to 0.1 MPa, and dissociation was monitored for 3 days at 268 K, 0.1 MPa. The measured dissociation rate is identical to those measured on samples that were depressurized within 15 seconds to 0.1 MPa.

- A porous hydrate-quartz sand mixture (1:3 by volume) dissociated at 268 K by rapid pressure release to 0.1 MPa released gas at a higher rate than 1:1 mixed or layered samples. This indicates that reducing hydrate-hydrate grain contacts by introducing sediment increases the rate of dissociation, and this factor will strongly impact the success of hydrate preservation in drill core materials with high sediment to hydrate ratios.

- Two hydrate-bearing samples were fabricated for testing of trial materials in the Mobile laboratory prior to its mobilization to Alaska. The first was a large volume, porous methane hydrate + quartz sand sample (30%:70% by volume) that was shipped directly to Tulsa in a chilled, pressurized vessel. The second was a pure, porous, methane hydrate sample that was sent to LBNL for computed tomography (CT) x-ray imaging tests in an instrument package built by LBNL for use in the Mobile Laboratory.

Introduction

Previously, a comprehensive set of experiments performed at 0.1 MPa CH_4 gas pressure and temperatures between 204 and 289 K (Stern et al., 2001) showed that methane hydrate dissociation rates are significantly depressed between 242 and 271 K. The optimum temperature for sample preservation is 268 K. Above 271 K, rates increase rapidly and systematically with increasing temperature (Circone et al., 2000). The introduction of 100 µm quartz sand into the methane hydrate sample in layers and in a homogeneous mixture (1:1 ratios by volume) resulted in higher, but still depressed, rates. Structure II methane-ethane hydrate (80% CH_4: 20% C_2H_6) did not exhibit anomalously depressed dissociation rates at 268 K.

At the request of the Maurer/Anadarko JIP, rapid depressurization experiments were performed at 1.0 and 2.0 MPa and temperatures between 250 and 283 K for the present report to determine: (1) if the optimum preservation temperature at 1 and 2 MPa is also at 268 K, and (2) if the complex temperature dependence of the dissociation rate at 0.1 MPa is also observed at elevated pressures. This information will provide recommendations for optimizing hydrate preservation by control of mud temperature during drill core recovery. An additional sample of porous methane hydrate was dissociated, following a slow depressurization pathway that was designed to emulate the depressurization pathway during retrieval of a drill core sample, to determine (3) if the depressurization rate affects the hydrate dissociation rate. (4) Finally, the dissociation rate of a 1:3 hydrate-quartz sand mixture at 268 K, 0.1 MPa was measured to determine what to expect in a similar experiment on a sample synthesized in our facility, which will be performed to test equipment and sample-handling protocol in the Mobile Laboratory prior to moving the lab to Alaska.

Experimental Method for Measuring Dissociation Rates

Experiments were performed on methane hydrate synthesized from 180-250 µm seed ice (packed to 40% porosity) and pressurized CH_4 gas by heating from 250 K to ~290 K, holding at 290 K for several hours at methane pressures above 22 MPa, then cooling to near 250 K (Stern et al., 1996; see Fig. 1). The resulting material is pure, sI methane hydrate with ~30% intergranular porosity and a measured stoichiometry of $n = 5.89 \pm 0.01$ (Circone et al., 2001).

Following synthesis, samples were thermally equilibrated at a fixed temperature between 250 and 283 K. Bath temperature T_{ext} was measured in the D-limonene bath surrounding the synthesis vessels, and internal sample temperatures were measured by thermocouples centered at the sample top, middle, and bottom and at the sample side (Setup #1, Fig. 1) or only at the sample middle (Setup #2). The pressure first was lowered to ~2 MPa above the equilibrium boundary. To start the dissociation experiment, the pressure was rapidly (~12 sec) decreased to the set point pressure, then opened to the back pressure regulator (Tescom ER 3000), which maintained the pressure within ±0.02 MPa of the set point.

Samples were held at constant temperature ($T_{iso} = T_{ext}$) for some time interval. As the hydrate sample dissociated, the back pressure regulator released methane to the flowmeter. The released gas was collected in our custom-built flowmeter at 0.1 MPa (gas flow rate is determined by monitoring the change in weight of an inverted, H_2O-filled cylinder as CH_4 gas displaces the H_2O; flow rate measurement capability ranges from 3000 to less than 0.1 cc/min; Circone et al., 2001). If $T_{ext} < 273$ K, the experiment was concluded by heating to 282 K to release any remaining methane gas and hence establish the gas content of the hydrate.

In addition, a methane hydrate sample, equilibrated at 268 K, was slowly depressurized from 2.34 MPa to 0.1 MPa at a rate of 0.17 MPa/minute while dissociation was monitored during and after the pressure release step (for 3 days at 0.1 MPa). The rate of pressure release was chosen to emulate the expected depressurization pathway during drill core retrieval at the "Hot Ice" site. The amount and rate of gas released from the hydrate was corrected for the amount of gas released from the free space in the vessel during the pressure release step.

Two porous hydrate-quartz sand mixtures (1:3 and 3:7 by volume, with ~35% porosity) were synthesized using the same technique but starting with a mixture of seed ice and 100 µm quartz sand to produce a 1-inch diameter by 14-inch long sample. For the dissociation experiment, the pressure was rapidly dropped to 0.1 MPa and then gas was released to the flowmeter, bypassing the back pressure regulator. The second sample was shipped to the Mobile Laboratory for testing.

Results

We measured the release of methane from methane hydrate samples held isothermally at 268, 273, 278, and 283 K and at 0.1, 1.0 and 2.0 MPa over time (Fig. 2 and Table 1). Three effects are clearly evident: (1) dissociation rates at 268 K are significantly slower than those at higher temperatures, (2) the samples completely dissociate within hours at $T_{iso} \geq 273$ K, and (3) rates of dissociation decrease with increasing pressure (at constant isothermal temperature). What is not evident from Fig. 2 is that, in the experiments at T ≥ 273 K, the internal sample temperatures plummet below 273 K following the depressurization step and are buffered for most of the dissociation event at 272 -273 K in the sample interior, as found by Circone et al. (2000) in experiments at 0 1 MPa. Additional experiments were performed at 250 to 263 K and 1.0 MPa to determine the effect of pressure over a wider temperature range for comparison with the previous results at 0.1 MPa.

Experimental results have been summarized in Fig. 3, in which the average rate of dissociation has been plotted as a function of isothermal hold temperature. This also shows that elevated methane pressure has depressed the dissociation rates both in the anomalous preservation regime and at the warmer temperatures. Furthermore, the rates remain significantly depressed at 268 K and elevated pressure. Note that in all experiments performed to date at 0.1 to 2.0 MPa, the dissociation rates decrease continually over time, never reaching a steady-state rate.

Also at the request of Anadarko, a methane hydrate/quartz sand sample (1:3 ratio, homogeneous mixture) was synthesized and shipped to their Mobile Laboratory then under development in Tulsa, Oklahoma. Synthesis took place in a newly acquired (with funding from this project) large, volume (1.5-inch diameter by 15-inch length) pressure vessel rated to 48 MPa (Fig. 4). The sample was to be rapidly depressurized to 0.1 MPa in a laboratory maintained at 268 K while undergoing testing of their equipment. In order to provide a reference time line for the sample composition while undergoing testing, an identical sample was dissociated in our laboratory by dropping the pressure from 4 to 0.1 MPa in 15 seconds while maintaining a constant external temperature of 268 K (Fig. 5). Our previous work shows that the hydrate dissociation rates increase with increasing volume fractions of sand, especially in homogeneous mixtures as opposed to layered hydrate/sand mixtures.

Finally, because the dissociation experiments that we have performed all followed a more rapid depressurization pathway than is anticipated during actual drill core recovery, we measured the dissociation rate on a sample that underwent the slower, expected depressurization rate (13 minutes vs. ~15 s). The results (Fig. 5) suggest that the rate of pressure release will not significantly affect the dissociation behavior if the drill core temperature is maintained near 268 K.

Summary

Based on the experimental results described in this report, the following observations can be made with respect to maximizing the preservation of a sI methane-rich hydrate during drill core retrieval:

1) Maintaining drill core mud near an optimum temperature of 268 K should greatly enhance the preservation of hydrate within the cores, as cores follow a P, T pathway of decreasing pressure (from $P > P_{equilibrium}$ to 0.1 MPa) and constant temperature.

2) Hydrate preservation will depend to large degree on the relative proportions and distributions of hydrate and sediment in the retrieved material. Hydrate preservation should be greater in hydrate-rich layers relative to sediment -rich layers.

References

Circone, S.; Kirby, S.H.; Pinkston, J.C.; Stern, L.A. *Rev. of Sci. Instrum.* **2001**, *72*, 2709.

Circone, S.; Stern, L.A.; Kirby, S.H.; Pinkston, J.C.; Durham, W.B. In *Gas Hydrates: Challenges for the Future*; Holder, G., Bishnoi, P., Eds.; **2000**; pp 544-555.

Stern, L.A.; Circone, S.; Kirby, S.H.; Durham, W.B. *J. Phys. Chem. B* **2001**, 105, 1756.

Stern, L.A.; Circone, S.; Kirby, S.H.; Durham, W.B. *Can. J. Phys.* **2003**, *in press*.

Stern, L.A.; Kirby, S.H.; Durham, W.B. *Science* **1996**, 273, 1843.

Table 1. Summary of rapid depressurization experiments performed at elevated pressures.

Sample ID	Sample weight (g)	T_{iso} (K)	P initial (MPa)	P final (MPa)	Time to drop P (s)	# of t.c.'s	Time at T_{iso} (h)	Gas Released At T_{iso} (%)	Gas Released Total (%)
040502B[a]	29.9	268.2	4.0	2.0		4	19.3	71.7	103.3
040502A[b]	34.5	268.2	4.0	2.0	98	none	188.9	30.2	98.4
042602A	29.9	273.2	5.0	2.0	34	1	22.5	98.0	98.1
042602B	29.9	277.8	7.0	2.0	17	4	2.6	92.9	92.9
120202B	29.9	283.2	9.6	2.0	13	4	2.0	96.6	96.6
053002B	29.9	249.5	3.0	1.0	14	4	18.9	57.9	100.2
072402A	29.9	253.2	3.0	1.0	15	1	886.1	41.2	98.4
091702A	29.9	257.8	3.5	1.0	12	1	460.0	52.5	99.2
012103B	29.9	262.8	4.0	1.0	15	4	382.7	51.1	100.1
010603A[c]	29.9	263.2	2.6	1.0	9	1	44.1	59.8	101.7
101502A	29.9	268.2	4.0	1.0	17	1	861.9	26.6	96.6
091702B	29.9	272.9	5.0	1.0	24	4	7.0	97.5	97.5
072402B	29.9	277.4	7.1	1.0	15	4	1.8	91.8	91.8
010603B	29.9	283.0	9.5	1.0	16	4	1.2	85.2	85.2
012103A[d]	29.9	268.3	2.3	0.1	753	1	72.5	26.3	101.3
112102[e]	37.4	268.3	4.0	0.1	15	none	21.0	49.3	93.3

Note: Total gas released includes that released upon heating from T_{iso} through 273 K and is based on a starting composition of $CH_4 \cdot 5.89\ H_2O$.

[a] During depressurization, P accidentally dropped to 1.2 MPa, then abruptly to 0.1 MPa, where sample dissociated at rates consistent with anomalous preservation. Then sample was pressurized to 2.0 MPa (up to this point, 13.0 mol% released), and the dissociation rate increased dramatically. Sample lost 58.7 % over next 19.1 h. This suggests that repressurizing samples to a CH_4 pressure below the equilibrium boundary may not decrease but instead enhance the dissociation rate.

[b] After 167 h at 2.0 MPa, P was dropped to 1.0 MPa for 8.1 h (lost 2.3 %), then increased to 2.0 MPa for 14.1 h (2.1%), before heating the sample to 282 K.

[c] Depressurization step complicated, as valve to gas booster was left open. This may have affected the dissociation rate, and the experiment will have to be duplicated.

[d] Sample slowly depressurized from 2.34 MPa to 0.1 MPa at a rate of 0.17 MPa/minute.

[e] Hydrate mixed with quartz sand, 33%:67% by volume.

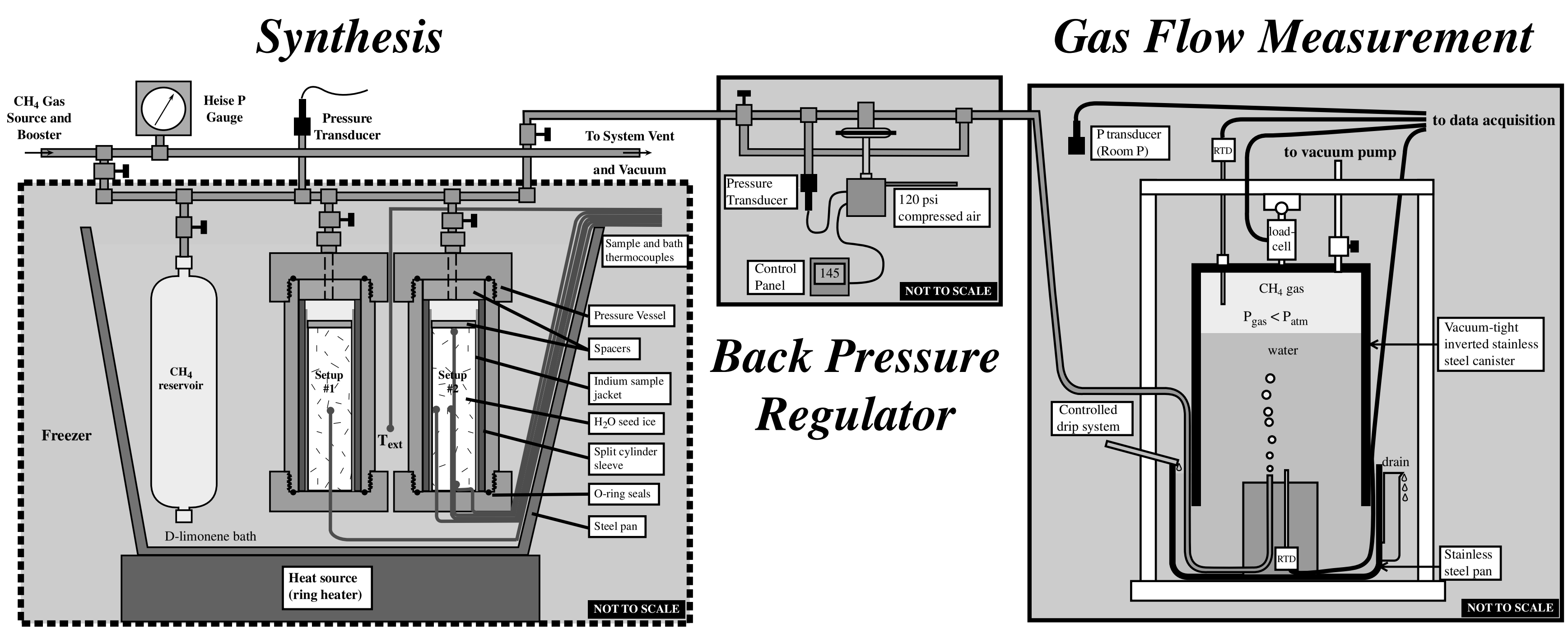

Figure 1. Schematic diagram of methane hydrate synthesis apparatus, back pressure regulator, and flowmeter apparatus.

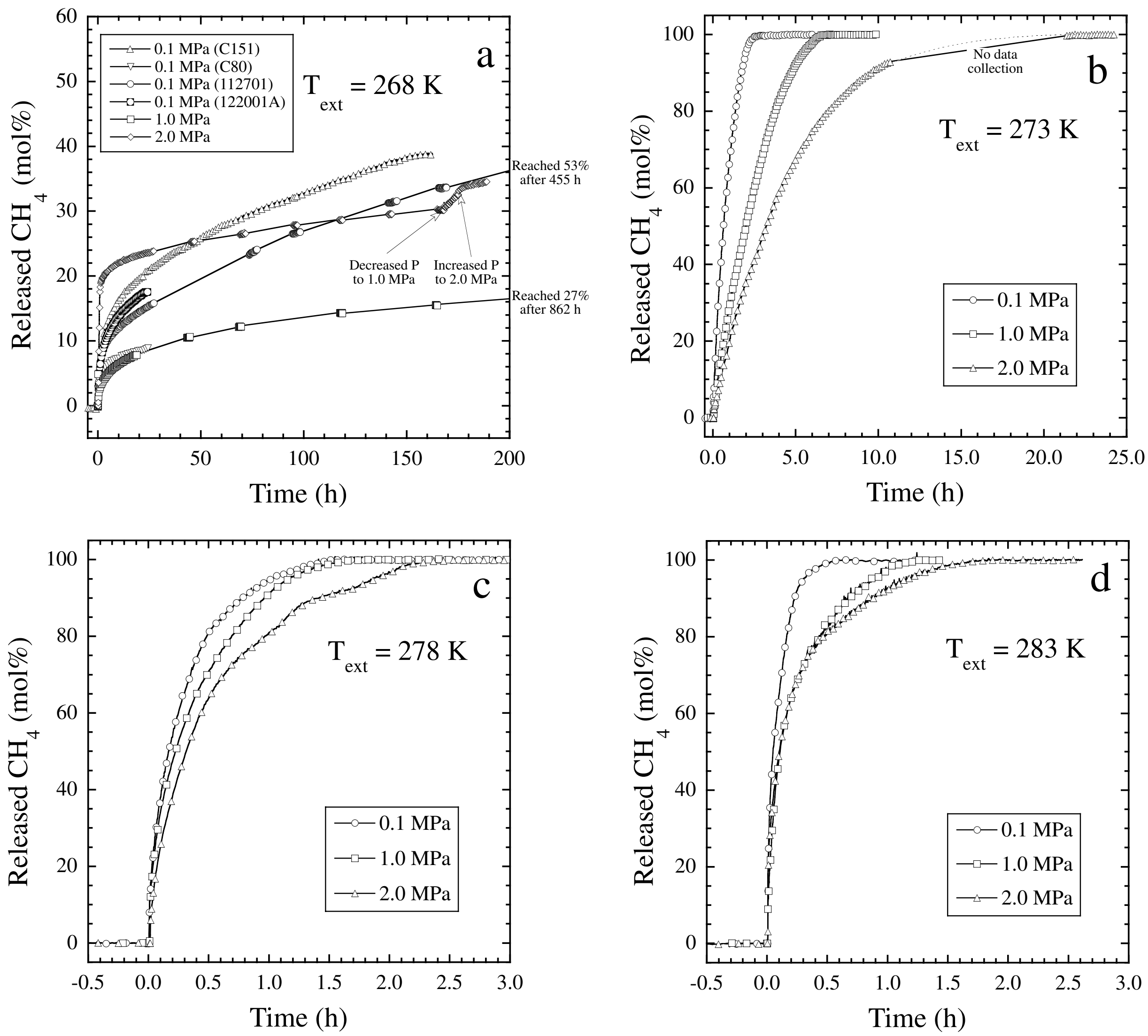

Figure 2. Evolution of methane gas from methane hydrate samples following rapid depressurization from elevated pressure to 0.1, 1.0, or 2.0 MPa at time t = 0 hours. Experiments were performed at isothermal bath temperatures of **(a)** 268 K, **(b)** 273 K, **(c)** 278 K, and **(d)** 283 K. Figure 1a includes curves of four dissociation experiments at 0.1 MPa. Note that the amount of dissociation in the first few hours is variable and does not appear to correlate with pressure. This variability significantly affects the amount of time to 50% dissociation but has little effect on the rate after the first few hours of dissociation, where the rates show a systematic decrease with increasing pressure. These experiments were concluded by heating to 282 K to release the remaining methane gas. In the 2.0 MPa experiment, we demonstrated that the pressure effect on the dissociation rate is reversible. Decreasing the pressure from 2.0 MPa to 1.0 MPa slightly increased the dissociation rate; returning to 2.0 MPa decreased the rate to near the prior value. At 0.1 MPa, similarly reversible rate changes were obtained by varying the temperature from 268 to as low as 251 K. In figures **(b)**, **(c)**, and **(d)**, the decrease in dissociation rate with increasing pressure is apparent, especially at 273 and 278 K.

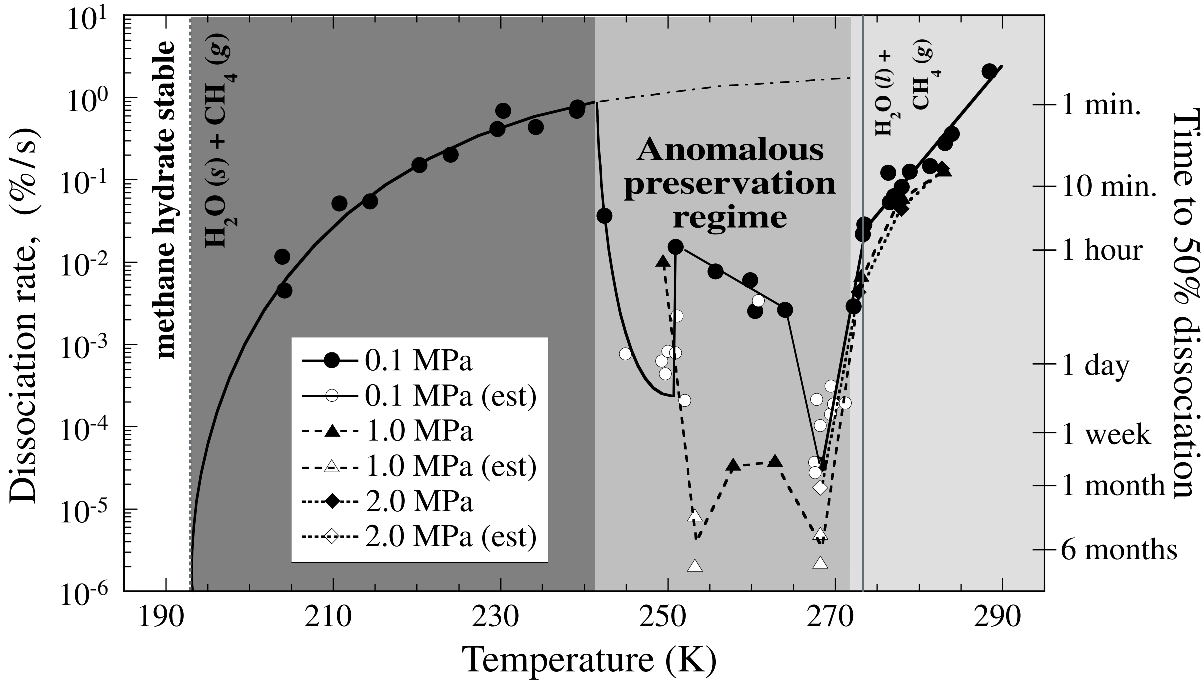

Figure 3. The average dissociation rate, as determined from the time (in seconds) required to release 50% of the gas content from the hydrate sample, as a function of the isothermal hold temperature. The right-hand axis shows the rates converted to relevant time scales. Solid symbols show results for experiments that reached 50% dissociation during the isothermal holds; open symbols show estimated times to 50% dissociation, based on extrapolations using the rates measured near the end of the isothermal hold (this extrapolation yields the minimum time to 50%; the two lowest rates at 253 and 268 K, 1.0 MPa were extrapolated assuming a continued decrease in the dissociation rate with time). Note that at 268 K, the average rate at 2.0 MPa appears higher than that at 1.0 MPa, due to the initially rapid release of methane at the start of the experiment (see Fig. 2a).

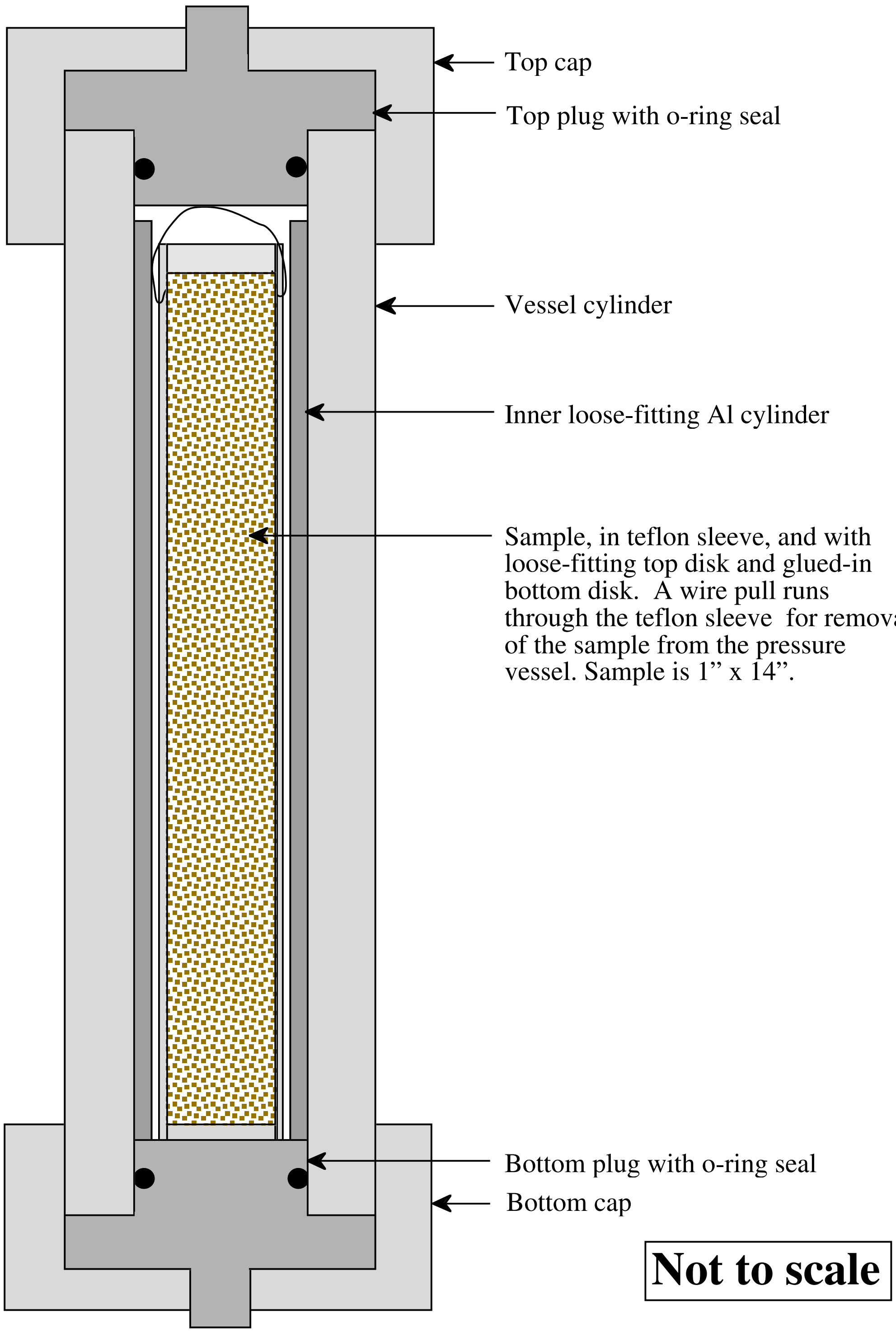

Figure 4. Schematic of vessel and sample of a porous hydrate-quartz sand mixture (30% hydrate: 70% sand by volume) synthesized at the U.S. Geological Survey and shipped for testing in the Mobile Laboratory at Anadarko in Tulsa, Oklahoma.

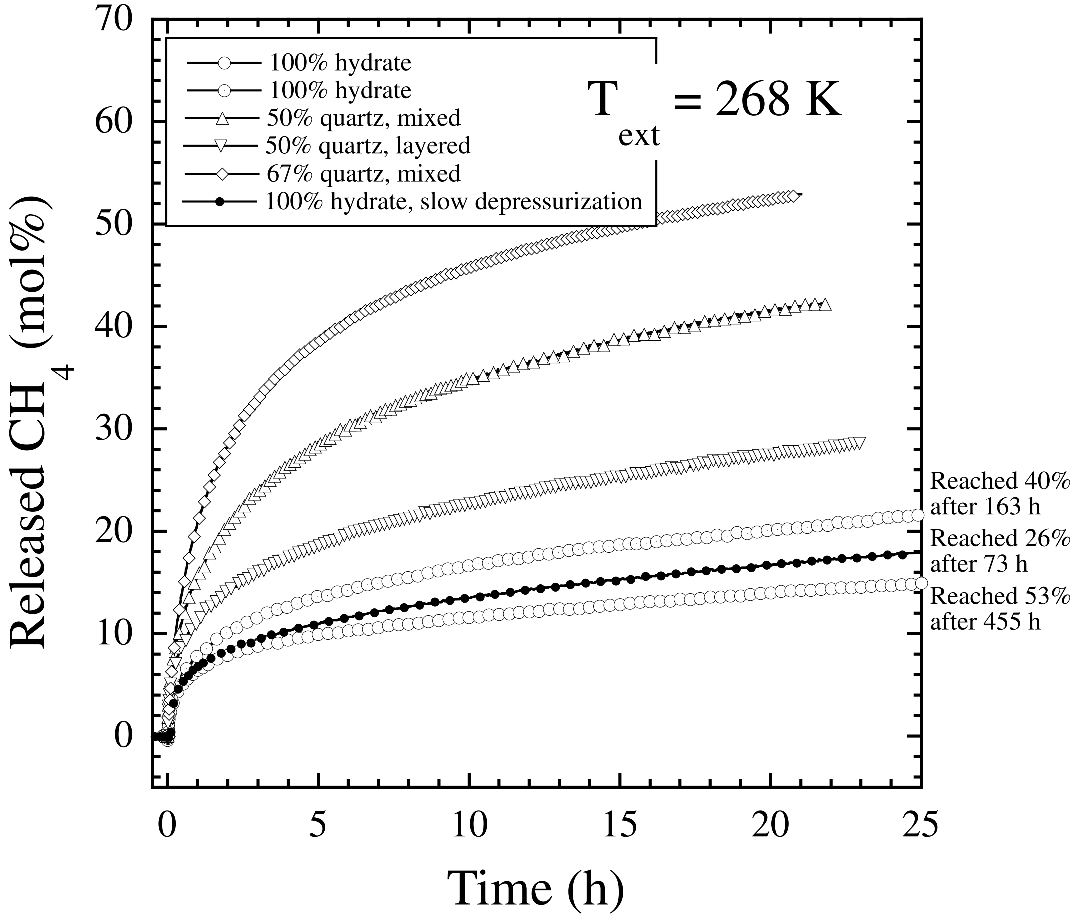

Figure 5. Release of methane from methane hydrate samples with varying amounts of quartz sand in layers (4 hydrate : 3 sand, 50% sand by volume) and in homogeneous mixtures (50% and 67% sand by volume). At 0 hours, the pressure was decreased in ~12 seconds to 0.1 MPa.